THE REDUCIBILTY OF CHROMITE ORE AND REACTIVITY OF CARBONACEOUS REDUCTANTS.

AMIT BHALLA

A dissertation submitted to the faculty of Engineering and the Built Environment, University of the Witwatersrand, Johannesburg, in fulfillment of the requirements for the degree of Master of Science in Engineering.

Johannesburg, 2012.

DECLARATION

I declare that this dissertation is my own work; unaided work. It is being submitted for the degree of Masters of Science to the University of the Witwatersrand, Johannesburg. It has not been submitted before for any degree or examination in any other university.

Amit Bhalla

21st day of August, 2012

ABSTRACT

The purpose of this dissertation is to study the reducibility of chromite ore and reactivity of carbonaceous reductants. The effect of temperature, particle size, composition, reducing agent and reducing atmosphere on the kinetics of the reduction of given chromite (obtained from Xstrata) was studied.using tga,and to test reactivity of the reductant, present experimental data was applied to Arrhenius model.

The ore is reduced by reductants namely coke, coal, charcoal and graphite at temperatures between 1000 ºC and 1300 ºC under argon atmosphere. Particle size range of as received, (+50µm-100µm), (+100µm-150 µm), (+150µm–200 µm) were used. For each experiment a calculated mixture of chromite and reductant was mixed with acetone and the mixture was reduced using a TGA furnace.The results indicated that the reduction rate was a function of temperature and particle size.The reduction at 1000 ºC under argon atmosphere is minimal.As temperature is increased to 1100 ºC, 1200 ºC and 1300 ºC it was observed that reduction rate of this chromite increased and sample having finer particle size fraction showed higher reduction rate at all temperature.

The effect of the type of reducing agent namely coal, coke, charcoal and graphite was variable.At lower temperatures: 1000ºC and 1100ºC coke, coal, charcoal and graphite was order of reduction from highest reduction to lowest whereas at higher temperatures: 1200 ºC and 1300ºC order was coal, coke, charcoal and graphite.The phases formed at the end of each reduction stage were studied using SEM and optical microscope which helped to confirm the experimental data.

To test reactivity of the reductant, present experimental data was applied to various models.A model which was found to be suitable was the Arrhenius model.The value of the activation energies obtained from fitting the data into the Arrhenius equation was used to determine the relative reactivity of the reductants, the values of the chemical reaction rate constants and effective diffusion constants were used to determine the relative speed at which the reductants can reduce the chromite ore.

The TGA test suggest that coke has the highest reactivity since its activation energies are lowest and require less energy to induce the reductants reaction The tests also suggest that the rate controlling mechanism is diffusion of species to the reactive site since the effective diffusion coefficients were of the order $10^{-11,}$ which were far less then

the chemical rate constant of the order 10^{-6} to 10^{-5}.Test also suggest that coal is fastest to react since its D_e values are high

DEDICATION

Dedicated to my parents Dr.T.N BHALLA and Mrs M.BHALLA for their ever lasting love.

ACKNOWLEDGEMENTS

Studies for the reduction of chromite ore are especially important for South Africa due to presence of large chromite ore reserves.The present study is undertaken to investigate the reducibility of chromite ore and the reactivity of carbonaceous reductants.

I wish to express my deep appreciation to my superviour Prof R.H Eric for his guidance, insight supervision and advice throughout the study, it was due to his help and advice which made research work contained in this dissertation possible.Prof C.S Kukukaragoz for his guidance, carefull questioning, patience and support which were invaluable to this study.The author wishes to express his gratefullness to Prof R.H Eric for bursary grant and financial support supplied for the project,university of witwatersrand for postgraduate merit scholarship.The author wishes to express sincere gratitude to Prof J.H Potieger, and Prof S.Iyuke, Heads of department of chemical and metallurgical engineering for the encouragement.Thanks are also due to the staff of workshop, lab managers and microscopic unit, the staff of the electron microscopic unit of the University of Witwatersrand for assistance with Scanning Electron Microscope.

Lastly but not the least, I wish to acknowledge the love of my parents, my brothers Dr Pankaj Bhalla and Dr Mohit Bhalla for their moral understanding and unparalled support during this period of my absence from home.

The Author obtained his B.TECH degree from Department of Materials and Metallurgical Engineering, Indian Institute of Technology, Kanpur, India.

TABLE OF CONTENTS Page

6.0 SUMMARY AND CONCLUSIONS

LIST OF TABLES: PAGE

LIST OF FIGURES PAGE

CHAPTER 1

INTRODUCTION

South Africa is the land of largest's chromite ore resource in the world, South African chromite ores reserves are all situated in the Transvaal province in the bushveld complex. This low quality chromite ore can act as a raw material for ferrochrome industry. The ferro chrome alloys are the principal alloys of the high carbon and low carbon ferrochromium.

The purpose of this dissertation is to study reducibility of chromite ore and reactivity of carbonaceous reductants, namely coal charcoal, coke, graphite, and thus to study the influence of composition, reducing atmosphere, particle size and temperature on the kinectis of reduction of the chromite ores. The chromite ore have been supplied by Xstrata. The ore was reduced with graphite, coal, coke and charcoal and the degree of the reduction have been obtained by measuring the losses in the weight of the samples as a function of time. The experiments were stopped each time after the desired weight losses were recorded. In this way the samples with varying degree of reduction were obtained, the phases in the reduced samples were observed under an optical microscope and scanning electron microscopy (SEM).

The overall reactions which could be taking place during reduction of chromite are shown in reaction scheme 1.

$$FeO_{(S)} + C_{(S)} = Fe + CO_{(g)}$$

$$Cr_2O_{3\,(S)} + 3C_{(S)} = 2Cr + 3CO_{(g).}$$

Scheme 1. Reactions taking place during reduction of chromite

The escape of CO as a product gas causes the masses of the sample to decrease during reduction.The mass loss recorded during reduction were used after for calculating the values of percent reduction as a function of time, the calculation related to the degree of reduction were based on assumption that CO was the only product escaping from the sample, and the amount of mass loss recorded for the sample was equal to the amount of CO escaped. With these assumptions, the relation between oxygen loss and mass loss become oxygen loss = 16/ 28 * mass loss.

To test reactivity of the reductant, present experimental data was applied to Arrhenius model, the value of the activation energies obtained from fitting the data into

the Arrhenius equation was used to determine the relative reactivity of the reductants; the values of the chemical reaction rate constant and effective diffusion constants were used to determine the relative speed at which the reductants can reduce the chromite ore.

The TGA test suggest that coke has the highest reactivity since its activation energies are lowest and require less energy to induce the reductants reaction The tests also suggest that the rate controlling mechanism is diffusion of species to the reactive site since the effective diffusionis of the order $10^{-11,}$ which is far less then the chemical rate constant of the order $10^{-}6$ to 10^{-5}, previous studies by Godfrey and Eric [45] confirms the similar rate control mechanisms.Tests also suggest that coal is fastest to react as its D_e values are high

CHAPTER 2

LITERATURE REVIEW

The reducibility of chromite ore and reactiveness of carbonaceous reductants have been studied in this thesis experimently and then a mathematical model for solid state reaction have been applied to the experimental data to determine rate of reaction and its control.

2.1 Structure of the chromite spinel:

Chromite ores comprise of pure chrome spinels combined with physically separable gangue minerals; pure chromite have a spinel structure (figure 2.1) and it can be represented as AB_2O_4 which is its chemical formula where A^{2+} divalent cation(Fe and Mg) in are in tetrahedral sites, B^{3+} trivalent cations (Cr, Al, and Fe) are in octrahedral sites. Distribution of the cations between tetrahedral A sites and octrahedral B sites give rise rise to two type of structure: (1) normal spinel which has eight divalent cations in the tetrahedral A sites and sixteen trivalent cations in octrahedral B sites, and (2) inverse spinel which have eight of the sixteen trivalent cations in tetrahedral A sites and the octrahedral B sites are occupied with eight trivalent and eight divalent cations.

2.2 Reduction Behavior of the Chromite spinels.

Chromite ore provided by Xstrata contained following oxide constituents: Cr_2O_3 (39.46%), FeO (23.1%), CaO (0.9%), SiO_2 (9.1%), Al_2O_3 (13.8%), MgO (12%), moisture (1.1%) and Cr/Fe =1.5%. Chrome ore has pure chrome spinel and physically separable gangue minerals. Reduction of chrome ore requires migration of atoms or ions in the spinel, which is possible if imperfections are present in the chromite spinel; the oxygen ion sublattice is rather perfect as compared to the cation sublattice. 1) Initially at the first stage of reduction, the removal of oxygen from surface of a chromite particle is accomplished by electrically balanced by reduction of Fe^{3+} to Fe^{2+} by the reductant. 2) In second stage, reduction will continue at the surface, by reduction of Fe^{2+} ions to the metallic states. It causes a concentration gradient of Fe^{2+} between the surface and interior of the particle which causes Fe^{2+} ions to diffuse out of the particle leaving behind a vacancy in the unit cell, because of the removal of Fe^{2+}, the ratio of the divalent cations to the trivalent cations in the unit cells underneath surface decreases, hence, the spinel

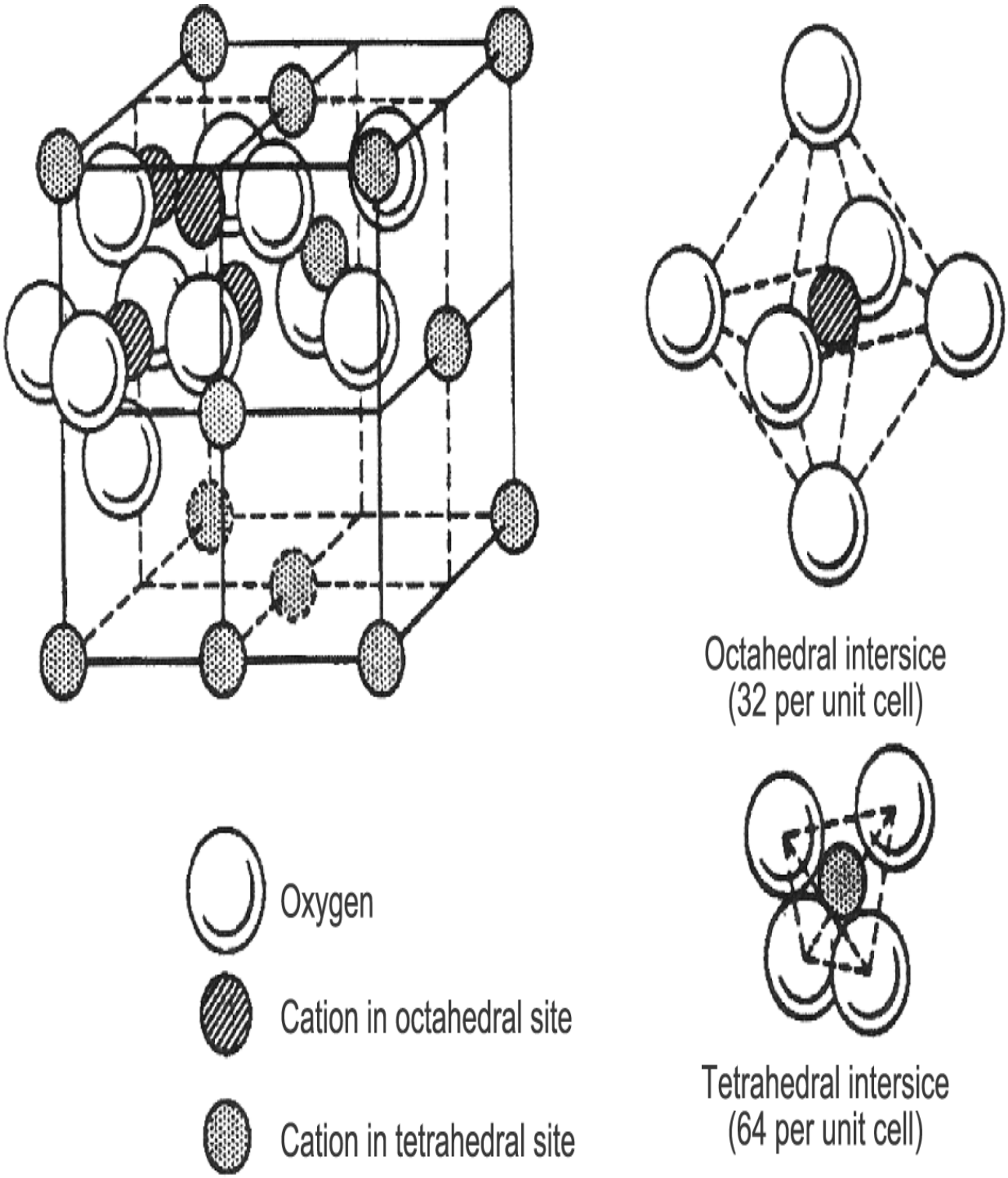

Figure 2.1 Structure of spinel

becomes saturated with trivalent oxides, and removal of iron from the system can be considered as addition of trivalent cations; Cr^{3+}, Al^{3+}, Fe^{3+} to the spinel.

2.3 Fe-O-Cr system:

The reducibility of a Chromite Ore depends on various factors such as composition, grain size of the oxides present in Chromite ore, smelting temperature and

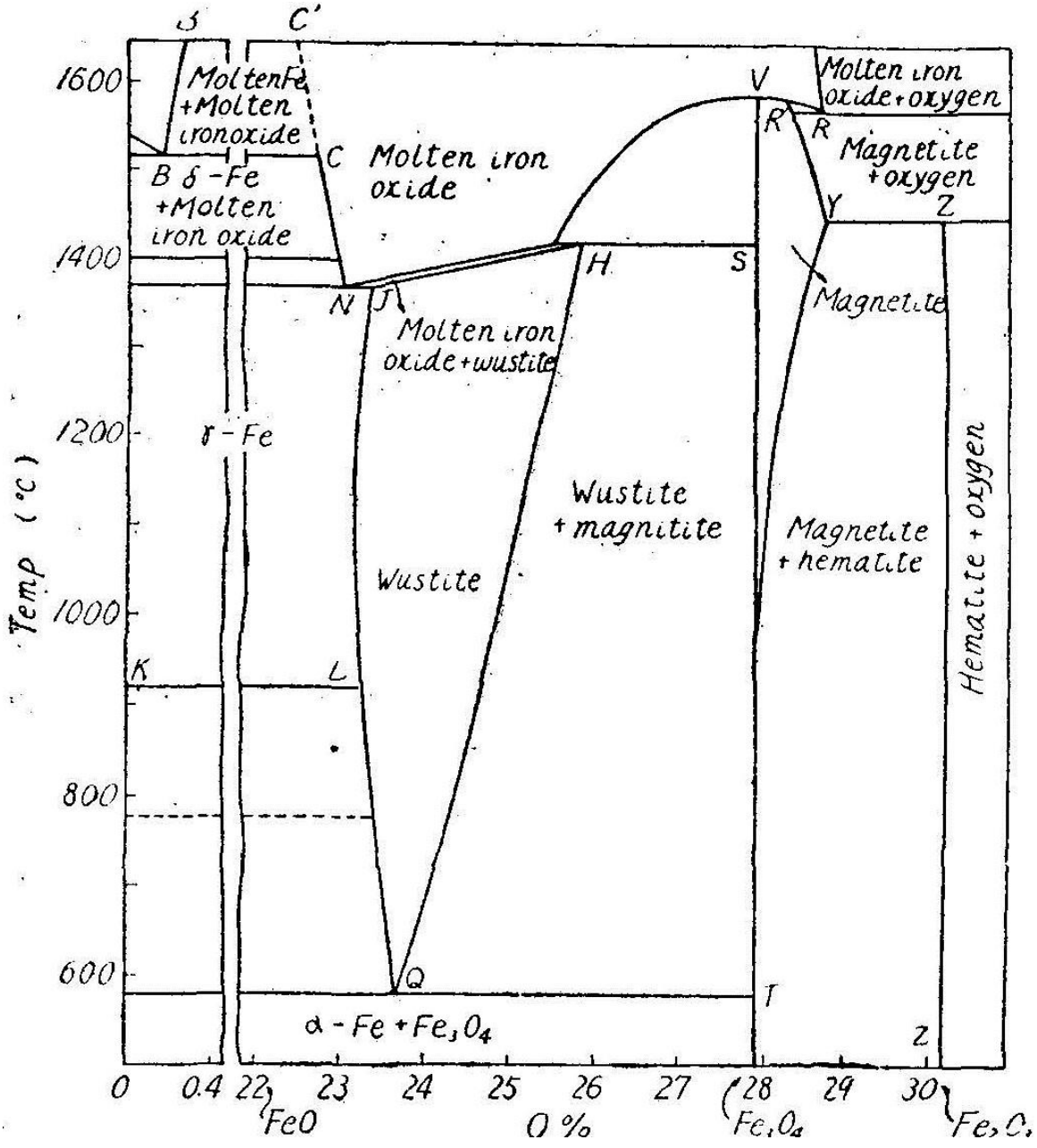

Figure 2.2 Equilibrium diagram of Fe-O system

type of reductants used. Of the oxides present in chromite ore, FeO and Cr_2O_3 can be reduced by carbonaceous reductant at normal temperatures, where as MgO and Al_2O_3 are practically irreducible. Since FeO and Cr_2O_3 are reducible at normal smelting temperature, the study of Fe-O-Cr system is important for this work. The system Fe-O was studied by Darken and Gurry [16] and later by Philips and Muan [87]. They found that during reduction of Fe_2O_3, first Fe_3O_4 and then FeO are formed as intermediate oxides; they also found that the stiochiometry of FeO changes with temperature and oxygen partial pressure at temperatures above 560 ºC. Figure 2.2 illustrates the Fe-O phase diagram. The system Cr-O was studied by Muan[78]. He noted that no intermediate crystalline phase between Cr and Cr_2O_3 is stable in the binary system. After that, Muan and Somiya [79] studied the system FeO- Cr_2O_3 in air. In this system the stable crystalline phases were the solid solutions formed between Fe_2O_3 and Cr_2O_3 and also between FeO and Cr_2O**.**

2.4 Types of carbonaceous materials used and their characteristics:

Carbonaceous materials are complex systems, which are generally heterogeneous in nature. They exhibit a wide variety of physical and chemical properties. While chemical characteristics control the reactivity of the reductant and influence the amount of reduction material used, product quality and energy consumption in the smelting process, physical properties affect the efficiency and productivity of operations to a certain extent. Specific details about main carbonaceous materials are given below:

a) **Coal**:

Coal is composed of mainly carbon, nitrogen, hydrogen, sulfur and inorganic matter. Coal is characterised by its rank, type and grade. The degree of metamorphism of coal is characterized by rank and for determining the technological usage of coal also it is also an important criterion. Type and grade of coal is determined by the amount of impurities, maceral composition and calorific value. Factors which also affect coal quality are texture, porosity, and density. Traditionally, coal selection criteria for ferroalloy production are volatile matter content, ash content and chemistry and (SiO, CO_2) reactivity. Since other reduction materials char and coke are produced from coal their properties will be derived and affected by properties of parent coal material. This is employed in prediction of coke properties and selection of coals in coke making.

(b) Coke:

Coke is produced by heating coal blend in the absence of oxygen to about 1100 °C. Quality and properties of coke are affected by the coal-rank, fluidity, maceral and mineral matter composition as well as processing conditions. Traditionally chemistry, particle size, reactivity (CRI) and strength after reaction (CSR) are considered as the most important properties of metallurgical coke for blast furnace operations. Electric furnace coke requires higher reactivity, lower strength and proper electrical resistivity.

(c) Charcoal:

Production of charcoal is from plant-derived biomass material and its properties depend on the type of wood from which it is obtained as well as the carbonisation process. As compared to coal and coke, charcoal has higher fixed carbon content and reactivity and has lower sulfur and ash content.The amount of volatile matter in charcoal is an important factor affecting charcoal properties. High volatile charcoal is less friable but more hygroscopic and easy to ignite. In comparison to fossil fuels, charcoal is a renewable and sustainable resource but is one of the most expensive raw materials.

(d) Graphite: Graphites in synthetic and natural form represent highly ordered form of carbonaceous materials. Due to cost considerations, graphite is generally not used as reductants but is used in special applications such as electrodes for the arc furnace etc.

2.5 Carbothermic Reduction Behaviour of the Metal Oxide:

During reduction of metal oxide direct reactions between oxygen and carbon are possible which can be given as following

$MeO_{(s)} + C_{(s)} = Me + CO_{(g)}$ and

$2MeO_{(s)} + C(s) = 2Me + CO_{2\,(g)}$.

According to the work done by RaO[91], direct reduction is only possible when CO and CO_2 are completely removed from the the system, this is achieved under very low pressures. It was also noted that in the reduction process the rate limiting step is diffusion of carbon atoms through the reacted shell. Where as, carbon and metal can react to form carbide as in following reaction: $xMe + yC = Me_xC_y$ and the carbide can act as a carbon carrier to the reaction interface.Therefore, the actual reduction reaction takes place

between carbide and metal oxide. It was proposed by Kolchin [63] that the reduction of metal oxides by carbon is a complex process. It is not correct to explain the mechanism of reduction by one single reaction; the possible mechanisms of reduction are classified by Kolchin [63] as follows

2.5.1. Indirect reduction of metal oxide by CO.

$$MeO_{(s)} + CO_{(g)} = Me_{(s)} + CO_{2\,(g)}$$

$$CO_{2\,(g)} + C_{(s)} = 2CO_{(g)}$$

2.5.2. Dissociation of oxide into its metal or its suboxide and oxygen followed by subsequent oxidation of carbon

$$2MeO_{(s)} = 2Me_{(s)} + O_{2\,(g)}$$

$$C_{(s)} + 1/2\ O_2 = CO_{(g)}$$

$$C_{(s)} + O_{2\,(g)} = CO_{2\,(g)}$$

2.5.3. Direct reduction of metal oxide with solid carbon.

$$MeO_{(s)} + C_{(s)} = Me_{(s)} + CO_{(g)}$$

Identification of reactions is very important for determining the rate controlling steps taking place in a reduction process.

2.6 Thermodynamics of Chromite reduction:

Perry [88] (1986) gave with help of the formula of the composition of natural chromite

$$(1\text{-}z)\ (Fe^{2+}_{x}Mg^{2+}_{(8\text{-}x)})[Cr^{3+}_{y}Al^{3+}\ (16\text{-}y)]O^{2-}_{32} + z\ (Fe^{2+}_{8})\ [Fe^{3+}_{16}]\ O^{2-}_{32}$$

Where x = (0 to 8), y = (0 to 16) and z = 0 to 1

Perry [88] expressed the total free energy of the solution as

$$\Delta G = \sum_i n_i\ \Delta G^\circ + RT \sum_i n_i\ \ln a_i.$$

Where n refers to the number of moles of end member component i. ΔG° is standard Gibbs free energy of pure component i and a_i = is the activity of component i relative to the standard state which is pure component at absolute temperature T. R is the universal gas constant. Since the solid solution is assumed to be ideal, Soykan [100] in his study calculated the Gibbs free energy for respective spinel unit cell using the above expression and thus established the thermodynamic feasibilty of the reduction reaction. He proved that phases present in order of increasing extent of reduction were found to be more stable than the previous ones. Dawson [18] (1989) in order to get iron and chromium

metallization proposed a thermodynamic model and used it effectively to get results. To express reduction process, he used following equations.

$$Fe_3O_4+4CO = 3Fe+4CO_2.$$

$$2(FeO*Cr_2O_3) +8O/7CO = 2Fe +4/7Cr_7C_3+68/7CO_2$$

$$7(MgO*Cr_2O_3) +33CO = 7MgO+2Cr_7C_3+27\ CO_2.$$

He then said that reduction of chromite can be taken as a kinetic process and considered thermodynamic 'pathway' in terms of an equilibrium between metal /carbide, oxides (spinel) and gas atmosphere at specific oxygen potentials (or CO_2/CO ratios).

2.7 The work on the development of the reduction mechanism for Chromite: Barnes, A.R and Eric, R.H [8]:

One of the most detailed studies about reduction of chromite ores by carbonaceous reductants was done by Barnes and Eric[8]. Various ores namely Henry Gould chromite, Zimbabean,Wcm lumpy, Wcm screened, Lefco concentrate were used and reductants namely Electrographite, Phoenix Coal, New Castle Coke, Vryheid Coke, Eikeboom coal were used.

Table 2.1 Composition of various ores used in study

Description	Cr_20_3	FeO	Al_2O_3	MgO	SiO_2	CaO
Henry Gould	45.8	26.5	15.4	9.2	1.5	0.35
Zimbabwean	55.2	8.7	12.9	15.2	4.6	1.0
Wcm lumpy	37.6	22.8	14.7	11.4	9.4	0.9
Wcm screened	38.7	22.8	15.0	10.7	8.6	0.9
Lefco Concentrate	39.6	25.5	15.9	10.3	5.05	0.6

Table 2. 2 Composition of various reductants used in study

Description	Fixed C	Vol	Al_2O_3	SiO_2	MgO	CaO	S	P
Electrgraphite	100							
Phoneix Coal	55.3	29.7	4.0	7.4	0.2	0.5		0.05
Castle Coke	79.6	1.4	3.7	10.3	0.6	0.5		
Vryheid Coke	78.4	1.1	6.2	10.7	0.4	0.5	0.01	
Eikeboom Coal	58.0	26.3	5.2	9.6	0.1	0.5	0.01	

Their study showed that very little reduction occurred at temperature below 1200 ºC while at 1500 ºC most chromite exhibit substantial (close to 100 %) reduction, so a temperature somewhere between these extremes was indicated. Although 1400 ºC appeared to give better discrimination, it was realized that this temperature was probably above the maximum operating temperature for solid state reduction and 1300ºC was consequently selected in order to extend the potential applicability of the technique to many laboratory facilities.

Table 2.3 Metallization results on reductants in study

Description	% Reduction	% Cr Metallization	% Fe Metallization	% Total Metallization
Vryheid coke	80	70.81	98.21	82
Newcastlecoke	58	39.86	99.03	65
Eikeboomcoke	69	58.71	91.59	72
Phoenixcoke	50	28.95	89.52	54

Nafziger, R.H, et al [80]: This study shows that that coal char is generally the preffered reductant among commercially available carbonaceous material in laboratory scale reduction experiments in argon between 1100 ºC and 1500 ºC on a domestic metallurgical grade chromite with respect to degree of reduction and metallization. They also found that for a domestic high iron chromite, coal char is preferred between 1100 ºC

and 1300 ºC where as metallurgical coke is the reductant at 1400 ºC and 1500 ºC. Both domestic chromites display generally similar reduction characteristics, the degree of reduction and metallization are proportional to the time and /or temperature used and generally reduction is greatest during first 15 min. The high iron chromite is more easily reduced, especially at the higher temperatures. They found that relatively simple kinectic equations can not adequetly describe the reduction mechanism for both of the chromites. The reduction may be nucleation controlled, especially under condition of interest of commercial operations. **Chakraborty, D et.al [13]:** they did experimental studies on the reducibility of two different chromite ores using different carbonaceous reducing agents in the temperature range 1173 to 1573K, friable lumpy and hard lumpy ore were used in the experiments. Petroleum coke, devolatised coke (DVC) and graphite were used as reducing agents. It was found by them that iron was practically completely reduced before commencement of the reduction of chromium in the ore. The reduction of iron was controlled by diffusion. The reduction of chromium was controlled either by chemical reaction or nucleation. Rate of reduction was highest when raw petroleum coke was used as reducing agent.The dvc was less effective to raw coke where rate of reduction was lowest when graphite was used as a reducing agent. **Fukagawa, S et.al [46]:** they did a study on smelting reduction mechanism of chromium ore sinter by solid carbon. Experiments were carried out at 1650 ºC to investigate the smelting reduction mechanism of chromium ore sinter by graphite. Chromium ore sinter was made from chromium ore and fluxes such as lime stone, silica sand and serpentine. The following results were obtained:

(a) Chromium ore particles are dispersed in the molten slag until they are entirely dissolved at the terminal stage of the reduction.

(b) The reduction rate is controlled by the following steps

  (i) The dissolution of chromium ore particle into the molten slag.

  (ii) The reduction of Cr and Fe oxide in the slag at slag graphite interface.

(c) The contents of Al_2O_3 and MgO in the molten slag increases as the reduction proceeds with dissolution of chromium particle.

(d) Reduction rate seemed to be decreased by the increase of Al_2O_3.

Godfrey, M and Eric, R.H [48]: authors did a study on selection of reductants. A variety of carbonaceous reductant materials are being used in the production of ferrochromium. Reductant materials include coal, coke and char. The selection of the most appropriate reducing agent depended on a number of considerations such as availability of raw material and associated costs, product and process requirements. To match the correct carbon reductant for each specific process and product requirements has become a vital function of the ferrochrome industry. This selection process however, has become increasingly difficult. In many cases, the substitution of new reductant, despite being similar in all relevant chemical specification characteristics to previous material, has resulted in different performance properties relative to that expected. An investigation prior to the usage of the substituting reductant in the submerged arc furnace was done in order to obtain required performance properties. In this investigation authors main concern was the search for a more reliable model in characterizing the reductant according to their reactivity performance, and using the model parameters to choose the appropriate reductant. The model chosen for this investigation was the Arrhenius model. Sintered chromite ore was reduced with the reductant under investigation in a Thermogravimetric analyzer TGA at different temperatures. The resultant data was then fitted into the Arrhenius model to obtain the indication of the reactivity of the reductant. The TGA tests suggest that the Vietnamese anthracite has the highest reactivity since its activation energies are the lowest and requires less energy to induce the reductant reaction. The tests also suggest that the rate controlling mechanism is the diffusion of species to the reactive site since the effective diffusion constant is of the order 10^{-10} to 10^{-11}, which is far less than the chemical rate constant of the order 10^{-6}. A generalized rate model developed by authors was used to describe the reduction of chromite which shows that at a given particle size and up to a reduction of 40%, the rate of reduction is controlled mainly by interfacial-area chemical reaction, and after which the rate is dominated by diffusion. **Perry, K.P.D.et.al [88]** studied ionic diffusion mechanism of chromite reduction. The occurrence of the various phases that form during the solid-state carbothermic reduction of chromite is explained by the use of a point-defect model. In this model each chromite particle is considered to be comprised of concentric layers of spinel unit cells ($Fe^{2+}$and Mg^{2+}occupy tetrahedral sites, Cr^{3+}, Al^{3+}, and Fe^{3+} occupy

octahedral sites). The phases that form is a result of the interchange of cations between unit cells within the particle affected by the presence of carbon monoxide at the surface of the particle. Four stages of reduction were identified by authors: (1) the formation of a slightly iron-enriched core comprising distorted spinel unit cells surrounded by a region of normal spinel unit cells, effected by the reduction of Fe^{3+} to Fe^{2+}; (2) the formation of Cr-Al sesquioxide and Mg-Cr-Al spinel phases effected by the metallization of Fe^{2+} ions and subsequent production of Cr^{2+} ions; (3) reduction of Fe^{2+} interstitials in the spinel core; and (4) metallization of chromium ions via the Cr^{2+} intermediate.

Atasoy and Sale [2]: They carried out solid state reduction of chromite concentrate. Turkish chromite concentrate was reduced with metallurgical coke between 1000-1500 ºC. Microstructure and the reduction mechanism of the chromite were looked into. Relationships between the sample morphology and reduction of chromite were investigated, such as the surface area and the porosities and cracks of the particle which have positive effect on the metallization of iron and chromium oxides. It was seen that the reduction of the iron chromite spinel started at 1000 ºC, where as reduction of picrochromite started at temperature around 1300 ºC.The formation of iron carbide phases accelerates the reduction of chromium at lower temperatures. The formation of carbon monoxide also affected on the reduction of chromite spinel, especially around imperfections of grain where porosity, cracks and fractures act as diffusion channel for the reducing gas. X-ray diffraction techniques, SEM and EDAX were used for the characterisation of the reaction products. **Hiroshi, G [50]:** he investigated under different atmosphere and with flowing CO reduction behaviour of chromite with carbon. The difference in reduction behavior was studied for pure chromite from South Africa when it was reduced with graphite powder in the atmospheres of CO, Ar, and a vacuum. Then, the reduction with flowing CO gas was also studied to compare with the former. The results are as follows: during the reduction process of the chromite with graphite the following features were observed: 1) during first two stages of the reduction, rate was much lower in vacuum but for CO and Ar atmosphere it was same, in the 3rd stage the rate was the highest in vacuum, followed by Ar, and finally by CO atmospheres. 2) In CO atmosphere and with flowing CO gas, carbon deposition was observed during the reduction with graphite at temperature below 1100 ℃, 3) It was also observed that upto

temperature 1200 ℃ the amount of carbon dissolved in metal during the reduction with flowing CO gas increased, but decreased above 1250 ℃. The reduction with the flowing CO gas was much slower with graphite. The reduction in this process indicated a preference of the iron oxide over the chromic oxide. **Sahajwalla, V et al [93]:** authors studied reductant characterization and selection implications for ferro alloys processing. A variety of carbonaceous reducing materials are being used for the production of ferroalloys. The reductant materials include not just carbons such as coke, coal, char but also bio-carbons in form of charcoal produced from different types of wood. This paper discusses critical properties and reactions of carbonaceous materials and their significance in dictating reductant performance. Main considerations include among others, gasification of reductant, dissolution of carbon into molten metal, and direct reduction of slag by solid carbon. These were discussed in this paper in relation to material properties such as structural order, mineral matter content, composition, physical characteristics etc. A brief review of both conventional and novel approaches towards characterisation of carbonaceous materials has been included. Due to complexity and heterogeneity of carbonaceous reducing materials and a wide range of process requirements, the selection of the most appropriate reducing agent will depend on a number of considerations such as the availability of raw material and associated costs, product and process requirements and environmental aspects of waste gas emissions.

Lekatou, A and Walkar.D [72]: The solid state reduction of a chromite concentrate from Northern Greece in the temperature range 1100-1470 °C has been studied. The degree of reduction of chromite by graphite was found to increase with increasing temperature, time, and carbon addition. The maximum reduction percentage attained was 75%. The maximum metallisation of iron and chromium was 91% and 67%, respectively. The main reduction products were: (i) metallic products, in order of succession of formation, Fe-C alloy, $(Cr, Fe)_7C_3$, and $(Cr, Fe)_{23}C_6$ and (ii) non-metallic products; spinels rich in MgO and Al_2O_3 that contain chromium in the divalent state. Melting of chromite, prereduced to 72.5% reduction level at 1550°C for 1.5h, led to 97.5% chromium recovery and 100% iron recovery. Satisfactory silicon and carbon contents of the metallic products were attained. **Zhang, C.Y. et al [123]:** they did a study on reduction mechanism of chromium ore pellets with carbonaceous breeze reductants and in order to clarify mechanism of

carbothermic reduction of Cr ore pellets mixed with carbonaceous breeze reductants such as coke, graphite and activated carbon samples were heated in various atmospheres at different reaction temperatures. The carbothermic reduction process of Cr ore consists of four stages. Chromite can not be reduced at low temperature, reducibility is about the same as that in CO atmosphere, the reduction of Cr ore pellets is intiated from the inside and spread gradually toward the surface, finally a stiff and compact shell is formed. At lower temperature, the carbothermic reactivity of the three kinds of carbonaceous reductants employed decreases in order of activated carbon, coke and graphite. However at higher temperature, the influence of carbonaceous reductants becomes weaker and weaker. **Khallafalla, S.E et al [62]:** They used the reacted pellets of chromite and carbonaceous reductants mixtures at pressure of 0.1 -1 torr and temperature of 1230 - 1320 ºC. The extent of reduction increased with increased temperature and decreased pressure; they found however that operating condition was limited due to onset of significant Cr vaporization at higher temperature and lower pressure. Foundary coke, anthracite and carbon black were found to be superior to graphite as reductants. **Byun, K.Y.et al [11]:** they studied the reduction rate of chromium oxide in slag phase under operating conditions of EAF process. Steel was melted in a graphite crucible under Ar atmosphere by high frequency induction furnace. The synthetic slag was placed on the steel melt and was reduced by carbon saturated melt, reduction rate were measured by analyzing both steel and reacted slag sample. Microscopic analysis showed that chromium oxide in EAF slag existed largely in spinel form of FeO and MgO, reduction yield was significantly increased by increasing temperature. The optimum temperature was found to be 1650 ºC. Experimental results indicated that the reduction rate was controlled by diffusion of Cr ions through the liquid slag phase; rate of reduction of chromium oxide increased by slag foaming at the later stage of reaction. It was also observed that SiC powder was far more effective then carbon powder as reductants at the intial stage of reaction.**Mistusuka, T. et al [77]:** They did a study on thermodynamic estimation on the reduction behaviour of iron chromium ore with carbon and it was found that the lowest temperature for reduction of FeO, Cr_2O_3 into iron chromium was 1390 K and a temperature higher than 1470K would be necessary to reduce Cr_2O_3 in $(CrAl)_2O_3$ in the pre reduction process of iron chromite ore. The composition of liquid Fe-Cr-C

alloy in equilibrium with iron- chromium ore was also estimated under 1atm of CO at steel making temperature. **Barcza** [4] studied the reduction of Bushweld Complex chromite ore with carbon. According to his work, same degree of reduction was obtained under carbon monoxide and argon atmosphere, the formation of Fe_3C was possible. Cr_2O_3 was reduced preferencially to chromium carbide. The final product was a mixed iron and chromium carbide. The reduction mechanism was diffusion controlled through the reduction products. Once the iron carbide or mixed carbide of iron and chromium are formed, these reduction products act as carbon carrier agents. **Chakraborty, D. et al** [14] studied pre-reduction of chromite outside the submerged-arc furnace (SAF) which can significantly lower the specific power consumption. Conventional processes for the pre-reduction of the ore operate at relatively high temperatures, at 1400-1500 ^oC. It is possible to enhance the rate of reduction at low temperatures by optimizing the flow rate of inert gas over the reaction site. The influence of the flow rate of inert gas on the rate of reduction of chromite ore was investigated. The rate of reduction initially decreased with the flow rate of the gas. It increased subsequently at higher flow rates to be followed by a decrease again. There was an optimum flow rate at which maximum reduction could be obtained. It was possible to achieve high levels of reduction at 1200 ^oC by optimising the flow rate of the gas. The degree of reduction obtained was comparable to that obtained at 1400-1500 ^oC, by conventional process routes.

Table 2.4 Percentage Composition of chromite ore used in their study

Cr_2O_3	Fe_2O_3	Al_2O_3	MgO	SiO_2
43	23	2.38	2.47	15.30

Experimental investigations show that high degrees of reduction of chromium and iron in chromite ore can be achieved by optimising the flow rate of argon gas over the reaction site. There is an optimum flow rate where maximum reduction can be obtained. **Van Deventer, J.S.J et al** [111] studied effect of additives on the reduction of chromite under argon atmosphere, mixtures of chromite, graphite and various additives were reacted isothermally and the loss in mass was recorded continuously. It was seen that most of the additives influenced the boudouard reaction positively. These additives were, SiO_2, Al_2O_3, K_2CO_3, Na_2O_2 CaO, MgO, Fe and Cr, and of these, only MgO and Al_2O_3 revealed

an inhibiting effect during the carbothermic reduction of chromite. During reduction it was seen that the X-ray diffraction peaks characteristic of the additives decreased in intensity, which could indicate that the additives reacted in some way. In most of the reduction products olivine (MgO Al_2O_3), Fe, Fe_3C and (Cr, Fe) $_7C_3$ could be identified. It appears as though MgO plays an inhibiting role in the decomposition of the chromite spinel. A decrease in the particle size of the chromite accelerated the reduction kinetics when CaO was used as additive; the activation energy of 192 kJ mol^{-1} for the reduction reaction without any additives is of the same order of magnitude as that measured by other authors. **Ataei, A. et al [1]** studied solid state reduction of chromite in high carbon ferrochromium chromite composite pellets. They investigated solid state reduction of high carbon ferrochromium-chromite composite pellets in the temperature range of 900-1350°C. A two stage reduction mechanism is proposed. In the first stage it was chemical reaction with activation energy of 127.2kJ/mol which was rate controlling. In second stage, rate control was by solid state diffusion of carbon through the reaction product layer.The activation energy of this stage was calculated to be 93.1 kJ/mol. It was found that high temperature and high vaccum favoured the reduction process. The results also show that pre-milling of initial mixture has a negative effect on the reduction degree. **Takano,C et al [103]** studied chromite reduction reaction mechanism in carbon chromite composite agglomerates at 1773 K. Fe–Cr–C production is a very high electrical energy consuming process. When self-reducing agglomerates are used, it is expected to decrease by up to 10% of this electrical energy. This paper presents the fundamental aspects of the reactions involved in reduction of chromites by use of self-reducing agglomerates. Brazilian chromite containing 41.2% Cr_2O_3 was mixed with petroleum coke and agglomerated with cement as the binder. The concept of 'initial slag' was introduced and it was assumed that this 'initial slag' is formed of fluxing agents, coke ash, silica formed, binder and dissolution of only 5% of the gangue from the chromite. This concept is important since the gangue of chromite is composed mainly by refractory oxides (MgO + Al_2O_3), which are difficult to dissolve into slag. The effects of 'initial slag' composition, one with low liquidus temperature (~1700 K) and the other with high liquidus temperature (~1750 K) were investigated. The mixture was pelletized, dried and submitted at the temperature of 1773 K until completion of the reactions and also the

fractional reaction as a function of time was determined. The results showed that the pellets in which liquid slag phase was formed at high temperature presented significantly better reduction behavior than the pellets in which the liquid slag phase was formed at low temperature. The microscopic analysis showed that a liquid phase was formed but the pellet did not collapse, and indicated that the coalescence of the metallic phase depended on the dissolution of the pre-reduced particles of the chromite into slag. **Xiao,Y. et al** [120] studied solid state reduction of chromite with CO. The chromite pellets (industrial and laboratory made) and lumpy ore were reduced with CO as reducing agent, with the presence of graphite in proximity to Chromite. The experiments were carried out at both rising temperature and constant temperature in the range of 1450°C - 1550°C. When reducing industrial pellets, temperature and CO flow rate had positive influence on the reduction rate. For the lab-made chromite pellets, the effects of particle size and bentonite addition on the reduction behaviour were studied. The pellet with smaller particle size gave a higher reduction rate. Bentonite addition had slightly negative effect on the reduction rate. Reduction of lumpy ore took place slower than reduction of a pellet. For all the samples, chromite reduction proceeded longer in the outer part of the sample than in the centre part. Both before and after the experiments the porosity of the chromite samples was determined. The porosity of lumpy chromite increased significantly during the reduction. However, the porosity of lab-made chromite pellet decreases due to sintering effect. Scanning electron microscopy was employed to observe and analyse the structure and composition changes of the chromite samples. **Kekkonen, M et al** [61] studied the kinetics of solid state reduction of chromite pellets and lumpy ores. The kinetics of solid state CO reduction of chromite pellets and lumpy ores were studied by thermogravimetric analysis (TGA) in the temperature range 1420-1595 °C. Generally, the reduction rate increased with the temperature. In the case of lumpy ores, at the highest temperature the kinetic conditions changed due to partial melting of the surface and thus the reduction degree remained lower. In the case of sintered pellets, the effect of surface melting was not so remarkable even at the highest temperature and the reduction rate further increased. In addition the reduction of sintered pellets with rising temperature was studied. Results showed that the reduction rate increased rapidly when the temperature reached about 1000 °C. And the final reduction was almost the same as it was in constant

temperature experiment at 1520 °C. Optical and scanning electron microscopy and microanalysis were used to obtain information on the structural changes of the partly reduced samples. Optical photographs and microanalysis showed that the reduction degree was higher in the outer zone of the samples. **Xuemin, Y et al** [121]studied effect of coal types on reduction rate of iron ore pellets containing coal. The effect of coal size, iron ore concentrate size, temperature and carbon oxygen mole ratio on the reduction rate of iron ore pellets containing high, middle, low volatile coals as reductant has been investigated in nitrogen at temperature range of 1223～1473 K by using a thermal weight loss balance. The reduction rate of iron ore pellets has been increased with decreasing the coal and iron ore concentrate size, increasing temperature and carbon oxygen mole ratio, but the above mentioned four factors have greater effect on reduction rate for pellets containing low volatile coal. Most of the experimental data can be successfully represented by four well known kinetics equations based on carbon gasification, gas diffusion and phase boundary reaction as rate controlling step and the rate constant can be evaluated, then the activation energy for pellets containing different volatile coals can be calculated by Arrhenius equation. It has been concluded that gas diffusion should be the reduction controlling step of composite pellets as the calculated activation energy based on the assumption that gas diffusion is the rate controlling step is the greatest. The higher the volatile content of coal is, the easier the pellets are reduced because the activation energy for gas diffusion is smaller for composite pellets containing higher volatile coal**.** **Ding, Y.L et al** [25] studied catalytic reduction of carbon-chromite composite pellets by lime. The catalytic effect of lime on the reduction of carbon-chromite composite pellets was investigated at 1270-1433^{o}C under CO-argon atmospheres. It was found that the data for the early stage of reduction, up to a reduction level of 30-60%, fit both an exponential law for nucleation control and an equation for chemical control with an apparent activation energy ranging from139 to161 kJ/mol depending on the amount of lime addition. In the late stage (after about 65% reduction), solid diffusion of chromium in the oxide phase is the most likely rate-controlling step with an apparent activation energy of 410 kJ/mol. Besides the possibility of it being able to go into the spinel lattice and release the FeO, lime is also suggested to catalyse the chromite reduction through enhancing the nucleation and/or interfacial reaction in the early stage, and facilitating the solid-diffusion

process in the late stage. The results of this study also indicate that heat treatment of chromite has a significant effect on the reduction kinetics.

3. EXPERIMENTAL.

Experimental details on

1) Chromite ore, 2) Reducing agents, 3) Selection of Experimental technique, 4) Atmosphere, 5) Experimental Setup, 6) Furnaces, Controller and Balance, 7) Measurement of loss of Mass, 8) Sample preparation reductions runs, 9)Particle size Analyser, 10) Metallographic techniques and Optical Microscopy, 11) Definitions of terms.

are given below.

3.1 CHROMITE ORE:

Chromite ore from Xstrata were used in the experiments conducted to determine the effects of various factors on the kinetics of reduction. It was ground in a crusher and sieved to different sizes namely as received, +50µm-100 µm,+100 µm -150 µm,+150 µm -200 µm.

Table 3.1: Composition of the chromite ore sample used in this study:

Oxide	Cr_2O_3	FeO	Cao	SiO_2	AL_2O_3	MgO	Moist	Cr/Fe
%	39.46	23.1	0.9	9.1	13.8	12.0	1.1	1.5

3.2 REDUCING AGENTS:

Reductants were procured from Xstrata namely coal, coke and, charcoal. These were coke (81.7% fixed carbon,16.9% ash, 0.9%volatiles), charcoal (74.8 fixed carbon, 18.9% ash, 4.6 volatiles), coal (58.2%fixed carbon 17.8 % ash, 22.7% volatiles). Graphite was taken from the chemical stores of the pyrometallurgy laboratory at the University of the Witwatersrand. Reductants were also ground in a crusher and sieved to different sizes namely as received,+50µm-100 µm,+100 µm -150 µm,+150 µm -200 µm. where µm is size in micron and (+) indicate size higher than the value and (-) indicates smaller than the value i.e,+50µm-100 µm indicate size greater than 50 but less then 100.

3.3 PARTICLE SIZE ANALYSIS:

Particle size analysis of the chromite was initially done to see in which range there is concentration of the particles, it was found, concentration was around 100µm.

3.4 SELECTION OF EXPERIMETAL TECHNIQUE:

Barnes (1981) [7] in his review work on the technique used to examine reduction behavior said that thermogravimetric analysis (TGA) gives a total picture of the rate of reduction of the sample at that temperature; it is basically a measurement of mass change as a function of time. Finn and Kucukkaragoz (1980) [41], Searle and Finn (1983) [94] also used the TGA technique to study reduction of the BC chromite. They concluded that by thermogravimetric analysis the runs could easily be duplicated and provision could easily be made for controlling the atmosphere.

Eric and Barnes [8] did a detailed study about reduction of chromite ores by carbonaceous reductants using TGA technique. Various ores namely Henry Gould chromite, Zimbabean, Wcm lumpy, Wcm screened, Lefco concentrate were used and reductants namely Electrographite, Phoenix Coal, New Castle Coke, Vryheid Coke, Eikeboom coal were used. Hence it was decided to examine the reduction mixtures of chromite and various reductants by thermogravimetric technique.

3.5 ATMOSPHERE:

The rate of reduction is influenced by the atmosphere in which reduction is carried out, though overall reaction may not involve the surrounding gas. In carbon monoxide atmosphere in the presence of solid carbon the reaction sequence for reduction of metal oxide MO is:

$$MO_{(s)} + CO_{(g)} = M_{(s)} + CO_{2\,(g)}$$

$$CO_{2\,(g)} + C_{(s)} = 2CO_{(g)}$$

The overall reaction is

$$MO_{(s)} + C_{(s)} = M_{(s)} + CO_{(g).}$$

Here, there was no consumption of carbon monoxide from atmosphere. Rankin (1979) [89] said this is valid for chromite reduction.

For inert atmosphere, the reaction path involves first reduction by solid carbon and then reduction by carbon monoxide. In this case the intial reduction step will involve carbon at points of direct contacts between the oxide and the solid carbon followed by carbon monoxide reduction and eventually the generation of carbon monoxide.

In this study an inert argon atmosphere is selected as a safe and convienient atmosphere. Argon is dried in a drying chamber and passed through a copper chips furnace operating at $500^{o}C$ to remove any residual oxygen before entering the system as spectroscopic argon contains 5 ppm oxygen and water vapour.

3.6 EXPERIMETAL SETUP:

Experimental setup was made with a furnace, balance, capillary flowmeters, argon cylinder, gas inlet/outlet connections, temperature controller and Pt –Rh thermocouple. Through drying system, argon gas was passed and regulated before being passed into the furnace, reagents used in drying units were 1) magnesium perchlorate and 2) sulphuric acid.

3.7 FURNACE, CONTROLLER AND BALANCE:

3.7 (a) FURNACE

A Kanthal wound resistance furnace with a recrystallised alumina work tube, which had a inside diameter of 60mm, was used. First the furnace was prepared by setting the thermal cotton wool inside the Furnace and fitting the outer cylinder in the container. Inner cylinder with kanthal wire was prepared by placing kanthal wire on the inner cylinder at a calculated distance and by using alumina cement the wire was set in. Once the assembly has dried, the cylinder with kanthal wire was placed inside the outer cylinder in the furnace. Temperature was controlled by A (Pt-Rh) thermocouple placed from the opening at the back of the furnace, so that the thermocouple is touching the alumina cement on winded kanthal tube.

Once the thermocouple was placed the space between the outer cylinder and inner cylinder was filled with sand to the top of the furnace, then furnace lid was closed. Furnace work tube was set in with proper care in order to avoid breaking of the worktube. The length and diameter of the furnace worktube were 1000mm and 60mm respectively.

The inlet and outlet pipe for the gases were connected at the bottom of the furnace and at the top of the furnace work tube. Argon cylinder was connected through capillary flowmeter to inlet pipe of the furnace, so that flow rate of gasses could be regulated.

3.7 (b) CONTROLLER

Temperature was controlled by a Eurotherm type temperature controller; the temperature controller had connections for the thermocouple and furnace supply.

3.7 (c) BALANCE

Balance was made by setting Ohaus balance in a sealed perspex box, such that alumina rod opening is at right place. Alumina rod was attached to the balance and it was adjusted for reading. A flexible tube was attached at the top of the balance which was connected to the lower part of the furnace work tube when balance was moved toward the work tube of the furnace at the start of the run. The furnace was water cooled at the top and bottom. The furnace was fixed and balance was free to move vertically along the rod attached. A rubber tube was attached at the top of the balance which was connected to the lower part of the tube when balance was moved toward the tube at the start of the run. Once connected it was sealed, so that no gas leak could take place.

3.8 MEASUREMENT OF LOSS OF MASS (TGA):

Weight loss measurements during reduction were continuously monitored on computer interfaced to balance, weight loss values were continuously stored in memory and weight loss was converted to reduction percentage.

3.9 SAMPLE PREPARATION AND REDUCTION RUNS:

3.9 (a) SAMPLE PREPARATIONS:

Reduction runs were performed with charge consisting of a mixture of chromite ore and reductants in an alumina crucible. The mixture was prepared in an agate mortar under acetone. Acetone was later removed in a drying oven. The amount of chromite and the reductant was calculated as shown in Appendix B.

3.9 (b) REDUCTION RUNS

The prepared charge was put in alumina crucible, the alumina crucible containing sample was placed on the top of balance pedestal. Argon flow into the worktube was started.The recorder was switched on and the zero level was adjusted according to total weight of the crucible plus sample and argon flow was let to continue in order to prevent oxidation.The alumina crucible along with the rod was slowly pushed to the hotzone and the mass change was started as soon as the sample was raised into the hot zone after zeroing of weight reading on the balance. Reduction runs were conducted at temperatures 1000 ºC, 1100 ºC, 1200 ºC and 1300ºC. Experimental runs were allowed to proceed up to 120 minutes, where upon they were stopped by lowering the balanced to the cold end of the furnace. To determine whether there was any air leaking into the system a carbon blank run was carried out at the end of each set of 10 runs which proved that the system was free of air leaks. After cooling, the reduced samples were mounted with epoxy resins, polished and examined under optical microscope. Scanning electron Microscopy was done for selected samples at various stages.

3.10 METALLOGRAPHIC TECHNIQUE AND OPTICAL MICROSCOPY:

Standard metallographic technique and optical microscopes were used for preliminary optical examination of product samples. Samples were prepared in the metallographic lab by putting the reduction charge with additives and pressing it to make epoxy samples, which were then polished using diamond wheel polisher and were examined under optical microscope to get optical image for various samples at various runs.

3.11 DEFINITION OF TERMS:

Slatter (1981) [97] stated that, reducibility is a measure of the relative ease with which an ore can be reduced to metal and it is defined as the measured weight loss of the ore during reduction with carbon, after a time at a given temperature, expressed as a percentage of the theoretical weight loss for total reduction of the ore.Therefore the degree of reduction of chromite, R%, could be described as:

R% = [mass of oxygen removed /mass of original removable oxygen]*100.

Three major oxide components, in naturally occurring chromite spinels, namely ferric and ferrous iron oxides and chromium oxide were considered to be reducible, whereas the other oxide components, namely alumina and magnesia, were all classed as non–reducible under the conditions of solid state reduction of chromite with carbon.

The thermodynamics of the Boudouard reaction $C+CO_2=2CO$ indicates that CO is the only stable gas above 900ºC. The measurement of the mass loss by thermogravimetry during reduction therefore indicated the quantity of CO released during the reaction and was directly proportional of oxygen lost from the oxides, and hence to the degree of reduction.The degree of reduction was therefore defined as:

R%= [mass of CO evolved / (28/16) * mass of original removable oxygen]*100.

This definition was used in this investigation.

3.11 (a) STIOCHIOMETRIC CARBON:

The stiochiometric amount of carbon was defined as the amount required for complete reduction of the iron and chromium oxides in the chromite spinels to form the carbide, $(Fe,Cr)_7C_3$, the presence of which was reported in the reduced chromite by Rankin (1979) [89].

CHAPTER 4

EXPERIMENTAL RESULTS AND DISCUSSIONS

The results of all reduction runs of chromite with different reductants at different temperature are presenred in following chapter. The reduction is defined as loss of oxygen from chromite and degree of reduction then equals to the ratio of oxygen loss to total reducible oxygen.

Reduction % = [oxygen loss/ total reducible oxygen]*100

Total reducible oxygen indicates the total amount of oxygen present in the reducibile oxides of the chromite. The total amount of reducibile oxide is calculated as 4.0392g (Appendix A). It is possible to replace oxygen loss with mass loss. In order to calculate the degree of reduction from the mass loss

Reduction % = [mass loss/ total possible mass loss] *100

Where total possible mass loss is calculated as (28*4.0392/16) of the sample and formula become reduction % = 13.96 * mass loss.

In experiments both chromite and reductants of sizes 1) as received, 2)(+50µm-100µm), 3)(+100µm-150µm),4) (+150µm-200µm)were taken. In this chapters for sake of understandibilty of experimental results, details of a sample group of chromite sizes (+100µm-150µm) and reductants of sizes, (+50µm-100µm), (+100µm-150µm), (+150µm-200µm) and as received is discussed in graphical form. Also effect of variation of particle size and effect of variation of temperature on all results is discussed. Graphs of others size are added into Appendix (D). The reduction curves of sample (figure 4.1 to figure 4.27) were obtained by plotting the degree of reduction obtained from the above formula as a function of time.

The effect of particle size and temperature on the reduction can clearly be seen in the curves (Figure 4.28 to figure 4.39). According to results obtained the reduction rate is a function of temperature and particle size, increasing with temperature and decreasing with particle size. The xstrata chromite with size fraction as received.(+50 µm -100 µm),(+100 µm -150 µm),(+150 µm –200 µm) was reduced at temperatures 1000 ºC, 1100 ºC, 1200 ºC and 1300 ºC. It was observed that reduction rate of this chromite increased

with temperature and sample having finer particle size fraction showed higher reduction rate at all temperature.

The effect of reducing agent namely coal, coke, charcoal and graphite is quite apparent from the behaviour shown at lower temperatures of 1000 ºC and 1100 ºC where coke, coal,charcoal and graphite was order of reduction whereas at higher temperatures of 1200 ºC and 1300 ºC order was coal, coke, charcoal and graphite. The reducing atmosphere was kept the same through out at all temperature and the reduced samples were examined under optical microscope. Metallisation could not be observed at reduction level <4%.

Nucleation of metallic phases was observed with samples having higher than 4% reduction. Nuclei grew in size as the degree of reduction increased.The growth of nuclei continued until the particle was completly covered by an alloy shell at high levels of reduction.

4.1 Reduction at 1100 ºC.

From the mass loss recorded at 1100 ºC for different reductants for sizes varing from as received, +50µm-100µm, +100µm-150µm,+150µm-200µm for both chromite and reductants; namely coke, charcoal, graphite and coal, reduction % was calculated as: reduction % = 13.96 * mass loss. Following table gives % reduction at this temperature.

Table 4.1 Experimental Results of Reduction Runs at 1100 ºC

Runs	Chromite size	Reductant	Reductant size	Time(min).	Red^{n} (%)
33	(+50 µm -100µm)	Coke	(+50 µm -100µm)	120	16.43
34	(+50 µm -100µm)	Coke	(+100 µm -150µm)	120	16.31
35	(+50 µm -100µm)	Coke	(+150 µm -200 µm)	120	14.12
36	(+100 µm -150µm)	Coke	(+50 µm -100µm)	120	16.16
37	((+100 µm -150µm)	Coke	(+100 µm -150µm)	120	16.01
38	(+100 µm -150µm)	Coke	(+150 µm -200 µm)	120	13.16
39	(+150 µm -200µm)	Coke	(+50 µm -100µm)	120	16.11
40	(+150 µm -200µm)	Coke	(+100 µm -150µm)	120	15.43
41	(+150 µm -200µm)	Coke	(+150 µm -200 µm)	120	10.17
42	(+50 µm -100µm)	Charcoal	(+50 µm -100µm)	120	11.40
43	(+50 µm -100µm)	Charcoal	(+100 µm -150µm)	120	9.39
44	(+50 µm -100µm)	Charcoal	(+150 µm -200 µm)	120	9.35
45	(+100 µm -150µm)	Charcoal	(+50 µm -100µm)	120	9.34
46	((+100 µm -150µm)	Charcoal	(+100 µm -150µm)	120	8.18
47	(+100 µm -150µm)	Charcoal	(+150 µm -200 µm)	120	6.72
48	(+150 µm -200µm)	Charcoal	(+50 µm -100µm)	120	5.61
49	(+150 µm -200µm)	Charcoal	(+100 µm -150µm)	120	5.59
50	(+150 µm -200µm)	Charcoal	(+150 µm -200 µm)	120	3.96
51	. (+50 µm -100µm)	Graphite	(+50 µm -100µm)	120	3.99
52	(+100 µm -150µm)	Graphite	(+150 µm -200 µm)	120	3.14
53	(+100 µm -150µm)	Graphite	(+50 µm -100µm)	120	4.32
55	(+50 µm -100µm)	Coal	(+50 µm -100µm)	120	9.98
56	(+50 µm -100µm)	Coal	(+100 µm -150µm)	120	9.36
57	(+50 µm -100µm)	Coal	(+150 µm -200 µm)	120	9.10
58	(+100 µm -150µm)	Coal	(+50 µm -100µm)	120	9.81
59	(+100 µm -150µm)	Coal	(+100 µm -150µm)	120	9.59
60	(+100 µm -150µm)	Coal	(+150 µm -200 µm)	120	9.21
61	(+150 µm -200µm)	Coal	(+50 µm -100µm)	120	12.81

4.1.2 Effect of particle size

In order to determine the influence of particle size of reductants and chromite at 1100 ºC, it was investigated for all sizes of chromite and all sizes of reductants. From this investigation, following conclusion were drawn, which in general can be stated that decreasing the particle size results in an increase of reduction rate, a finding which is confirmed in a number of previous studies (Barcza[4], Soykan[100]).

4.1.3 Change in reduction (%) with change in size of chromite, coke, charcoal, graphite and coal at 1100 ºC. (Showing effect of particle size).

1)At 1100ºC, as the chromite size decreases from +150µm-200µm to +50µm-100µm with varing coke size, reduction % increases from 10.17 %(min) to 16.43%(max) as shown in figures 4.1 to 4.3 and figures D.1 to D.4(appendix D) and table 4.1.

2) At 1100ºC, as the chromite size decreases from +150µm-200µm to +50µm-100µm with varing charcoal size, % reduction increases from 3.96%(min) to 11.40%(max) as shown in figures 4.4 to 4.6 and figures D.5 to D.10(appendix D) and table 4.1

3) At 1100 ºC**,** as the chromite size decreases from +150µm-200µm to +50µm-100µm with varing graphite size, %reduction increases from 3.14 % (min) to 3.99% max. Not much can be deduced from graphite reduction as % of reduction is very low as shown in figures D.11 to D.13 (appendix D) and table 4.1

4)With Coal, at 1100 ºC as the chromite size decreases from +150µm-200µm to +50µm-100µm with varing coal size, % reduction increases from 9.21%(min) to 9.98% max. The effect of reductant coal at this size with chromite of size (+150 µm -200µm) is shown in figures D.14 to D.16 (appendix D) and table 4.1

So it can be concluded that at 1100 ºC, coke as a reductant gives maximum reduction of 16.43 % for smallest chromite and coke size, each being (+50 µm -100µm), whereas graphite shows the least; 4.32%(max) reduction, followed by 11.40 % (max) of charcoal and coal 12.81%(max). Hence order of reductants is coke, coal, charcoal and graphite in terms of % reduction, coke being highest % and graphite being lowest.

4.1.4. Reduction curves of how reduction proceeds at 1100 ºC.

For sample group (chromite size (+100-150) and reductants size increasing from (+50-100) to (+150-200) graphs are given below.

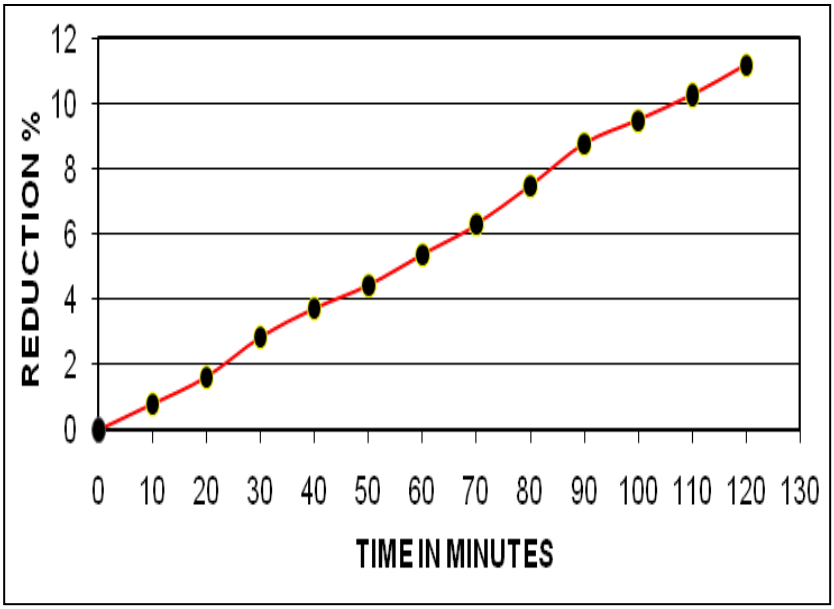

Figure 4.1 Effect of coke (+50µm-100µm) addition on the reduction of xstrata chromite (+100µm-150µm) at 1100 ºC

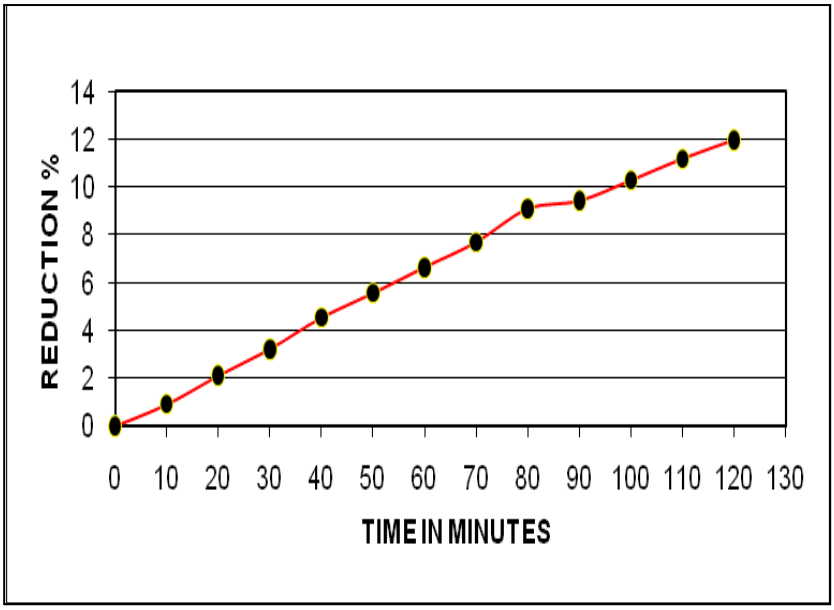

Figure 4.2 Effect of coke (+100µm-150µm) addition on the reduction of xstrata chromite (+100µm-150µm) at 1100 ºC

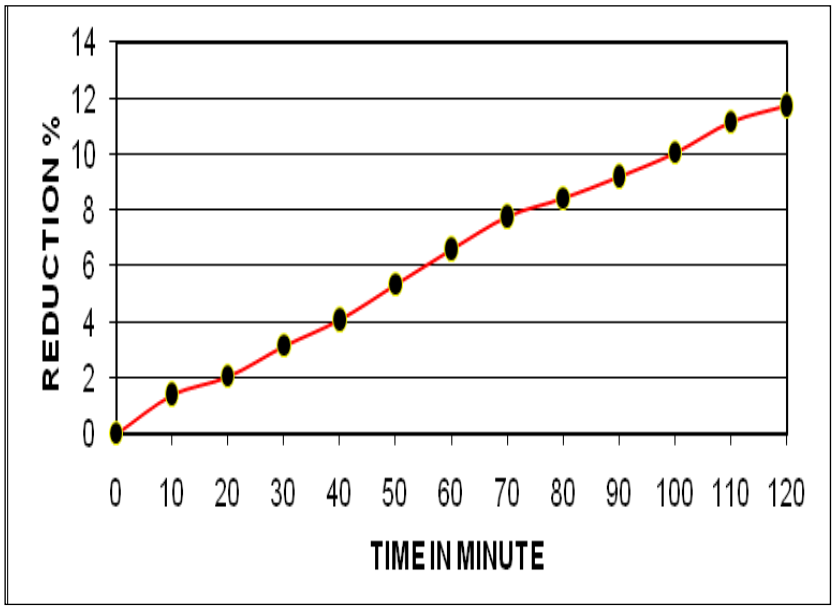

Figure 4.3 Effect of coke (+150µm-200µm) addition on the reduction of xstrata chromite (+100µm-150µm) at 1100 ºC

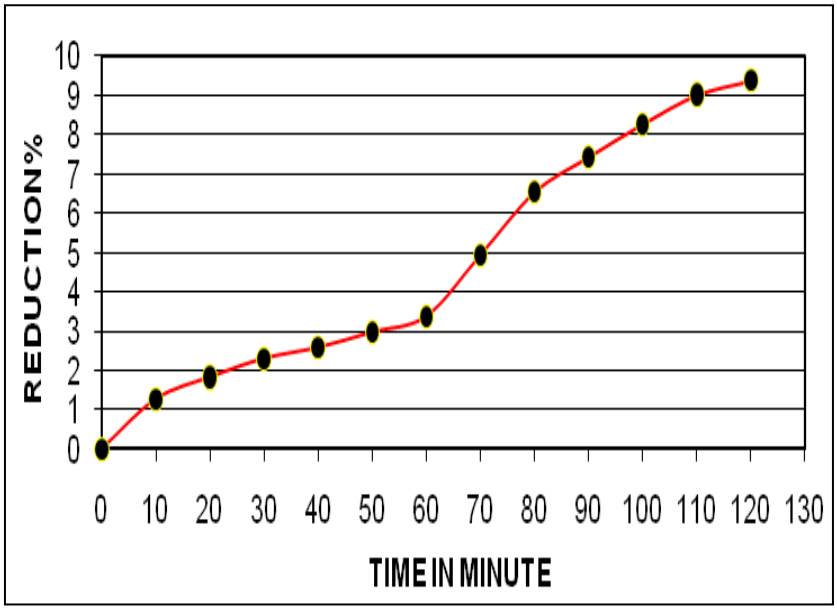

Figure 4.4 Effect of charcoal (+50µm-100µm) addition on the reduction of xstrata chromite (+100µm-150µm) at 1100 ºC

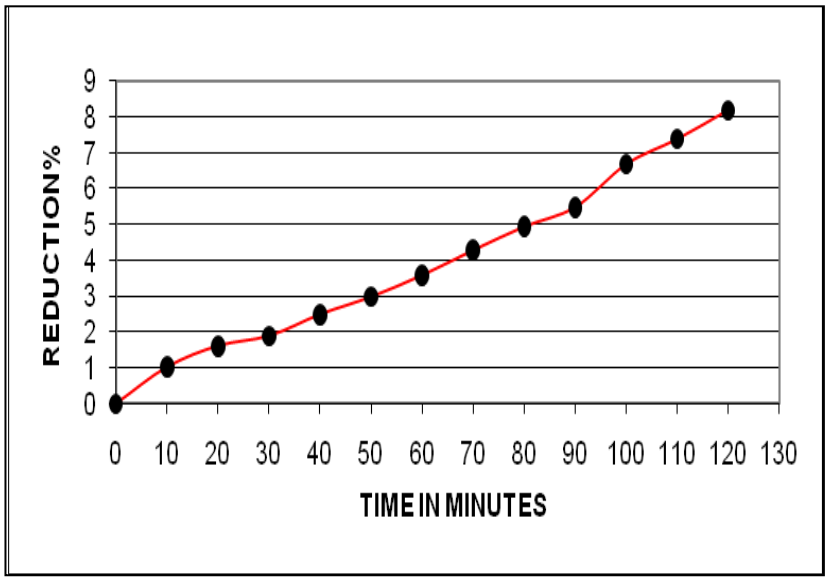

Figure 4.5 Effect of charcoal (+100µm-150µm) addition on the reduction of xstrata chromite (+100µm-150µm) at 1100 ºC

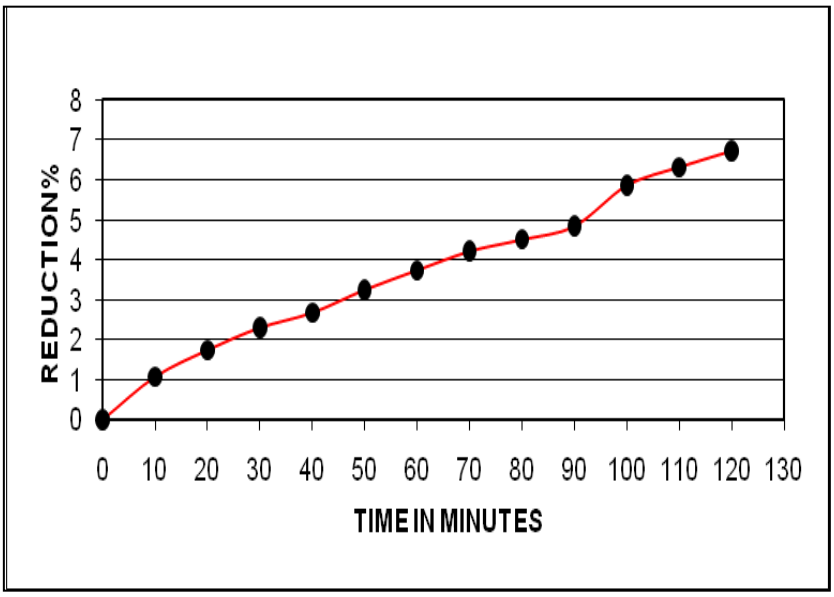

Figure 4.6 Effect of charcoal (+150µm-200µm) addition on the reduction of xstrata chromite (+100µm-150µm) at 1100 ºC

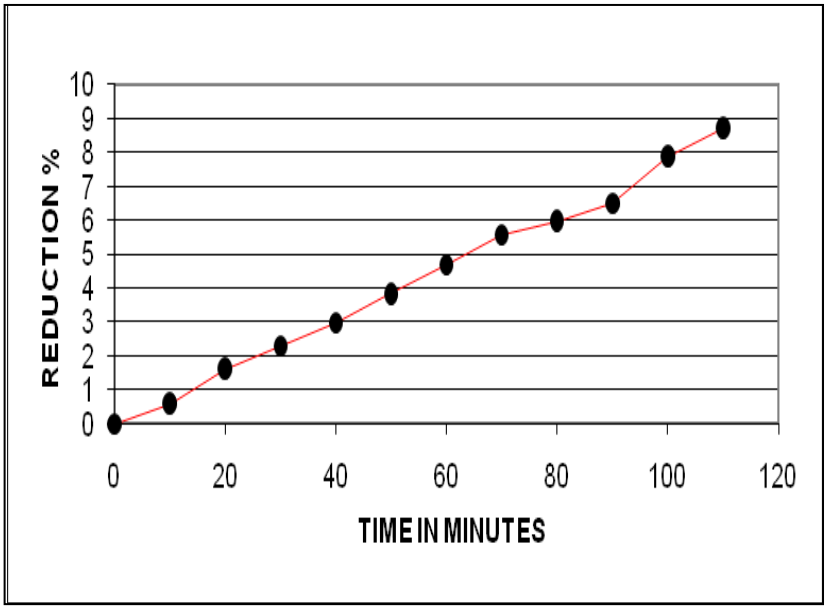

Figure 4.7, Effect of coal (+100µm-150µm) addition on the reduction of xstrata chromite (+100µm-150µm) at 1100 ºC.

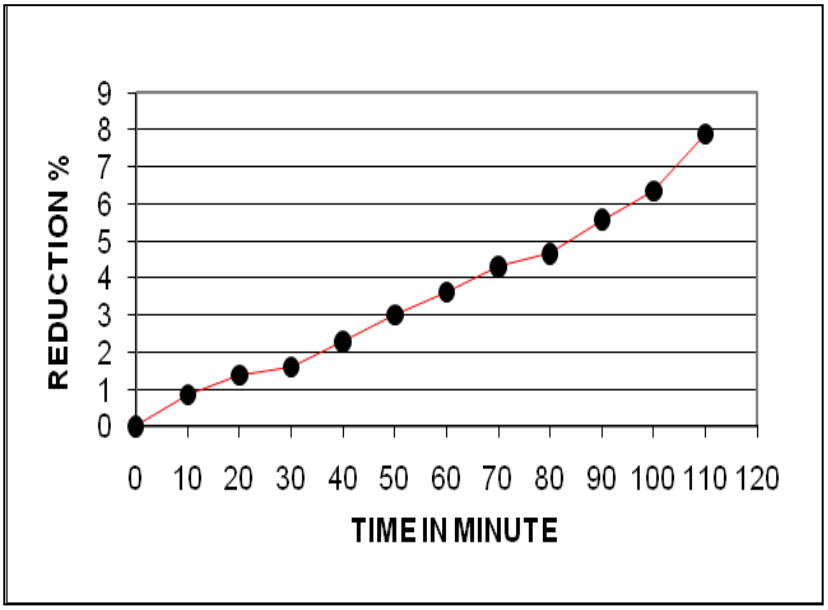

Figure 4.8, Effect of coal (+150µm-200µm) addition on the reduction of xstrata chromite (+100µm-150µm) at 1100 ºC

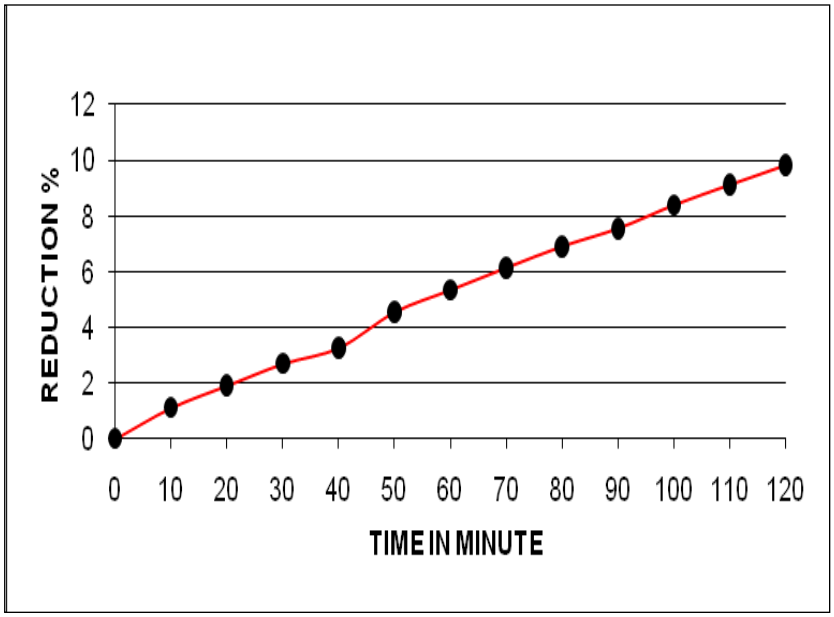

Figure 4.9, Effect of coal (+50µm-100µm) addition on the reduction of xstrata chromite (+100µm-150µm) at 1100 ºC

TABLE 4.2 1Experimental Results of Reductions at 1200 ºC

Runs	Chromite size	Reductant	Reductant size	Time (min)	Red ^{n} (%)
62	(+50 µm -100µm) º	Coke	(+50 µm -100µm)	120	19.89
63	(+50 µm -100µm)	Coke	(+100 µm -150µm)	120	19.75
64	(+50 µm -100µm)	Coke	(+150 µm -200 µm)	120	14.58
65	(+100 µm -150µm)	Coke	(+50 µm -100µm)	120	14.79
66	(+100 µm -150µm)	Coke	(+100 µm -150µm)	120	12.90
67	(+100 µm -150µm)	Coke	(+150 µm -200 µm)	120	12.70
68	(+150 µm -200µm)	Coke	(+50 µm -100µm)	120	11.03
69	(+150 µm -200µm)	Coke	(+100 µm -150µm)	120	10.61
70	(+150 µm -200µm)	Coke	(+150 µm -200 µm)	120	9.91
71	(+50 µm -100µm)	Charcoal	(+50 µm -100µm)	120	6.61
72	(+50 µm -100µm)	Charcoal	(+100 µm -150µm)	120	6.35
73	(+50 µm -100µm)	Charcoal	(+150 µm -200 µm)	120	5.69
74	(+100 µm -150µm)	Charcoal	(+50 µm -100µm)	120	7.84
75	((+100 µm -150µm)	Charcoal	(+100 µm -150µm)	120	7.44
76	(+100 µm -150µm)	Charcoal	(+150 µm -200 µm)	120	5.07
77	(+150 µm -200µm)	Charcoal	(+50 µm -100µm)	120	6.31
78	(+150 µm -200µm)	Charcoal	(+100 µm -150µm)	120	4.71
79	(+150 µm -200µm)	Charcoal	(+150 µm -200 µm)	120	4.21
84	(+50 µm -100µm)	Graphite	(+50 µm -100µm)	120	4.66
85	(+50 µm -100µm)	Graphite	(+150 µm -200 µm)	120	3.35
88	(+150 µm -200µm)	Graphite	(+50 µm -100µm)	120	4.24
89	(+150 µm -200µm)	Graphite	(+150 µm -200 µm)	120	4.116
80	(+50 µm -100µm)	Coal	(+50 µm -100µm)	120	31.78
81	(+50 µm -100µm)	Coal	(+100 µm -150µm)	120	31.39
82	(+100 µm -150µm)	Coal	(+50 µm -100µm)	120	30.29
83	((+100 µm -150µm)	Coal	(+100 µm -150µm)	120	30.19

87	(+100 µm -150µm)	Coal	(+150 µm -200 µm)	120	29.73
83A	(+150 µm -200µm)	Coal	(+50 µm -100µm)	120	30.02
83B	(+150 µm -200µm)	Coal	(+100 µm -150µm)	120	30.19
86	(+150 µm -200µm)	Coal	(+150 µm -200 µm)	120	27.04

4.2.2 Change in reduction(%) with change in size of chromite, coke, charcoal, graphite and coal at 1200 ºC.(**showing effect of particle size**).

In order to determine the influence of particle size of reductants and chromite at 1200 ºC, it was investigated for all sizes of chromite and all sizes of reductants. From this investigation following conclusion were drawn, which in general can be stated that decreasing the particle size results in an increase of reduction level, a finding which is confirmed in a number of previous studies (Barcza[4], Soykan[100]).

1)At 1200 ºC, as the chromite size decreases from +150µm-200µm to +50µm-100µm with varing coke size, reduction % increases from (10.61 %)(min) to (19.89 %)(max) as shown in figures 4.10 to 4.12 and D.17 to D.18 (appendix D) and table 4.2.

2) At 1200 ºC, as the chromite size decreases from +150µm-200µm to +50µm-100µm with varing charcoal size, % reduction increases from (4.71%)(min) to (6.61%)(max) as shown in figures 4.12 to 4.15 and table 4.2.

3) At 1200 ºC, as the chromite size decreases from +150µm-200µm to +50µm-100µm with varing graphite size, percentage reduction increases from (3.35 %)(min) to (4.66 %) max. Not much can be deduced from graphite reduction as percentage of reduction is very low as can be seen from table 4.2.

4)With Coal, at 1200 ºC as the chromite size decreases from +150µm-200µm to +50µm-100µm with varing coal size, percentage reduction increases from (27.04%)(min) to 31.78 (%) max as shown in figures 4.16 to 4.18 and table 4.2.

5) It can also be noted that at 1200 ºC, coal as a reductant gives a maximum reduction of 31.78% for smallest chromite and coal size, each being (+50 µm -100µm), whereas graphite shows least % reduction of 3.35%, followed by 6.61 % of charcoal and coke with 19.89%. Hence order of reductants is coal, coke, charcoal and graphite in terms of percentage reduction, coke being highest and graphite being lowest.

4.2.3 REDUCTION CURVES OF HOW REDUCTION PROCEEDS AT 1200 ºC.

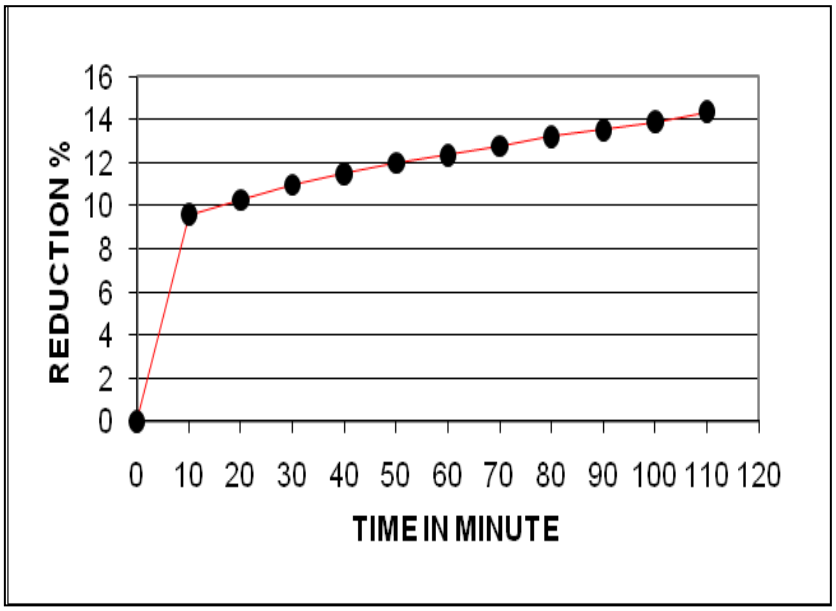

Figure 4.10, Effect of coke (+50µm-100µm) addition on the reduction of xstrata chromite (+100µm-150µm) at 1200 ºC

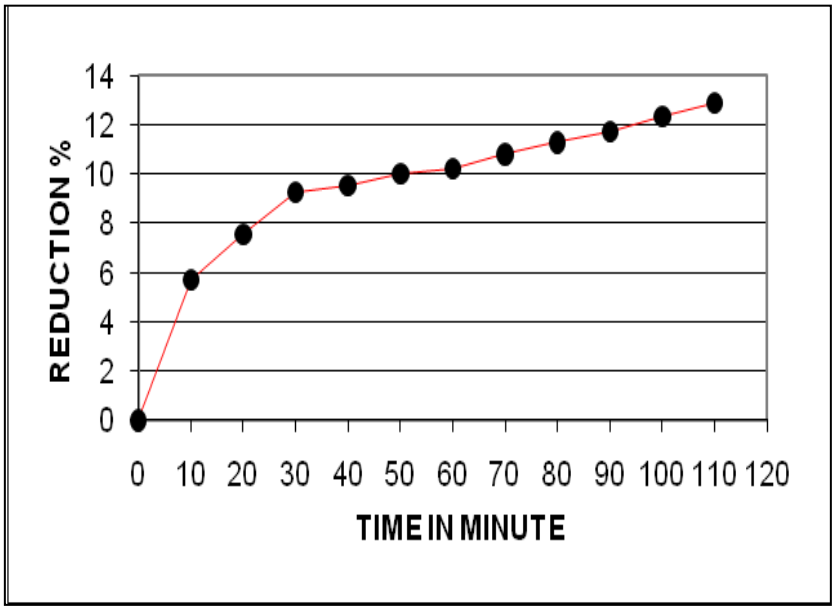

Figure 4.11 Effect of coke (+100µm-150µm) addition on the reduction of xstrata chromite (+100µm-150µm) at 1200 ºC

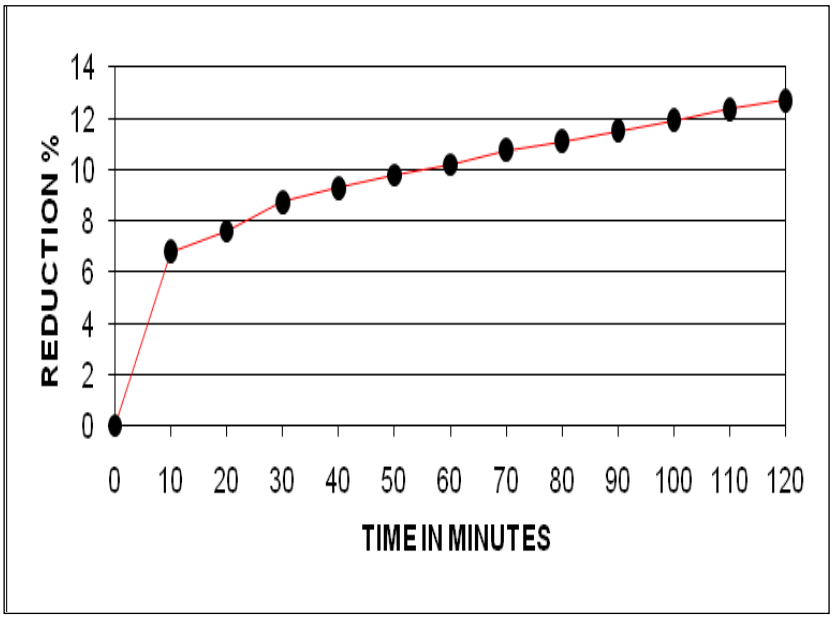

Figure 4.12 Effect of coke (+150µm-200µm) addition on the reduction of xstrata chromite (+100µm-150µm) at 1200 ºC

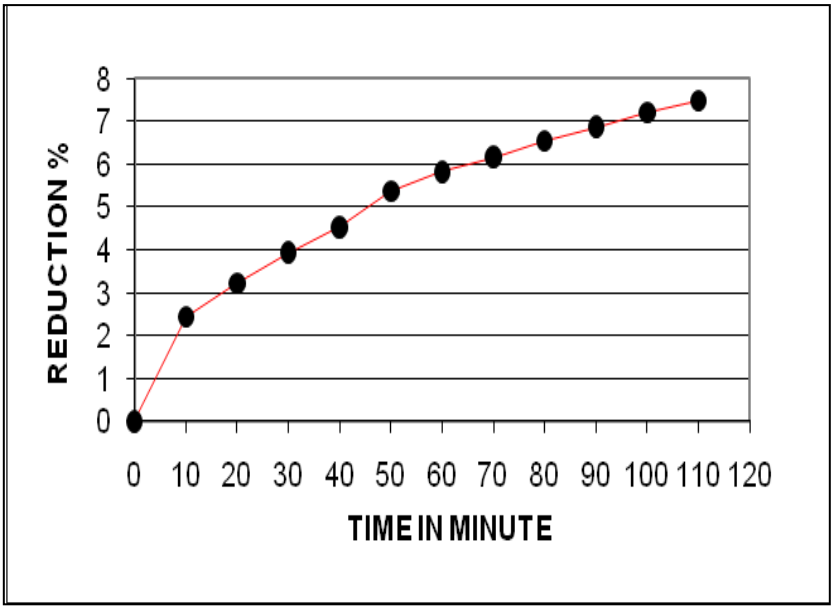

Figure 4.13 Effect of charcoal (+50µm-100µm) addition on the reduction of xstrata chromite (+100µm-150µm) at 1200 ºC

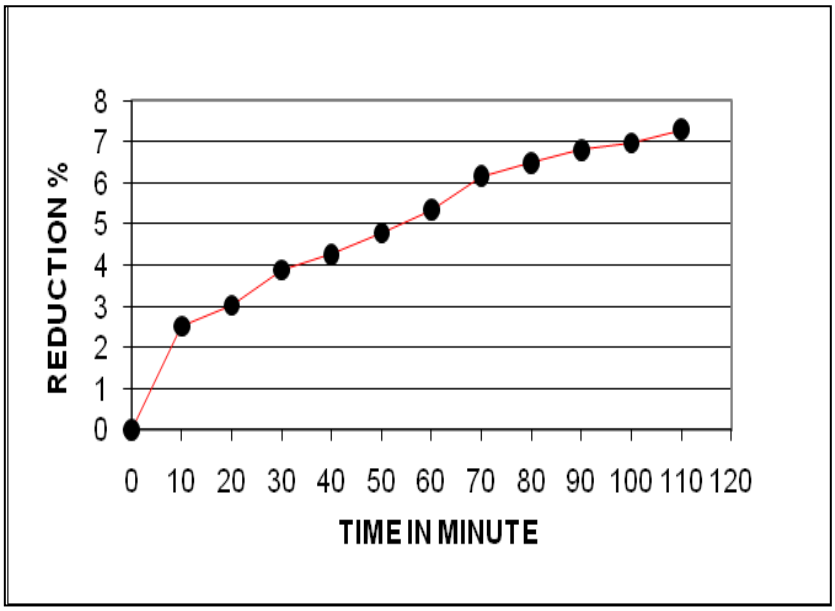

Figure 4.14 Effect of charcoal (+100µm-150µm) addition on the reduction of xstrata chromite (+100µm-150µm) at 1200 ºC

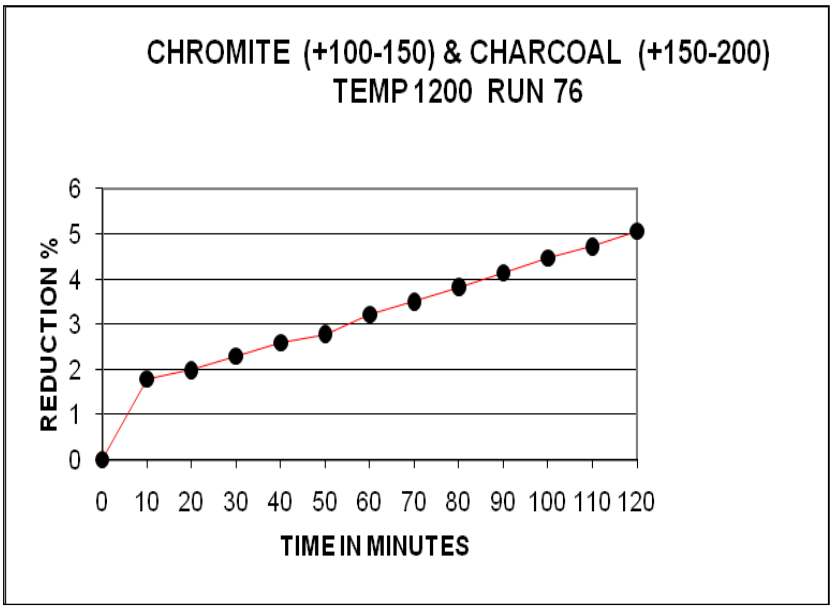

Figure 4.15 Effect of charcoal (+150µm-200µm) addition on the reduction of xstrata chromite (+100µm-150µm) at 1200 ºC

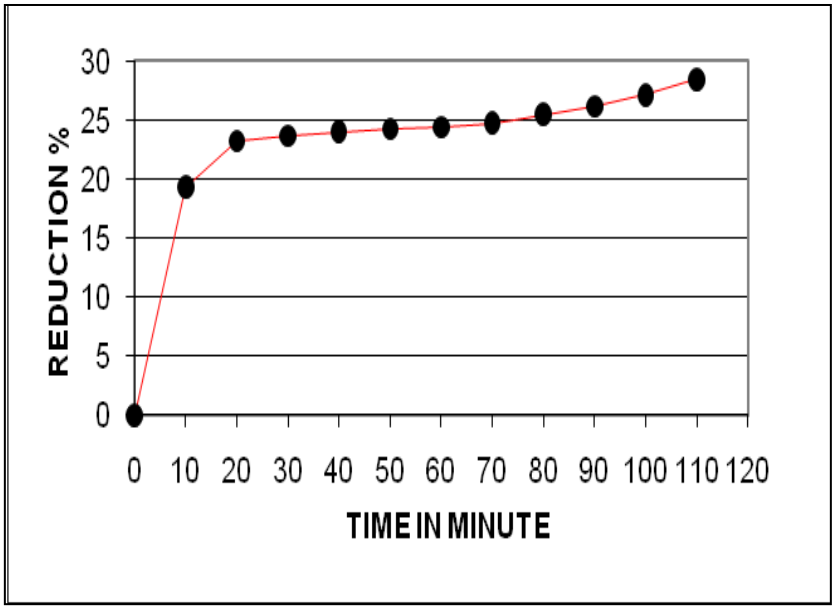

Figure 4.16 Effect of coal (+50µm-100µm) addition on the reduction of xstrata chromite (+100µm-150µm) at 1200 ºC

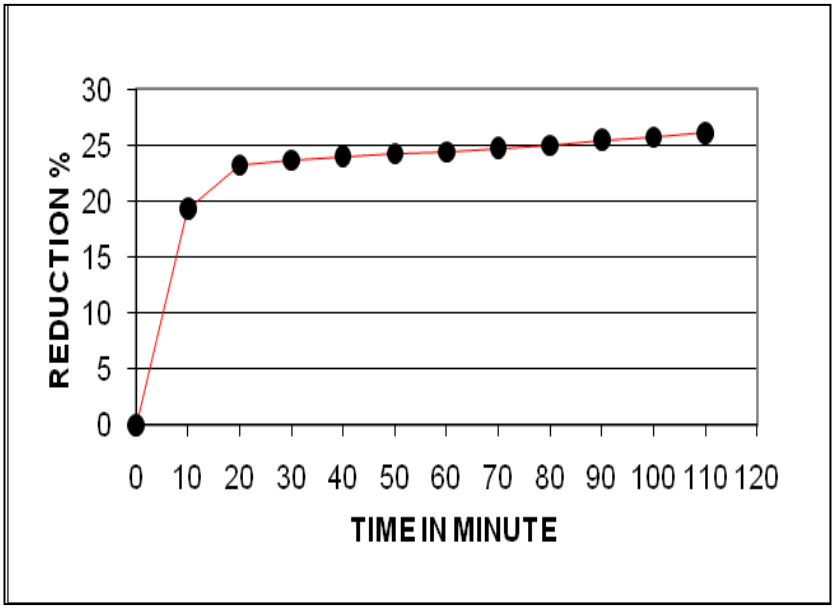

Figure 4.17 Effect of coal (+100µm-150µm) addition on the reduction of xstrata chromite (+100µm-150µm) at 1200 ºC

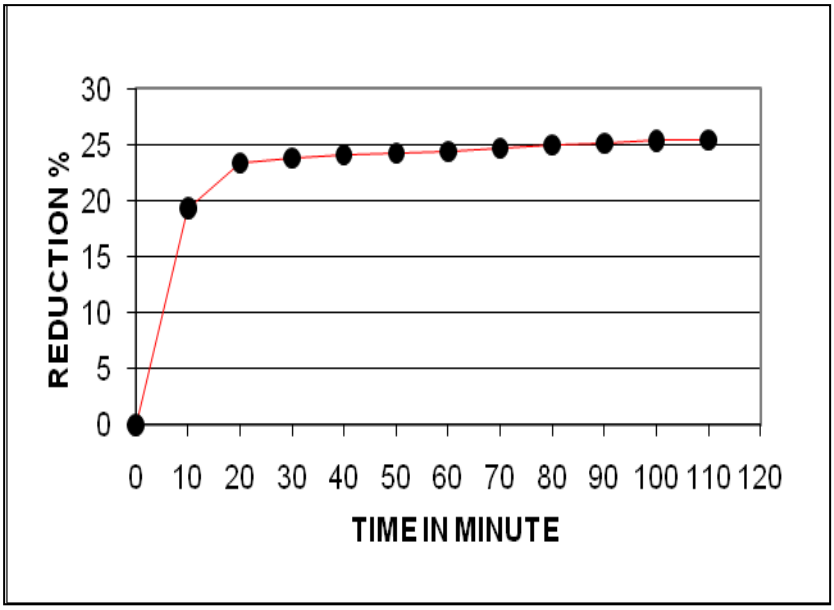

Figure 4.18 Effect of coal (+150µm-200µm) addition on the reduction of xstrata chromite (+100µm-150µm) at 1200 ºC

Table 4.3 1Experimental Results of Reductions at 1300 ºC

Runs	Chromite size	Reductant	Reductant size	Time (min)	Red^{n}(%)
90	(+50 µm -100µm)	Coke	(+50 µm -100µm)	120	42.28
91	(+50 µm -100µm)	Coke	(+100 µm -150µm)	120	19.47
92	(+50 µm -100µm)	Coke	(+150 µm -200 µm)	120	14.49
94	(+100 µm -150µm)	Coke	(+50 µm -100µm)	120	18.70
97	((+100 µm -150µm)	Coke	(+100 µm -150µm)	120	17.92
95	(+100 µm -150µm)	Coke	(+150 µm -200 µm)	120	13.02
98	(+150 µm -200µm)	Coke	(+50 µm -100µm)	120	16.75
99	(+150 µm -200µm)	Coke	(+100 µm -150µm)	120	15.66
96	(+150 µm -200µm)	Coke	(+150 µm -200 µm)	120	13.54
106	(+50 µm -100µm)	Coal	(+50 µm -100µm)	120	45.06
100	(+50 µm -100µm)	Coal	(+100 µm -150µm)	120	43.27
101	(+50 µm -100µm)	Coal	(+150 µm -200 µm)	120	36.30
132	(+100 µm -150µm)	Coal	(+50 µm -100µm)	120	37.21
102	((+100 µm -150µm)	Coal	(+100 µm -150µm)	120	34.27
103	(+100 µm -150µm)	Coal	(+150 µm -200 µm)	120	31.49
133	(+150 µm -200µm)	Coal	(+50 µm -100µm)	120	38.73
104	(+150 µm -200µm)	Coal	(+100 µm -150µm)	120	34.07
105	(+150 µm -200µm)	Coal	(+150 µm -200 µm)	120	31.17
107	. (+50 µm -100µm)	Charcoal	(+50 µm -100µm)	120	20.29
112	(+50 µm -100µm)	Charcoal	(+100 µm -150µm)	120	19.57
113	(+50 µm -100µm)	Charcoal	(+150 µm -200 µm)	120	15.76
108	(+100 µm -150µm)	Charcoal	(+50 µm -100µm)	120	16.32
114	(+100 µm -150µm)	Charcoal	(+100 µm -150µm)	120	16.17
115	(+100 µm -150µm)	Charcoal	(+150 µm -200 µm)	120	11.09
109	(+150 µm -200µm)	Charcoal	(+50 µm -100µm)	120	15.25
110	(+150 µm -200µm)	Charcoal	(+100 µm -150µm)	120	9.17
111	(+150 µm -200µm)	Charcoal	(+150 µm -200 µm)	120	8.41
112	(+150 µm -200µm)	Graphite	(+150 µm -200 µm)	120	4.12

4.3.2 Change in reduction(%) with change in size of chromite, coke, charcoal, graphite and coal at 1300 ºC.(showing effect of particle size).

In order to determine the influence of particle size of reductants and chromite at 1300 ºC, it was investigated for all sizes of chromite and all sizes of reductants. From this investigation, following conclusion were drawn, which in general can be stated that decreasing the particle size results in an increase of reduction level, a finding which is confirmed in a number of previous studies (Barcza[4], Soykan[100]).

1) At 1300 ºC, as the chromite size decreases from +150µm-200µm to +50µm-100µm with varing coke size, reduction % increases from 13.02 %(min) to 42.28% (max) as shown in the figures 4.19 to 4.21 and table 4.3

2) At 1300 ºC, as the chromite size decreases from +150µm-200µm to +50µm-100µm with varing charcoal size, % reduction increases from 8.41%(min) to 20.29%(max) as shown in figures 4.22 to 4.24 and figure D.22 and table 4.3

3) With coal, at 1300 ºC as the chromite size decreases from +150µm-200µm to +50µm-100µm with varing coal size, % reduction increases from 31.17%(min) to 45.06% except with particle size of chromite of (+150 µm -200µm) and coal size of (+50 µm -100µm) where it is 12.81%. The effect of reductant coal at this size with chromite of size (+150 µm -200µm) are shown in figures 4.25 to 4.27, figures D.19 to D.21, figure D.30 and D.33 and table 4.3.

5) It can also be noted that at 1300 ºC, coal as a reductant gives maximum reduction of 45.06 % for smallest chromite and coal size, each being (+50 µm -100µm), whereas graphite shows the least 4.12% (max) reduction, followed by 20.29 % (max) of charcoal and coke 42.28% (max). Hence order of reductants is coal, coke, charcoal and graphite in terms of % reduction, coal being highest % and graphite being lowest.

4.3.3 REDUCTION CURVES OF HOW REDUCTION PROCEEDS AT 1300 ºC,

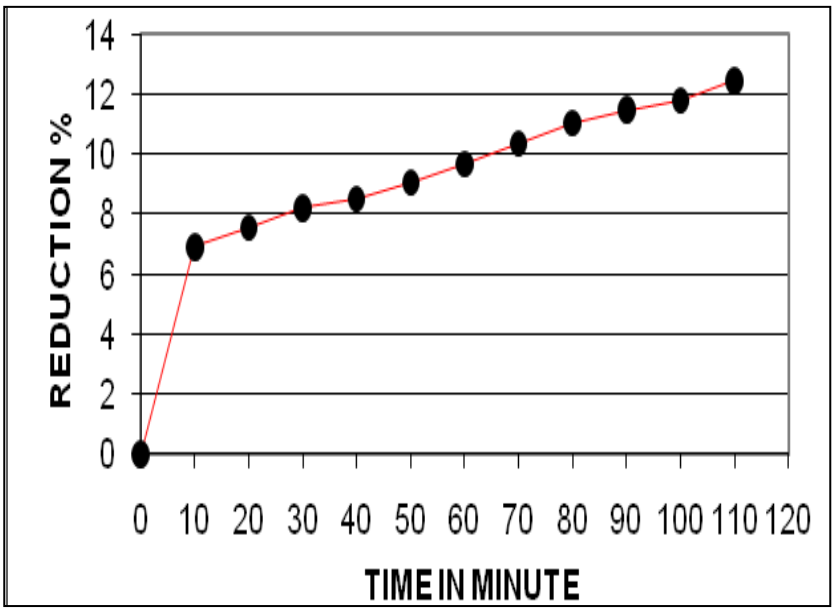

Figure 4.19 Effect of coke (+50µm-100µm) addition on the reduction of xstrata chromite (+100µm-150µm) at 1300 ºC

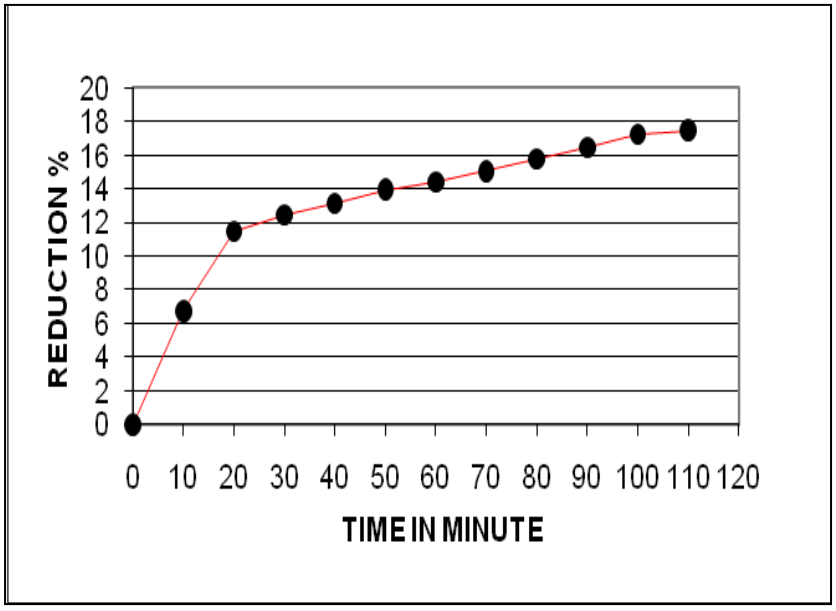

Figure 4.20 Effect of coke (+100µm-150µm) addition on the reduction of xstrata chromite (+100µm-150µm) at 1300 ºC

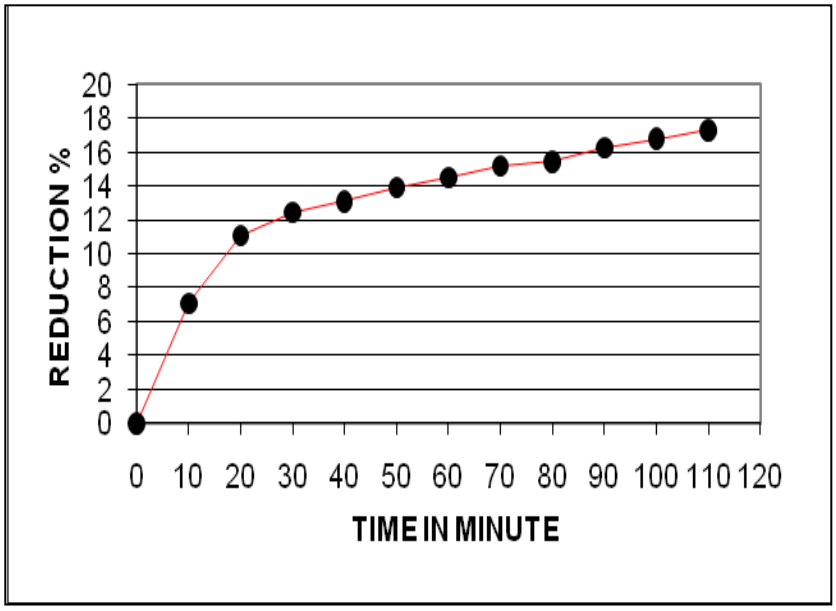

Figure 4.21 Effect of coke (+150µm-200µm) addition on the reduction of xstrata chromite (+100µm-150µm) at 1300 ºC

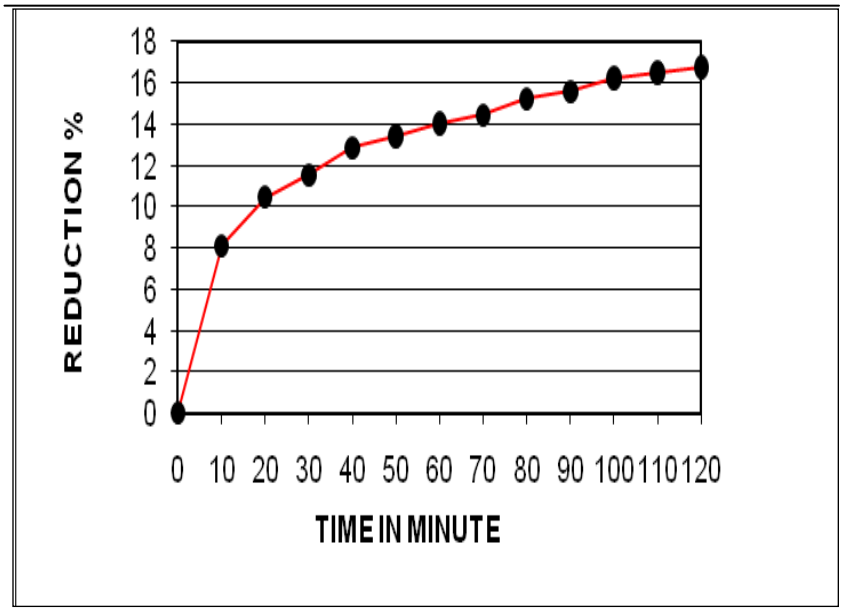

Figure 4.22 Effect of charcoal (+50µm-100µm) addition on the reduction of xstrata chromite (+100µm-150µm) at 1300 ºC

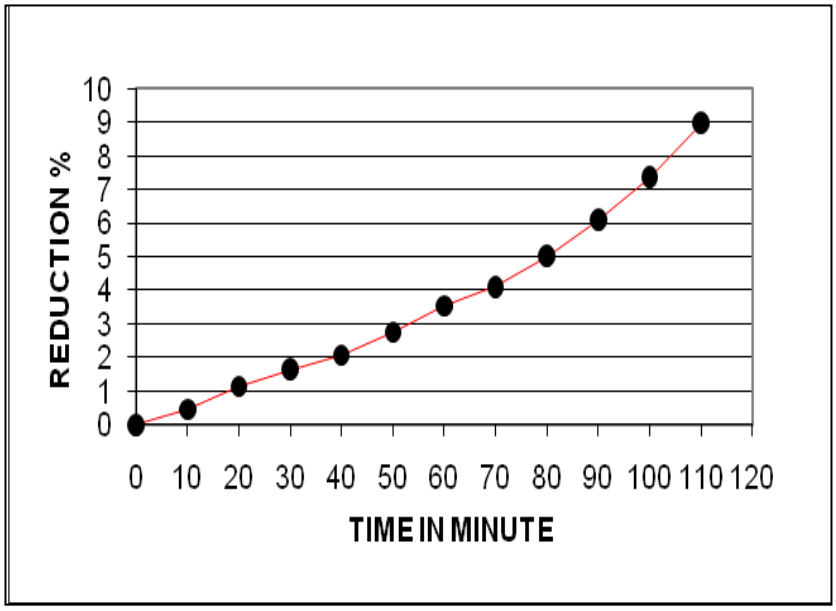

Figure 4.23 Effect of charcoal (+150µm-200µm) addition on the reduction of xstrata chromite (+100µm-150µm) at 1300 ºC

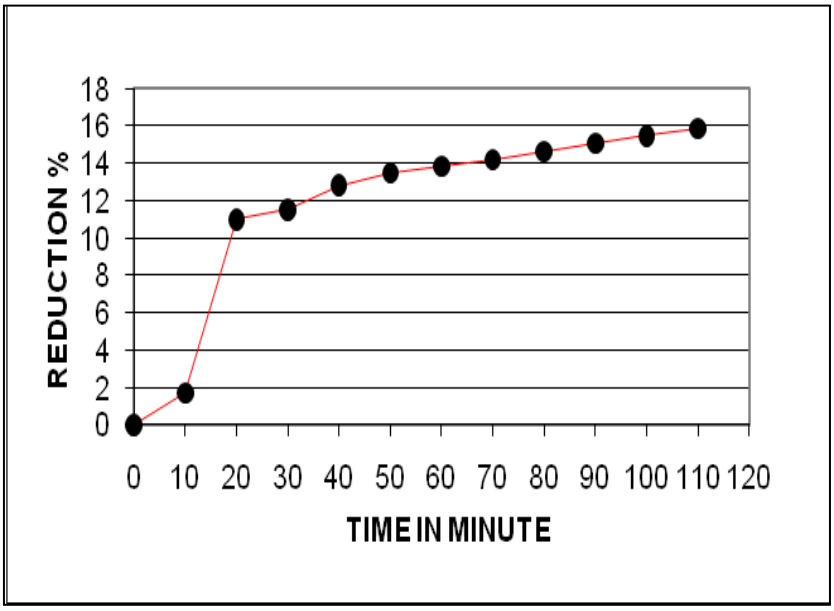

Figure 4.24 Effect of charcoal (+100µm-150µm) addition on the reduction of xstrata chromite (+100µm-150µm) at 1300 ºC

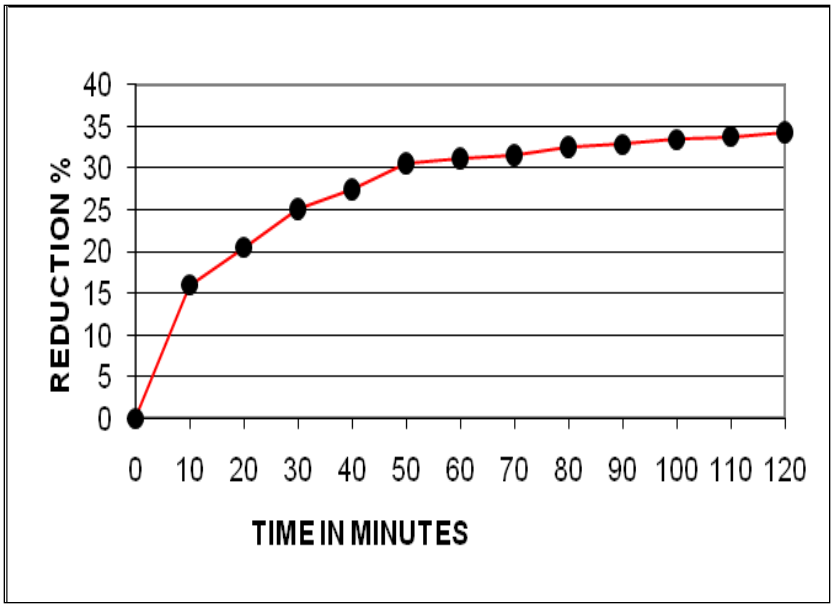

Figure 4.25 Effect of coal (+100µm-150µm) addition on the reduction of xstrata chromite (+100µm-150µm) at 1300 ºC

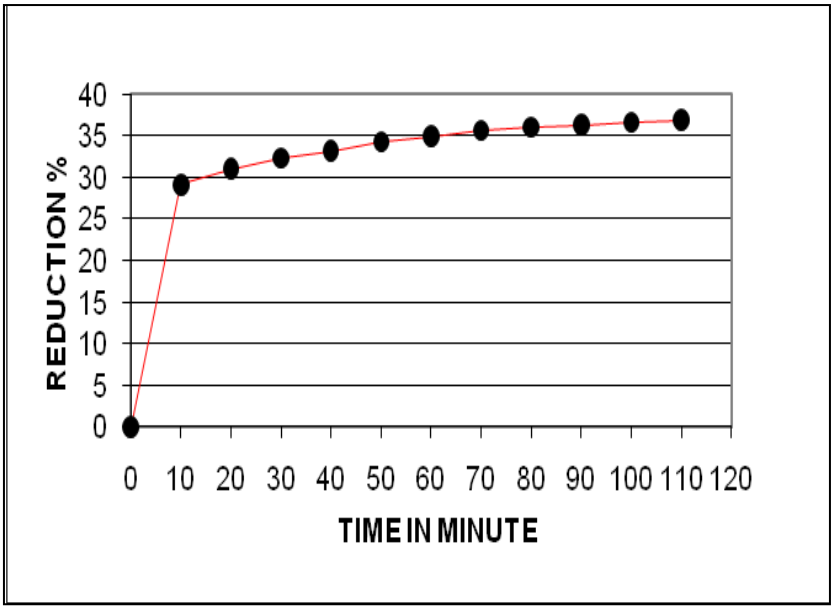

Figure 4.26 Effect of coal (+50µm-100µm) addition on the reduction of xstrata chromite (+100µm-150µm) at 1300 ºC

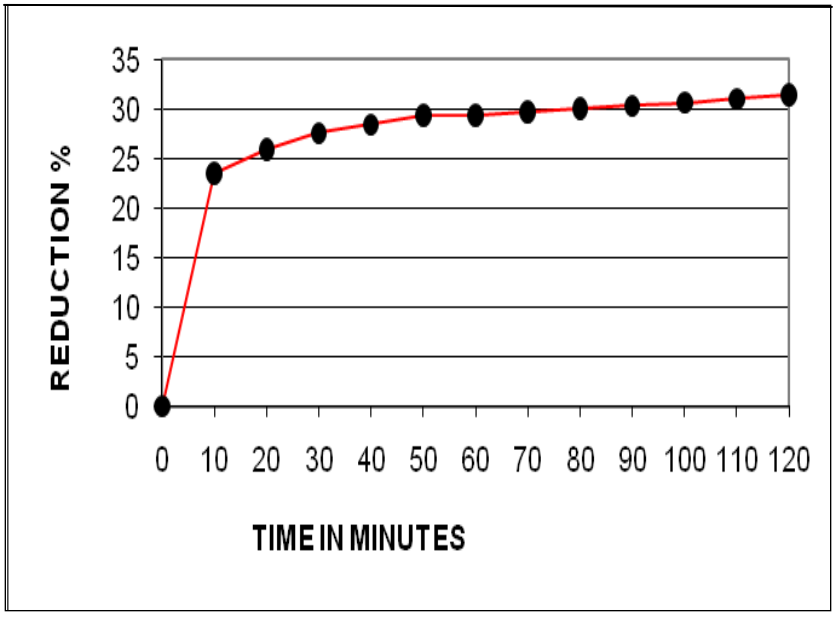

Figure 4.27 Effect of coal (+150µm-200µm) addition on the reduction of xstrata chromite (+100µm-150µm) at 1300 ºC

Table 4.4 1Experimental results of reductions at 1000 ºC

Runs	Chromite size	Reductant	Reductant size	Time(min)	Red^n(%)
1	As-Received	Coke	As-Received	120	6.60
2	As-Received	Coke	(+50 µm -100µm)	120	6.90
3	As-Received	Coke	(+100 µm -150 µm)	120	10.70
5	(+50 µm -100µm)	Coke	As-Received	120	6.17
6	(+50 µm -100µm)	Coke	(+150 µm -200 µm)	120	10.70
7	(+50 µm -100µm)	Coke	(+50 µm -100µm)	120	13.05
8	(+50 µm -100µm)	Coke	(+100 µm -150µm)	120	12.52
9	(+100 µm -150µm)	Coke	As-Received	120	9.14
10	(+100 µm -150µm)	Coke	(+50 µm -100µm)	120	11.12
11	((+100 µm - 150µm)	Coke	(+100 µm -150µm)	120	7.82
12	(+100 µm -150µm)	Coke	(+150 µm -200 µm)	120	8.49
13	(+150 µm -200µm)	Coke	As-Received	120	9.54
14	(+150 µm -200µm)	Coke	(+50 µm -100µm)	120	11.03
16	(+150 µm -200µm)	Coke	(+150 µm -200 µm)	120	10.32
21	As-Received	Graphite	As-Received	120	6.22
22	(+50 µm -100µm)	Graphite	As-Received	120	6.30
23	(+100 µm -150µm)	Graphite	As-Received	120	3.49
24	(+150 µm -200µm)	Graphite	As-Received	120	6.46
25	As-Received	Charcoal	(+150 -200µm)	120	6.46
26	As-Received	Coal	(+150 µm -200 µm)	120	7.95
27	As-Received	Coke	(+150 µm -200 µm)	120	11.94
28	(+100 µm -150µm)	Charcoal	(+100 µm -150µm)	120	7.84

TABLE 4.5Experimental results of reduction at 1300 ºC of as-receivedsamples.

Runs	Chromite size	Reductant	Reductant size	Time(min)	Red^n(%)
116	As-Received	Charcoal	As-Received	120	9.54
117	As-Received	Coal	As-Received	120	44.78
118	As-Received	Coke	As-Received	120	15.24
119	As-Received	Graphite	As-Received	120	7.67

TABLE 4.6 Experimental results of reduction at 1200 ºC of as-received samples

Runs	Chromite size	Reductant	Reductant size	Time(min)	Red^n(%)
120	As-Received	Charcoal	As-Received	120	8.15
121	As-Received	Coke	As-Received	120	13.54
122	As-Received	Coal	As-Received	120	35.03
123	As-Received	Graphite	As-Received	120	9.32

TABLE 4.7 Experimental results of reduction at 1100 ºC of as-received samples

Runs	Chromite size	Reductant	Reductant size	Time(min)	Red^n(%)
125	As-Received	Coke	As-Received	120	10.03
126	As-Received	Charcoal	As-Received	120	7.65
127	As-Received	Graphite	As-Received	120	4.25

TABLE 4.8 Experimental results of reduction at 1200 ºC of as-received samples

Runs	Chromite size	Reductant	Reductant size	Time(min)	Red^n(%)
128	As-Received	Charcoal	As-Received	120	8.18
129	As-Received	Coke	As-Received	120	11.12
130	As-Received	CoaL	As-Received	120	8.19
131	As-Received	Graphite.	As-Received	120	6.22

4.5.1 Comparision of the reduction behavior of different chromite sizes and reductants sizes at different temperature.

(1) Following graph shows that at 1100 ºC for chromite (+50 µm -100µm) as coke size decreases from (+150 µm -200µm) to (+50 µm -100µm), % reduction increases from 14.12% to 16.43 %.

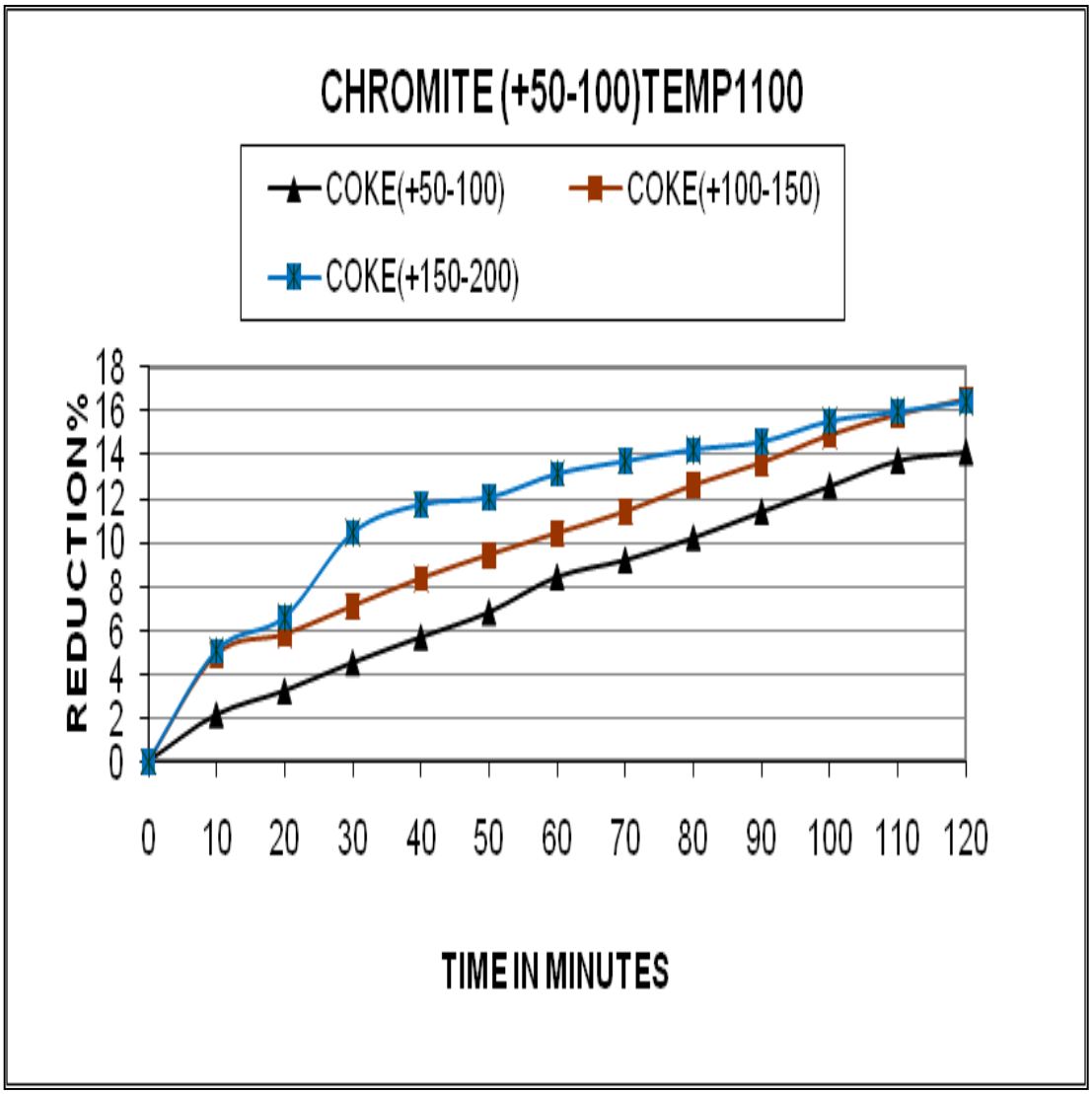

Figure 4.28 Effect of particle size on reduction of xstrata chromite (+50µm-100µm) with changing coke size at 1100 ºC.

(2)Following graph shows that at 1100 ºC for chromite (+150 µm -200µm) as coke size decreases from (+150 µm -200µm) to (+50 µm -100µm), % reduction increases from 10.17 % to 16.11 %.

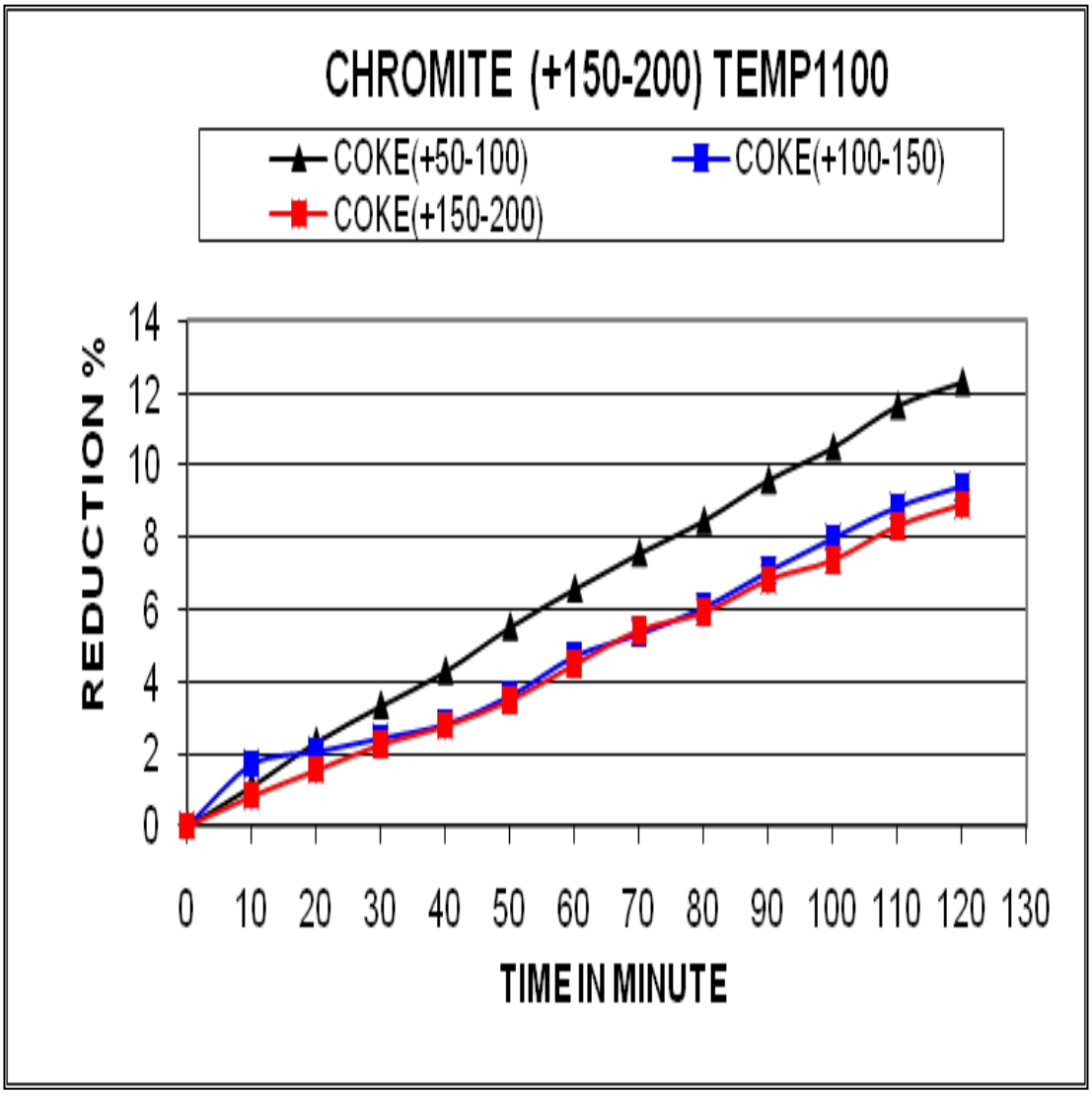

Figure 4.29 Effect of particle size on reduction of xstrata chromite (+150µm-200µm) with changing coke size at 1100 ºC

(3) Following graph shows that at 1100 ºC for chromite (50 µm -100µm) as charcoal size decreases from (+150 µm -200µm) to (+50 µm -100µm), % reduction increases from 9.35% to 11.40%.

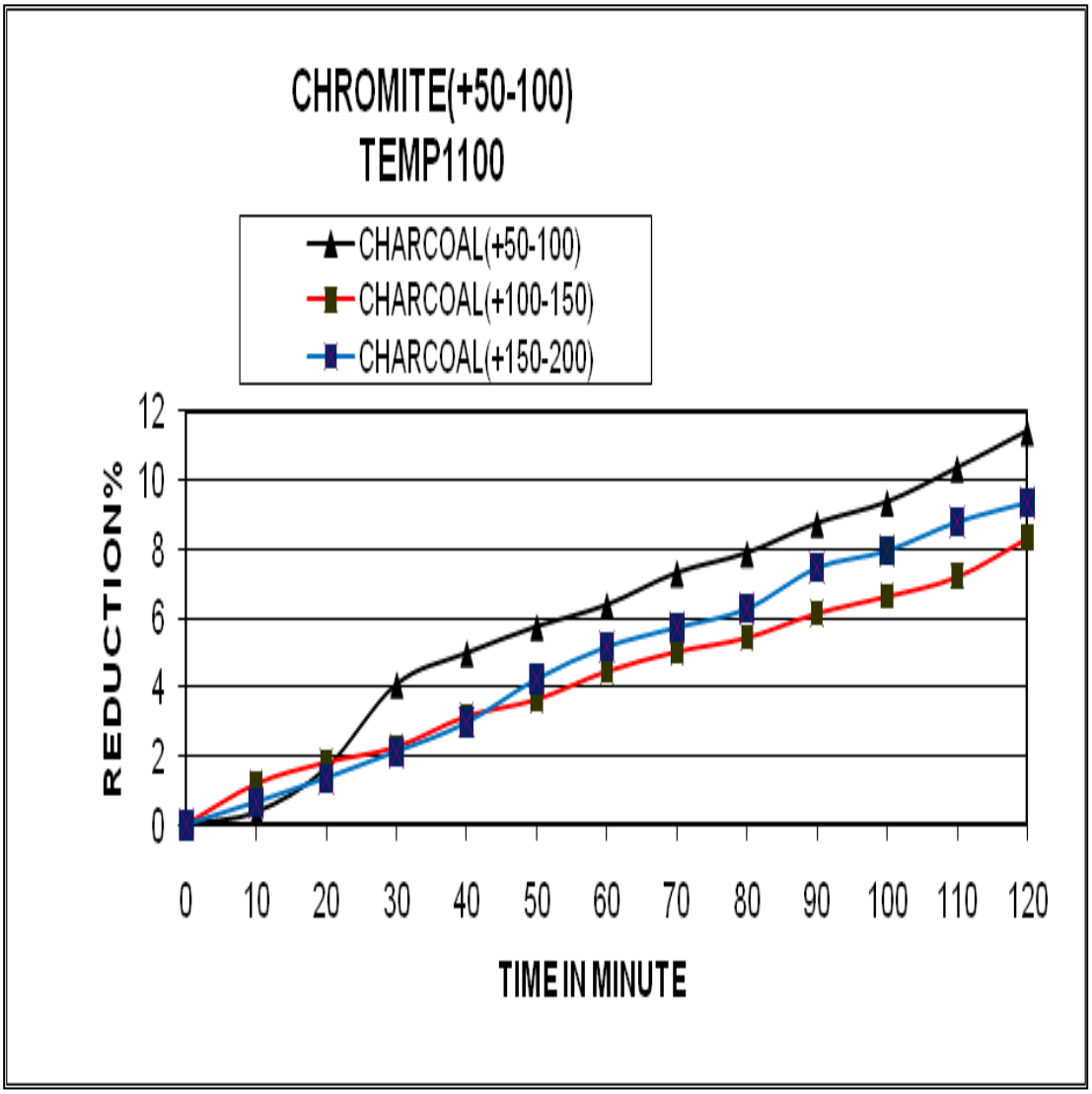

Figure 4.30 Effect of particle size on reduction of xstrata chromite (+50µm-100µm) with changing charcoal size at 1100 ºC**.**

(4) Following graph shows that at 1100 ºC for chromite (+150 µm -200µm) as charcoal size decreases from (+150 µm -200µm) to (+50 µm -100µm), % reduction increases from 3.96% to 5.61%.

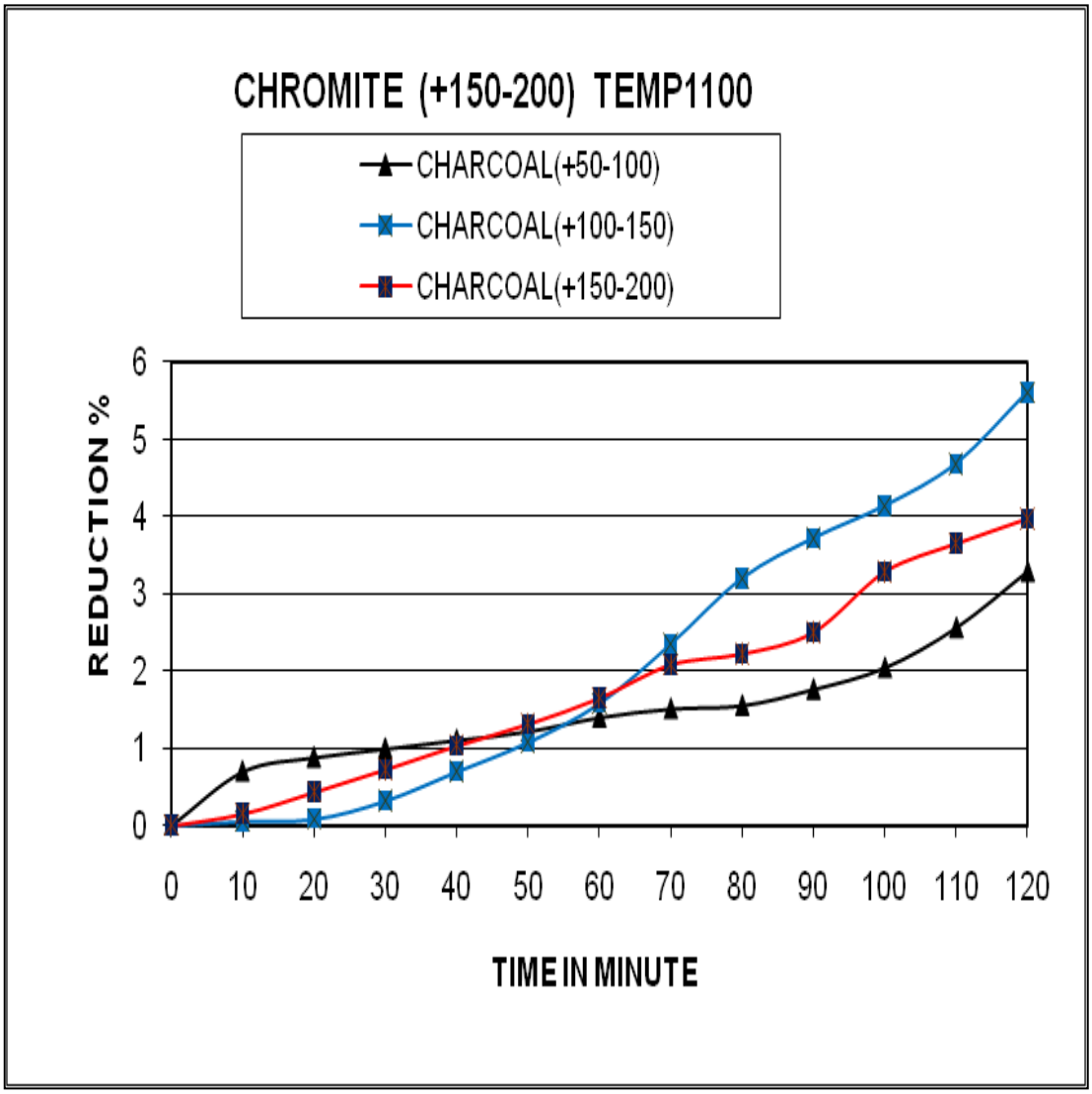

Figure 4.31 Effect of particle size on reduction of xstrata chromite (+150µm-200µm) with changing charcoal size at 1100 ºC.

(5) Following graph shows that at 1200 ºC for chromite (+50 µm -100µm) as charcoal size decreases from (+150 µm -200µm) to (+50 µm -100µm), % reduction increases from5.69% to 6.61%.

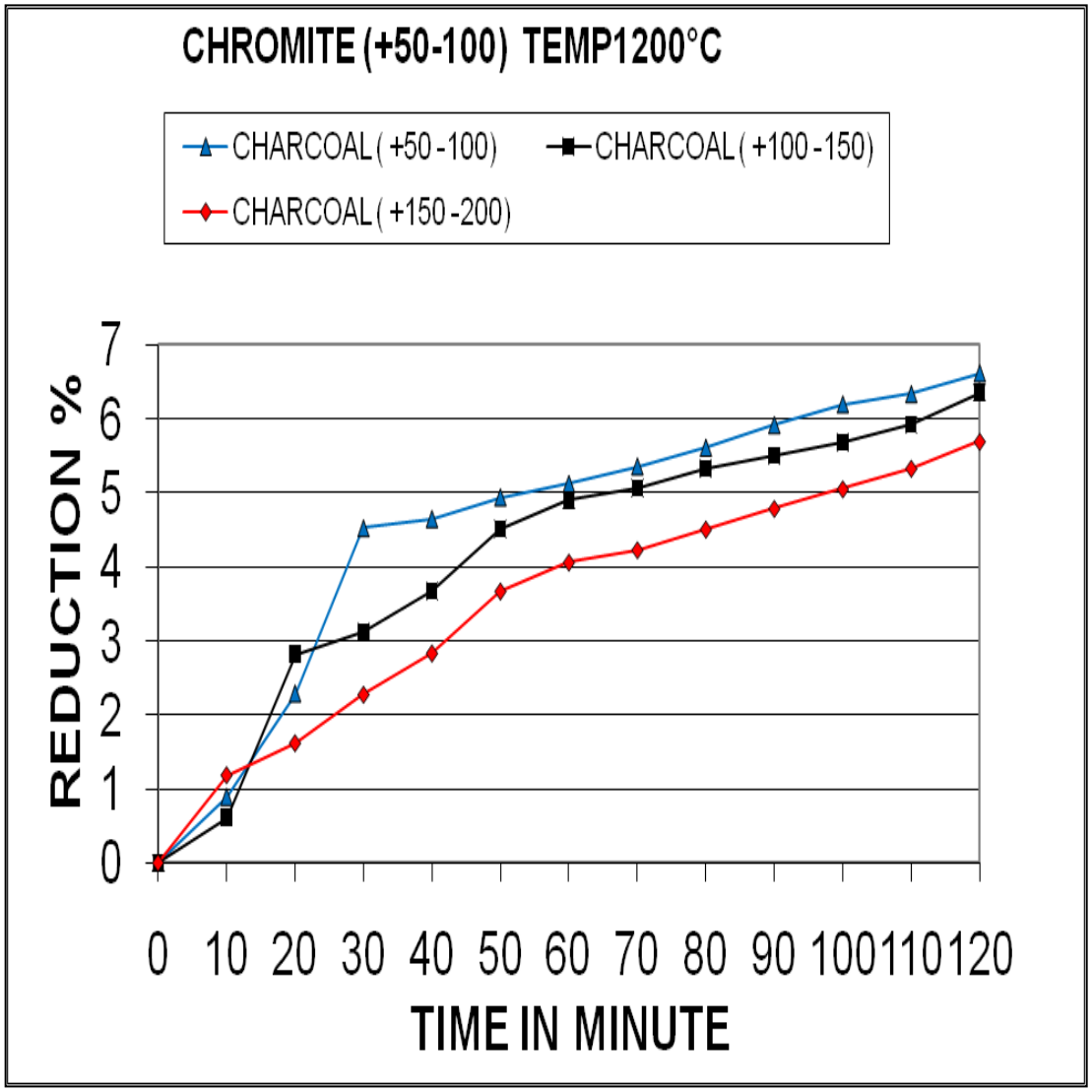

Figure 4.32 Effect of particle size on reduction of xstrata chromite (+50µm-100µm) with changing charcoal size at 1200 ºC**.**

(6) Following graph shows that at 1200 ºC for chromite (+150 µm -200µm) as charcoal size decreases from (+150 µm -200µm) to (+50 µm -100µm), % reduction increases from 4.21 % to 6.31%

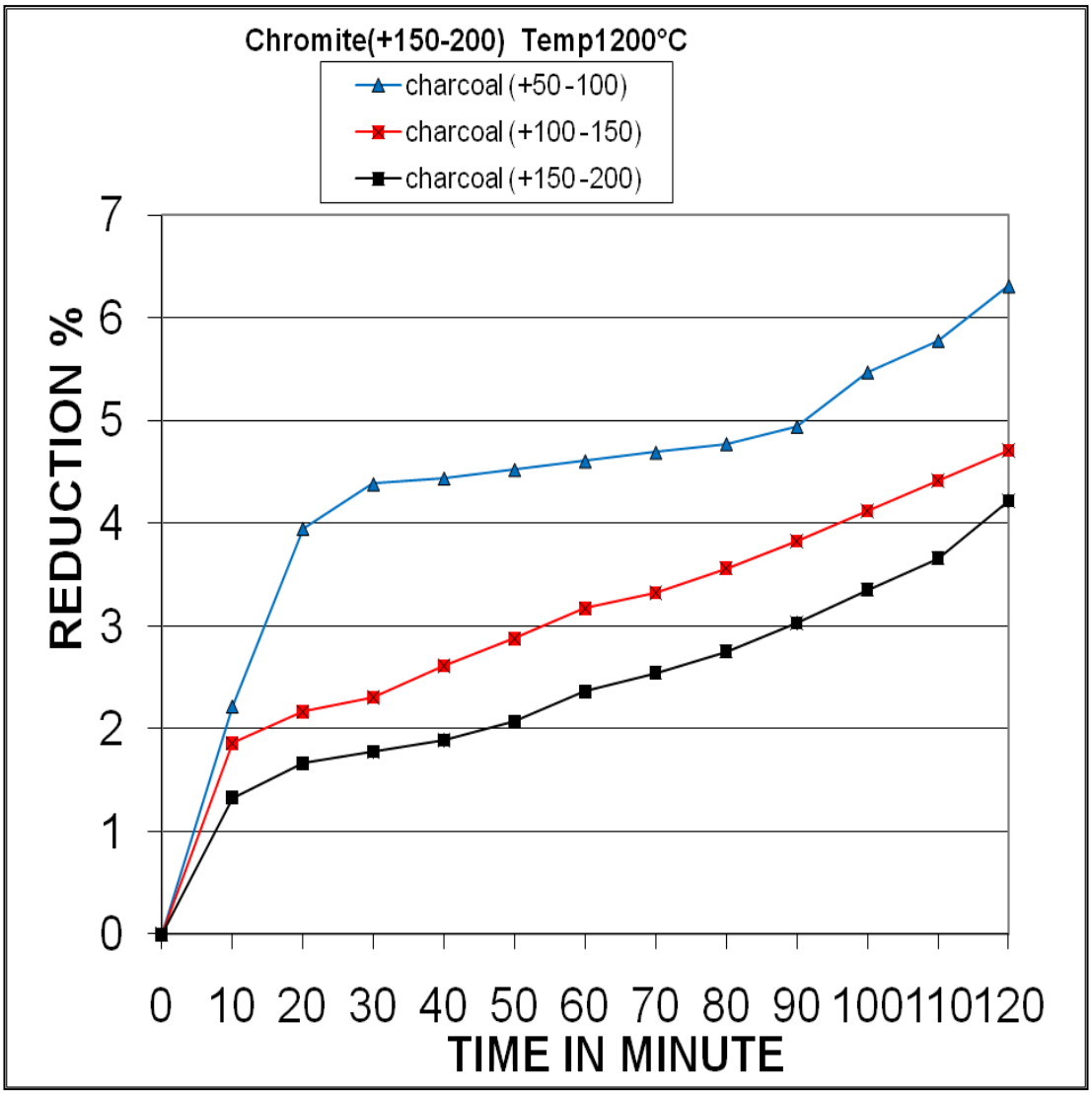

Figure4.33 Effect of particle size on reduction of xstrata chromite (+150µm-200µm) with changing coke size at 1200 ºC.

(7) Following graph shows that at 1300 ºC for chromite (+50 µm -100µm) as charcoal size decreases from (+150 µm -200µm) to (+50 µm -100µm), % reduction increases from15.76% to 20.29%

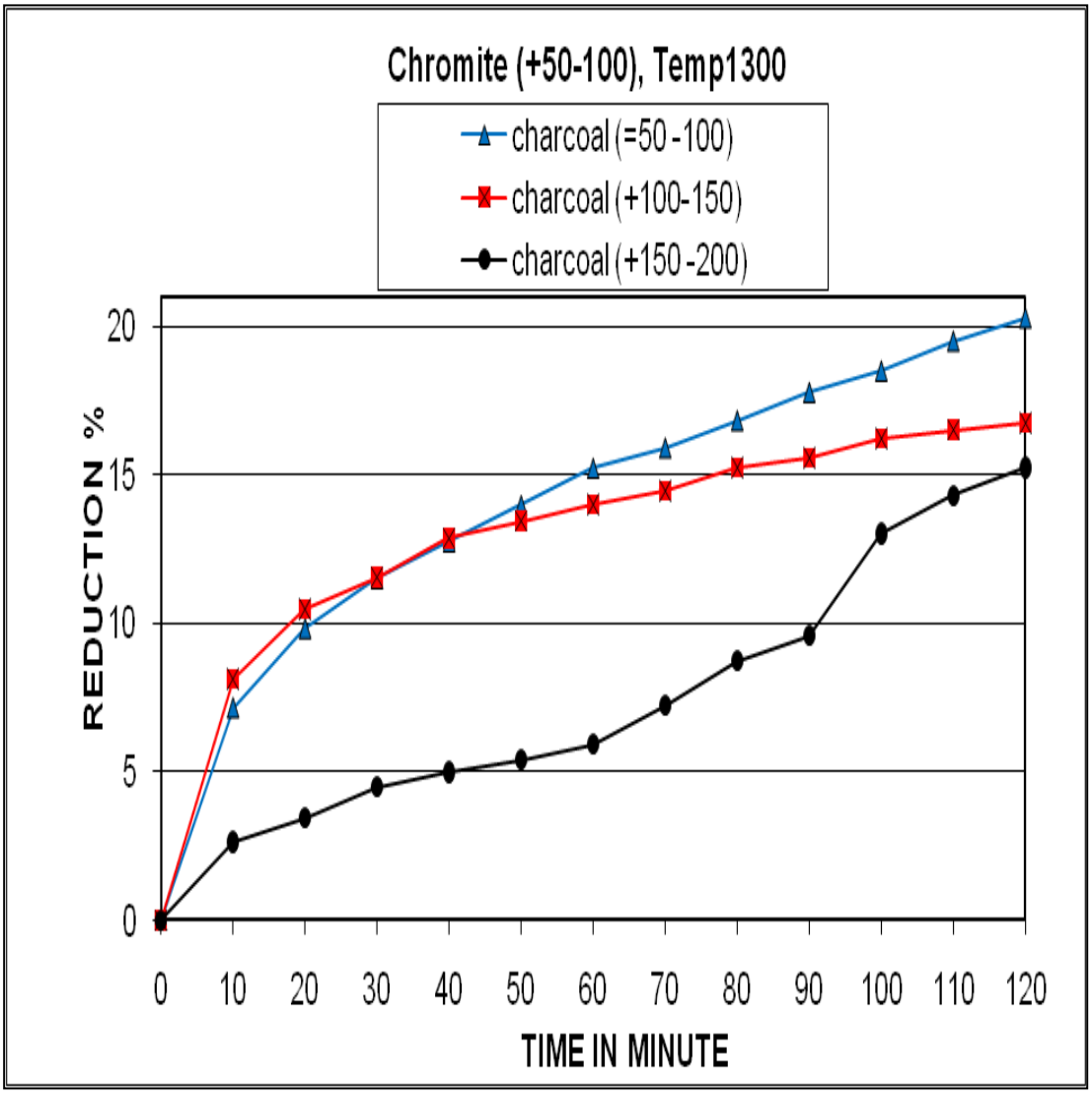

Figure 4.34 Effect of particle size on reduction of xstrata chromite (+50µm-100µm) with changing charcoal size at 1300 ºC**.**

(8**)** Following graph shows that at 1200 ºC for chromite (+100 µm -150µm) as coal size decreases from (+150 µm -200µm) to (+50 µm -100µm), % reduction increases from 29.73 % to 30.29%

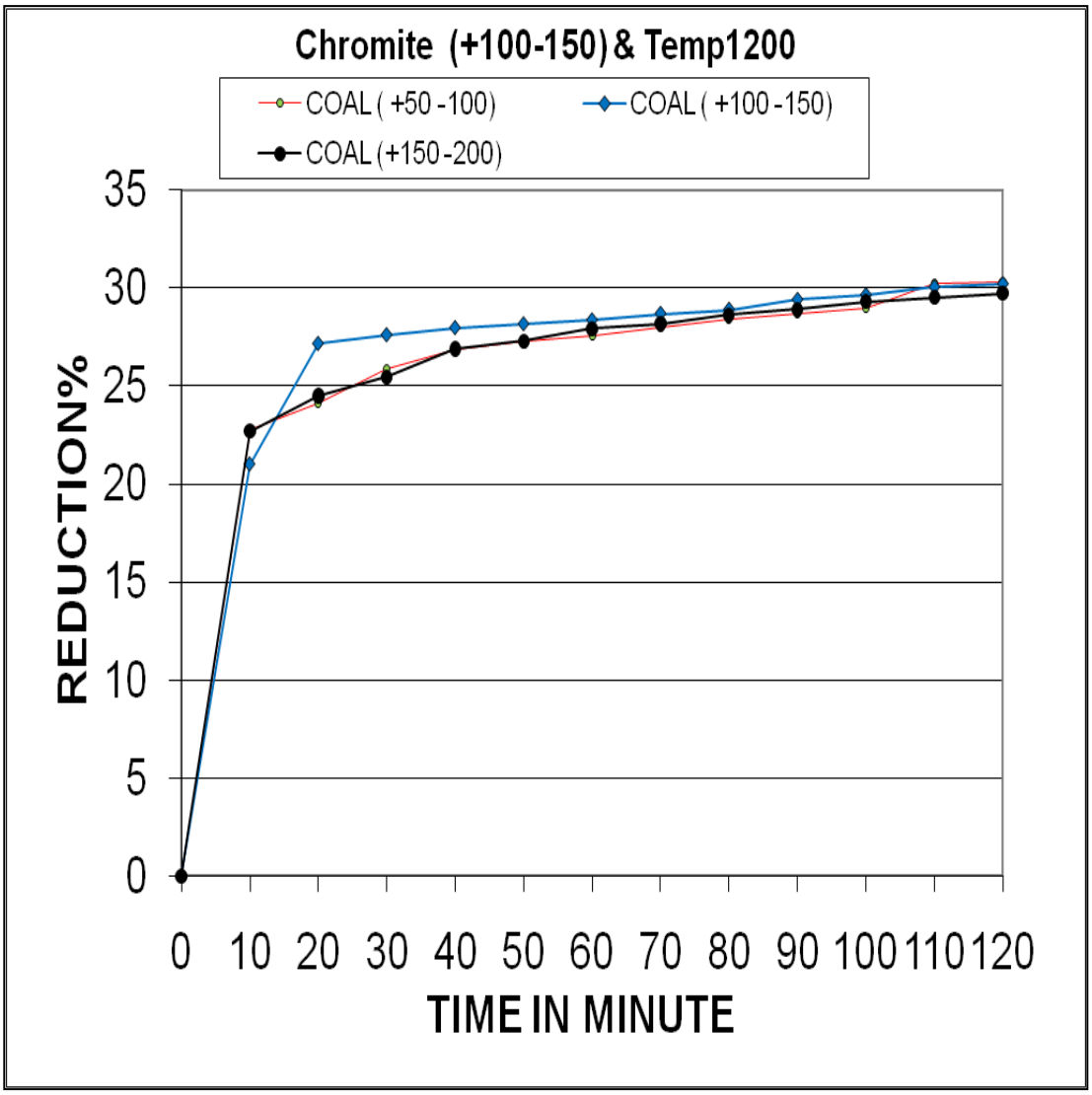

Figure 4.35 Effect of particle size on reduction of xstrata chromite (+100µm-150µm) with changing coal size at 1200 ºC**.**

(9) Following graph shows that at 1200 ºC for chromite (+150 µm -200µm) as coal size decreases from (+150 µm -200µm) to (+50 µm -100µm), % reduction increases from 27.04% to 30.02%

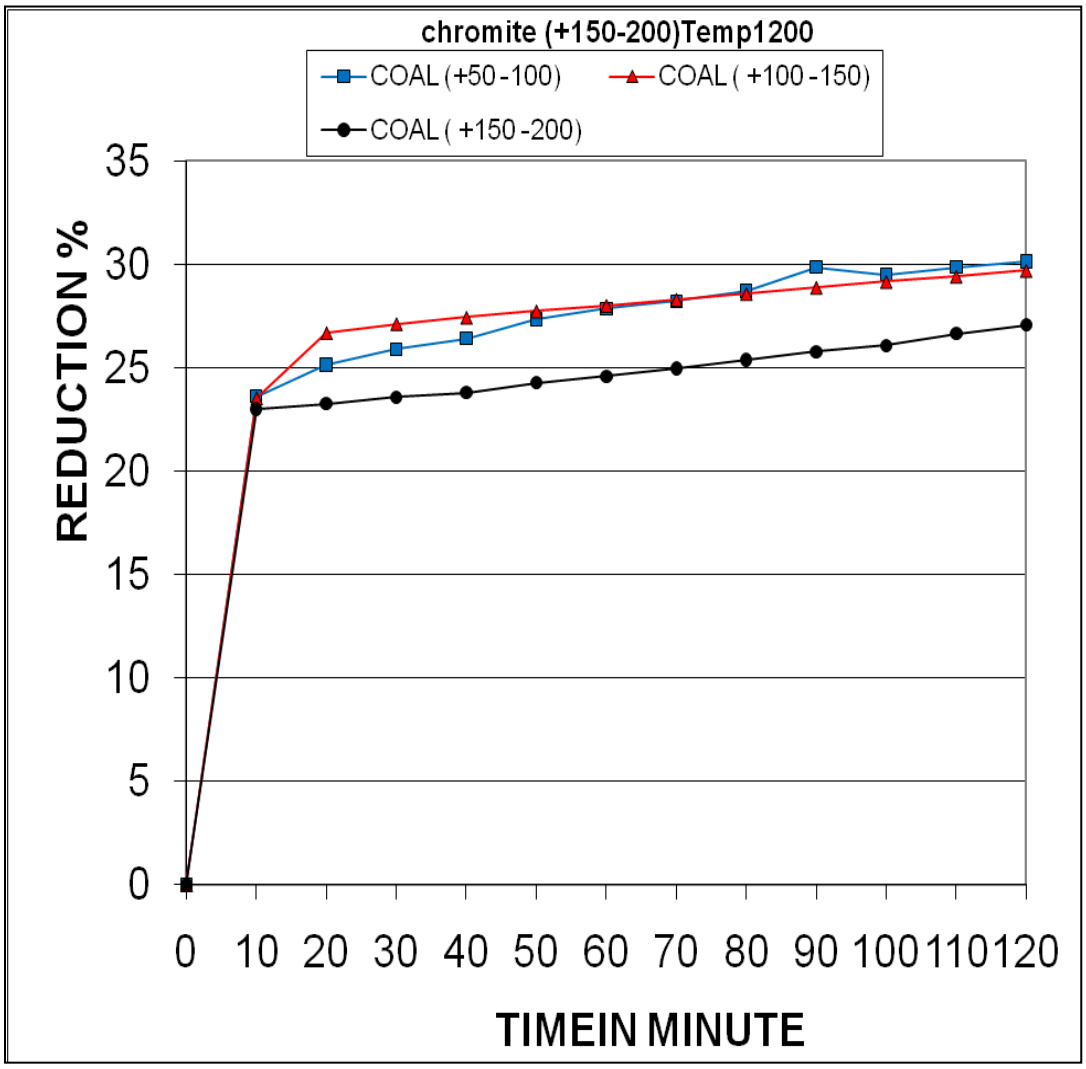

Figure 4.36 Effect of particle size on reduction of xstrata chromite (+150µm-200µm) with changing coal size at 1200 ºC.

(10) Following graph shows that at 1200 ºC for chromite (+50 µm -100µm) as graphite size decreases from (+150 µm -200µm) to (+50 µm -100µm), % reduction increases from 3.35% to 4.66 %.

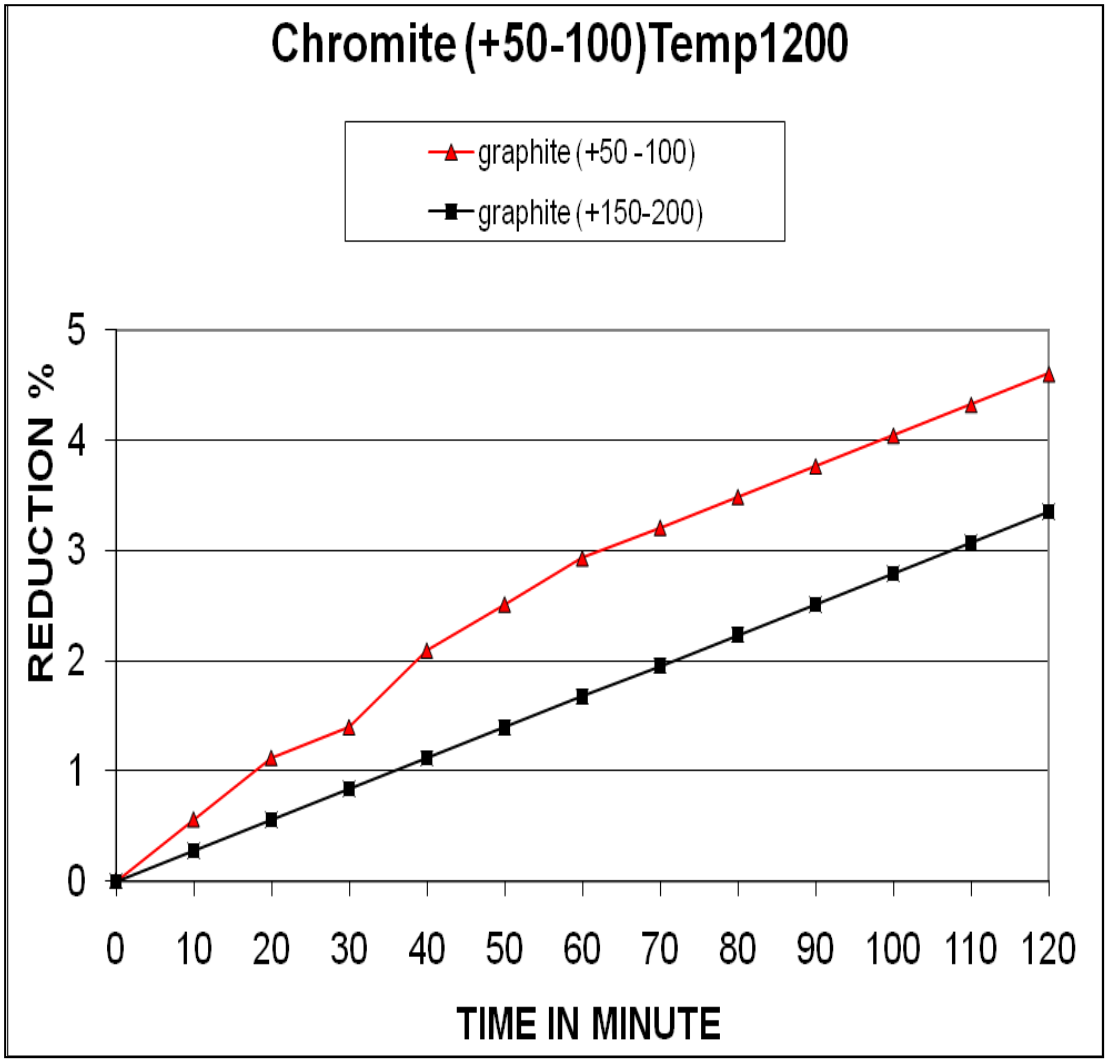

Figure 4.37 Effect of particle size on reduction of xstrata chromite (+50µm-100µm) with changing graphite size at 1200 ºC.

(11) Following graph shows that at 1200 ºC for chromite (+150 µm -200µm) as graphite size decreases from (+150 µm -200µm) to (+50 µm -100µm), % reduction increases from 4.116 % to 4.24 %.

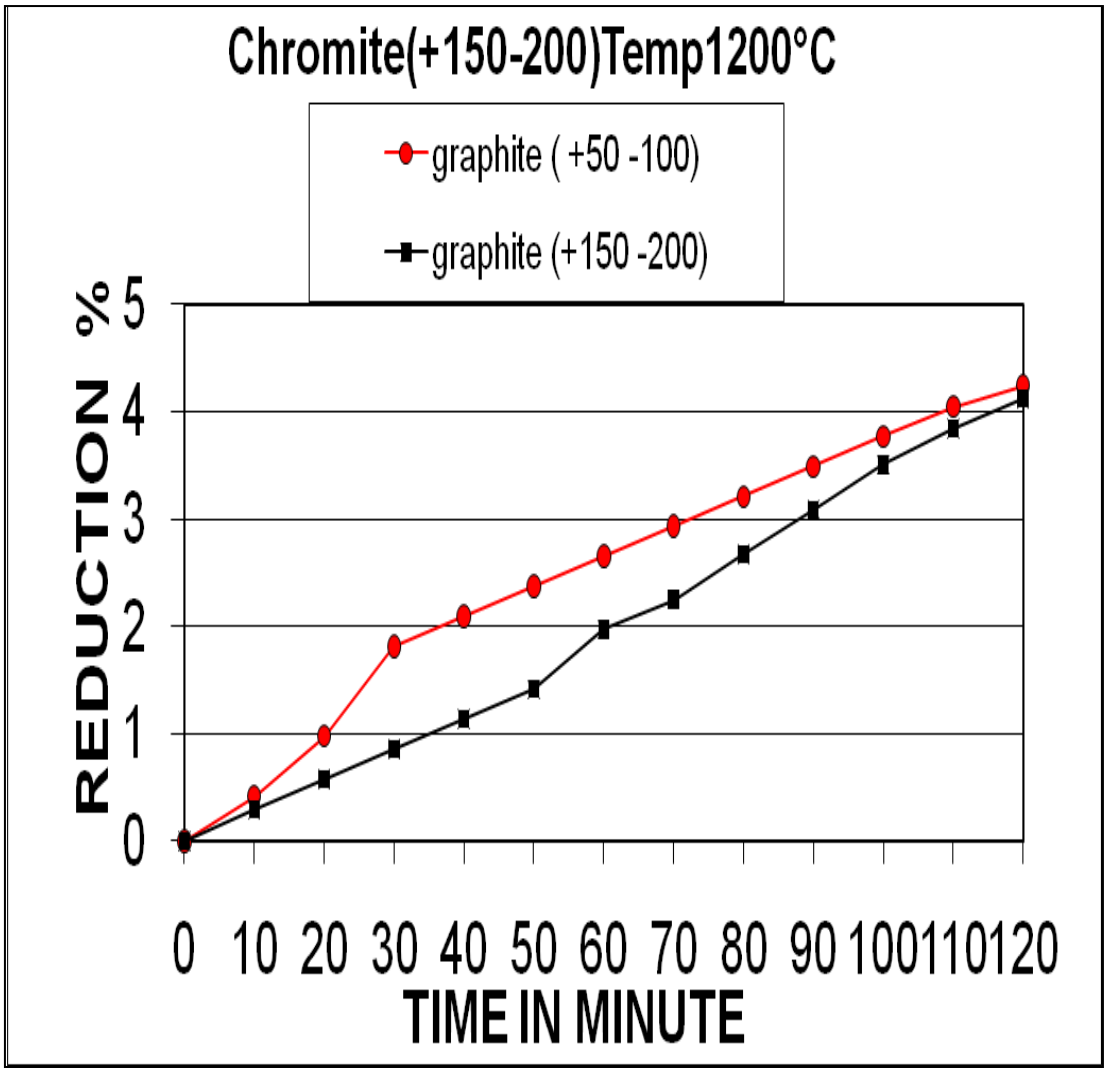

Figure 4.38 Effect of particle size on reduction of xstrata chromite (+150µm-200µm) with changing graphite size at 1200 ºC.

(12) Following graph shows comparison of reductant behavior at 1100 ºC. For chromite size of (+50 µm -100µm) and all reductants of size (+50 µm -100µm), coke gives 16.43%, charcoal gives 11.40 % whereas coal gives 9.98% and grahite 3.99% reduction.

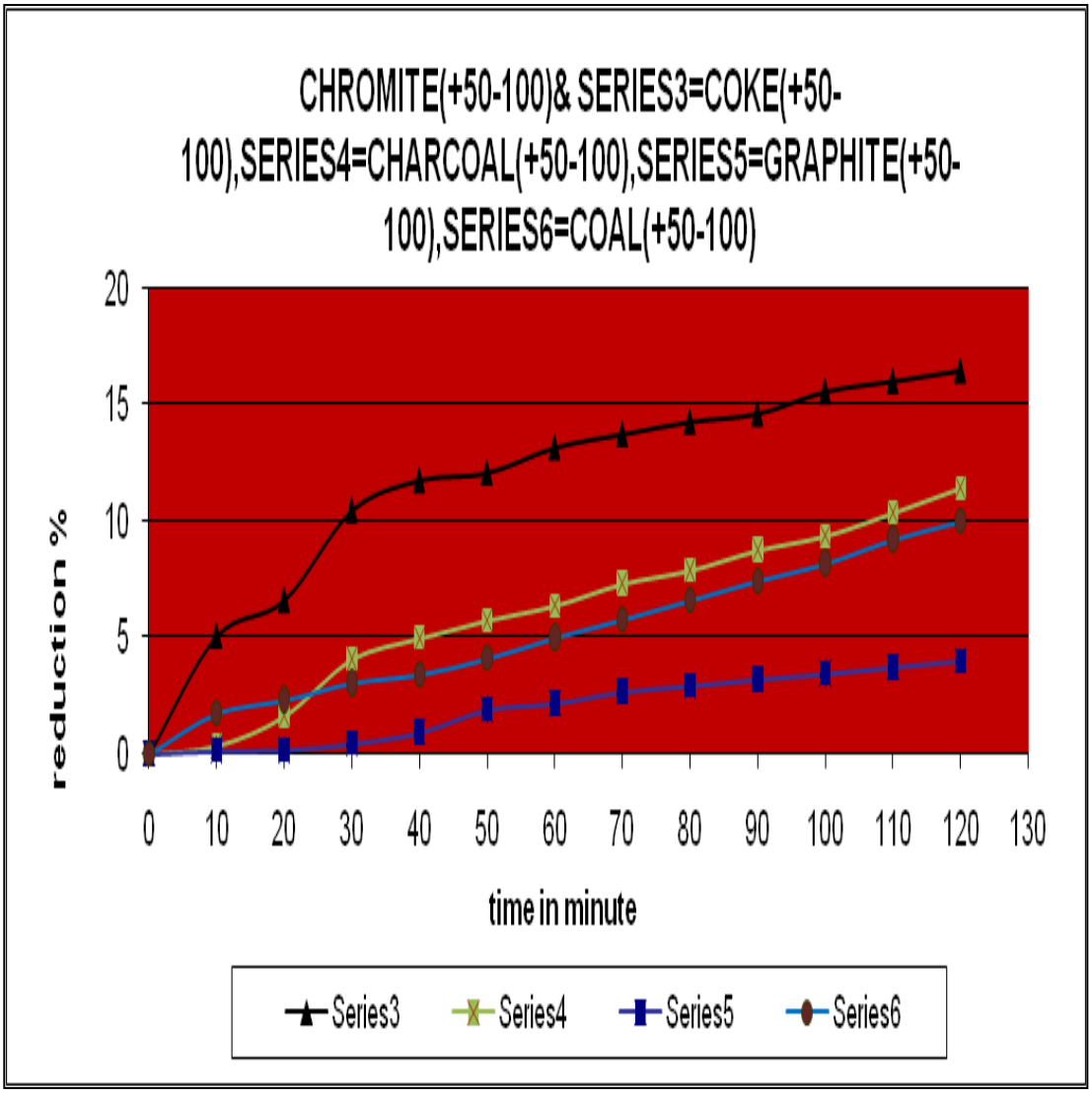

Figure 4.39 Comparasion of reductant behaviour for same sizes of chromite (+50 µm -100µm) and all reductants (+50 µm -100µm) at 1100 ºC.

4.6 EXPLAINATION OF EFFECT OF PARTICLE SIZE

Experimental results show that, the reduction rate increases with decrease in the particle size of the reactants. This effect is explained as follows, decrease in particle size of both the chromite and reductant results in

1. Higher total surface area of both chromite and reductant particle exposed to the reducing atmosphere.
2. Larger number of contact points between the chromite and the reductants particle
3. Shorter diffusion paths for Cr^{3+} and O^{2-} ions in the chromite particle. Higher reactants surface area, larger the number of contact points and shorter diffusion path all give rise to increased reaction rate.

4.7 EFFECT OF REDUCING AGENTS

The effect of the type of reducing agent namely coal, coke, charcoal and graphite is quite apparent. At at lower temperatures of 1000 ºC and 1100 ºC coke, coal,charcoal and graphite was order for reductions from highest to lowest where as at higher temperatures of 1200 ºC and 1300 ºC order was coal, coke, charcoal and graphite.

4.8 EFFECT OF COMPOSITION

Reduction rate of the ore depends on the amount of Fe, Cr, Mg, Al present in the ore. Iron and chromium oxides are reducible where as magnesium and aluminum oxides are practically irreducible. The higher concentration of Feand Cr ions increases the reaction rate and level of reduction.

4.9 EFFECT OF TEMPERATURE

The experiment results show that the reduction level and rate of the chromite increases as the reaction temperature increases. This result is expected as it is known that increase in reaction temperature increases the rate of all reactions in general.

Effect of graphite on the reduction behavior of xstrata chromite at 1000 ºC

In order to test the system initially blank runs were done in which furnace is initially tested using only graphite to check the leakage,once it was established that reduction is taking place with no leakages, then calculated amount (Appendix B) of chromite was added to calculated amount of graphite (Appendix B). Results indicated

that at 1000 ºC graphite was reducing chromite from 3.49 percent to 6.46 percent (Table 4.4), which was according to expectation.

Effect of charcoal on the reduction behavior of xstrata chromite at 1000 ºC

To investigate the effect of charcoal addition on the reduction at 1000 ºC, charcoal of all sizes (namely as received,(+50µm-100µm), (+100µm-150µm), (+150µm-200µm) (whereever all sizes are refered in this thesis, it will refer to all of these sizes)) was added in calculated amount (appendix B) to the all sizes of chromite and reduction run was performed**.** It was observed that reduction at this temperature by charcoal was fairly low of around 6.46 percent: Table (4.4).and figure D.28.

Effect of coal on the reduction behaviour of xstrata chromite at 1000 ºC

When coal was added to xstrata chromite in calculated amount the reduction level was around 7.95 percent, as can be seen in Table 4.4 and figure D.31, which is again fairly low.

Effect of coke on the reduction behavior of xstrata chromite at 1000 ºC

Lastly, at this temperature when coke behavior on reduction rate was investigated by adding chromite (of all sizes) to coke of all sizes (according to Table 4.4) in calculated amounts (according to appendix B), it was seen that reduction percent varied from 6.6 percent to 13.05 percent (figure D.29). At this temperature maximum reduction was observed with coke but still nothing much was happening at this temperature. Next approach was to increase the temperature to 1100 ºC and then investigate possible effect of reductants on the reduction behavior.

Effect of graphite on reduction behavior of xstrata chromite at 1100 ºC

Reduction of graphite with chromite (table 4.1) at 1100 ºC was again obtained through weight loss measurements. It can be gathered that reduction with graphite was low around 3.14 percent to 4.32 percent as can be seen from table 4.1, figures D.11 to D.13, figure D.27 and figure D.32.

Effect of charcoal on the reduction behavior of xstrata chromite at 1100 ºC

At 1100 ºC, when calculated amount (appendix B) of charcoal of all sizes were added to calculated amount(appendix B) of xstrata chromite of all sizes, it was observed that reduction was lowest for combination of largest size for chromite (+150µm-200µm)

and largest size of charcoal (+150µm-200µm) which was around 3.96 percent and reduction was maximum for combination of smallest size of chromite (+50µm-100µm) and smallest size of charcoal (+50µm-100µm) which was around 11.40 percent as given in table 4.1, figuresD.5 to D.10, figure D.26 and table 4.1.

Effect of coal on the reduction behavior of xstrata chromite at 1100 ºC

When various combination of all sizes of coal and xstrata chromite were mixed, it was observed that as compared to 1000 ºC coal shows a slightly higher reduction of around 9.98 percent (max), which was with smallest size chromite and coal (+50µm-100µm) as seen in figures D.14 to 16 and table 4.1

Effect of coke on the reduction behavior of xstrata chromite at 1100 ºC

Lastly, at this temperature behavior of coke was investigated (table 4.1). It was seen that reduction increased to around 16.43 percent (which was again for smallest size chromite and coke), it was more from reduction achieved at 1000 ºC of about 13.05 percent as given in table 4.1,figures D.1 to D.4 and figure D.25.

As the effect of reductants addition in enhancing the reduction was relatively small at 1100 ºC, the working temperature was raised to 1200ºC.

Effect of graphite on reduction behavior of xstrata chromite at 1200 ºC

Graphite continues its behavior even at 1200ºC and as expected and shows a low reduction of 4.66 percent for smallest size of graphite and chromite as given in table 4.2 and figres D.23.

Effect of charcoal on reduction behavior of xstrata chromite at 1200 ºC

At 1200 ºC, charcoal shows low levels of reduction which was minimum of 4.71 percent and maximum of 7.84 percent. Hence it can be seen that charcoal is not doing much as a reductant at this temperature as given in table 4.2 and figure D.24.

Effect of Coal on reduction behavior of xstrata chromite at 1200 ºC

In contrast to charcoal, addition of coal at 1200 ºC resulted in higher reduction levels as it increases the extent of reduction by 22 percent with the smallest sizes of coal and chromite (+50µm-100µm) to about 31.78 percent as compared to 9.98 percent at 1100 ºC for same sizes as given in table 4.2 and figures D.19 to D.21.

Effect of coke on the reduction behavior of xstrata chromite at 1200 ºC

When behavior of coke was investigated at 1200 ºC with addition of different sizes of coke and chromite it was observed that percent reduction increased to a maximum of 19.89 percent (table 4.2) and minimum being 9.91 percent. This percentage of reduction for coke (19.89) was higher than what was achieved for 1000ºC (13.05 percent) and 1100ºC (16.43 percent) as given in table 4.2 and figures D.17 to D.18. Hence it was deduced that coke is showing increasing reduction behavior at higher temperature. At this temperature highest percent reduction was for coal followed by coke then charcoal and then graphite being the least. Still maximum reduction percent of 31.78 by reductants (namely coal) was considered not suitable enough and with varying behavior of reductants, it was thought suitable to investigate further and so it was decided to raise the temperature to 1300 ºC.

Effect of graphite on the reduction behaviour of xstrata chromite at 1300 ºC

Graphite being hardest to reduce chromite, gives a low 4.12 percent reduction on its addition to chromite at 1300 ºC as given in table 4.3.

Effect of charcoal on the reduction behaviour of xstrata chromite at 1300 ºC

As can be seen from table 4.3 and figure D.22 addition of charcoal of all sizes to all sizes of chromite resulted in a maximum of 20.29 percent and a minimum of 8.41 percent. Behaviour of charcoal changes at higher temperature of 1300 ºC as compared to 1200 ºC, where at 1200 ºC maximum reduction achieved was 7.84 percent (Table 4.2).

Effect of coal on reduction behaviour of xstrata chromite at 1300 ºC

Coal had showed maximum reduction achieved among all reductants in all runs. Again this was achieved by addition of coal of size +50µm -100µm to chromite of size +50µm -100µm which was 45.06 percent (table 4.3) as can be seen in figures D.30, D.31 and D.33 showing that finest coal and finest chromite are the best suitable combination to

achieve maximum reduction possible. With coal at this temperature the least percent of reduction was for largest sizes of coal and chromite (table 4.3) of 31.17 percent as expected. Raising temperature from 1200 ºC to 1300 ºC has enhanced reduction (max) percent to 45.06 at 1300 ºC as compared to 31.78 (max) percent (table 4.3) achieved for same size at 1200 ºC.

Effect of coke on reduction behaviour of xstrata chromite at 1300 ºC

When behaviour of coke was investigated at 1300 ºC with addition of different size coke and chromite, it was observed that coke also enhanced the reduction percent from what was achieved at 1200 ºC (19.89 percent max), 1100 ºC (16.43 percent max),and 1000 ºC (13.05 percent max) to 42.28 percent max at 1300 ºC. It was also observed that this maximum reduction of 42.28 percent was achieved for smallest size coke and chromite where largest size coke and chromite shows 13.54 percent.

It can be deduced that at higher temperature of 1300 ºC coal will show higher percent reduction as compared to coke. Hence at higher temperatures of 1300 ºC and 1200 ºC order of reduction is coal, coke, charcoal and graphite where as at 1100 ºC it was coke, coal, charcoal and graphite and at 1000 ºC coke give highest percent reduction and graphite gives lowest while coal and charcoal give similar percent reduction.

4.10 GENERAL DISCUSSION

The discussion done here is to shed some light into the behaviour of various reductants on the chromite. Examination of reduced sample under optical microscope revealed that at 1000ºC where reduction is around 3 % -11%, there is very little metallic phase. At 1100 ºC where reduction % increases to maximum of 14-16 %, the metallic phase was observed in the form of nuclei over the particle surface. At 1200 ºC when reduction level increases to a maximum of 36 % the metallic nuclei have been observed to grow. At 1300 ºC where reduction level increases to a maximum of 45% metallic nuclei tend to grow till it forms a complete alloy shell, around the particle.

4.11 MICROSCOPY

Microstructure evolution of the reduced sample was studied by a series of reductions at different temperatures for 120 minutes. At higher temperatures of 1200°C – 1300 °C, the microstructure consists of metallic (Fe-Cr carbides) globules and even shells formed due to solid state reaction (chemical reaction and phase boundary diffusion of reducible Fe and Cr ions). At lower temperatures (1000°C – 1100 °C) where percent reduction is less only small amount of small metallic globes are seen as shown in Figures 4.41 to 4.45).Where alloy (Fe –Cr) indicated in figures is $(Fe\ Cr)_7C_3$.

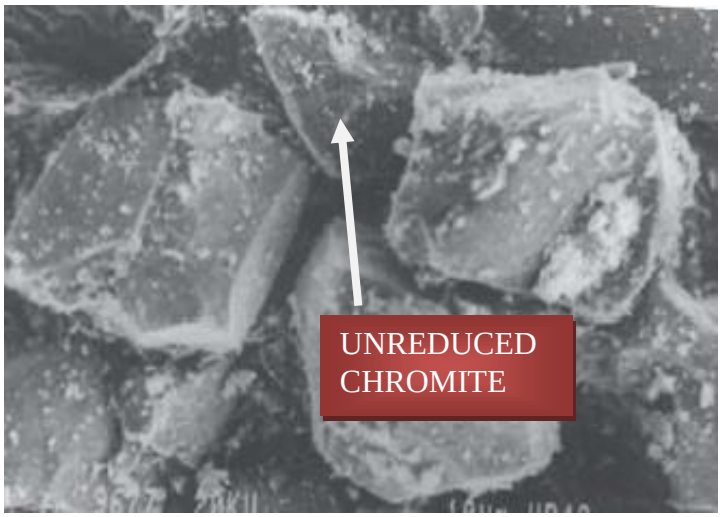

Figure 4.40.Scanning electron microscopic image of unreduced chromite

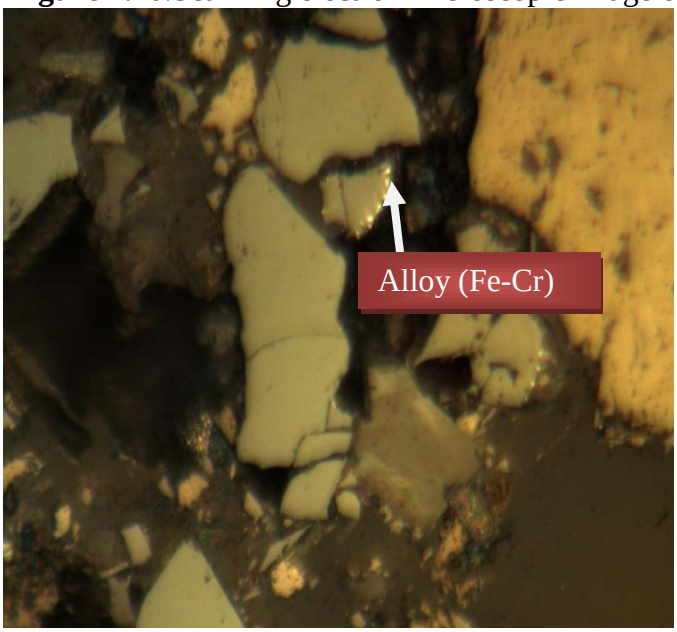

Figure 4.41 Chromite (150 µm -200 µm) and coke (+150 µm -200 µm) at 1000 ºC, run 4

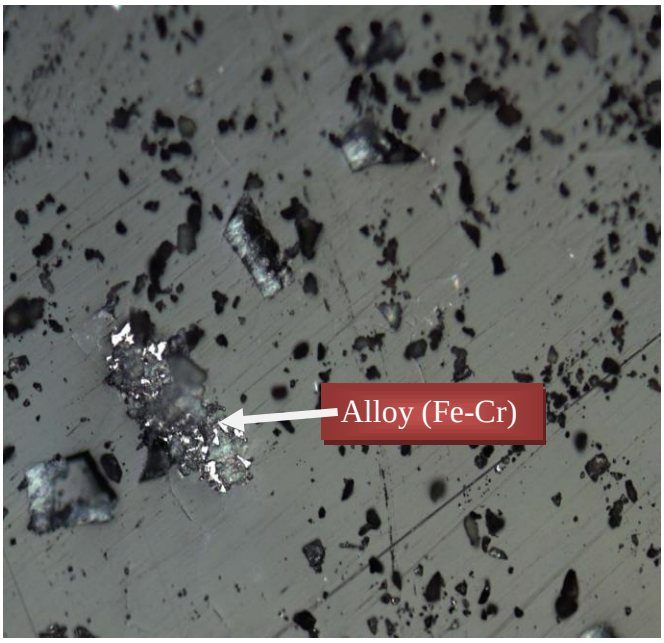

Figure 4.42, Chromite (+50 µm -100 µm) and as received coke, at 1000 ºC, run 5.

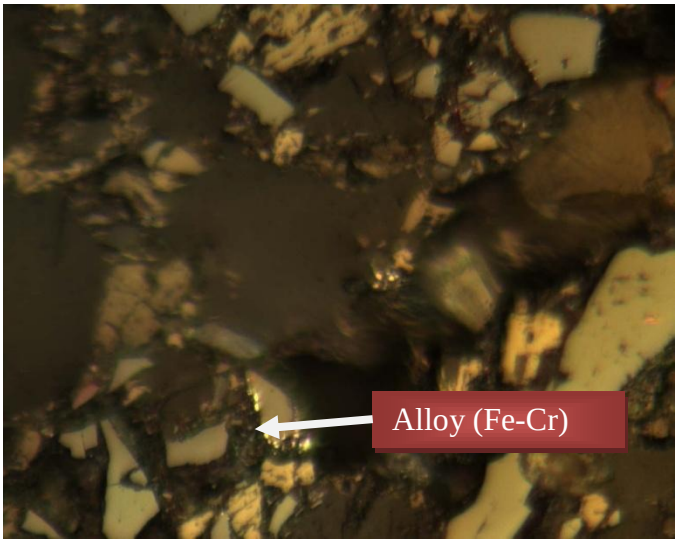

Figure 4.43 As received chromite and coke (+50 µm -100 µm) at 1000 ºC, run 2

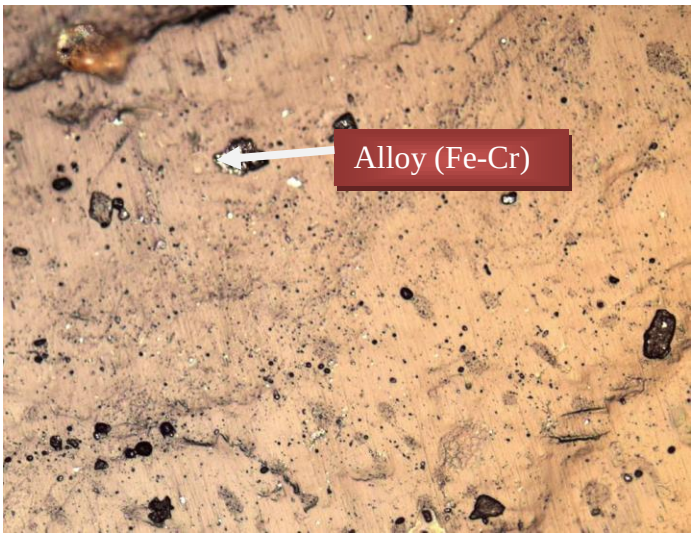

Figure4.44 As received chromite and coke (+150 µm -200 µm) at 1000 ºC, run 27.

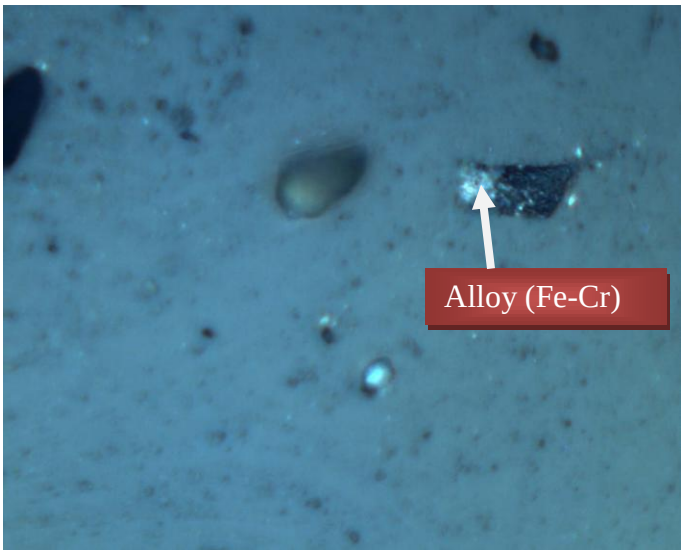

Figure 4.45, Chromite (+100 µm -150 µm) and coke (+150 µm -200 µm) at 1100 ºC**,** run 38.

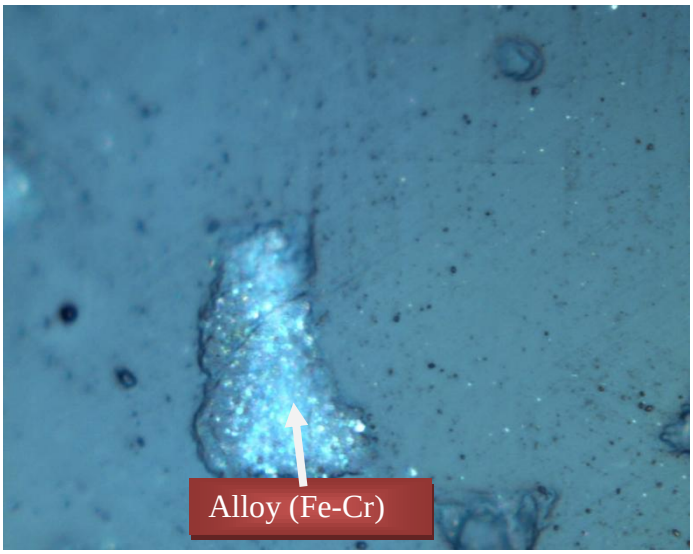

Figure 4.46, Chromite (+150 µm -200 µm) and coal (+150 µm -200 µm) at 1200 ºC**,** run 86.

CHAPTER 5

MATHEMATICAL ANALYSIS OF THE REDUCTION RATE DATA

Many theorital kinetic equations have been derived over past 73 years for solid state reactions. The merits of these equations have been reviewed by several authors (Bamford and Tipper,[3] 1980). Basically, the models for solid state reaction are classified into three major groups:

1) diffusion of the reactants and or products through a contionous product layer,
2) nuclei and growth, and
3) phase boundary reactions.

These are reviewed in the following.

5.1.1 Diffusion models:

When a solid state non porous reaction product is formed on the reacting solid, the kinetics of the reaction will be goverened by the resistance through the solid product layer. then y=kw, where k is a rate constant.The diffusion through the solid product layer will then be given by the equation,

$$dw/dt=\alpha\,[(DAC)/Y] = (\alpha/K)[\,(DAC)/W] \quad \text{.....5.1}$$

Where

α: is the stiochiometry factor,

C: is constant,

D: is diffusion coefficient,

A: is cross sectional area

Y: is the thickness of this product layer,

W: is the weight of the solid reaction product at time t,

K: is a rate constant,

If there is a continous supply of the reagent, that is when C is constant,

Then

$$w\int (dw) = (\alpha/k)\, DAC \int (dt) \quad \text{.....5.2}$$

$$w^2/2=k't +\text{constant}$$

$y^2 = 2kt + constant.$

Choosing the boundary condition y=0 when t=0 gives

$Y^2 = 2k_D t = K_P T$……...5.3

Equation 5.3 is a well known parabolic rate law, where K_P is the parabolic rate constant. This equation was first deduced by Tammann[104] and was found to apply for the oxidation kinetics of a number of metals.

In 1927, Jander[54] applied the parabolic rate law and developed a model for planer interface reactions, applicable to powdered compacts. Jander came up with an equation relating the fraction of reaction completed to time, where the fraction of reaction completed is defined R = [Weight of oxygen removed / weight of removable oxygen]

$2k_j t = 2kDt/r_o^2 = [1-(1-R)^{1/3}]2$……..5.4

k_j is the rate constant.

The equation developed from the Jander model for solid state reactions state that the rate constant is proportional to the diffusion coefficient of the species being transported and inversely proportional to the square of the initial radius. Jander model is based on the following assumption:

1 The reaction under consideration can be classified as an additive reaction
2 The reacting particle is all spheres of uniform radii.
3 Nucleation, followed by surface diffusion, occurs at a temperature below that needed for bulk diffusion, so that a coherent product layer is present when bulk diffusion does occur.
4 Bulk diffusion is unidirectional.
5 The chemical reaction at the phase boundary is considerably faster than the transport process and thus the solid state reaction is bulk diffusion controlled.
6 The surface of the component in which reaction take place is completely and continuously covered with particle of the other component as though the former particle were immersed in a melt of the latter. This assumption is approximately true when the ratio of (r_A/r_B) is very large and the amount of component B is greatly in excess of that of component A.
7 The product phase is not miscible with any of the reactant phase.

8 The ratio of the volume of the product layer to the volume of the material reacted is unity

9 The diffusion coefficient of the species being transported is not a function of time.

10 The activity of the reactants remains constant on both sides of the reaction interface.

Some other researchers who worked under different conditions and made contribution to this field were Kroger and Ziegler[64], Zhuravlev and Lesokhin [124], Carter[12], Valensi[110], Dunwald and Wagner[23], Serin and Ellickson [95] and Ginstling and Brounshtein[47].

Ginstling and Brounshtein[47] arrived at a model using Jander's assumptions with the exception of the parabolic rate law. They indicated that the parabolic rate law asserted that the reaction surface remained constant; however, when they considered spherical particles, this surface actually decreased in area as the reaction proceeded. They discarded the parabolic rate law in favour of an equation relating the growth of the product layer to Barrer's equation for steady –state heat transfer through a spherical shell. Equation 5.5 is the Ginstling and Brounshtein equation.

$$k_{gb}t=2kDt/r_o^2=1-2/3R-(1-R)^{2/3} \quad \ldots\ldots 5.5$$

5.1.2 NUCLEI GROWTH MODELS

Model discussed so far assumed that initially a continous product layer coats the surface of the reacting particle so that further reaction occurs by the transport of matter to the reaction zone through this product layer. However, there is another way of looking at the intial product formation and subsequent growth.This approach considers the nucleation of products at active sites and the rate at which the nucleated particles grow.

According to Welch[118] such mechanism is possible whenever the product phase is partially miscible in one of the reactants.All the nuclei growth equation developed are of the general form:

$$\ln [1/ (1-R)] =kt^m \quad \ldots\ldots 5.6$$

Where m is a parameter which is a function of:

1 Reaction mechanism.

2 Nucleation Rate.

3 Geometry of the Nuclei.

If a solid state reaction can be represented by a nuclei- growth model, according to equation 5.6, a plot of ln [1/ (1-R)] versus lnt (nuclei growth analysis) should yield a straight line with slope m and intercept mlnk.

5.1.3 PHASE BOUNDARY MODELS:

According to Laidler[69], when a discountinous product phase occurs, the rate determining step may be the chemical process occurring at the phase boundary. Under these circumstances, the rate is determined by the available interface area, and such processes are reffered to as topochemical.

Rate equations have been derived for topochemical system assuming that:

1. The reaction rate is phase boundary controlled.
2. The reaction rate is proportional to the surface area of the fraction of unreacted material.
3. The nucleation step occurs virtually instantaneously, so that the surface of each particle is covered with a layer of product.

The models developed from the foregoing boundary conditions are termed phase – boundary kinetic models.

For spherical particles:

$$K_{pb}t=kt/r_o=1-(1-R)^{1/3} \quad \ldots\ldots\ldots\ldots\ldots\ldots\ldots\ldots\ldots\ldots\ldots\ldots\ldots\ldots 5.7$$

Where k=dr/dt

The radius thus recedes at a constant rate which is k. According to equation 5.7, the rate constant for a phase boundary controlled reaction, K_{pb} is equal to the velocity at which the interface advances into the reactants divided by the intial radius of the particles. It should be noted that the rate constants for phase –boundary kinectics models are inversely proportional to the radius, whereas for transport controlled kinetics models they are inversely proportional to the square of the radius.

Equations analogous to classical rate equations have often been applied to the solid state reactions.The integrated form of the general kinetics equation based on the concept of an order of reaction is

$$K_t= [1/(n-1)][(1/(1-R)^{(n-1)})-1]\ldots\ldots\ldots\ldots..5.8$$

5.2 1Application of the model to the experimental data

To test reactivity of the reductant, the definition of reactivity of reductant according to present experiments should be considered as the inherent capacity of the reductant to induce the reduction reactions of the ore. On the basis of this definition, present experimental data was fitted to the Arrhenius equation which gives the temperature dependence of the rate through activation energy:

$$R_T = R_{To} \exp [-\Delta E/R\ (I/T-I/T_o)].\text{----------5.9}$$

Where R_T and R_{To} are rates (in units / sec) at temperature T and T_o respectively,

ΔE(J/mol) is the activation energy of the reaction which here will be the measure of the capacity of the reductant to induce the reduction reactions of the ore (its reactivity), and

R (J/ (mol.K)) is the gas constant.

Previous study by R.H Eric[33] on the solid state reduction of chromite ore suggested that reaction mechanism of the reduction of the ore involves both the chemical reactions and the diffusion of the ionic species ($Fe^{3+,}$ $Fe^{2+,}$ $Cr^{3+,}$ $Cr^{2+,}$ $Mg^{2+,}$ Al^{3+}) from and to the reactions sites. This has prompted the use of a mixed rate control model to describe the kinetics of the reduction process of the ore:

$$t_i = \tau \mathcal{G}_f(X_i) + \tau \sigma^2 \mathcal{P}_f(X_i), \text{ mixed control.----------5.10}$$

$$\mathcal{G}_f(X_i) = 1-(1-X_i)^{1/3}, \text{ chemical rate control conversion factor. ----------5.11}$$

$$\mathcal{P}_f(X_i) = 1-3(1-X_i)^{2/3}+2(1-X_i), \text{ diffusion rate control conversion factor.---5.12}$$

$$\tau = (t / t^*). \text{----------5.13}$$

Where

t^* = is the dimensionless time for a chemical reaction controlled process.

σ^2 =is the ratio of dimensionless time for a chemical reaction controlled process to dimensionless time for diffusion controlled process.

X_i =is the fraction reduction of the ore and was calculated by use of the following equation:

$$X_i = [\text{Mass of CO evolved}] / [(28.01/15.99) * \text{Mass of original removable oxygen}]\text{----5.14}$$

$$k = \rho F_p V_p / \tau b A_p = \text{Chemical reaction rate constant----------5.15}$$

$$D_e = k V_p / 2 \sigma^2 A_p = \text{Effective diffusion coefficient---------- ----------5.16}$$

Where:

ρ is the density (kgm^{-3}).

F_p is the shape factor (3 for spherical particles)

V_p is the volume (m^3) = $4/3\pi r^3$(r is the particle radius)

A_p is the cross sectional area (m^2) = $4\ \pi r^2$(r is the particle radius)

b is the stiochiometric factor (¼ for the reduction of $FeCr_2O_4$ spinel

The chemical reaction rate constants (k, in s^{-1}), and the effective diffusion coefficient (D_e, in m^2s-1) obtained at different temperatures are then fitted into the Arrhenius equation.The reactivity of the reductant will then be obtained from the fit of the data to the Arrhenius equation**.**

5.3 1Method of least square

A Statistical regression tool known as the method of least square was used to determine the values of the parameters (τ and σ^2) of the above model equation.And this was done with the help of Microsoft excel.

Method of least square is a parameter estimation technique in which the parameters of the system are estimated by minimizing the sum of the square of the differences between the observed values (experimental data) and the fitted or predicted values from the system.

$$s^2= \Sigma(f(x_{exp})-f(x_i))^2 \text{----------5.17}$$

Where

s^2 is the sum of the square of the differences between the observed value (experimental data) and the fitted values from the system.

$f(x_{exp})$-observed values from tga runs

$f(x_i)$- fitted values to be predicted by equation 5.10 above.

Thus each parameter is assigned a predicted value initially, then to obtain their correct values one of the parameter is varied while others are kept constants until minimum s^2 value was reached, thus at that minimum s^2 value is where the correct value of the parameter is obtained. Then that value is kept constant, while following the same procedure to determine the other parameter. After all the parameters are determined, they are put in the equation 5.10 called fitted equation now.

Values of all parameters were substituted into fitted equation to predict time for mixed control process, these predicted time for mixed control where converted to fraction loss for model (as given below). Then the fractional loss (model) and fractional loss

(experimental) were plotted and agreement on values obtained from experiments were verified with the value obtained from model, i.e how well does mixed control model describes the fractional loss results obtained from experimental data. It was seen that a good agreement is observed in all cases except for some sizes of coal which showed larger variations while other sizes of coal had shown considerable agreement.

5.3.2 Application of experimental data from tga to rate control model.

To apply this model to experimental data, tga experimental results were used, using Microsoft excel, tga results were uploaded on excel sheets, formulas were inbuilt on excel sheet to calculate the fraction loss(experimental), chemical rate conversion factor, diffusion rate control conversion factor. Value of variable τ and σ^2 were calculated using mixed control model to describe the kinetics of the reduction process equation (5.10) and appling method of least square(iteration method).

Formulae were calculated as following; Fractional loss (experimental)=0.1396×mass loss, Chemical rate conversion factor from equation 5.11, diffusion rate conversion factor from equation 5.12, time model from equation 5.10,

As described in section 5.2, while fitting into equation 5.10 values of τ and σ^2 were calculated from the least square iteration method. Then this value of t_{model} was used to calculate fraction loss= $(1-(1-t_{model}/\ \tau)^3$. Then fractional loss (model) and fractional loss (experimental) were plotted and agreement on value's obtained from experiment's were verified with the value obtained from model.

Following plot's of chromite size (+100µm -150µm) and reductants sizes (+50µm-100µm), (+100µm-150µm), (+150µm-200µm) are given as main part of dissertation, namely for coke (figure 5.1 to figure 5.8), for charcoal (figure 5.15 to figure 5.21) and for coal (figure 5.28 to 5.34). For other chromite sizes namely (+50µm-100µm), (+150µm-200µm), as received) and reductants sizes ((+50µm-100µm), (+100µm-150µm), (+150µm-200µm) are given in appendix figures from D.34 to D.104. All results are given in tabular form in Appendix E from table E1 to table E71.

5.4. Activation energy.calculations

Values of τ, σ^2 (given below in figures 5.1 to 5.8, 5.15 to 5.21 and 5.28 to 5.34), K (calculated from equation 5.15) and D (calculated from equation5.16) (given in appendix B) for chromite size (+100µm -150µm) and reductants sizes (+50µm-100µm),

(+100µm-150µm), (+150µm-200µm) were put in tabular form in tables 5.1 to 5.9, against each temperature (1100 ºC, 1200 ºC, 1300 ºC).

Variation of chemical rate and diffusion rate with temperature for chromite size (+100µm -150µm) and reductants sizes (+50µm-100µm), (+100µm-150µm), (+150µm-200µm) were plotted and are in main part of this dissertation namely for coke (figures 5.9 to 5.14) for charcoal (figures 5.22 to 5.27) and for coal (figures 5.35 to 5.40) where as variation of chemical rate and diffusion rate with temperature of chromite namely (+50µm-100µm), (+150µm-200µm), as received and reductants sizes (+50µm-100µm), (+100µm-150µm), (+150µm-200µm) are parts of appendix from figures D.105 to D.122.

5.5 Results and Discussions of Modelling.

The microsoft excel sheets for calculation of fractional loss model and time model using iteration method is given in appendix E From table E1 to table E71, the results from these tables for all runs indicate that fractional loss model and fractional loss experiment are in generally good agreement except in case of coal where large variation between fractional loss model and fractional loss experiment is seen.

The results suggest that the coke has highest reactivity since its activation energies are lowest.The results also suggest that the likely rate controlling mechanism is diffusion of species to the reaction site since the effective diffusion constants are much smaller than reaction rate constants. The tests also suggest that coal is fastest to react since its D_e value is high.

5.5(a) Determinationof τ and σ^2 at 1100 ºC for coke

The generated data in appendix C is fitted into equation 5.10 using sum of least squares as follows

$$s^2 = \Sigma (\text{error})^2_i = \Sigma [a_1 \tau \mathcal{G}_f (X_i) + a_2 \mathcal{P}_f (X_i) - t_i]^2 \quad \ldots\ldots\ldots\ldots\ldots\ldots 5.17$$

Where

$a_1 = \tau$

And $a_2 = \tau.\sigma^2$

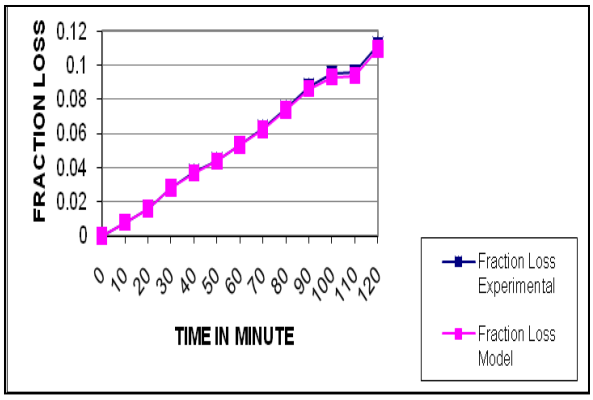

Figure 5.1 Comparison of experimental and model fractional loss vs time on addition of coke (+50µm-100µm) to chromite (+100µm-150µm) at 1100 ºC

The fit yields

τ=3200

σ^2=0.187

s^2=100.264325

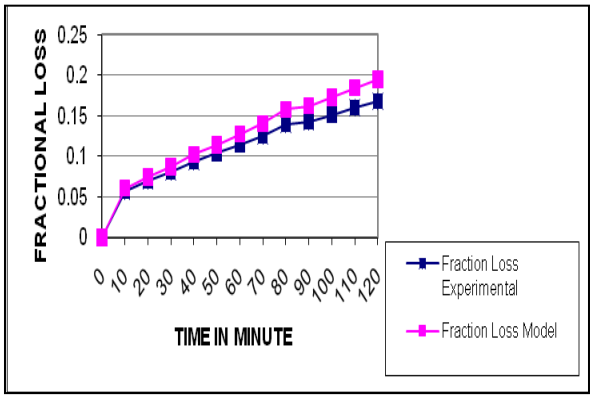

Figure 5.2 Comparison of experimental and model fractional loss vs time on addition of coke (+100µm-150µm) to chromite (+100µm-150µm) at 1100 ºC

The fit yields

τ=3700

σ^2=1.0

s^2=1522.55138.

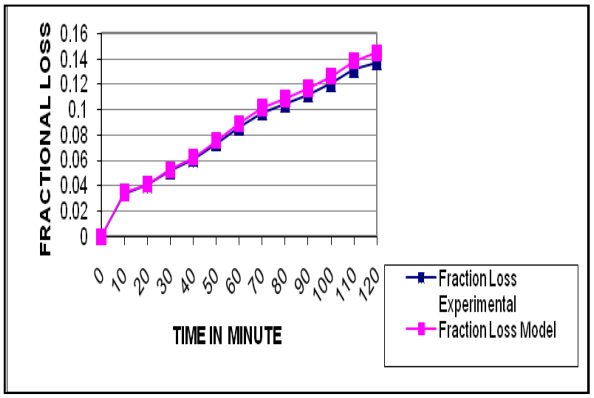

Figure 5.3 Comparison of experimental and model fractional loss vs time on addition of coke (+150µm-200µm) to chromite (+100µm-150µm) at 1100 ºC

The fit yields

τ=2200

σ^2=0.409

s^2=742.1946

5.5(b) Determination of τ and σ^2 at 1200 ºC for coke

The generated data in appendix C is fitted into equation 5.10 using sum of least squares as follows through eqation [5.17]

$$s^2=\Sigma\ (\text{error})^2{}_i = \Sigma[\ a_1\ \tau \mathcal{G}_f(X_i) + a_2\ \mathcal{P}_f(X_i) - t_i\ ]^2$$

Where

$a_1 = \tau$

and $a_2 = \tau\ \sigma^2$

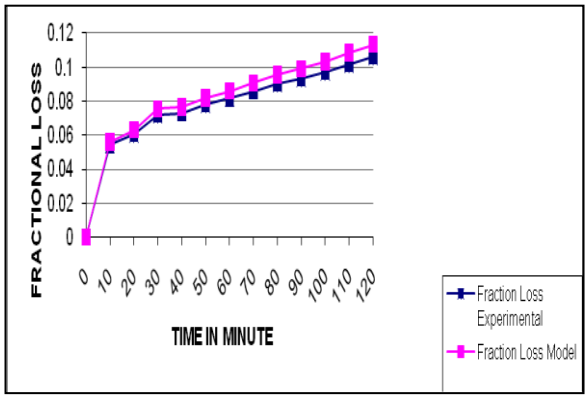

Figure 5.4 Comparison of experimental and model fractional loss vs time on addition of coke (+50µm-100µm) to chromite (+100µm-150µm) at 1200 ºC

The fit yields

τ=2400

σ^2=0.6666

s^2=5588.420912.

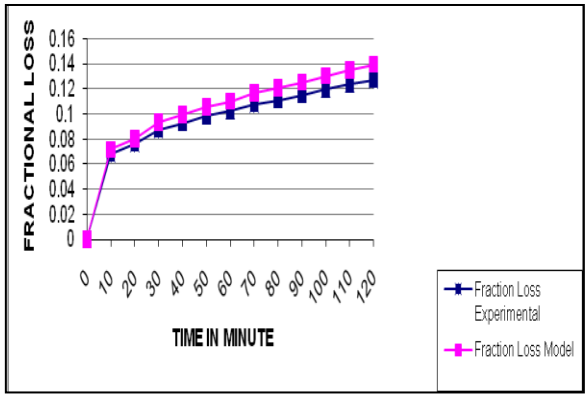

Figure 5.5 Comparison of experimental and model fractional loss vs time on addition of coke (+150µm-200µm) to chromite (+100µm-150µm) at 1200 ºC

The fit yields

τ=1900

σ^2=0.789

s^2=5944.551632.

5.5(c) Determination of τ and σ^2 at 1300 ºC for coke

The generated data in appendix C is fitted into equation 5.10 using sum of least squares as follows through equation [5.17]

$$s^2=\Sigma(\text{ error })^2_i =\Sigma[\ a_1\ \tau\mathcal{G}_f(X_i)+\ a_2\ \mathcal{P}_f(X_i) - t_i\ ]^2$$

Where

$a_1= \tau$

and $a_2= \tau\ \sigma^2$

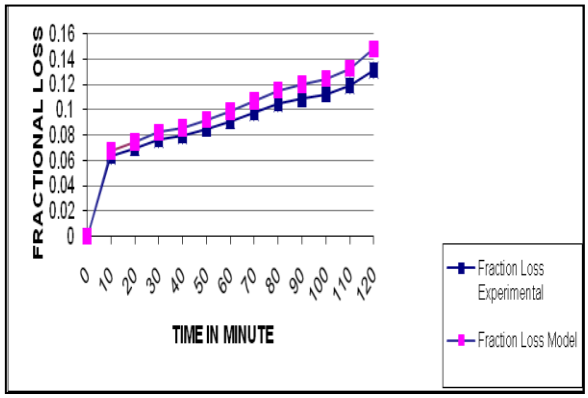

Figure 5.6 Comparison of experimental and model fractional loss vs time on addition of coke (+50µm-100µm) to chromite (+100µm-150µm) at 1300 ºC

The fit yields

τ=2000

σ^2=1.0

s^2=4349.784

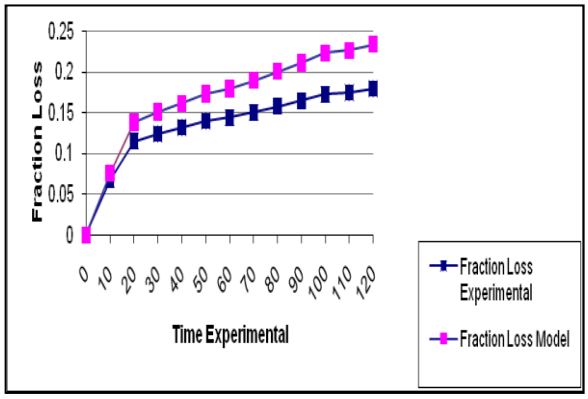

Figure 5.7 Comparison of experimental and model fractional loss vs time on addition of coke (+100µm-150µm) to chromite (+100µm-150µm) at 1300 ºC

The fit yields

τ=1100

σ^2=1.8181

s^2=4465.158.

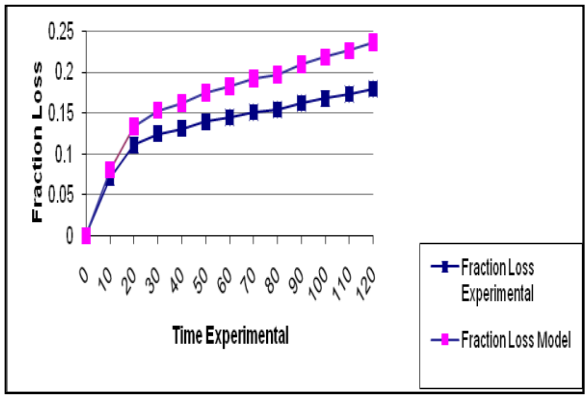

Figure 5.8 Comparison of experimental and model fractional loss vs time on addition of coke (+150µm-200µm) to chromite (+100µm-150µm) at 1300 ºC

The fit yields

τ=1100

σ^2=1.9090

s^2=4541.1687

5.5(d) Determination of ΔE (for chemical reaction) and ΔE (for diffusion) for coke

From equations 5.15 and 5.16 the values of the chemical rate constants K (s^{-1}) and the effective diffusion coefficient De (m^2s^{-1}) are obtained at different temperature and are as follows:

Table 5.1 Diffusion rate and chemical rate for chromite (+100 -150) and coke (+50 - 100)

Temp.°C	*τ(min)*	*τ* (sec)	σ^2	K(s^{-1})	D_e (m^2s^{-1})
1100 °C	3200	192000	0.187	0.60416E-06	5.555E-11
1200 °C	2400	144000	0.6666	3.47222E-06	2.17036E-11
1300 °C	2000	120000	1.0	4.1666E-06	1.7361E-11

The values of K at different temperatures were fitted into equation [5.9] (as shown in figure 5.9) using the sum of least square as follows:

$$s^2=\sum [K_o \exp (\Delta E/R \{1/T_i - 1/T_o\})-K_i]^2 \text{----------5.18}$$

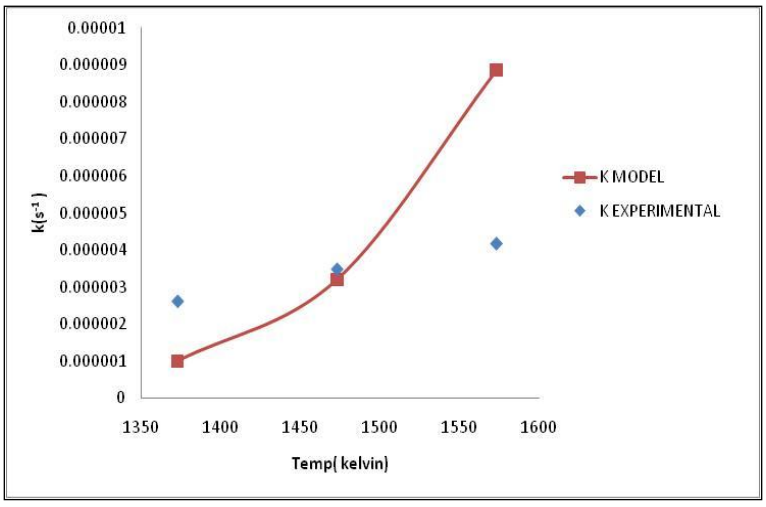

Figure 5.9 Variation of chemical rate constant with temperature on addition of coke (+50µm-100µm) to chromite (+100µm-150µm)

The fit yields:

ΔE=196,000 J/mol
T_o=1373 °K
K_o=1.05E-06 s^{-1}
s^2=2.468E-11

Table5.2 Diffusion rate and chemical rate for chromite (+100-150) and coke (+100-150)

Temp.ºC	τ *(min)*	τ (sec)	σ^2	K (s^{-1})	D_e (m^2s^{-1})
1100 ºC	3700	222000	1.0	2.25225E-06	2.5363E-11
1200 ºC	2100	126000	0.47619	3.960E-06	3.473E-11
1300 ºC	1100	66000	1.818	8.333E-06	1.05219E-11

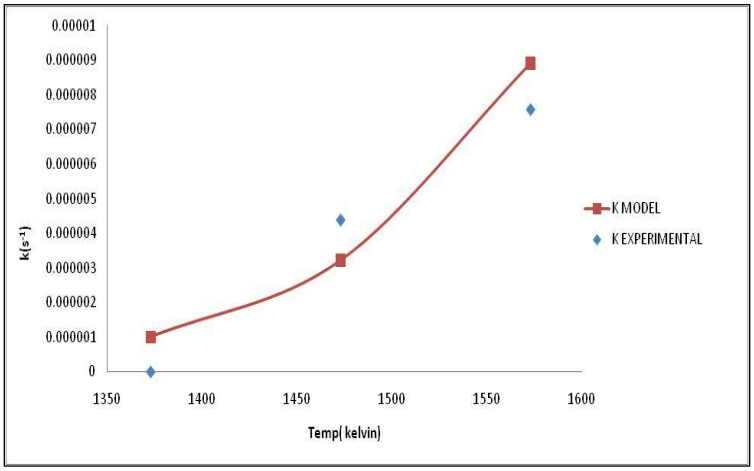

Figure 5.10 Variation of chemical rate constant with temperature on addition of coke (+100µm-150µm) to chromite (+100µm-150µm)

The fit yields:

ΔE=196,500 J/mol
T_o=1373 ºK
K_o=1.006E-06 s^{-1}
s^2=4.1512E-12

Table 5.3 Diffusion rate and chemical rate for chromite (+100-150) and coke (+150-200)

Temp ºC	$\tau(min)$	τ (sec)	σ^2	K(s^{-1})	D_e (m^2s^{-1})
1100 ºC	2200	132000	0.409	1.72775E-09	1.754E-14
1200 ºC	1900	114000	0.789	4.3859E-06	2.3148E-11
1300 ºC	1100	10000	1.900	7.575E-06	1.6535E-11

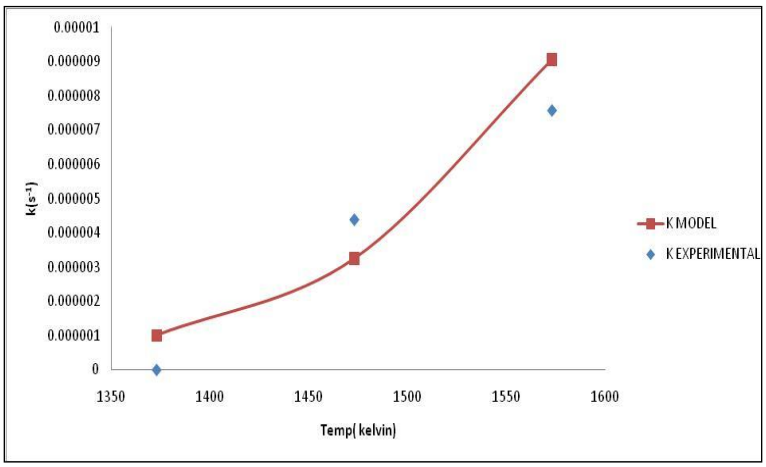

Figure 5.11 Variation of chemical rate constant with temperature on addition of coke (+150µm-200µm) to chromite (+100µm-150µm)

The fit yields:

ΔE=198,000 J/mol
T_o=1373 ºK
K_o=1.009E-06 s^{-1}
s^2=4.5074E-12

5.5.1(d)Determination of ΔE (for diffusion) for coke

The values of D_e at different temperatures were also fitted into equation [5.19] (as shown in graph) using the sum of least squares as follows:

$$s^2=\sum [D_o \exp (- \Delta E/R \{I/Ti- 1/T_o\}) - D_i]^2 \text{----------5.19}$$

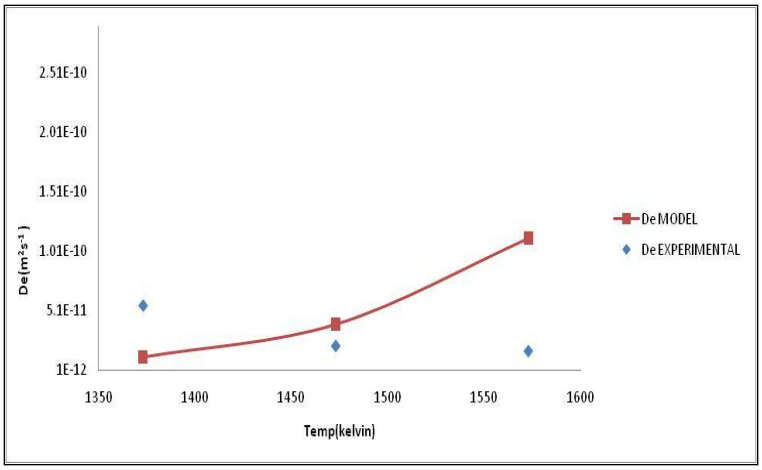

Figure 5.12 Variation of effective diffusion rate constant with temperature on addition of coke (+50µm-100µm) to chromite (+100µm-150µm)

The fit yield:
ΔE=200,000 J/mol
T_o=1373 ºK
D_o=1.25E-11 $m.s^{-1}$
s^2=1.11846E-20

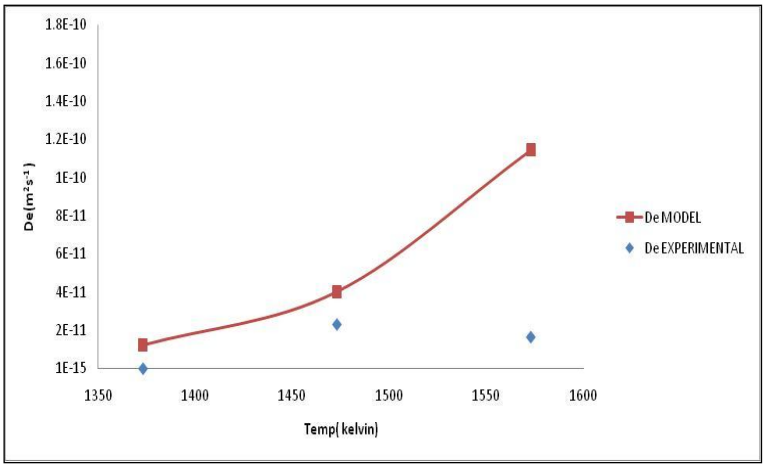

Figure 5.13 Variation of effective diffusion rate constant with temperature on addition of coke (+100µm-150µm) to chromite (+100µm-150µm)

The fit yields:
ΔE=200,100 J/mol
T_o=1373 ºK
D_o=1.23E-11 ms^{-1}
s^2= 1.0522E-20

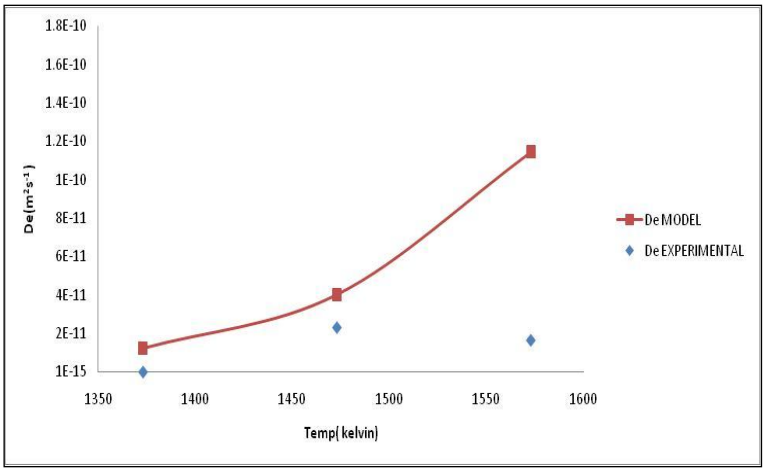

Figure 5.14 Variation of effective diffusion rate constant with temperature on addition of coke (+150µm-200µm) to chromite (+100µm-150µm)

The fit yields:

ΔE= 200,200 J/mol

T_o=1373 ºK

D_o= 1.21E-11 m s^{-1}

s^2= 1.00643E-20

5.6(a) Determinatio of τ and σ^2 at 1100 ºC for charcoal

The generated data in appendix C is fitted into equation 5.10 using sum of least squares as follows through equation [5.17]

$$s^2 = \Sigma \text{ (error)}^2_i = \Sigma [\ a_1\, \tau \mathcal{G}_f(X_i) + a_2\, \mathcal{P}_f(X_i) - t_i\ ]^2$$

Where

$a_1 = \tau$

and $a_2 = \tau\, \sigma^2$

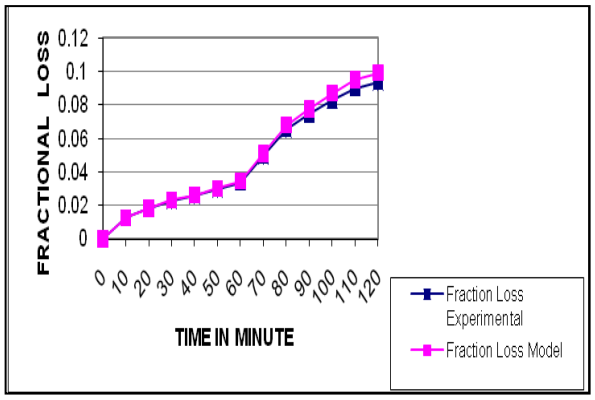

Figure 5.15 Comparison of experimental and model fractional loss vs time on addition of charcoal (+50µm-100µm) to chromite (+100µm-150µm) at 1100 ºC

The fit yields

τ=3500

σ^2=0.6571

s^2=837.8305

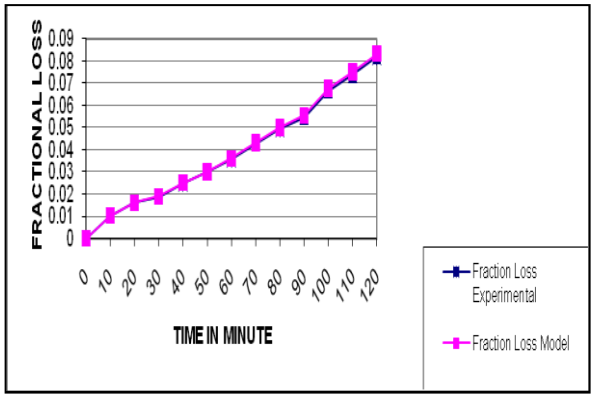

Figure 5.16 Comparison of experimental and model fractional loss vs time on addition of charcoal (+100µm-150µm) to chromite (+100µm-150µm) at 1100 ºC

The fit yields

τ=4400

σ^2=0.22727

s^2=288.3909

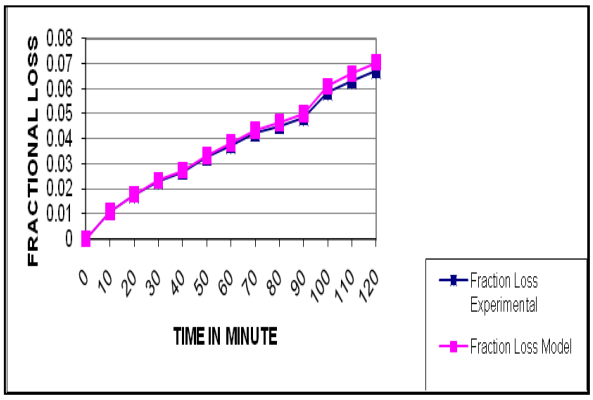

Figure 5.17 Comparison of experimental and model fractional loss vs time on addition of charcoal (+150µm-200µm) to chromite (+100µm-150µm) at 1100 ºC

The fit yields

τ=4900

σ^2=0.69387

s^2=342.284

5.6(b) Determination of τ and σ^2 at 1200 ºC for charcoal

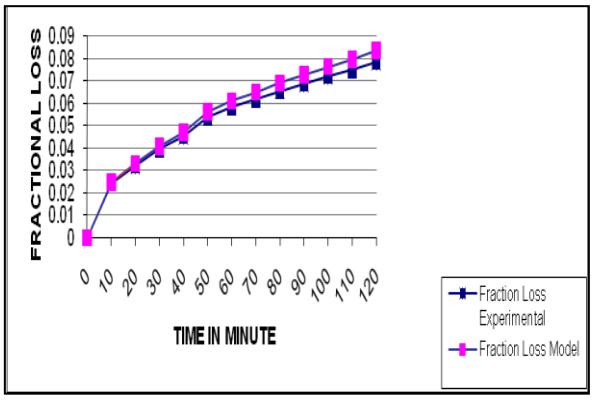

Figure 5.18 Comparison of experimental and model fractional loss vs time on addition of charcoal (+50µm-100µm) to chromite (+100µm-150µm) at 1200 ºC

The fit yields

τ=3500

σ^2=0.85714

s^2=2505.196

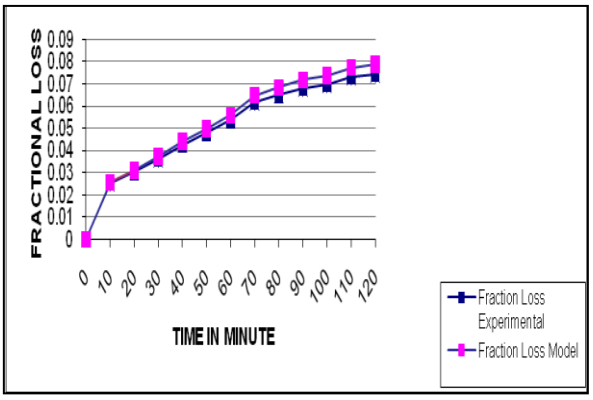

Figure 5.19 Comparison of experimental and model fractional loss vs time on addition of charcoal (+100µm-150µm) to chromite (+100µm-150µm) at 1200 ºC

The fit yields

τ=3600

σ^2 =0.83333

s^2=2269.463

5.6(c).Determination of τ and σ^2 at 1300 ºC for charcoal

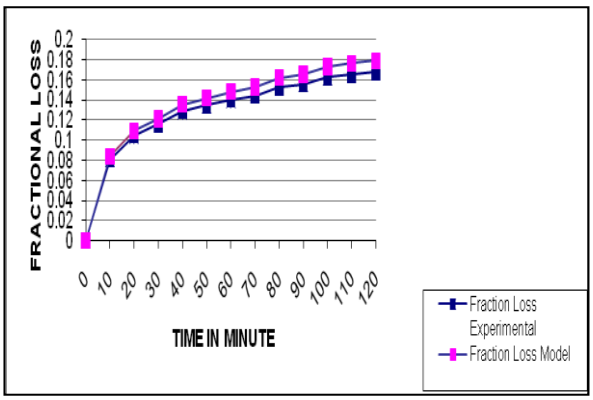

Figure 5.20 Comparison of experimental and model fractional loss vs time on addition of charcoal (+50µm-100µm) to chromite (+100µm-150µm) at 1300 ºC

The fit yields

τ=1400.

σ^2=0.428571

s^2=5832.39798

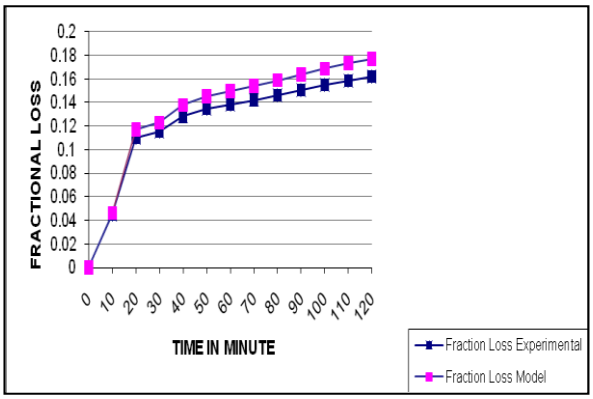

Figure 5.21 Comparison of experimental and model fractional loss vs time on addition of charcoal (+100µm-150µm) to chromite (+100µm-150µm) at 1300 ºC

The fit yields

τ=1400

σ^2=0.6071428

s^2=5785.495

5.6(d) Determination of ΔE (for chemical reaction) and ΔE (for diffusion) for charcoal
From equations 5.15 and 5.16 the values of the chemical rate constants K (s^{-1})
and the effective diffusion coefficient De (m^2s^{-1}) are obtained at different temperatures as follows:

Table 5.4 Diffusion rate and chemical rate for chromite (+100-150) and charcoal (+50-100)

TEMP ^oC	*τ(min)*	*τ* (sec)	σ^2	K(s^{-1})	D_e (m^2s^{-1})
1100 ^oC	3500	210000	0.6571428	2.38095E-06	1.50966E-11
1200 ^oC	3500	210000	0.85714	2.38095E-06	1.1574E-11
1300 ^oC	1400	84000	0.428571	5.952E-06	5.7 7E-

Using the sum of least squares as follows:

$$s^2=\sum (K_o\exp [- \Delta E/R \{I/Ti- 1/T_o\}]-K_i)^2 \text{----------5.18}$$

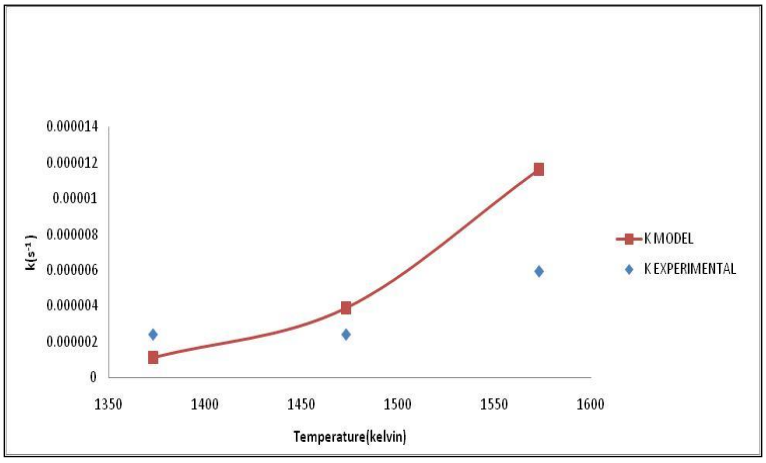

Figure 5.22 Variation of chemical rate constant with temperature on addition of charcoal (+50μm-100μm) to chromite (+100μm-150μm)

The fit yields:

ΔE=212,000 J/mol
T_o=1373º K
K_o=1.25E-06 s^{-1}
s^2=3.62954E-11

Table 5.5 Diffusion rate and chemical rate for chromite (+100-150) and charcoal (+100-150)

Temp.^{o}C	τ(min)	τ (sec)	σ^2	K(s^{-1})	D_e (m^2s^{-1})
1100 ^{o}C	4400	264000	0.22727	1.89393E-06	3.47227E-11
1200 ^{o}C	3600	216000	0.833333	2.3148E-06	1.12526E-11
1300 ^{o}C	1400	84000	0.6071428	5.9152E-06	4.08498E-11

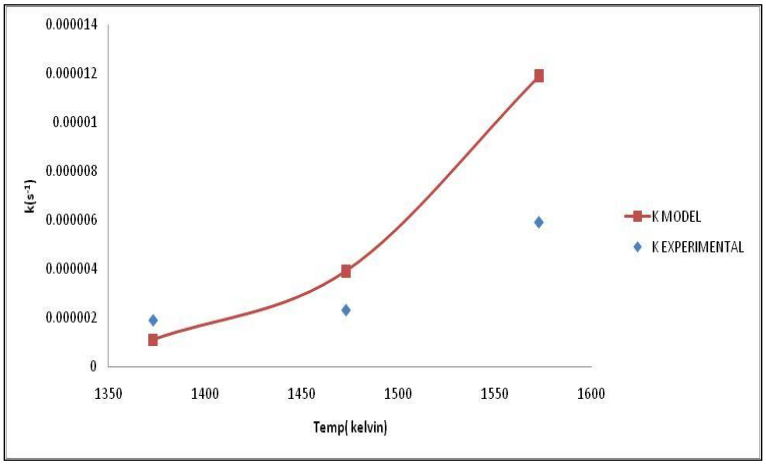

Figure 5.23 Variation of chemical rate constant with temperature on addition of charcoal (+100µm-150µm) to chromite (+100µm-150µm)

The fit yields:

ΔE=214,000 J/mol
T_o=1373^{o}K
K_o=1.2E-06 s^{-1}
s^2=3.9125E-11

Table 5.6 Diffusion rate and chemical rate for chromite (+100-150) and charcoal (+150-200)

Temp ^{o}C	τ(min)	τ (sec)	σ^2	K(s^{-1})	D_e (m^2s^{-1})
1100 ^{o}C	4900	294000	0.6938775	1.70068E-06	1.02124E-14
1200 ^{o}C	5500	330000	0.6545	1.515E-06	0.96457E-11
1300 ^{o}C	3200	192000	6.875	2.6041E-06	1.57828E-12

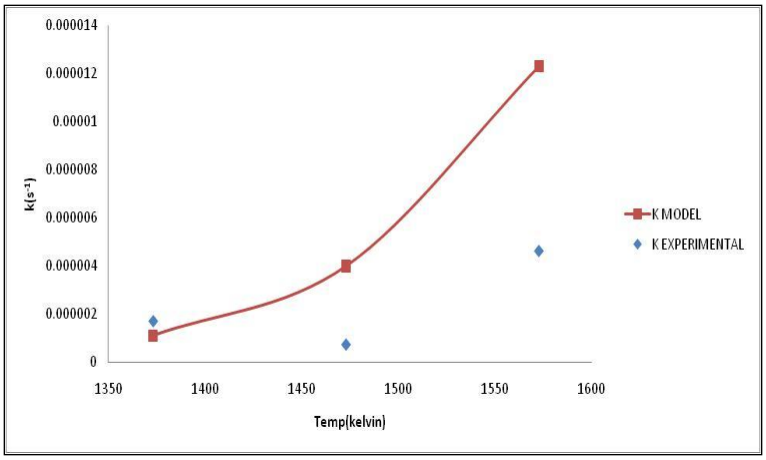

Figure 5.24 Variation of chemical rate constant with temperature on addition of charcoal (+150µm-200µm) to chromite (+100µm-150µm)

The fit yield:

ΔE=217,000 J/mol
T_o=1373 ºK
K_o=1.1E-06 s^{-1}
s^2 =7.00665E-11

5.6.1(d)Determination of ΔE (for diffusion) for charcoal

The values of D_e at different temperatures were also fitted into equation [5.19] (as shown in figure 5.25) using the sum of least squares as follows:

$$s^2=\sum [D_o \exp(\Delta E/R\{ I/Ti- 1/T_o\})- D_i]^2 \text{----------5.19}$$

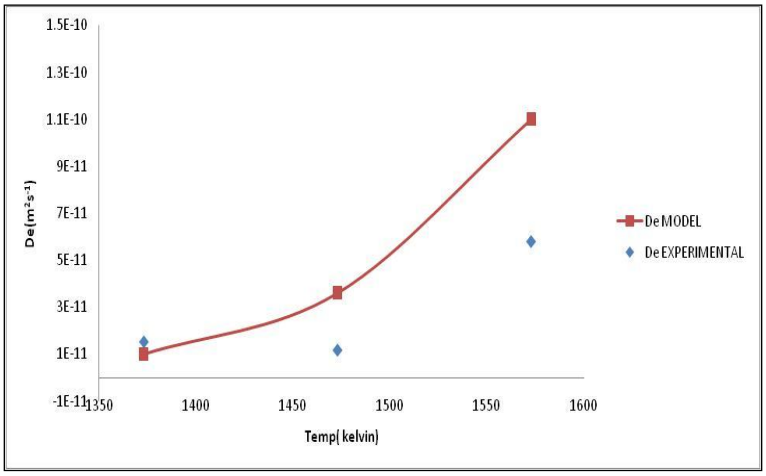

Figure 5.25 Variation of effective diffusion rate constant with temperature on addition of charcoal (+50µm-100µm) to chromite (+100µm-150µm)

The fit yields:

ΔE=215,000.J/mol

T_o=1373 ºK

D_o=1.01E-11.m s^{-1}

s^2=3.35924E-21

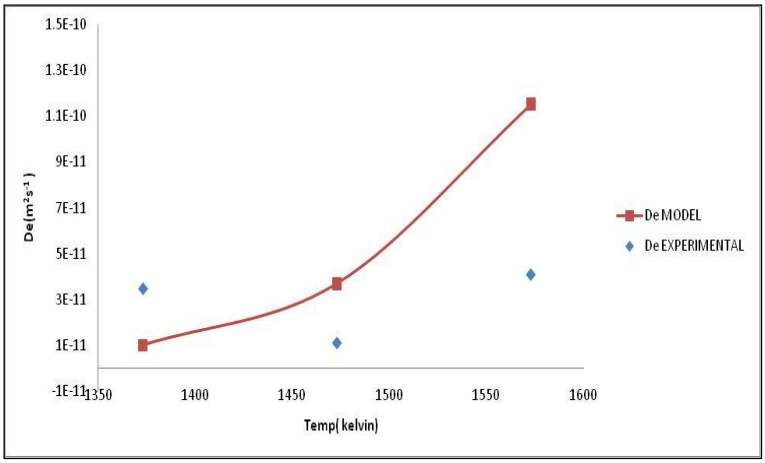

Figure 5.26 Variation of effective diffusion rate constant with temperature on addition of charcoal (+100µm-150µm) to chromite (+100µm-150µm)

The fit yields:

ΔE=219,000.J/mol

T_o=1373.ºK

D_o=1.005E-11.ms^{-1}

s^2=6.7918E-21.

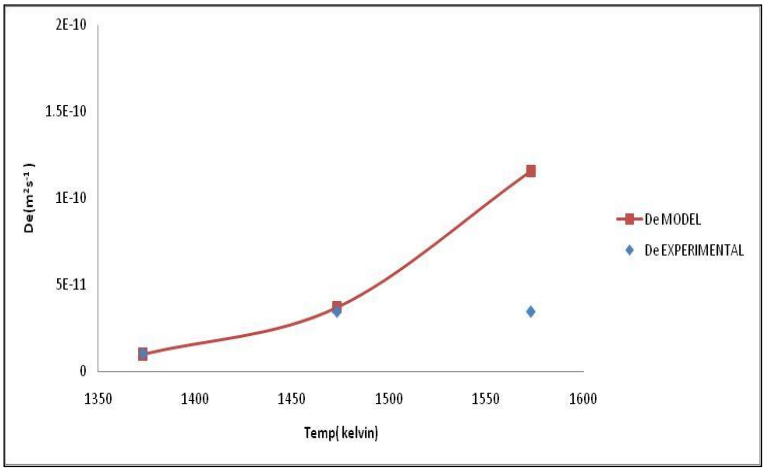

Figure 5.27 Variation of effective diffusion rate constant with temperature on addition of charcoal (+150µm-200µm) to chromite (+100µm-150µm)

The fit yields:

ΔE=219,500.J/mol

T_o=1373.ºK

D_o=1.006E-11.ms^{-1}

s^2=5.25083E-21.

5.7(a) Determination of τ and σ^2 at 1100 ºC for coal

The generated data in appendix C is fitted into equation 5.10 using sum of least squares as follows through equation [5.17]

$$s^2 = \Sigma \text{ (error)}^2_i = \Sigma \left[a_1 \tau \mathcal{G}_f (X_i) + a_2 \mathcal{P}_f (X_i) - t_i \right]^2$$

Where

$a_1 = \tau$

and $a_2 = \tau \sigma^2$

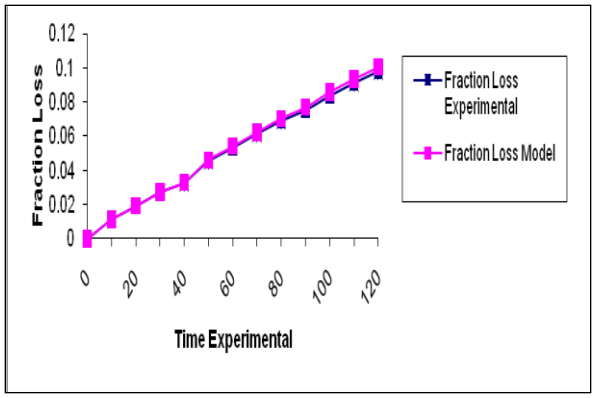

Figure 5.28 Comparison of experimental and model fractional loss vs time on addition of coal (+50µm-100µm) to chromite (+100µm-150µm) at 1100 ºC

The fit yields

τ=3400

σ^2=0.2647058

s^2=45.3565

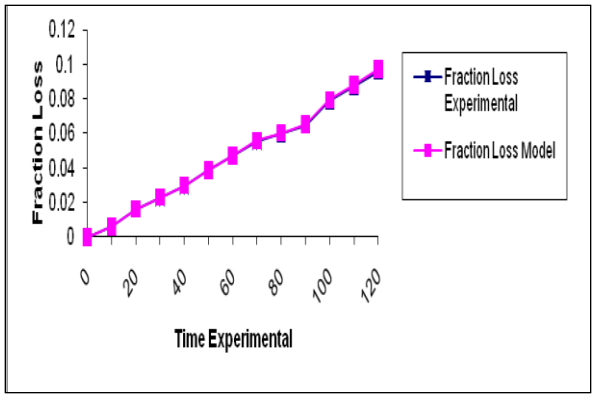

Figure 5.29 Comparison of experimental and model fractional loss vs time on addition of coal (+100µm-150µm) to chromite (+100µm-150µm) at 1100 ºC
The fit yields
τ=3700.
σ^2=0.1351351
s^2=113.4391

5.7(b) Determination of τ and σ^2 at 1200 ºC for coal

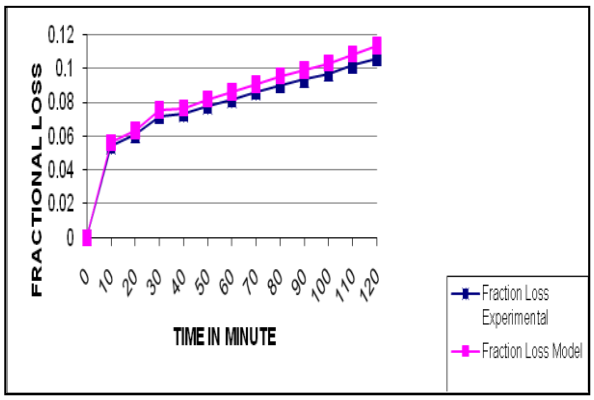

Figure 5.30 Comparison of experimental and model fractional loss vs time on addition of coal (+50µm-100µm) to chromite (+100µm-150µm) at 1200 ºC

The fit yields
τ=2400.
σ^2 =0.6666.
s^2=5588.420912**.**

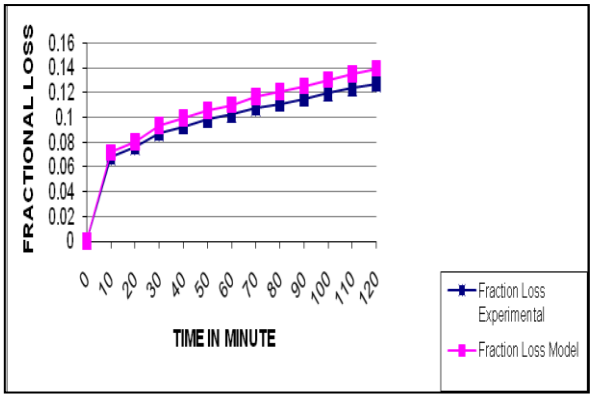

Figure 5.31 Comparison of experimental and model fractional loss vs time on addition of coal (+150µm-200µm) to chromite (+100µm-150µm) at 1200 ºC

The fit yields

τ=1900.

σ^2 =0.789473.

s^2=5944.551632.

5.7(c) Determination of τ and σ^2 at 1300 ºC for coal

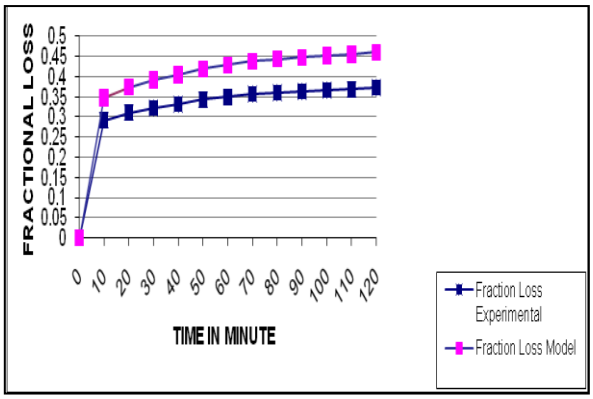

Figure 5.32 Comparison of experimental and model fractional loss vs time on addition of coal (+50µm-100µm) to chromite (+100µm-150µm) at 1300 ºC

The fit yields

τ=400.

σ^2 =0.75.

s^2=9956.014.

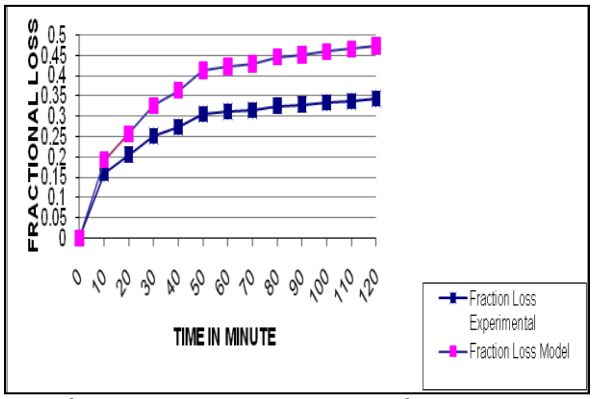

Figure 5.33 Comparison of experimental and model fractional loss vs time on addition of coal (+100µm-150µm) to chromite (+100µm-150µm) at 1300 ºC

The fit yields

τ=450.

$\sigma^{2=}$1.333.

s^2 =5017.32

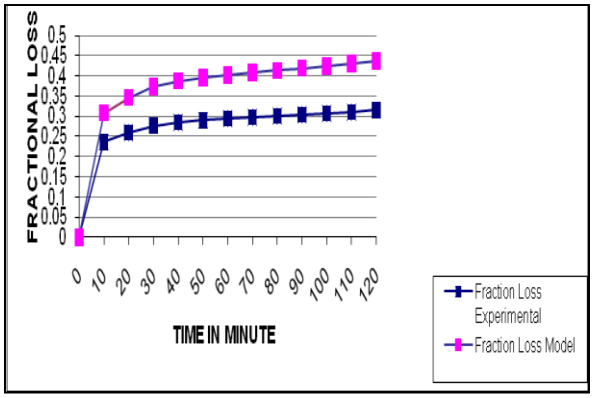

Figure 5.34 Comparison of experimental and model fractional loss vs time on addition of coal (+150µm-200µm) to chromite (+100µm-150µm) at 1300 ºC

The fit yields

τ=450.

σ^2=1.44444.

s^2=9508.32038.

5.7(d) Determination of ΔE (for chemical reaction) and ΔE (for diffusion) for coal

From equations 5.15 and 5.16 the values of the chemical rate constants K (s^{-1}) and the effective diffusion coefficient De (m^2s^{-1}) are obtained at different temperatures and are as follows

Table 5.7 Diffusion rate and chemical rate for chromite (+100-150) and coal (+50-100)

Temp ^oC	$\tau(min)$	τ (sec)	σ^2	K(s^{-1})	D_e (m^2s^{-1})
1100 ^oC	700	42000	31.428	1.10047E-05	1.578E-12
1200 ^oC	300	18000	2.0	2.777E-05	5.787E-11
1300 ^oC	400	24000	0.25	2.0833E-05	3.4723E-10

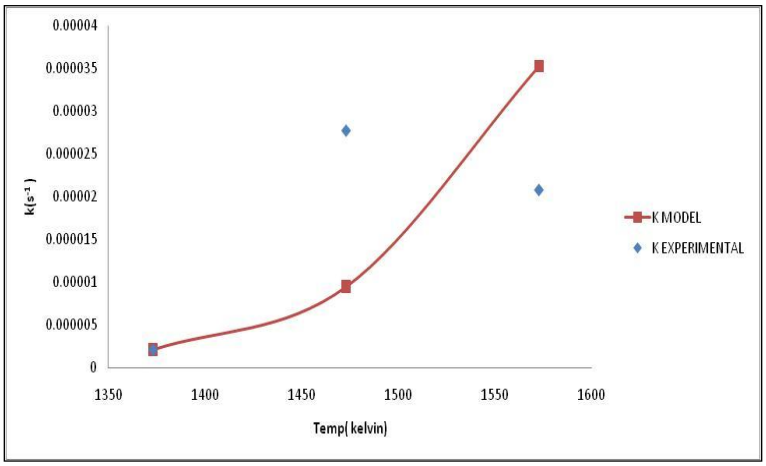

Figure 5.35 Variation of chemical rate constant with temperature on addition of coal (+50µm-100µm) to chromite (+100µm-150µm)

The fit yield:

ΔE=253,540 J/mol
T_o=1373.^oK
K_o=2.3E-06.ms^{-1}
s^2=5.4431E-10

Table 5.8 Diffusion rate and chemical rate for chromite (+100-150) and coal (+100-150)

Temp.^oC	$\tau(min$	τ (sec)	σ^2	K(s^{-1})	D_e (m^2s^{-1})
1100 ^oC	3700	222000	0.135135	2.25225E-06	6.9446E-11
1200 ^oC	800	48000	0.01250	1.04166E-06	4.1667E-11
1300 ^oC	450	27000	1.33340	1.8518E-05	5.787E-11

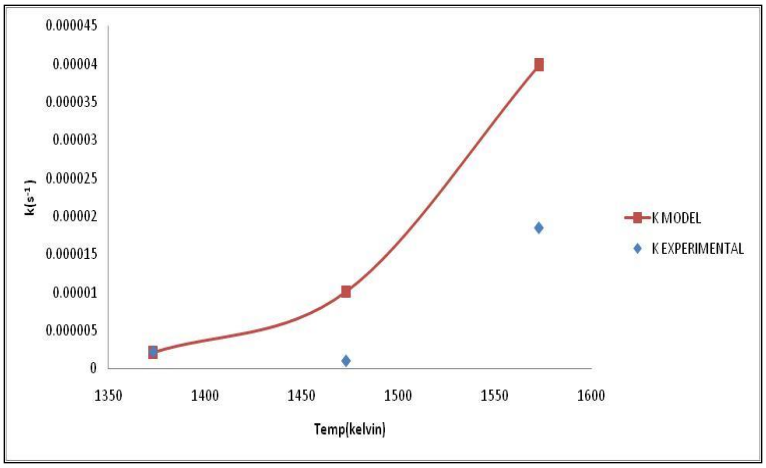

Figure 5.36 Variation of chemical rate constant with temperature on addition of coal (+100µm-150µm) to chromite (+100µm-150µm)

The fit yields:

ΔE=264,500 J/mol

T_o=1373ºK

K_o=2.2E-06 s^{-1}

s^2=5.3876E-10

Table 5.9 Diffusion rate and chemical rate for chromite (+100-150) and coal (+150-200)

TEMP ºC	*τ(min)*	τ (sec)	σ^2	K(s^{-1})	D_e (m^2s^{-1})
1100 ºC	4400	264000	0.6545	1.89389E-06	1.73262E-11
1200 ºC	600	36000	36.666	1.3889E-05	1.57831E-12
1300 ºC	450	27000	1.44444	1.8518E-05	7.265E-11

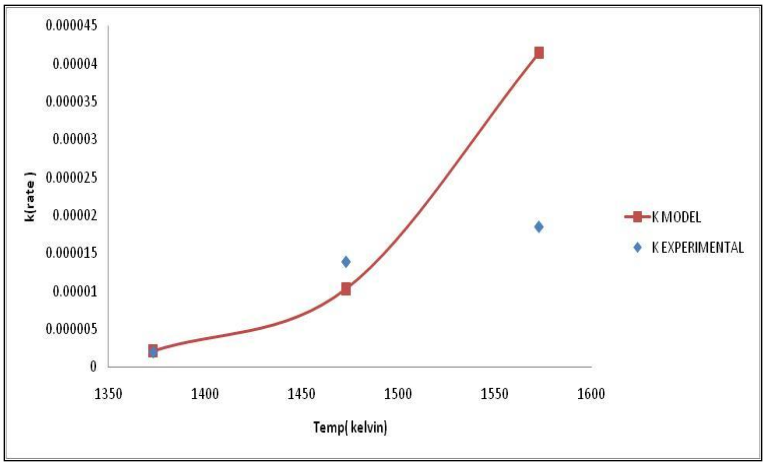

Figure 5.37 Variation of chemical rate constant with temperature on addition of coal (+150µm-200µm) to chromite (+100µm-150µm)

The fit yields:

ΔE=268,000 J/mol

T_o=1373.^oK

K_o=2.1E-06.s^{-1}

s^2=5.39227E-10

5.7.1(d)Determination of ΔE(for diffusion)for coal

The values of D_e at different temperatures were also fitted into equation [5.19] (as shown in figure 5.38) using the sum of least squares as follows:

$$s^2=\sum (D_o exp[- \Delta E/R\{ I/Ti- 1/T_o\}]- D_i)^2 \text{----------5.19}$$

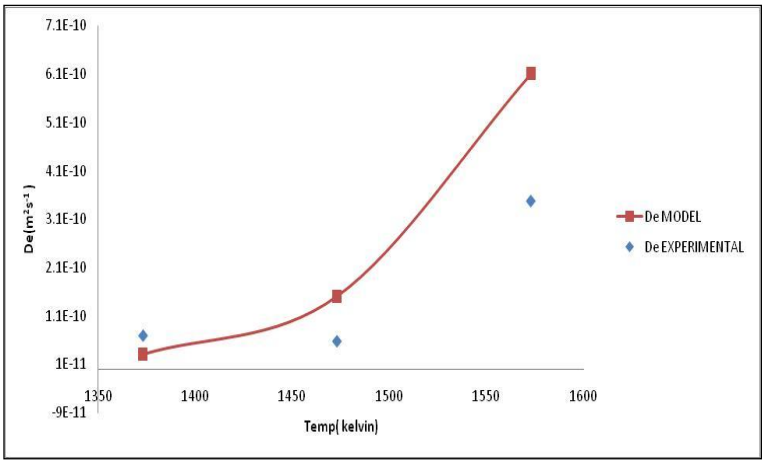

Figure 5.38 Variation of effective diffusion rate constant with temperature on addition of coal (+50µm-100µm) to chromite (+100µm-150µm)

The fit yields:

ΔE=270,000 J/mol

T_o=1373.^oK

D_o=3.03E-11.ms^{-1}

s^2=8.01494E-20

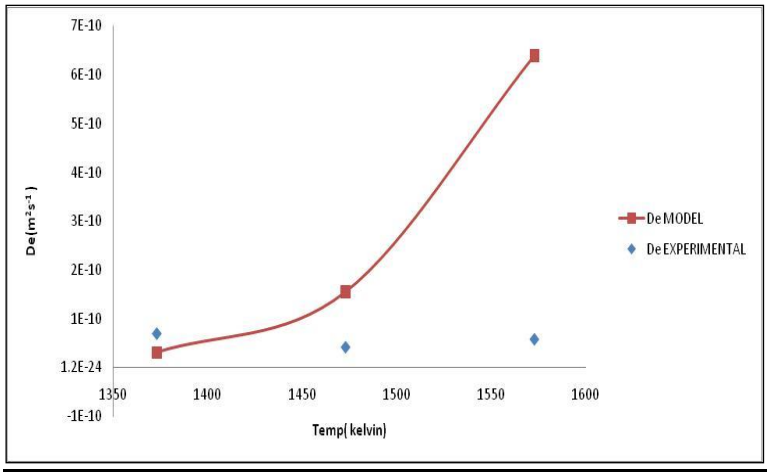

Figure 5.39 Variation of effective diffusion rate constant with temperature on addition of coal (+100µm-150µm) to chromite (+100µm-150µm)

The fit yields:

ΔE=274,000.J/mol

T_o=1373.^oK

D_o=3.025E-11.ms^{-1}

s^2=3.52707E-20.

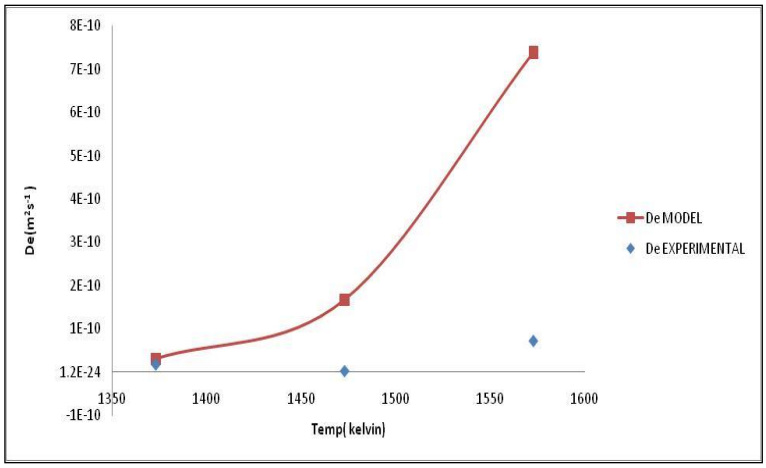

Figure 5.40 Variation of effective diffusion rate constant with temperature on addition of coal (+150µm-200µm) to chromite (+100µm-150µm).

The fit yields:

ΔE=287,000.J/mol

T_o=1373. ^oK

D_o=3.023E-11.ms^{-1}

s^2=4.71777E-20.

CHAPTER 6

SUMMARY AND CONCLUSIONS

Experiments were carried out at stiochiometric amount of various reductants namely coke, coal, charcoal and graphite. The xstrata chromite with size fraction as received, +50 µm -100 µm, +100 µm -150 µm, +150 µm -200 µm was reduced at temperatures 1000 ºC, 1100 ºC, 1200 ºC and 1300 ºC. It was observed that reduction rate of this chromite increased with temperature and samples having finer particle size fraction showed higher reduction rate at all temperature. The effect of reducing agent namely coal, coke, charcoal and graphite is quite apparent from the behaviour shown at lower temperatures 1000 ºC and 1100 ºC where coke, coal,charcoal and graphite was order of reduction whereas at higher temperatures 1200 ºC and 1300ºC order was coal, coke, charcoal and graphite.

The value of the activation energies obtained from fitting the data into the Arrhenius equation was used to determine the relative reactivity of the reductants. The values of the chemical reaction rate constants and effective diffusion constants were used to determine the relative speed at which the reductants can reduce the chromite ore. The summary of results of the TGA tests is as follows:

TABLE 6.1 Summary of the TGA tests results for chromite (+100µm-150µm) and reductant (+50µm-100µm)

Reductants	Chemical Reaction		Diffusion Reaction	
	ΔE(J/mol)	k(s^{-1})	ΔE(J/mol)	D_e(m^2s^{-1})
coke	196,000	1.05E-06	200,000	1.25E-11,
charcoal	212,000	1.25E-06	215,000	1.01E-11,
coal	253,540	2.3E-06	*270,000*	3.03E-11

TABLE 6.2.Summary of the TGA tests results for chromite (+100µm-150µm) and reductant (+100µm-150µm)

Reductants	Chemical Reaction		Diffusion Reaction	
	ΔE(J/mol)	k(s^{-1})	ΔE(J/mol)	D_e(m^2s^{-1})
coke	196,500	1.006E-06	200,100	1.23E-11
charcoal	214,000	1.2E-06	219,000	1.005E-11
coal	264,500	2.2E-06	274,000	3.025E-11

TABLE 6.3 Summary of the TGA tests results for chromite (+100µm-150µm) and reductant (+150µm-200µm)

Reductants	Chemical Reaction		Diffusion Reaction	
	ΔE(J/mol)	k(s^{-1})	ΔE(J/mol)	D_e(m^2s^{-1})
coke	198,000	1.0009E-06	202000	1.21E-11
charcoal	217,000	1.1E-06	219,500	1.006E-11
coal	*268,000*	2.1E-06	287,000	3.023E-11

The TGA tests suggest that coke has the highest reactivity since its activation energies are lowest and require less energy to induce the reduction reaction. The tests also suggest that the rate controlling mechanism is diffusion of species to the reaction site since the effective diffusions of the order 10^{-11}(m^2s^{-1}) are far less then the chemical rate constant of the order $10^{-}6$ to 10^{-5} (s^{-1}). The tests also suggest that coal is fastest to react since its D_e value is higher.

Further work can be done to to compare size-wise values of chemical rate constants and effective diffusion constants for each reductant in detail to understand variation according to sizes of reductants and chromite. That study will also give details of activation energy values for each size fraction of reductants and chromite thus showing the variation of reactivities according to size.

REFERNCES

[1].Ataei, A'etal' (2008) Solid state reduction of chromite in high carbon ferrochromium-chromite composite pellets, IJOMSE, vol 5, pp.22-28.

[2].Atasoy, A and Sale, F.R (2009) An investigation on the solid state reduction of chromite concentrate, solid state phenomena, vols.147-149, pp.752-757.

[3].Bamford, C.H and Tipper, C.F.H. (1980) Chemical kinetics, reactions in solid State, vol.22, Elseveir, N.Y.

[4].Barcza, N.A. 'etal'. (1971) The mechanism and kinetics of reduction of Transvaal chromite ores, *Electric Furnace Proceedings*, vol.29, pp.88-93.

[5].Barcza, N.A. (1972) Incipient fusion studies in the system chromites –CaO-MgO-Al_2O_3-SiO_2-C, M.Sc Thesis, *University of the Witwatersrand*, Johannesburg.

[6].Barnes, A.R. and Finn, C.W.P. (1980) The pre-reduction of chromites from the UG-2 reef, Johannesburg, *National Institute for Metallurgy*, Report no 207.

[7].Barnes, A.R. (1981) The prereduction and smelting of UG-2 chromite concentrates, M.Sc thesis, *University of the Witwatersrand*, Johannesburg.

[8].Barnes, A. R. and Eric R. H. (1995) The relative reducibilities of chromite ores and relative reactivity of carbonaceous reductants Proceedings of Seventh International Ferroalloy Congress, *INFACON*, pp 231-238.

[9].Biswas, A.K. (1981) Principle of blast furnace iron making, theory and practice, *Lootha Publishing House*, Brisbane, Australia.

[10].Born,O.S.and Muan,A.(1965) Phase equilibria among oxides in steel making, *Addison Wesley Publishing Co*, Reading, Massc, USA.

[11].Byun, K.Y.'etal'.(2000) Reduction rate of chromium oxide in stainless steel EAF slags by carbonaceous reductants, *Journal of the Korean Institute of Metal and Materials South Korea*, vol.38, No.4, pp.591-598.

[12].Carter R.E, "Mechanism of solid –state reaction between magnesium oxide and aluminium oxide and ferric oxide" J.Am.Ceram.soc, 44[3]116-20(1961).

[13].Chakraborty, D.'etal'.(2005) Investigation on the carbothermic reduction of chromite ores, *Metallurgical and Material Transaction B*, vol. 36, no.4, pp. 437 - 444.

[14].Chakraborty, D.'etal'.(2010) Carbothermic reduction of chromite ore under different flow rates of inert gasses, *Metallurgical and Materials Transactions B,* vol. 41B, pp 10 -18.

[15].Cousins, C.A. and Feringa, G.(1964) The chromite deposits of the Western belt of the BC, The geology of some ore deposits in southern africa, Johannesburg, *Geol.Soc.of SA*, Vol.2, pp.131-168.

[16].Darken, L.S.and Gurry, R.W. (1945) The system Fe-O the wustite field and related equlibria, *J.Am.Chem.Soc 67, 8,* pp. 1398 -1412.

[17].Darken, L.S. and Gurry, R.W. (1946) The system Fe-O, equilibrium and thermodynamics of liquid oxide and other phases, Am *chem..Soc 68, 5,* pp. 798 - 816.

[18].Dawson, N.F. (1989) Factors affecting the reduction rate of chromite, Ph.D Thesis, University *of Natal*, Durban, South Africa.

[19].Demir, O. (1992) Reduction of chromite in liquid Fe-Cr-C-Si alloys, Johannesburg, *University of the Witwatersrand*, M.Sc Thesis.

[20].De wall,S.A.and Hiemstra,S.A.(1971)The chromite of the Bushveld Ingeous complex,an assestment of published Information,Johannesburg, *National Institute of Metallurgy*, Report no 1203.

[21].Dewaal, S.A.and Hiemstra, S.A.(1972)The Interrelation of the chemical physical and other metallurgical properties of chrome spinel from the Bushveld Ingeous complex, Johannesburg, *National Institute for Metallurgy*, Report no 1415.

[22].Dewaal,S.A. and Hiemstra,S.A.(1975)The mineralogy, chemistry and certain aspects of reactivity of chromite from the Bushveld Ingeous complex,Johannesburg, *National Institute for Metallurgy*, Report no 1709.

[23].Dunwald.H and Wagner C, "Measurement of diffusion rate in the process of dissolving gases in solid phases" Z.Physik.Chem (Leipzig), B24 [1]53-58(1934).

[24].Dijs, H.M.and Smith, D.J. (2004) The characterization of carbon reductants in metallurgical industry, *Infacon X*, Capetown, SAIMM, pp.363-380.

[25].Ding,Y.L. and Merchant,A.J.(1999) Kinetics and mechanism of smelting reduction of fluxed chromite part 2 chromite –flux pellets in Fe-Si melts, *Iron and Steelmaking*,vol.26, no. 4, pp. 254 -261.

[26].Dyason, G.A. (1974) Direct stainless steel production, M.Sc Thesis, *University of the Witwatersrand*, Johannesburg.

[27].Edstrom, J.O. (1953) The mechanism of reduction of iron oxides, *J.Iron steel Inst, vol.175, pp.289*-304.

[28].Edstrom, J.O.and Bitsianes, G. (1955) Transactions Aime, *J.of Metals*, no.6, pp.760-764.

[29].Eric, R.H. 'etal'.(1989) The reduction of chromite spinels by solid carbon and carbon dissolved in liquid alloys,*Infacon,Proceedings of the 5th Inernational Ferro Alloys Congress*, New Orleans, vol.1,pp.77-87.

[30].Eric,R.H. 'etal'(1991)The reduction Mechanism of a natural chromite at 1416 ºC, *Metall TransB*, vol. 22 B, pp. 53 -63.

[31].Eric,R.H.'etal'.(1991)Kinetics of the reduction of Bushveld complex chromite ore at 1416 ºC, *Metall TansB*, vol. 22.B, pp.801 –810.

[32].Eric,R.H and Demir,O.(1992)Reduction of chromite in Fe-Cr-C-Si alloys, *Infacon6,Proceedings of the 6th International Ferroalloys Congress*,Capetown, South African Institute of Mining and Metallurgy,vol.1,pp.99-105.

[33].Eric, R.H.and Weber,P.(1992)Solid state fuxed reduction of LG-6 chromite from the Bushveld complex,*Infacon 6,Proceedings of the 6th International Ferroalloys Congress*, Capetown,South African Institute of Mining and Metallurgy,vol.1,pp.71-77.

[34].Eric, R.H. (1994) Reduction behavior of chromite at high temperature, XVth CMMI *Congress*, Johannesburg, SAIMM, vol.2, pp.221-230.

[35].Eric, R.H. and Jesl. (2002), High temperature carbothermic reduction of Fe_2O_3 – TiO_2 –M_xO_Y oxide Mixtures, *Pyromet '02,* Capetown, South Africa, pp. 971 -984.

[36].Eric, R.H. and Weber, P. (2006) The reduction of chromite in the silica flux, *Mineral. Engineering*, vol.19, no.3, pp. 318 -324.

[37].Eric, R.H. and Kucukkaragoz, C.S. "Prereduction of Chromite agglomerates", *TMS The Mineral, Metals and Material society*, pp. 623-630.

[38].Falcon,R. 'etal'.(2004)The characterization of carbon reductants in metallurgical Industry –A case study,*Infacon 2004 Proc.Tenth International Ferro Alloy Congress*, Capetown, South Africa, pp. 363 -380.

[39].Fernandes, T.R.C.'etal'. (1994)Microstructrural aspects of reduction of Zimbabe chromite to high–carbon ferro chromium, *Trans.Instn. MinMetall*, 103 September – December 1994, Institute of Mining and Metallurgy, pp. 177-187.

[40].Feng,B. 'etal'(2004)The behavior of coke in submerged arc furnace smelting of ferrochrome,*Infacon X*,CapeTown,SAIMM,pp.381-391.

[41].Finn, C.W.P. and Kucukkaragoz, C.S. (1980) Reaction mechanisms for the prereduction of winterveld chrome spinel, *Proceeding of 2 nd Int.Ferro-Alloys Congress, Lausanne, pp.149* -230.

[42].Finn, C.W.P and Kucukaragoz, C.S. (1981) Infacon 80, Proc. Of the 2nd Int.FerroAlloy Cong., Lausanne, Oct.1980, *Lousanne Inst.Des producers de Ferro-aliges d'Europe Occidental*, pp.130-149.

[43].Franke, H. and Duderstadt, G.(1974)Production of medium- carbon ferro-chromium in a bottom blowing convertor and its application to stainless- steel production, *Infacon* 7, Johannesburg.

[44].Freuhan, R.J. (1977) The rate of reduction of iron oxides by carbon, *Metall. Trans*, vol.8B, pp.279-286.

[45].Freuhan, R.J. (1977) Rate of reduction of Cr_2O_3 by carbon dissolved in liquid Iron alloys, *Metallurgical Transactions 8B*, pp. 429 –433.

[46]Fukagawa S. and Shimoda T (1987), "Smelting reduction mechanism of chromite ore sinter by solid carbon",Trans ISIJ, vol.27, pp.609-617.

[47] Ginstling, A. M.; Brounshtein, B. I. (1950) "Concerning the diffusion kinetics of reactions in spherical particles" J. Appl. Chem. USSR, 23, 1327-38.

[48].Godfrey, M (2007) Reduction characterisation and selection in ferrochromium production, Johannesburg, *University of the Witwatersrand*, M.Sc Thesis

[49].Gaskell, D.R. (1973) Introduction to metallurgical thermodynamics, *Mc-graw Hill Book Co*,Johannesburg,South Africa.

[50].Hiroshi, G. (1977) Reduction of chromite with carbon, chemical abstract, vol.86, pp158815 C.

[51].Hitunen, R. and Harliki, J. (2004) Reduction behaviour of the akanvaara chromite of northern finland, *Infacon 2004 Proc. Tenth International Ferro Alloy Congress*, Capetown, South Africa,pp. 36 -46.

[52].Hoffman, V.A Investigations Of equilibria in the system iron –oxide-chromium – oxide, *Arch –Esenhuttenwes 36,* pp. 155 -162.

[53].Honkaniem,M.'etal'.(1992)The importance of chromite pre treatment in the production of ferrochromium,*Infacon 6,*Capetown,SAIMM.

[54] Jander, W. Z. Anorg. Allg. Chem. 1927, 163, 1.

[55].Jochens,P.R. 'etal'(1971)The pyrometallurgical research Groups's Current research programme on ferro-alloys,Johannesburg,*National Institute of Metallurgy*,Report no1343,23rd Aug.

[56].Kamal, P. and Rankin,W.J (2004) The behaviour of coke in submerged arc furnace smelting of ferromanganese, *Infacon 2004 Proc.Tenth International Ferro Alloy Congress 1-4 Feburary 2004*,Capetown, South Africa, pp. 381-391.

[57].Katayama, H.G and Tanaka, A. (1974) The reduction process and reducibility of chromite with carbon, *Tetsu –To Hagane*, vol.60, no.9, pp.1289.(Tr.).

[58].Katayama, H. G (1977) Reduction of chromite ($FeCr_2O_4$) with carbon, *Nippon Kinzokugakkaishi*, vol.41, no.3, pp.275-280.

[59].Katayama, H.G. and Tokudu, M.(1979) The reduction behaviour of synthetic chromite by carbon, *Tetsu –To – Hagane*, vol.61,no. 3, pp. 331 - 340 (Tr.).

[60].Katsura, T. and Muan, A. (1964) Experimental study of equilibria in the system Feo –Fe_2O_3 –Cr_2O_3 at 1300 ºC, *Trans. AMIE, 230*,pp.77-84.

[61].Kekkonen, M. 'etal' (1995) Kinetic study on solid state reduction of chromite pellets, Infacon 7, Trondheim, Norway, pp.351-360.

[62].Khallafalla,S. E. and Pahlman, J.E.(1985)Direct method to prepare low carbon ferrochrome, *Physical Chemistry of Extractive Metallurgy*,New York,USA, pp. 433-456

[63].Kolchin, O.P. (1968)The Mechanism of reduction of metals from their oxides by carbon,*Mekhn.Kinet.Vosstanov,Metal.Mater.Simp,* pp. 40 -48.

[64]Kroger.C and Ziegler. G "Reaction rates of glass batch Melting, II".Glastech.Ber, 26[11]] 346-53(1953).

[65].Kroger, F.A. (1974) The chemistry of Imperfect crystals, v.2, Imperfection Chemistry of crystalline solids, *2nd Edn.North-holland/American Elsevier*, pp.251-255.

[66].Kucukkaragoz, C.S. (1983) The mechanism and kinetics of reduction of winterveld chromites fines, Johannesburg, *University of the Witwatersrand*, Ph.d Thesis.

[67].Kucukkaragoz, C.S. 'etal' (1984). *Mintek*, Rep.No.M154.

[68].Kulscar, F. (1959)*J.Am.Cer.Soc*, vol.42, pp.343.

[69].Laidler, K.J (1965) Chemical kinetics, McGraw *Hill Inc*., NY.

[70].Lekatou,A. and Veazarlis,H.G(1993)Pelletising,sintering,prereduction and smelting of greek chromite ores and concentrates,*Iron Making and Steel making*, vol.20, no.1, pp. 42 -53.

[71].Lekatou,A. and.Walker,R.D.(1995)Microstructural changes in chromite concentrate during calcination in air and argon atmospheres, *Iron and Steel Making*, vol.22, no.3, pp. 227 -238.

[72].Lekatou, A. and Walker,R.D.(1995)Solid state reduction of chromite concentrate melting pre- reduced chromite, *Iron and Steel Making*,vol. 22, no.5, pp. 378.

[73].Lekatou, A. and Walker, R.D. (1995) Mechanism of solid state reduction of Chromite concentrate, *Iron and steel Making*, 5, vol. 22, no. 5, pp. 393 –404.

[74].Monsen, B. 'etal'.(2004)Use of charcoal in silico manganese production, *Infacon 2004 Proc.Tenth International Ferro Alloy Congress*, Capetown, South Africa,pp. 392- 404.

[75].Morozov, A.N. 'etal'. (1963)Changes in the composition and structure of chrome ores during heating and reduction, *Steel USSR*, pp.119-122.

[76].Morning, J.L. (1977) Chromium mineral commodity profiles, *U.S.Dept. Of Interior, Bureau of Mines*.

[77].Mitsutaka, H. 'etal'(1998)Thermodynamics estimation on the reduction behaviour of Iron –chromium ore with carbon,*Metallurgical and Materials Transaction B*,vol. 29b, pp. 351 -360.

[78].Muan, A. (1975) Phase relations in chromium oxide containing systems at elevated temperature, *Geo Chimica Et Cosmochimica Acta*, vol. 39, pp.791 –802.

[79].Muan, A and Somiya, S. (1960) Phase relations in the system Iron oxide Cr_2o_3 in air, *J.Am.Cer.Soc*, vol.43, no.4, pp.204 -209.

[80].Nafziger, R.H. 'etal' (1979) Carbothermic reduction of domestic chromites, *Metallurgical and Material Transactions B*, vol.10, no.1, pp.5-14.

[81].Neuschutz,D.(1992)Kinetic aspects of chromite ore reduction with coal at 1200 to 1550 ºC,*Infacon 6*,Johannesburg,South African Institute of Mining and Metallurgy,vol.1,pp.65-70.

[82].Niayesh, M.J. (1990) The solid state reduction of chromite in a vertical shaft, Ph.d thesis, *University of Pretoria*, South Africa.

[83].Niemela, P.'etal'.(2004)Formation characteristics and utilization of Co – gas formed in ferrochromium smelting, *Infacon 2004 proc.Tenth International Ferro Alloy Congress*, Capetown, South Africa, pp. 68 -77.

[84].Oslen,S.E. and Lindstad,T.(1992)Solid state reduction of chromite,*Infacon6*,Capetown,SAIMM,pp.65-77.

[85].Ossin, D.I. 'etal' (1974) The production of medium carbon ferrochromium alloys by solid-state reduction,Johannesburg,*National Institute for Metallurgy*,Report No.1650.

[86].Otam, Y. and Ichikova, K. (1974) Infacon 74, *Proc 1st Inst. Ferro Alloy Congress The South African Institute of Mining and Metallurgy*, Johannesburg, South Africa, pp. 31-37.

[87].Philips, B. and Muan, A. (1960) Stability relations of Iron oxides phase equilibria in the system Fe_3O_4 –Fe_2O_3 at oxygen pressure upto 45 atmospheres, *J.Phy Chem*., vol. 64, pp.1451.

[88].Perry, K.P.D. (1986) Thermodynamical Analysis of the reduction of chromites, Phd thesis, University *of the Witwatersrand*, Johannesburg, South Africa.

[89].Rankin, W.J. (1979) The composition and structure of chromite during reduction with carbon, *Arch. Eisenhuttenwes*, vol. 50, pp. 373 -378.

[90].Rankin, W.J, 'et.al'. (1979)Solid state reduction by graphite and carbon Monooxide of chromite from the bushveld complex, Johannesburg, *National Institute for Metallurgy*, Report no1957.

[91].Rao, Y.K. (1971) The kinetics of reduction of hematite by carbon, *Metall. Trans*, vol.2, pp.1439-1447.

[92].Rao, Y.K. (1979) Mechanism and Instrinsic rates of reduction of metallic oxides, Metal *Trans*, vol. 10 B, pp. 243 -255.

[93].Sahajwalla,V. 'etal'.(2004)Reductant characterization and Selection Implification for Ferro Alloy Processing,*Infacon 2004 Proc.Tenth International Ferro Alloy Congress*, 1-4 Feburary 2004, Capetown, South Africa, pp. 351 -361.

[94].Searle, M.J. and Finn, C.W.P. (1983) The Mathematical Modelling of the reduction Behaviour of chromite from the upper chromite layer of BIC Randburg, *Mintek*, Report No M96.

[95].Serin.B and Ellickson, "Determination of diffusion coefficients,"J.chem.Phy, 9[10]742-7(1941).

[96].Shin, F. And Teruhisa, S.(1987)Smelting reduction mechanism of chromium ore sinter by solid carbon,*Transactions of the Iron and Steel Institute of Japan*, vol. 27, no. 8, pp. 609 -617.

[97].Slatter,D.del.(1980)The composition of zimbababean chromite ores and derivation of chemical and physicochemical ratings for smelting of the ores to high carbon ferrochromium, Salisbury, Zimbabwe,*Institute of Mining Research*, University of Rhodesia.Report no. 173.

[98].Snowdowne, A.C. (1993) Thermodynamic evalutation of the technored process for the production of ferrochromium, Randburg, *Mintek*.

[99].Smith, I.N. *(2004)* Aspects of submerged arc furnace smelting of ferrochrome and reductant selection, *InfaconX, Capetown, SAIMM, pp.1-14.*

[100].Soykan,O.(1988)The solid state reduction characteristics of the Bushveld complex chromites,Phd Thesis,*University of Witwatersrand*,*Johannesburg*,South Africa.

[101].Streicher,P.E.(1979)The marketing of chromite and ferrochromium from a south African point of view, *Inst.Min.and Metallurgy*, London. [102].Szekely, J. and Themelis, N.J. (1971) Rate phenomenon in process metallurgy, *Wiley Interscience*, New York.

[103].Takano, C.'etal' (2009) High carbon ferro chromium by self reducing process: Fundamentals, *Songklanakarin J.Sci.Technol*.vol.31, pp. 433-439.

[104].Tammann, Z (1920).Anorg. Chem.111, 78.

[105].Thiemelis, N.J. and Gauvin, W.H. (1962) Mechanism of reduction of iron oxides, *Trans.AMIE*, vol. 55, pp. 444 -456.

[106].Thiemelis, N.J. and Gaunvin, W.H. (1963) A generalized rate equation for the Reduction of Iron Oxide,*Trans.AMIE*, vol. 227, pp.290 -300.

[107].Tien, R.H. and Turkdogan, E.T. (1977) Mathematical analysis of reactions in metal oxide / carbon mixtures, *Met.Trans volB*, pp. 305 -313.

[108].Ulmer, G.C.(1969)Experimental Investigation of the chromite spinels,*Society for Economical Geology Symposium*, Monograph 4, Standford University, pp.114.

[109].Uslu,E.(1989)Reduction of chromite spinels by carbon dissolved in Fe-Cr alloys,Johannesburg, *University of the Witwatersrand*,M.Sc Thesis.

[110].Valensi, G. (1936) "Kinetics of the oxidation of metallic spherules and powders"*Compt.Rend*, vol.202, no.2, pp.309-12.

[111].Van Deventer, J.S.J (1988) The effect of additives on the reduction of chromite by graphite: An isothermal kinetic study, Thermochimica, vol.127, pp25-35

[112].Verwey, E.J.M. (1935) *Z.krstallog, vol.91, pp.65*-69.

[113].Visser,'etal'.(2004)Reductant characterization and selection*InfaconX*,capetown,SAIMM,pp.351-362.

[114].Vuuren,C.P.J.'etal'(1992)The reduction of synthetic iron chromite in the presence of various metal oxides,*Infacon 6*,capetown,SAIMM,pp.51-55.

[115].Waal, A.D.and Barker, I.J. (1992) Kinetics aspects of chromite ore reduction with coal and coke, *Infacon 6*, Capetown, SAIMM, pp.65-77.

[116].Wagner, J.P. (1971) Contribution to the thermodynamics of interstitial solid Solutions, *Acta Metallurgica*, vol.19, August, pp.843-849.

[117].Weber,P.(1992)Fundamentals of the solid state reduction of chromite in the presence of silica flux,Johannesburg, *University of the Witwatersrand*,Ph.d Thesis.

[118].Welch A.F.E.(1953)Solid state chemistry,Ed.WE Garner,*Butterworths Sci.Publ.*

[119].Wessel F.W. and Rasmussen R.T.C. (1950) Ferrochromium from low grade ores and concentrates, *J.Metals*, pp.984-988.

[120] Xiao, Y. (etal). (2004)Solid state reduction of chromite with Co, *Infacon 2004.Proc.Tenth International Ferro Alloy Congress*, Capetown, South Africa, pp. 26 -35.

[121].Xuemin,Y (1997) Effect of Coal type reduction rate of iron ore pellets containing coal, Journal of Iron and Steel Research, vol 9,pp.1-6

[122].Yang, Y. ‘etal’ (2004) Analysis of transport phenomena in arc furnaces for ferrochrome production, InfaconX, Capetown, SAIMM, pp.15-25.

[123].Zhang, C.Y. and, Xie, Y. (1993) Study on reduction mechanism of chromium ore pellets with carbonaceous breeze reductants, *Sel –Pap.Eng. Chem.Metall,* pp. 41 - 49.

[124].Zhuravlev, V.F, Lesokhin, I.G.and Templeman, R.G, “Kinetics of the reactions for the formation of aluminates and the role of mineralizers in this process”J, Appl.Chem.USSR, 21[9]887-902(1948).

APPENDIX A

Calculations and reactions involed in reduction process

Possible reaction:

$Fe_2O_3 + CO = 2FeO + 3CO_2$

$FeO + CO = Fe + 6CO_2$

$3Fe + C = Fe_3C$

$Cr_2O_3 + 3CO = 2Cr + 3CO_2$

$7Cr + 7/3Fe_3C + 2/3C = (FeCr)_7C_3$

$C + CO_2 = 2CO.$

Calculations related to the stiochiometric amount of carbon. The stiochiometric amount of carbon used in the sample can be calculated as follows:

Let weight of sample be 1 g

O in Cr_2O_3= [(wt% Cr_2O_3/100) *1 * (48/152)]

= 39.46 *1*48 /100*152

= 0.12461

O in Fe_2O_3 = ((wt% FeO/100)*1*(16/71.85))

= 23.1 *1*16 /100*71.85

= 0.05147

Total O = 0.12461 + 0.05147.

= 0.17608.

Reduction % = (16*Mass loss*100)/(0.17608*28)

For 10 g of chromite

W_{Fe} = 23.1 *55.85 *10 /100*71.85 =1.7955

N_{Fe} =1.7955/55.85 =0.03215

W_{Cr} = 39.46 *103.992*10 /100 *151.992=2.699758

$N_{Cr} = W_{Cr}/51.996$

=2.699758/51.996

= 0.05192.

So total moles of Fe Cr = 0.03215+0.05192=0.084

7Moles of Fe Cr require 3 mole of C

So 1 mole of Fe Cr require 3/7 mole of carbon

0.084 Mole of Fe Cr require (3*0.084)/7 moles of carbon =0.036

SO for 10 g of chromite = 0.036 moles of carbon is required

=0.036*12 g of carbon

=0.432 g of carbon is required.

$7NFe(FeO) +7N/2(Cr_2O_3) +(3C +7NFe +(7NCr/2*3))= (NFe NCr)_7C_3+(7NFe+(7NCr/2*3))CO$

NFe =0.03215

NCr =0.05192.

Total reducible oxygen = (7NFe +7/2*3NCr) of O

= (7NFe +7/2*3NCr)/2 for O_2

=7*0.03215 + (7*3/2) * 0.05192/2

= 0.77021 /2

=0.3851

Net number of carbon moles = 0.036 + 0.3851

= 0.4211

Grams of carbon required = 0.4211*12

= 5.053 g

So for 10 g of chromite 5.053 g of carbon is required.

Total reducible oxygen =.3851 *16

= 6.1616 g

In 15.0532 g of sample we require 6.1616 g of oxygen

In 10 g of sample (6.1616/15.0532)*10 =4.0932 g of oxygen.

In 15.0532 g of sample we have 10 g of chromite

In 10 g of sample we have 10*10 /15.0532 =6.643 g of chromite.

In 15.0532 g of sample we have 5.053 g of carbon

In 10 g of sample 5.0532 /15.0532 *10 = 3.35689g of carbon.

In coke fixed carbon =81.7

81.7 of carbon will be in 100 g of coke

1 g 100/81.7

3.35689 g in 100 /81.7 * 3.35689= 4.1112 g

In coal fixed carbon =58.2

58.2 of carbon will be in 100 g of coal

1 g 100/58.2

3.35689 Of carbon in 100/58.2 * 3.35689 = 5.7678

In charcoal

74.8 carbons will be in 100 g of charcoal

1 g will be in 100 /74.8

3.35689 will be in 100/74.8 * 3.35689 =4.48

APPENDIX B

Calculation of K and D values.

$K = \rho F_p V_p / \tau b A_p$ = Chemical reaction rate control-

$D_e = k V_p / 2 \sigma^2 A_p$ = Effective diffusion coefficient-

Where:

ρ is the density (kgm^{-3}).

F_p is the shape factor (3 for spherical particles)

V_p is the volume (m^3) = $4/3\pi r^3$(r is the particle radius)

A_p is the cross sectional area (m^2)= $4 \pi r^2$(r is the particle radius)

b is the stiochiometric factor (¼ for the reduction of $FeCr_2O_4$ spinel

$K = \rho F_p V_p / \tau b A_p$

$K= (5\times10^3\times3\times4/3\pi r^3)/(\tau\times 1/4\times4 \pi r^2)$

$K=20\times10^3\times r/ \tau$

Putting value of r

$K= 0.5/ \tau$

$D_e = k V_p / 2 \sigma^2 A_p$

$D_e= K\times4/3\pi r^3/2\times \sigma^2\times4 \pi r^2$

Putting value of K =0.5/ τ and r in this equation

$D_e= (2.08334/ \sigma^2\times \tau) \times10^{-6}$.

Once value of τ and σ^2 are calculated from iteration method of least square for each chromite (+100µm -150µm) and reductants sizes they were substituted to calculate value of K and De and are given in the table 4.6 to 4.14.From these values Variation of chemical rate and Variation of effective diffusion rate and activation energies are calculated.

APPENDIX C:Mass loss results

Table C.1 Mass loss results at 1100 ºC

Runs	Intial mass(g)	Final mass(g)	Mass loss	Time(min)
33	35.646	34.469	1.17	120
34	40.767	39.584	1.183	120
35	40.856	39.843	1.013	120
36	40.481	39.681	0.8	120
37	37.501	36.298	1.203	120
38	37.501	36.516	0.985	120
39	39.830	38.586	1.244	120
40	48.039	47.363	0.676	120
41	39.503	38.732	0.771	120
42	48.850	48.033	0.817	120
43	48.880	48.283	0.597	120
44	41.300	40.630	0.670	120
45	48.824	48.155	0.669	120
46	48.860	48.274	0.586	120
47	48.264	47.782	0.482	120
48	48.590	48.202	0.388	120
49	48.702	48.301	0.401	120
50	48.570	48.286	0.284	120
51	47.634	47.348	0.286	120
52	40.240	40.015	0.225	120
53	40.350	40.040	0.310	120
55	46.200	45.485	0.715	120
56	46.222	45.610	0.612	120
57	46.275	45.623	0.652	120
58	46.304	45.601	0.703	120
59	46.166	45.479	0.687	120
60	40.501	39.769	0.732	120
61	44.952	44.034	0.918	120
62	47.464	46.039	1.425	120

Table C.2 Mass Loss Results at 1200 ºC

Runs	Intial mass(g)	Final mass(g)	Mass loss	Time(min)
63	48.883	47.460	1.423	120
64	48.409	47.364	1.045	120
65	48.726	47.666	1.06	120
67	48.500	47.590	0.91	120
68	48.546	47.756	0.79	120
69	48.580	47.820	0.76	120
70	48.357	47.647	0.71	120
71	48.764	48.310	0.454	120
72	48.841	48.386	0.455	120
73	48.858	48.450	0.408	120
74	48.974	48.412	0.562	120
75	48.847	48.314	0.533	120
76	48.923	48.560	0.363	120
77	48.883	48.431	0.452	120
78	48.857	48.520	0.337	120
79	57.967	55.690	2.277	120
81	56.445	54.196	2.259	120
82	56.538	54.375	2.342	120
83	56.538	54.410	2.128	120
84	53.990	53.660	0.33	120
85	53.980	53.740	0.24	120
86	52.5400	50.6000	1.94	120
87	52.49000	50.3600	2.13	120
88	49.92	49.616	0.304	120

Table C.3 Mass loss result at 1300 ºC

Runs	Intial mass(g)	Final mass(g)	Mass loss	Time(min)
90	54.7111	51.682	3.0291	120
91	54.726	53.331	1.395	120
92	54.559	53.521	1.038	120
94	54.361	53.379	0.982	120
95	54.632	53.699	0.933	120
96	54.468	53.498	0.988	120
97	54.648	53.364	1.284	120
98	54.231	53.031	1.20	120
99	54.480	53.358	1.122	120
100	56.502	53.402	3.1	120
101	56.471	53.870	2.601	120
102	56.256	53.801	2.455	120
103	55.505	53.249	2.256	120
104	56.120	53.679	2.441	120
105	56.299	54.066	2.233	120
106	56.478	53.250	3.228	120
107	55.00	53.546	1.454	120
108	54.515	53.315	1.2	120
109	54.855	53.762	1.093	120
110	54.793	54.136	0.657	120
111	54.771	54.168	0.603	120
112	54.830	53.428	1.402	120
113	53.291	52.162	1.129	120
114	53.809	52.650	1.159	120
115	53.179	52.384	0.795	120

Table C.4 Mass loss result (as received sample) at 1300 ºC

Runs	Intialmass(g)	final mass(g)	loss of mass	Time(min)
116	53.279	52.596	0.683	120
117	55.303	52.095	3.208	120
118	52.834	51.742	1.092	120
119	52.301	51.751	0.55	120

Table C.5 Mass loss result (as received sample) at 1200 ºC

uns	Intialmass(g)	final mass(g)	loss of mass	Time(min)
120	53.355	52.771	0.584	120
121	53.530	52.560	0.97	120
122	54.859	52.350	2.509	120
123	52.1000	51.432	0.668	120

Table C.6 Mass loss result (as received sample) at 1100 ºC

Runs	Intialmass(g)	final mass(g)	loss of mass	Time(min)
125	52.764	52.045	0.719	120
126	53.524	52.976	0.548	120
127	53.308	52.003	1.305	120

Table C.7 Mass loss result (as received sample) at 1000 ºC

Runs	Intialmass(g)	final mass(g)	loss of mass	Time(min)
128	53.652	53.066	0.586	120
129	53.566	52.769	0.797	120

130	54.288	53.701	0.587	120
131	47.121	46.675	0.446	120
132	54.946	52.280	2.6666	120
133	55.267	52.492	2.775	120

Table C.8 Mass Loss Results at 1000 ºC

Runs	Intialmass(g)	final mass(g)	loss of mass	Time(min)
1	48.657	48.255	0.402	120
2	51.111	50.601	0.5101	120
3	41.23	39.881	1.349	120
4	57.565	57.123	0.442	120
5	57.565	57.123	0.442	120
6	39.86	38.41	1.45	120
7	37.89	36.20	1.69	120
8	39.316	37.80	1.516	120
9	29.393	28.24	1.152	120
10	39.754	38.660	1.094	120
11	36.669	35.92	0.749	120
12	40.6102	40.02	0.608	120
13	36.783	36.100	0.683	120
14	46.7901	46.000	0.7901	120
15	35.939	35.200	0.739	120
21	47.121	46.675	0.446	120
22	40.064	39.612	0.452	120
23	40.167	39.917	0.25	120
24	40.066	39.603	0.463	120
25	39.099	38.524	0.575	120
26	38.801	38.231	0.57	120
27	41.027	40.171	0.856	120
28	41.533	40.971	0.562	120
30	40.62	39.622	0.998	120
32	40.533	39.641	0.892	120

Appendix D

Graphs of reduction behavior of reductants

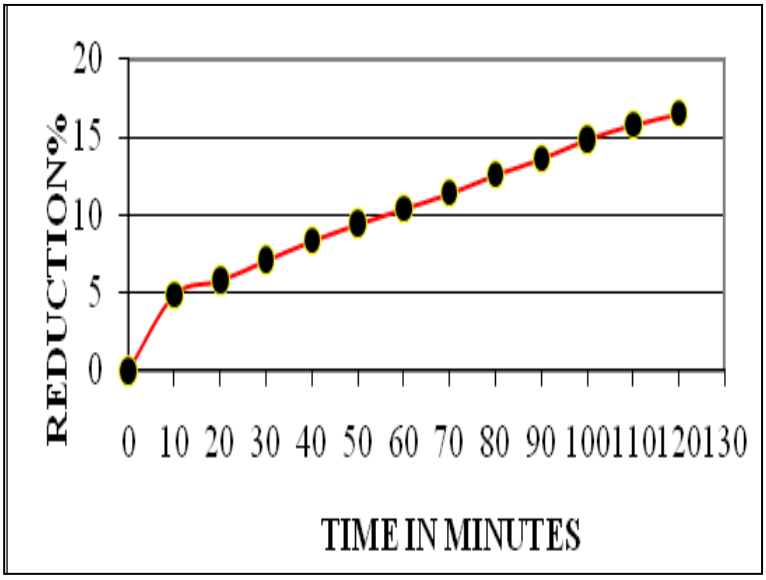

Figure D.1 Effect of coke (+50µm-100µm) addition on the reduction of xstrata chromite (+100µm-150µm) at 1100 ºC

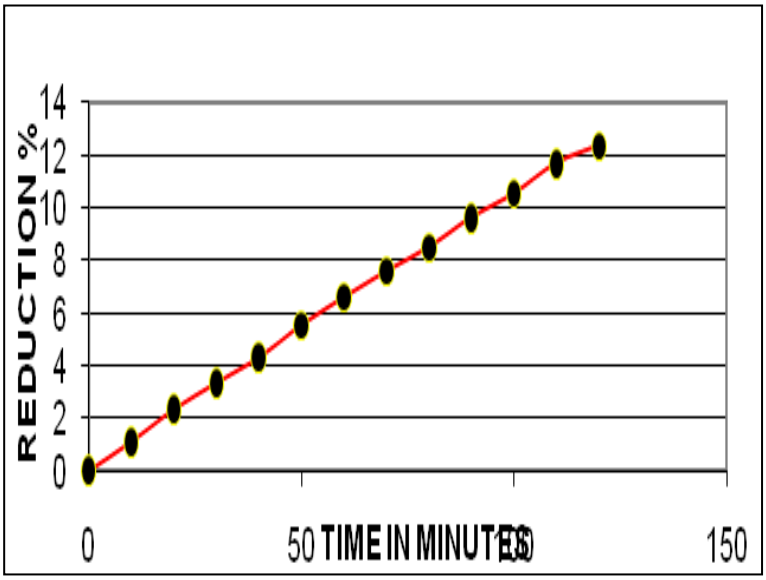

Figure D.2 Effect of coke (+50µm-100µm) addition on the reduction of xstrata chromite (+150µm-200µm) at 1100 ºC

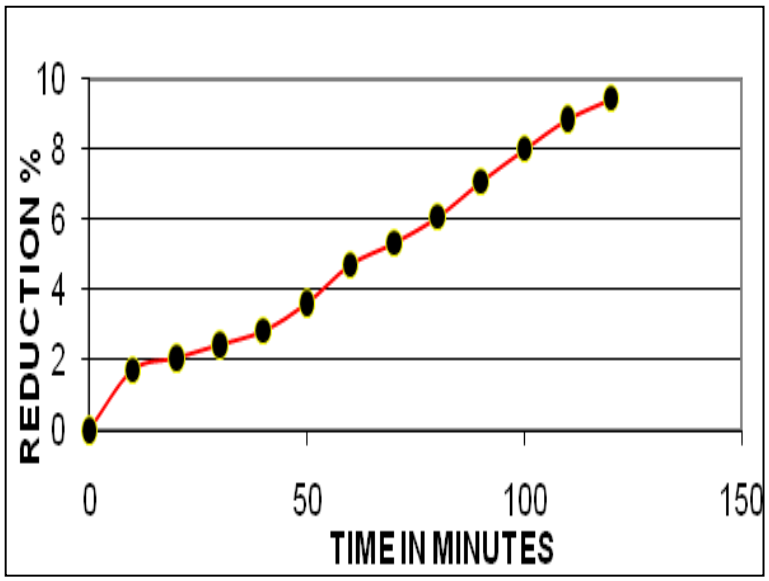

Figure D.3 Effect of coke (+100µm-150µm) addition on the reduction of xstrata chromite (+50µm-100µm) at 1100 ºC

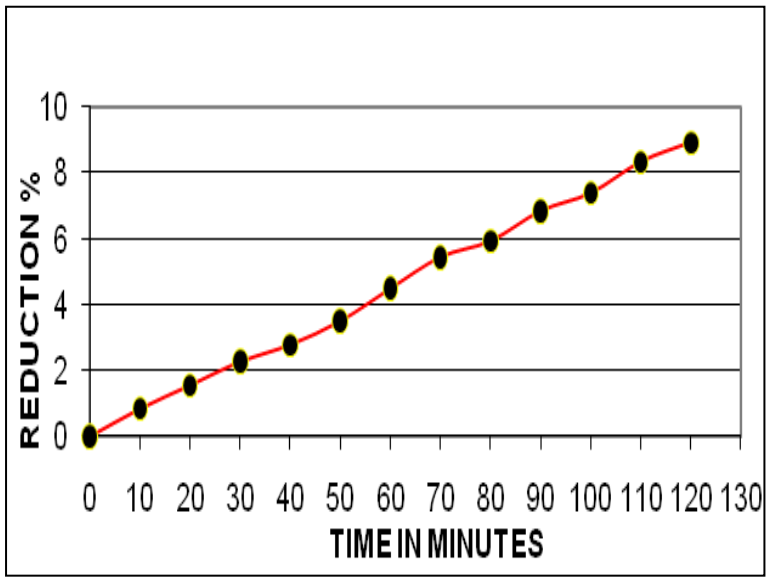

Figure D.4 Effect of coke (+150µm-200µm) addition on the reduction of xstrata chromite (+150µm-200µm) at 1100 ºC

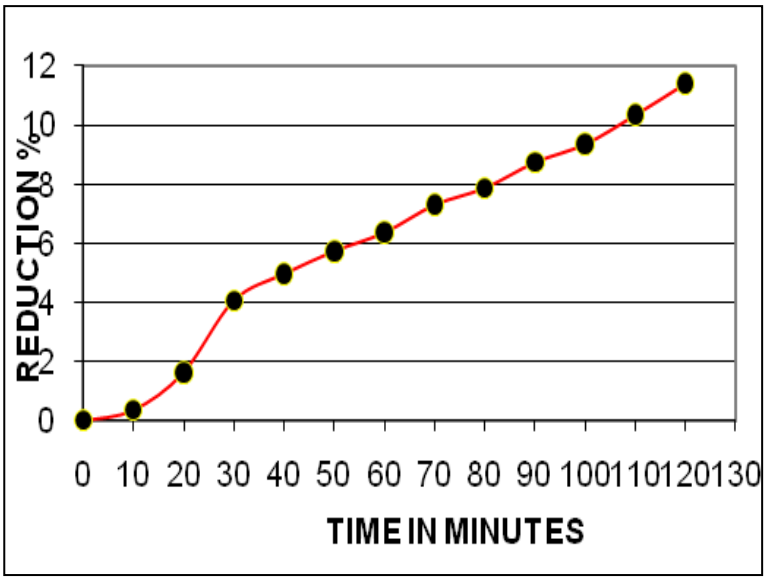

Figure D.5 Effect of charcoal (+50µm-100µm) addition on the reduction of xstrata chromite (+50µm-100µm) at 1100 ºC

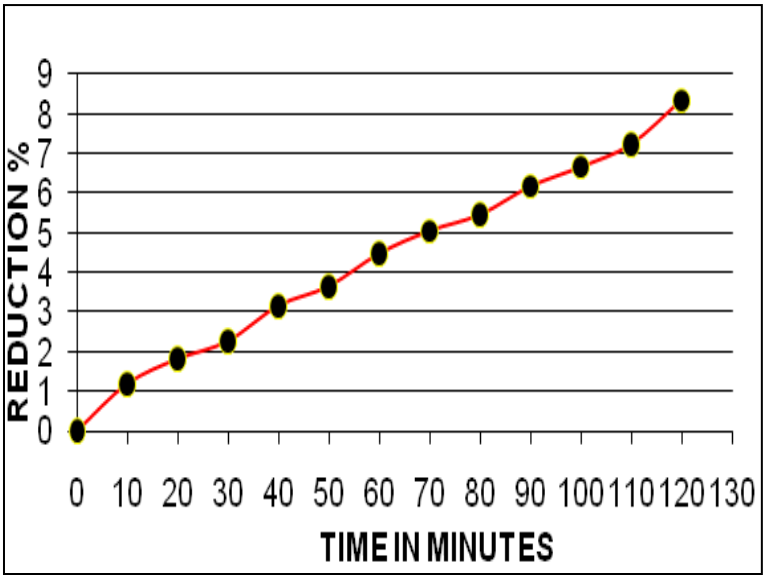

Figure D.6 Effect of charcoal (+100µm-150µm) addition on the reduction of xstrata chromite (+50µm-100µm) at 1100 ºC

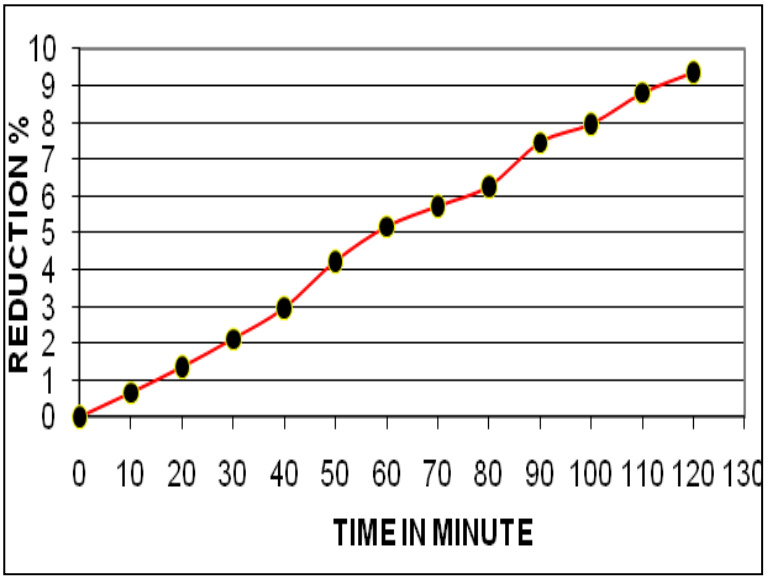

Figure D.7 Effect of charcoal (+150µm-200µm) addition on the reduction of xstrata chromite (+50µm-100µm) at 1100 ºC

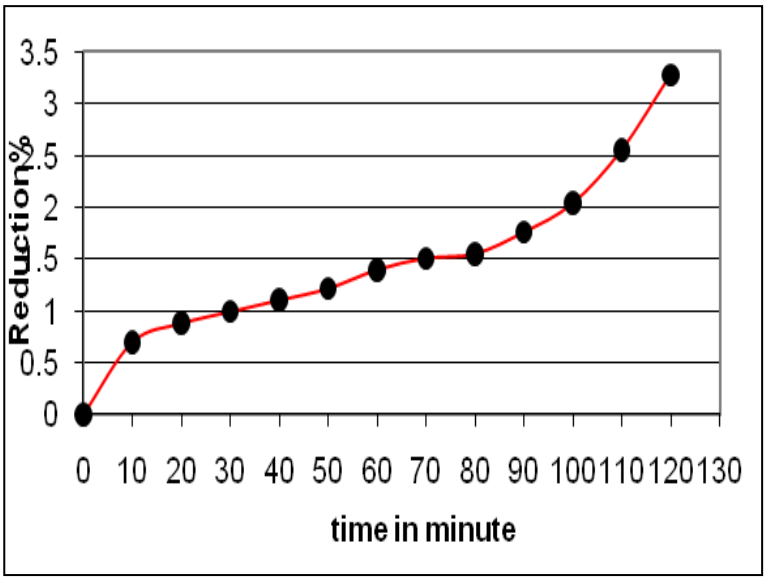

Figure D.8 Effect of charcoal (+50µm-100µm) addition on the reduction of xstrata chromite (+150µm-200µm) at 1100 ºC

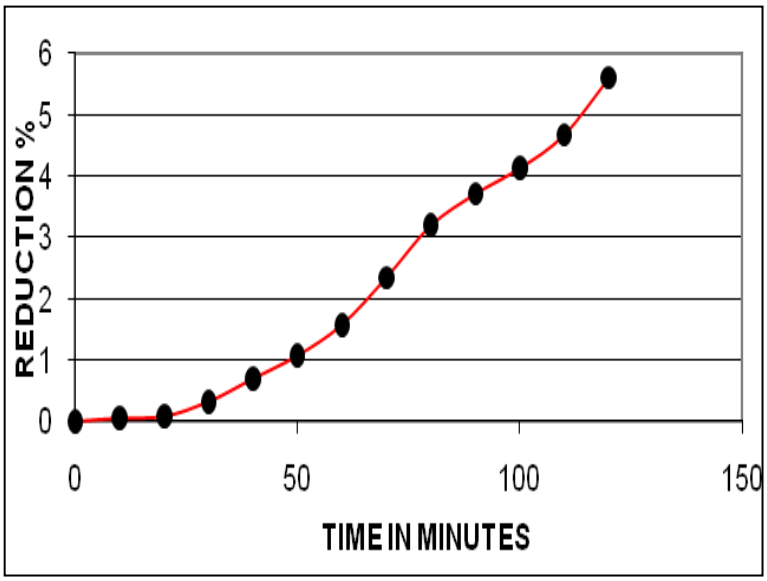

Figure D.9 Effect of charcoal (+100µm-150µm) addition on the reduction of xstrata chromite (+150µm-200µm) at 1100 ºC

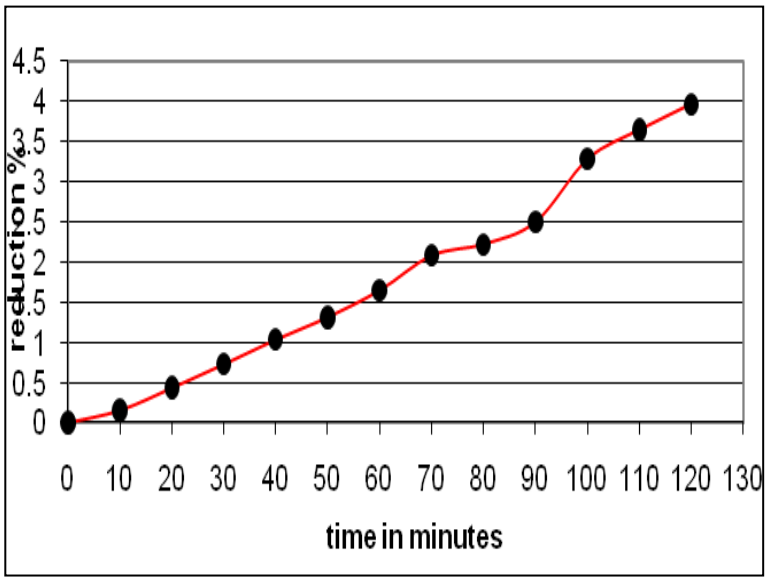

Figure D.10 Effect of charcoal (+150µm-200µm) addition on the reduction of xstrata chromite (+150µm-200µm) at 1100 ºC

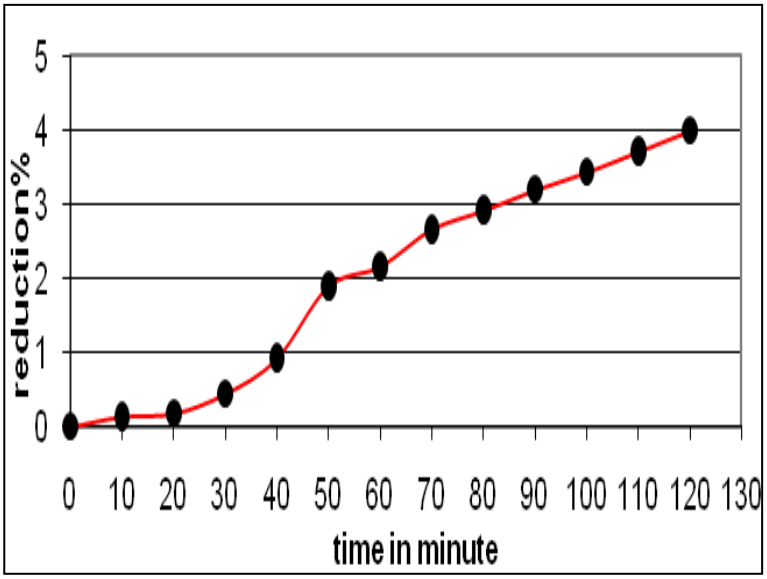

Figure D.11 Effect of graphite (+50µm-100µm) addition on the reduction of xstrata chromite (+50µm-100µm) at 1100 ºC

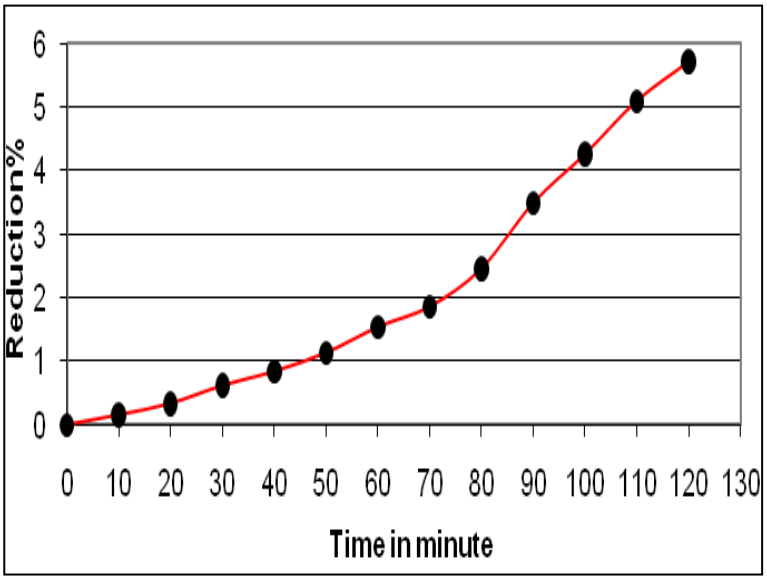

Figure D.12 Effect of graphite (+150µm-200µm) addition on the reduction of xstrata chromite (+50µm-100µm) at 1100 ºC

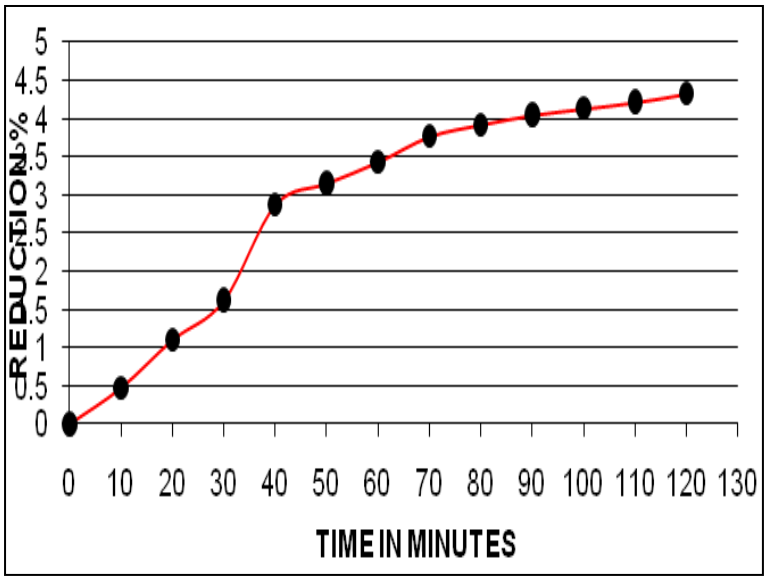

Figure D.13 Effect of graphite (+50µm-100µm) addition on the reduction of xstrata chromite (+100µm-150µm) at 1100 ºC

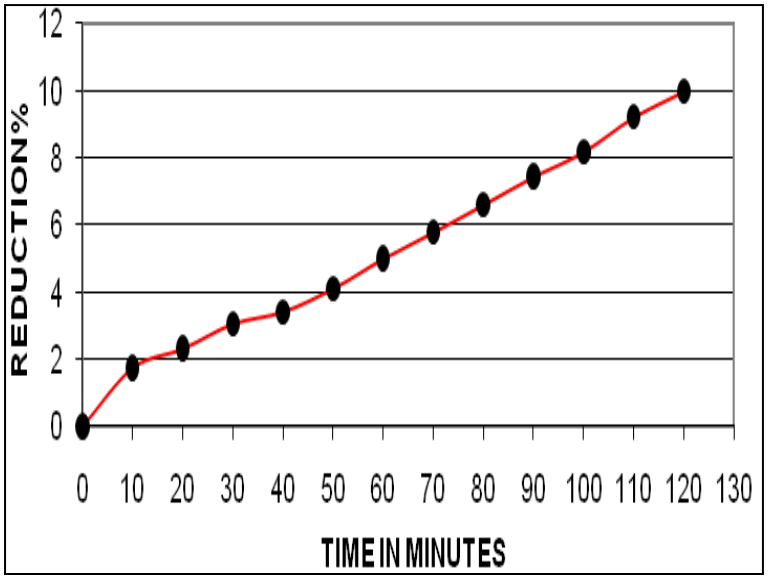

Figure D.14 Effect of coal (+50µm-100µm) addition on the reduction of xstrata chromite (+50µm-100µm) at 1100 ºC

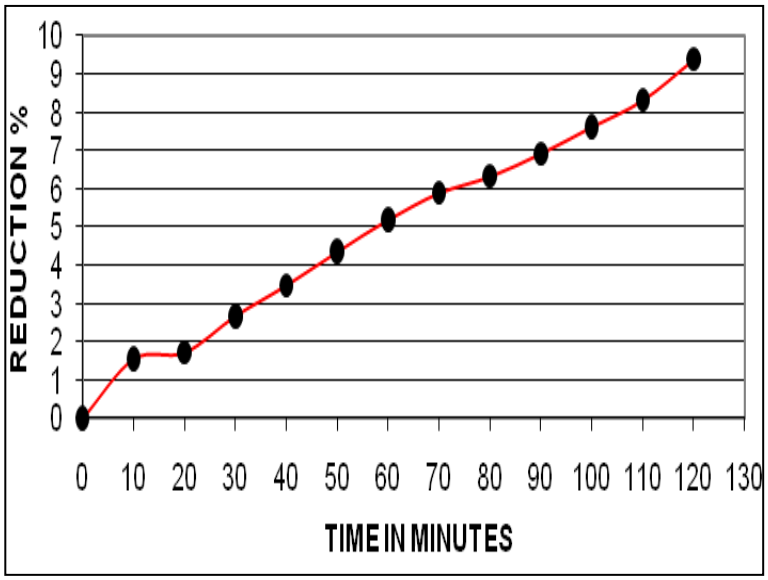

Figure D.15 Effect of coal (+100µm-150µm) addition on the reduction of xstrata chromite (+50µm-100µm) at 1100 ºC

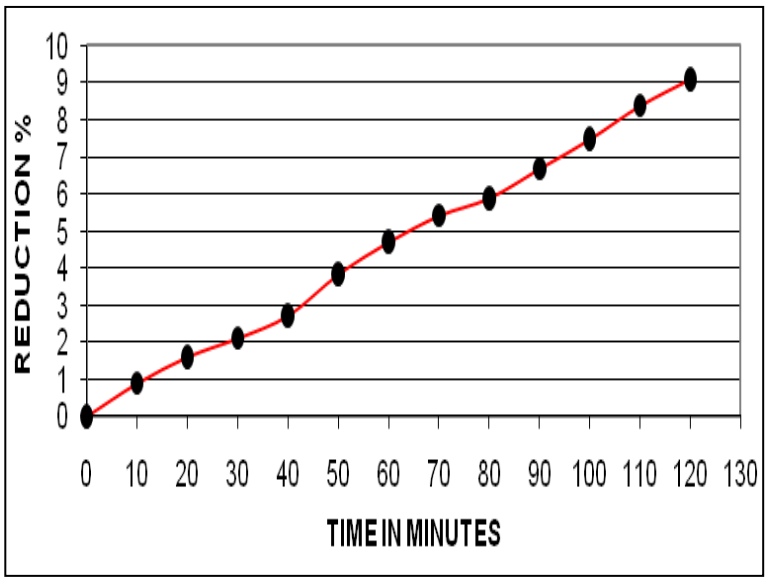

Figure D.16 Effect of coal (+150µm-200µm) addition on the reduction of xstrata chromite (+50µm-100µm) at 1100 ºC

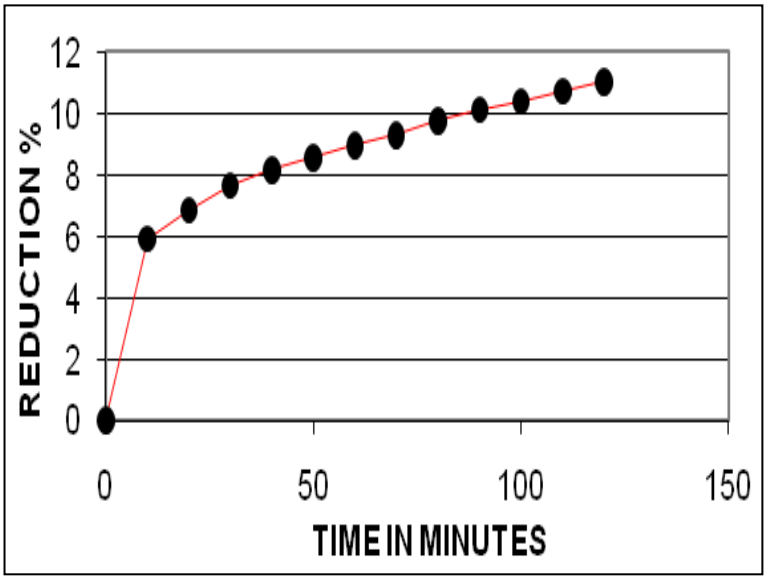

Figure D.17 Effect of coke (+50µm-100µm) addition on the reduction of xstrata chromite (+150µm-200µm) at 1200 ºC

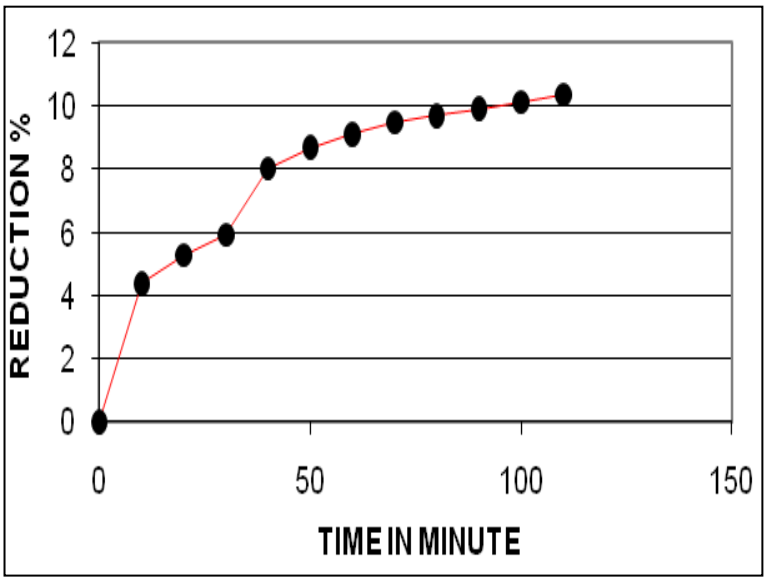

Figure D.18 Effect of coke (+100µm-150µm) addition on the reduction of xstrata chromite (+150µm-200µm) at 1200 ºC

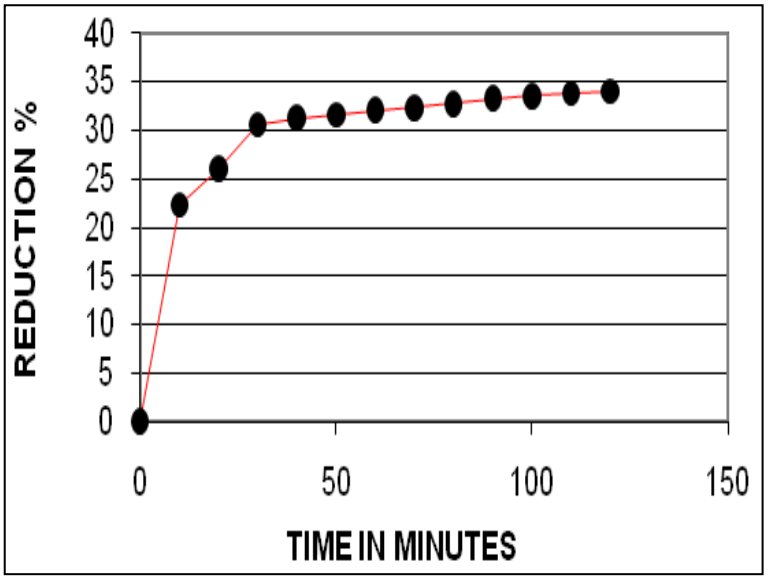

Figure D.19 Effect of coal (+100µm-150µm) addition on the reduction of xstrata chromite (+150µm-200µm) at 1300 ºC

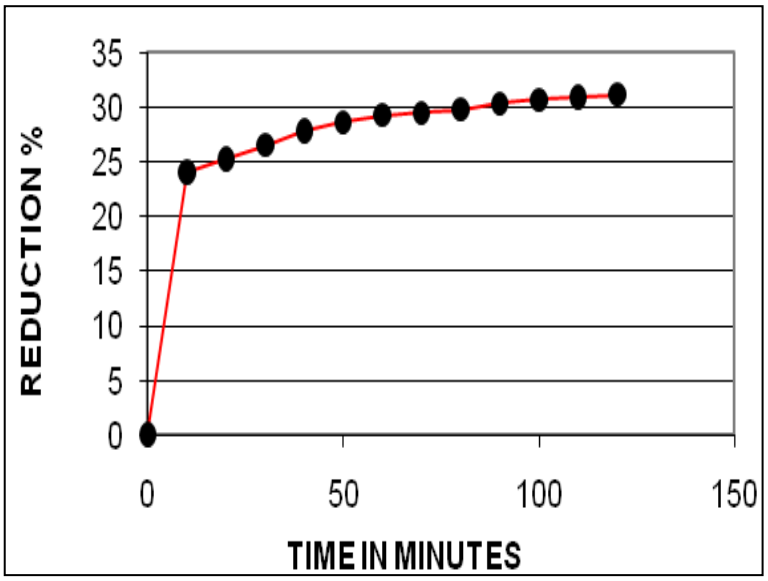

Figure D.20 Effect of coal (+150µm-200µm) addition on the reduction of xstrata chromite (+150µm-200µm) at 1300 ºC

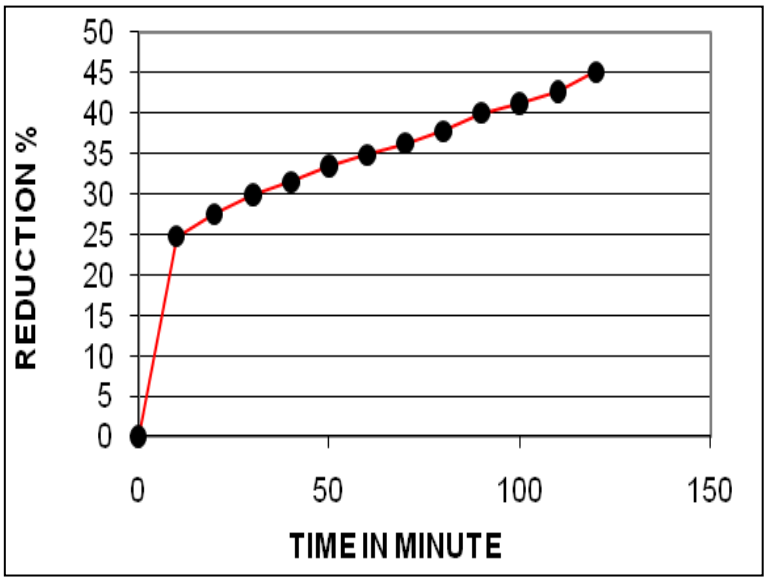

Figure D.21 Effect of coal (+50µm-100µm) addition on the reduction of xstrata chromite (+50µm-100µm) at 1300 ºC

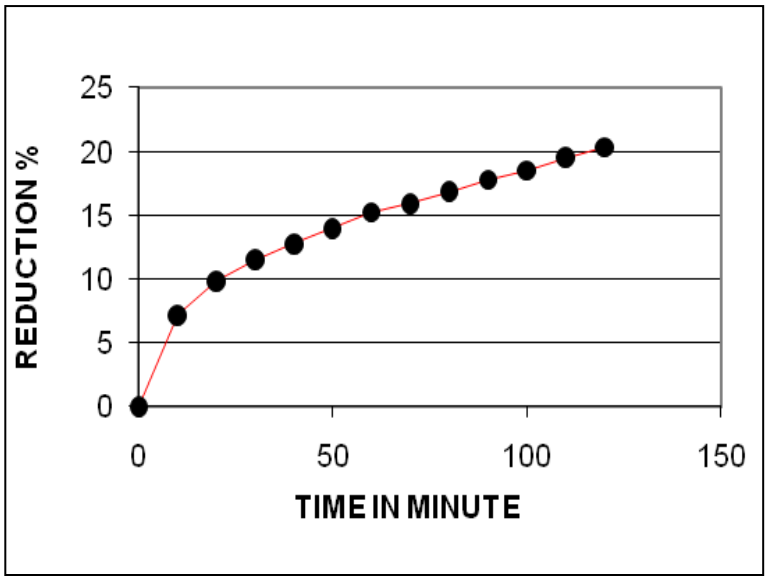

Figure D.22 Effect of charcoal (+50µm-100µm) addition on the reduction of xstrata chromite (+50µm-100µm) at 1300 ºC

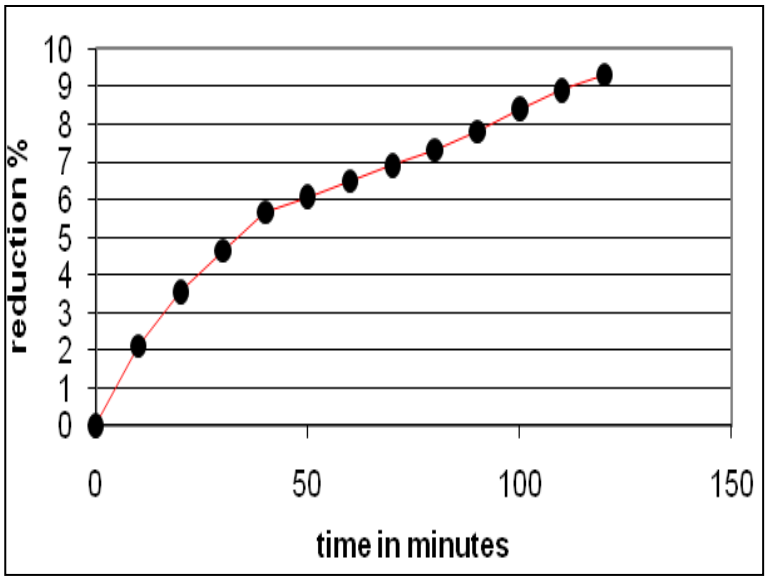

Figure D.23 Effect of graphite (as received) addition on the reduction of xstrata chromite (as received) at 1200 ºC

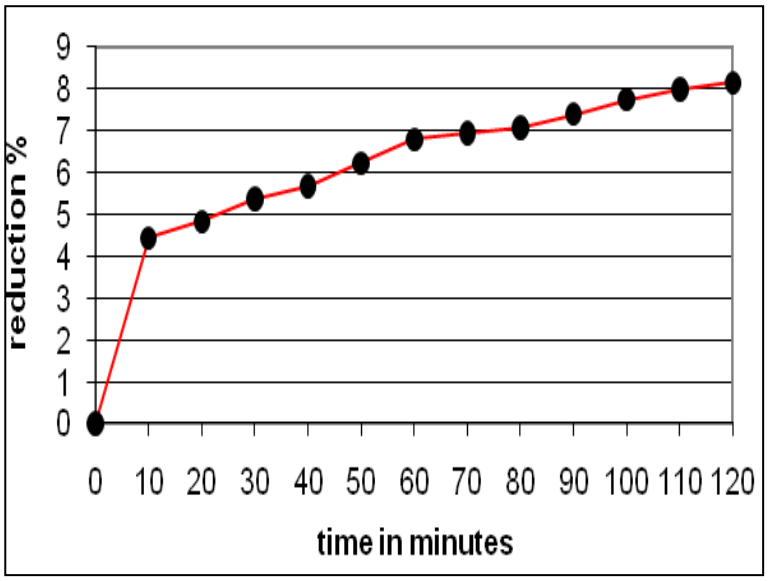

Figure D.24 Effect of charcoal (as received) addition on the reduction of xstrata chromite (as received) at 1200 ºC

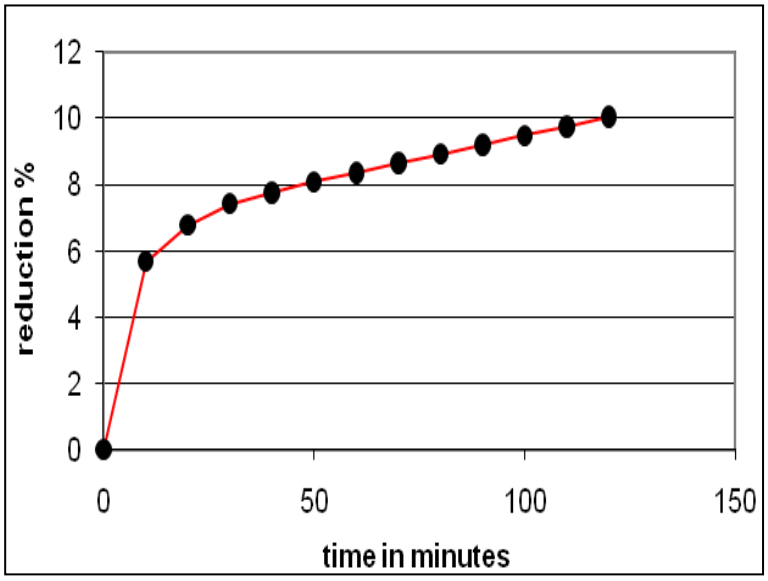

Figure D.25 Effect of coke (as received) addition on the reduction of xstrata chromite (as received) at 1100 ºC

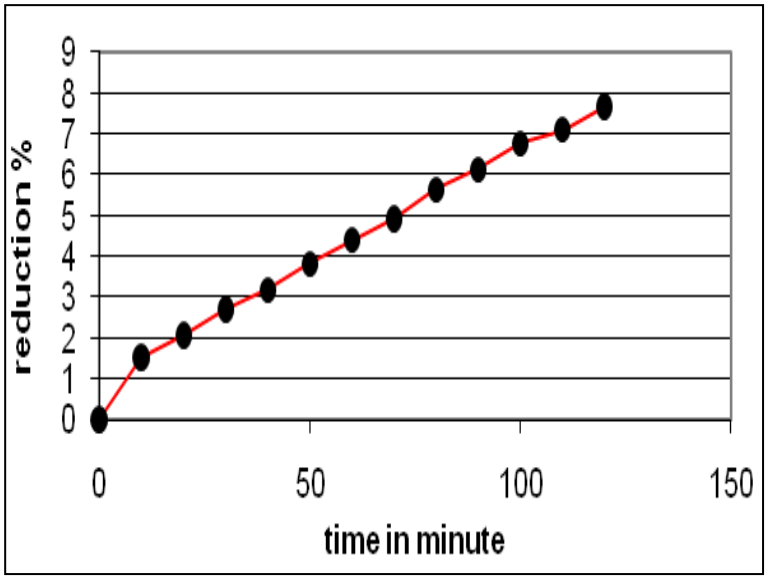

Figure D.26 Effect of charcoal (as received) addition on the reduction of xstrata chromite (as received) at 1100 ºC

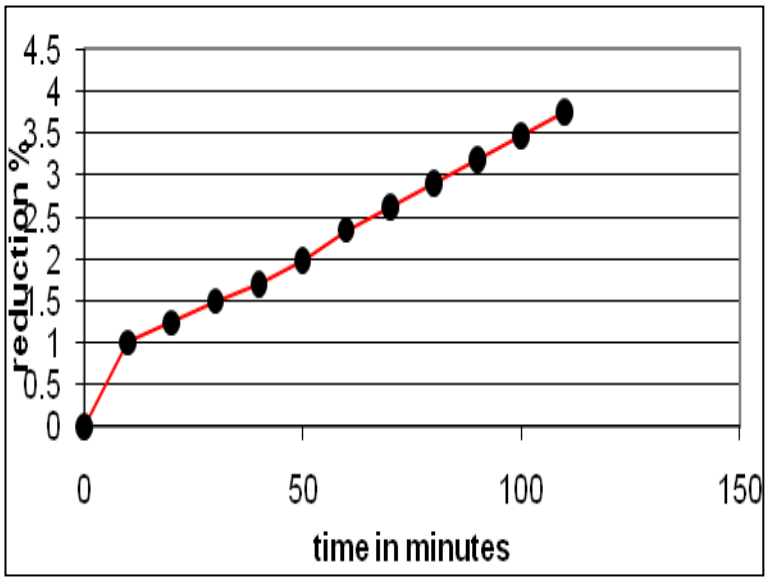

Figure D.27 Effect of graphite (as received) addition on the reduction of xstrata chromite (as received) at 1100 ºC

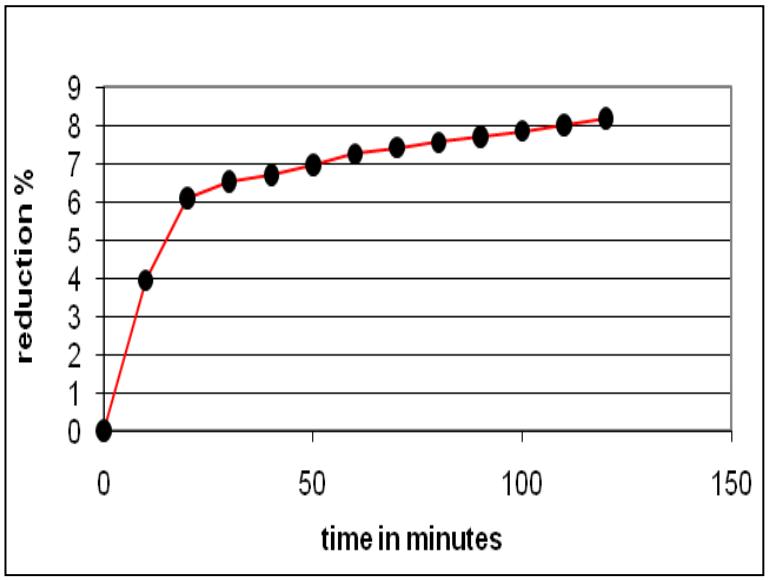

Figure D.28 Effect of charcoal (as received) addition on the reduction of xstrata chromite (as received) at 1000 ºC

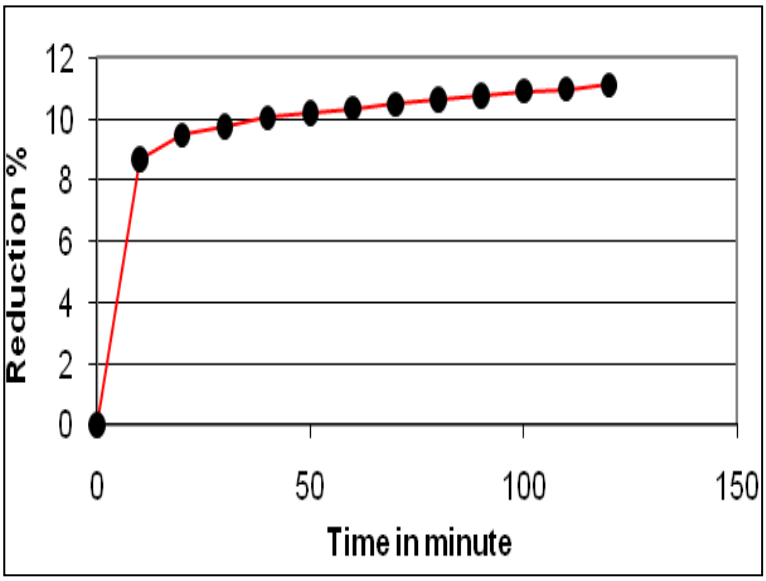

Figure D.29 Effect of coke (as received) addition on the reduction of xstrata chromite (as received) at 1000 ºC

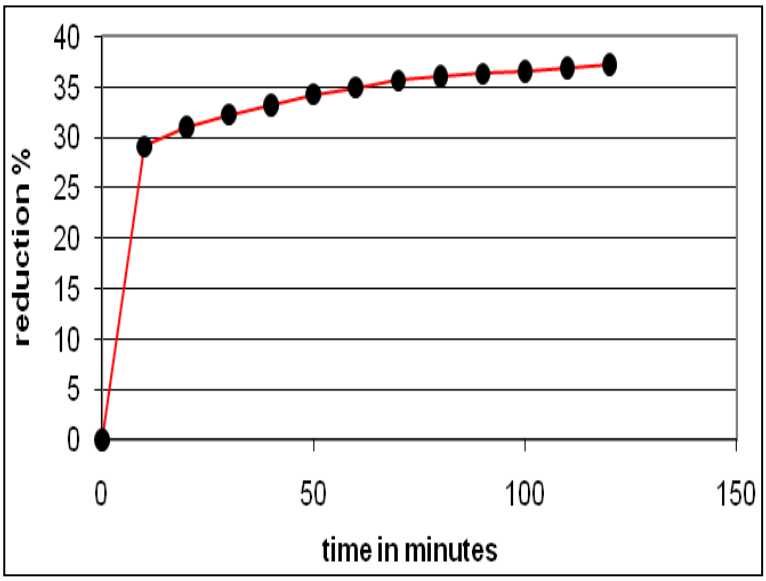

Figure D.30 Effect of coal (+50µm-100µm) addition on the reduction of xstrata chromite (+100µm-150µm) at 1300 ºC

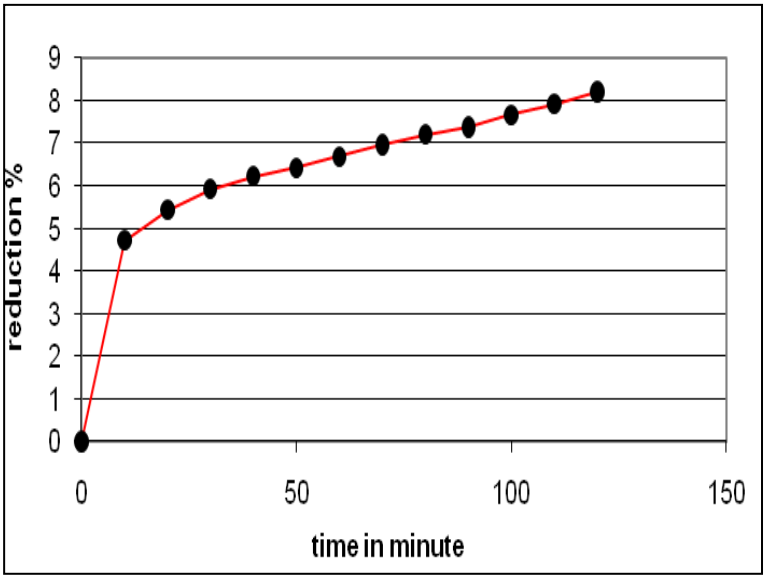

Figure D.31 Effect of coal (as received) addition on the reduction of xstrata chromite (as received) at 1000 ºC

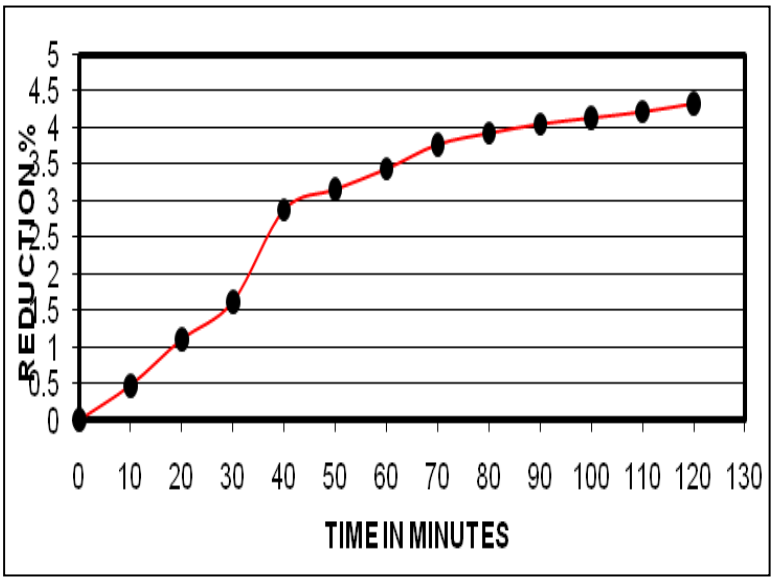

Figure D.32 Effect of graphite (+50µm-100µm) addition on the reduction of xstrata chromite (+100µm-150µm) at 1100 ºC

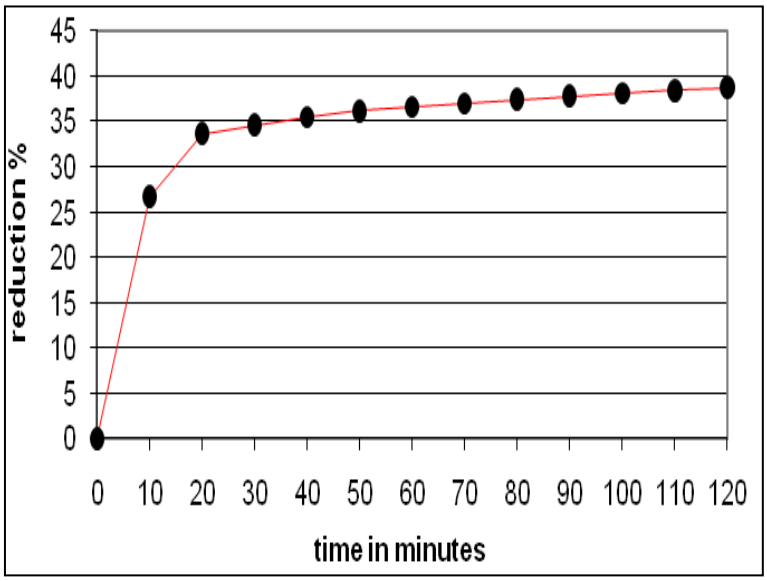

Figure D.33 Effect of coal (+150µm-200µm) addition on the reduction of xstrata chromite (+150µm-200µm) at 1300 ºC

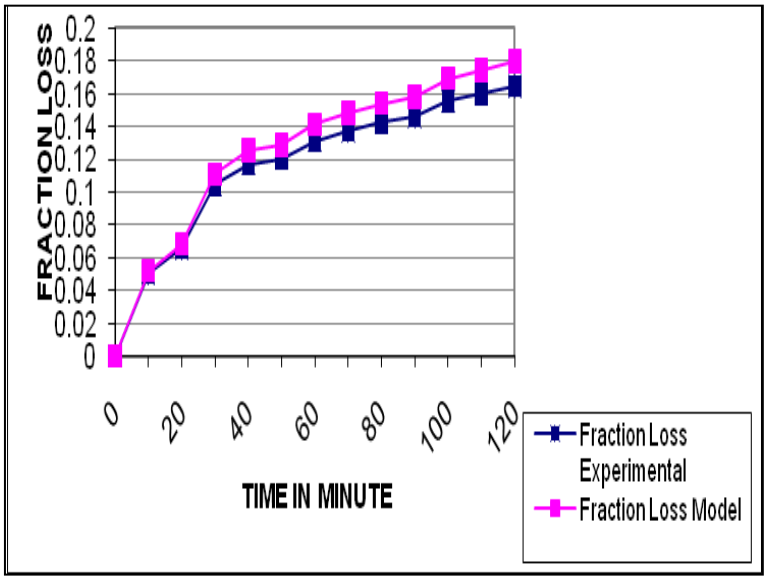

Figure D.34 Comparison of experimental and model fractional loss vs time on addition of coke (+50µm-100µm) to xstrata chromite (+50µm-100µm) at 1100 ºC

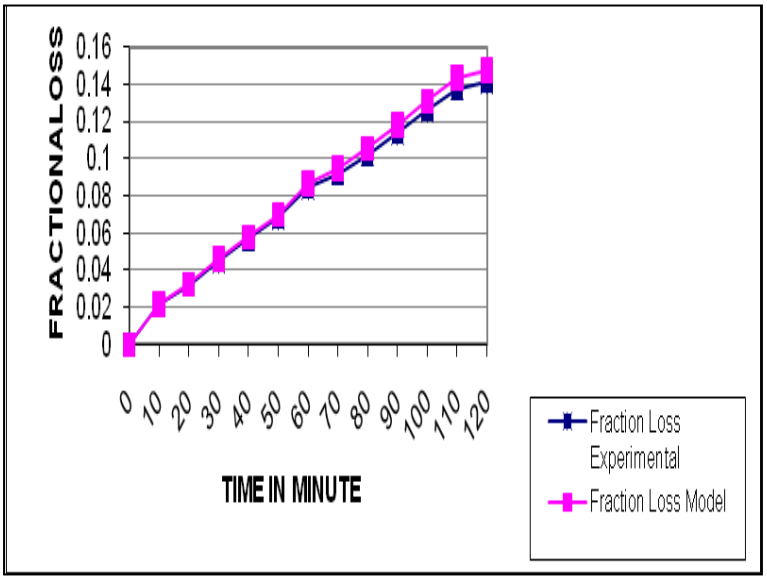

Figure D.35 Comparison of experimental and model fractional loss vs time on addition of coke (+50µm-100µm) to xstrata chromite (+100µm-150µm) at 1100 ºC

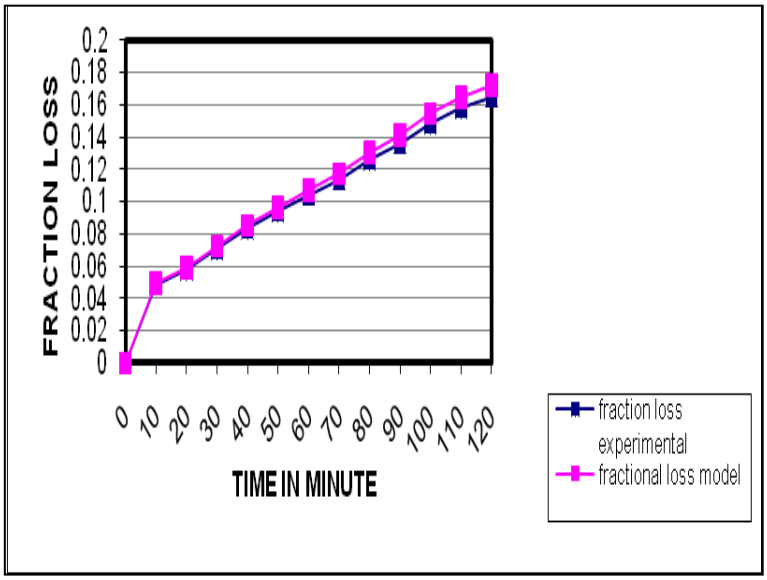

Figure D.36 Comparison of experimental and model fractional loss vs time on addition of coke (+100µm-150µm) to xstrata chromite (+100µm-150µm) at 1100 ºC

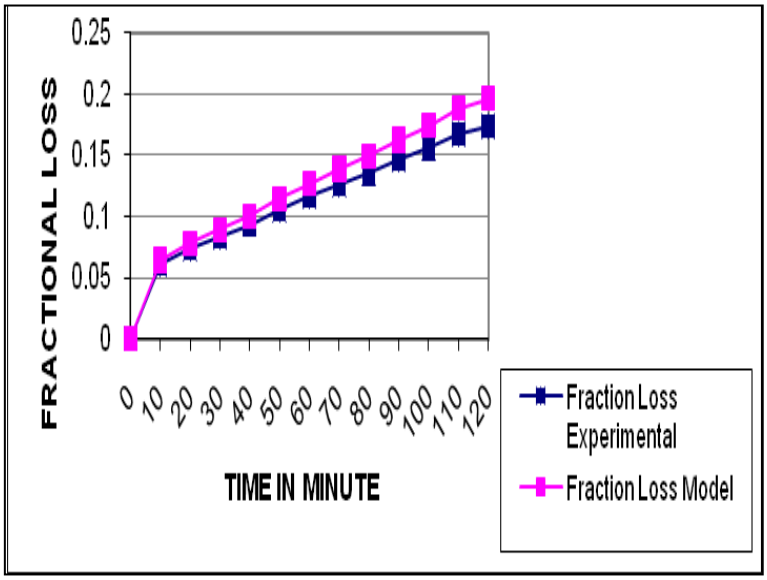

Figure D.37 Comparison of experimental and model fractional loss vs time on addition of coke (+50µm-100µm) to xstrata chromite (+150µm-200µm) at 1100 ºC

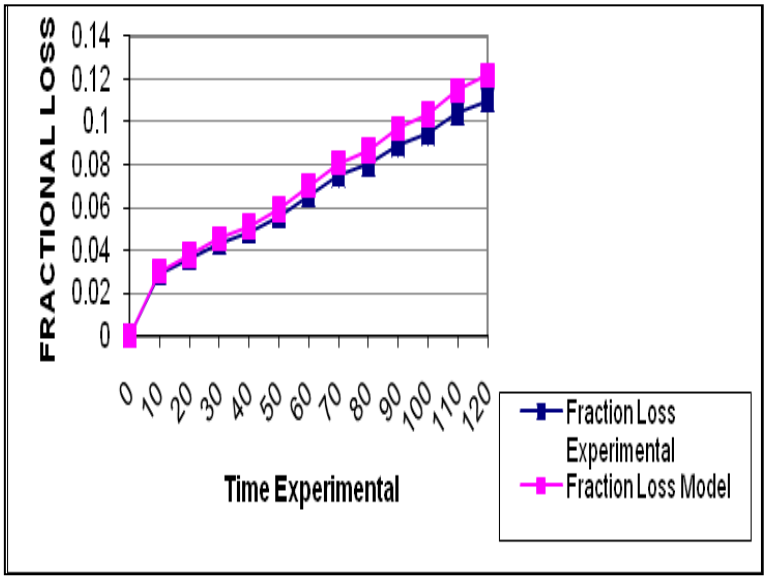

Figure D.38 Comparison of experimental and model fractional loss vs time on addition of coke (+150µm-200µm) to xstrata chromite (+150µm-200µm) at 1100 ºC.

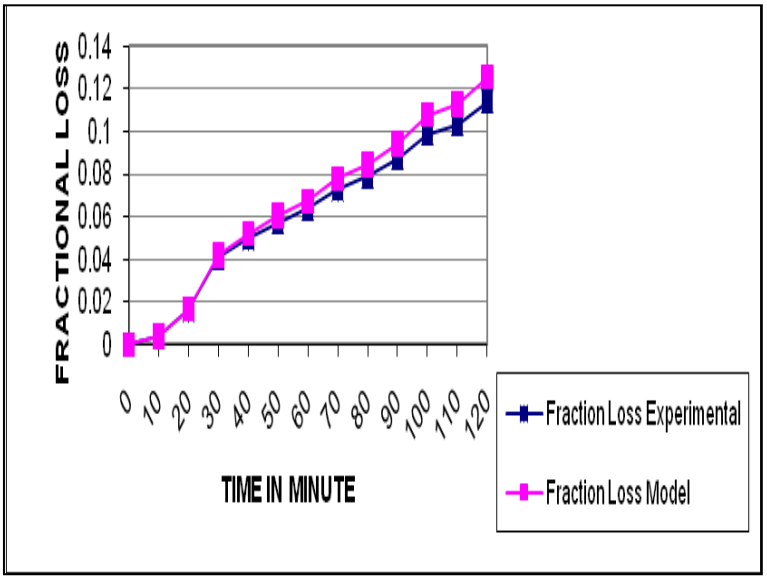

Figure D.39 Comparison of experimental and model fractional loss vs time on addition of charcoal (+50µm-100µm) to xstrata chromite (+50µm-100µm) at 1100 ºC

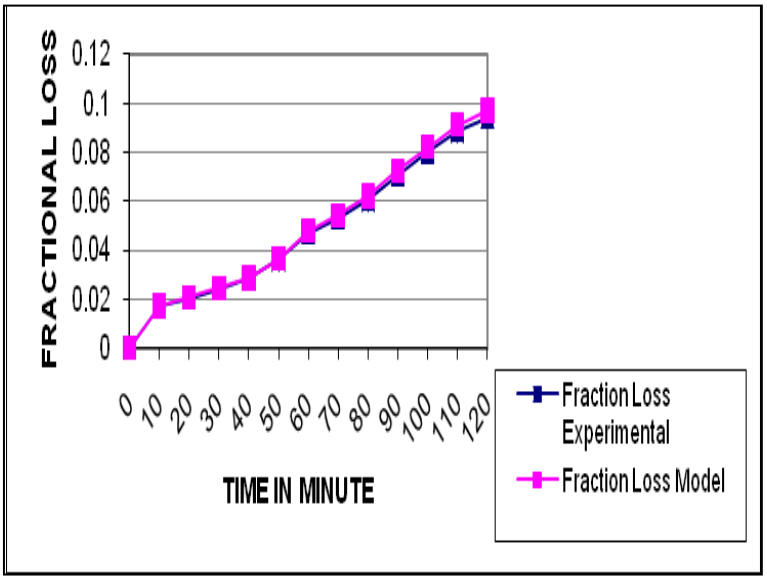

Figure D.40 Comparison of experimental and model fractional loss vs time on addition of coke (+100µm-150µm) to xstrata chromite (+50µm-100µm) at 1100 ºC

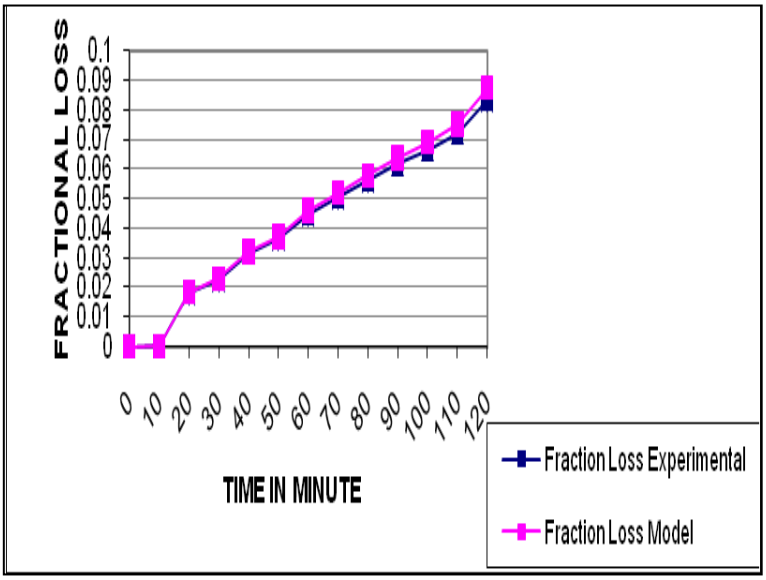

Figure D.41 Comparison of experimental and model fractional loss vs time on addition of charcoal (+100µm-150µm) to xstrata chromite (+50µm-100µm) at 1100 ºC

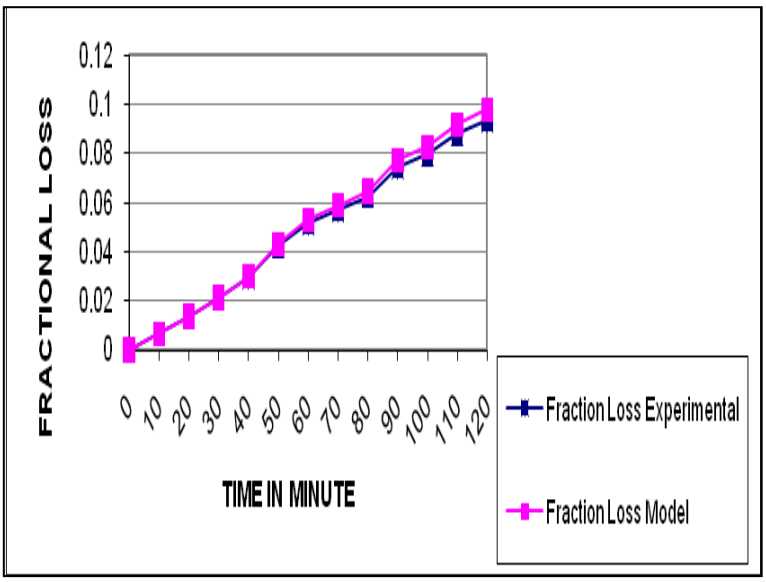

Figure D.42 Comparison of experimental and model fractional loss vs time on addition of charcoal (+150µm-200µm) to xstrata chromite (+50µm-100µm) at 1100 ºC

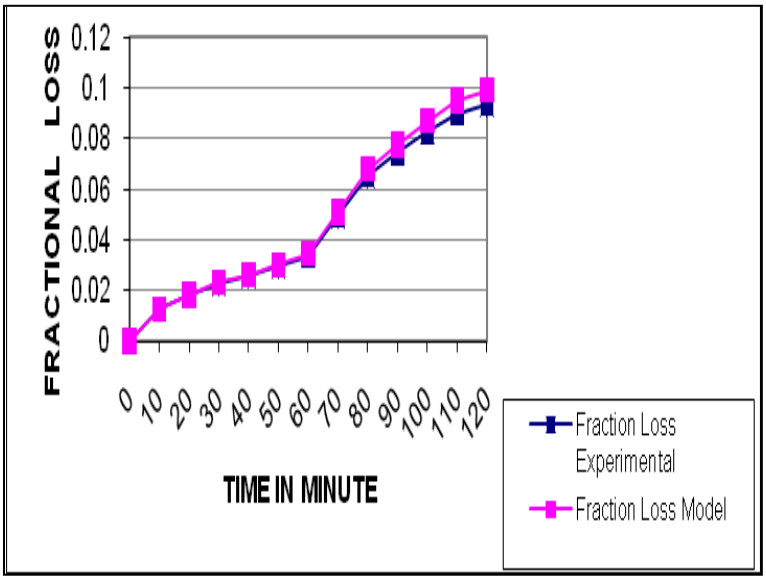

Figure D.43 Comparison of experimental and model fractional loss vs time on addition of charcoal (+50µm-100µm) to xstrata chromite (+100µm-150µm) at 1100 ºC

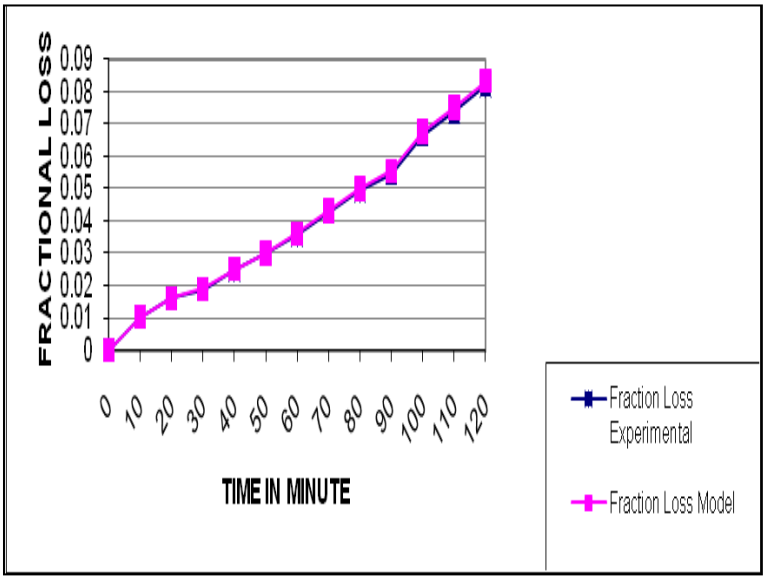

Figure D.44 Comparison of experimental and model fractional loss vs time on addition of charcoal (+100µm-150µm) to xstrata chromite (+100µm-150µm) at 1100 ºC

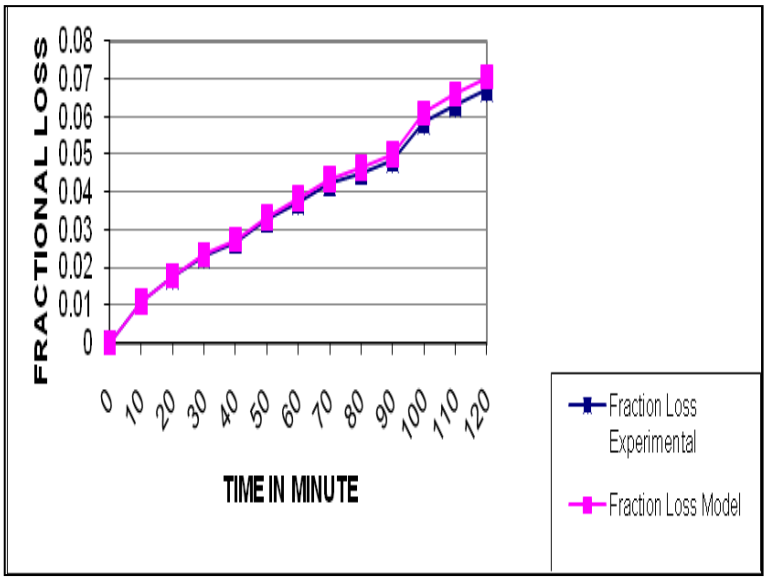

Figure D.45 Comparison of experimental and model fractional loss vs time on addition of charcoal (+150µm-200µm) to xstrata chromite (+100µm-150µm) at 1100 ºC

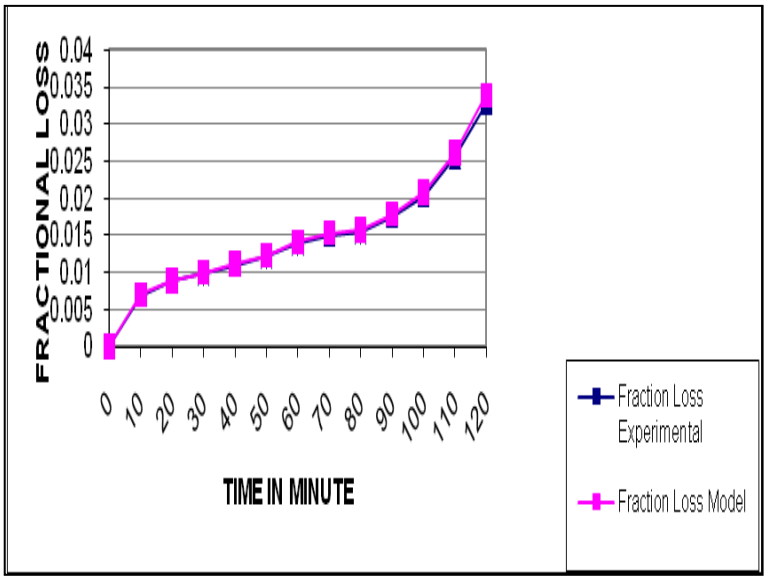

Figure D.46 Comparison of experimental and model fractional loss vs time on addition of charcoal (+50µm-100µm) to xstrata chromite (+150µm-200µm) at 1100 ºC

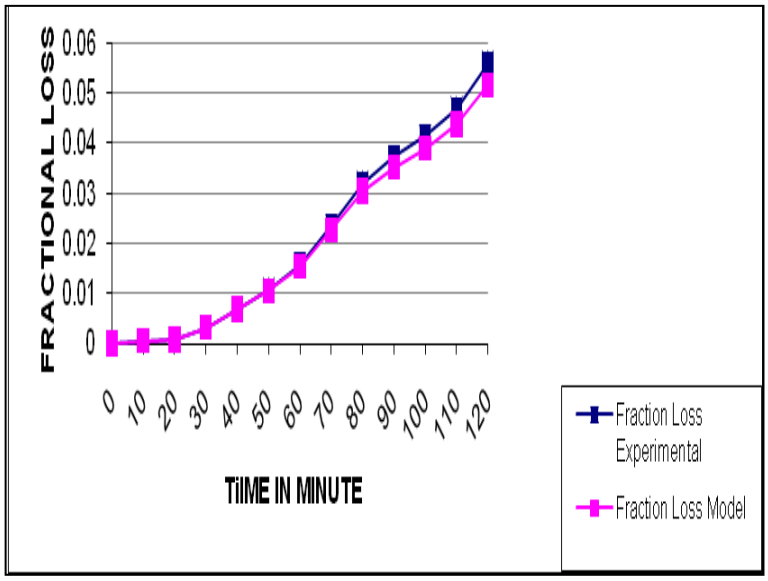

Figured D.47 Comparison of experimental and model fractional loss vs time on addition of charcoal (+100µm-150µm) to xstrata chromite (+150µm-200µm) at 1100 ºC

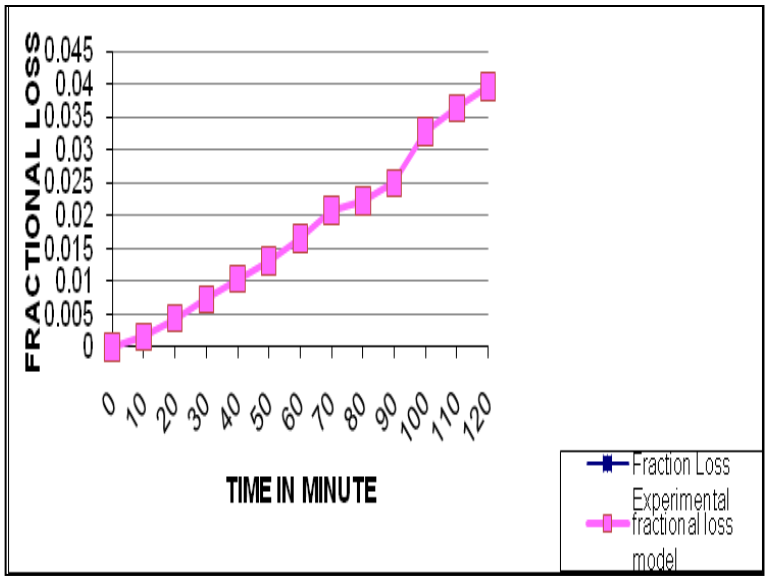

Figure D.48 Comparison of experimental and model fractional loss vs time on addition of charcoal (+150µm-200µm) to xstrata chromite (+150µm-200µm) at 1100 ºC

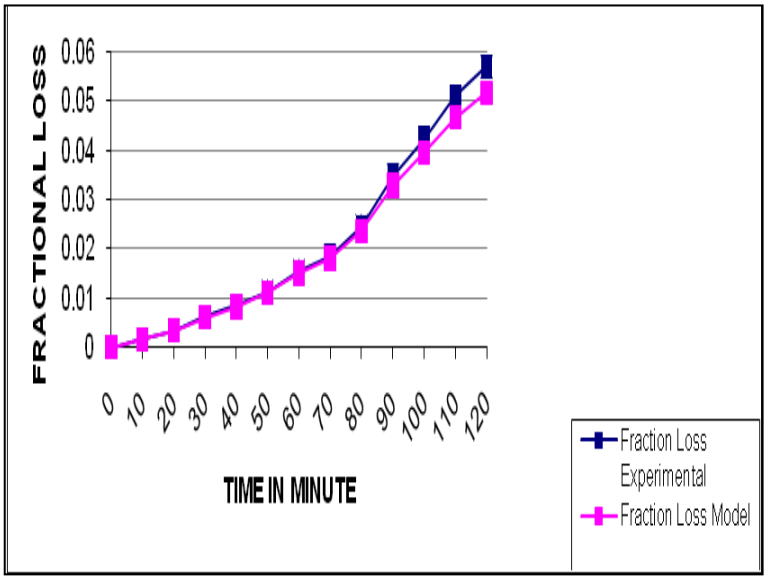

Figure D.49 Comparison of experimental and model fractional loss vs time on addition of graphite (+150µm-200µm) to xstrata chromite (+50µm-100µm) at 1100 ºC

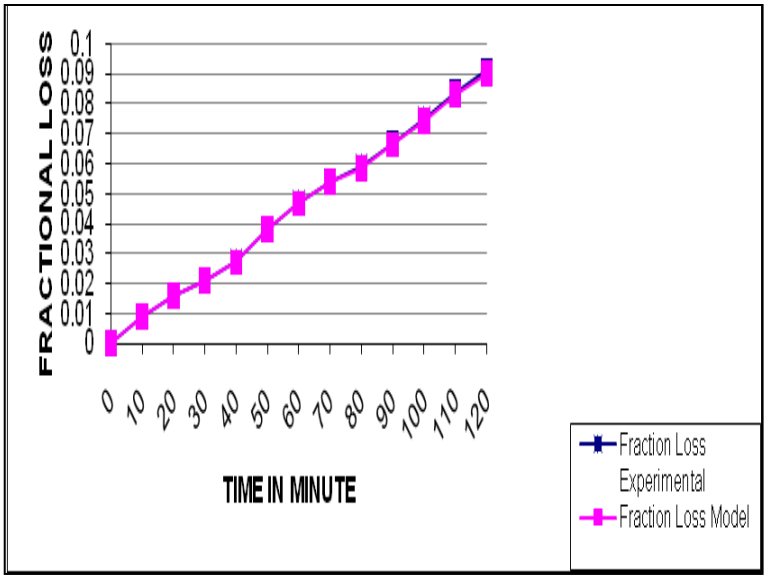

Figure D.50 Comparison of experimental and model fractional loss vs time on addition of coal (+150µm-200µm) to xstrata chromite (+50µm-100µm) at 1100 ºC

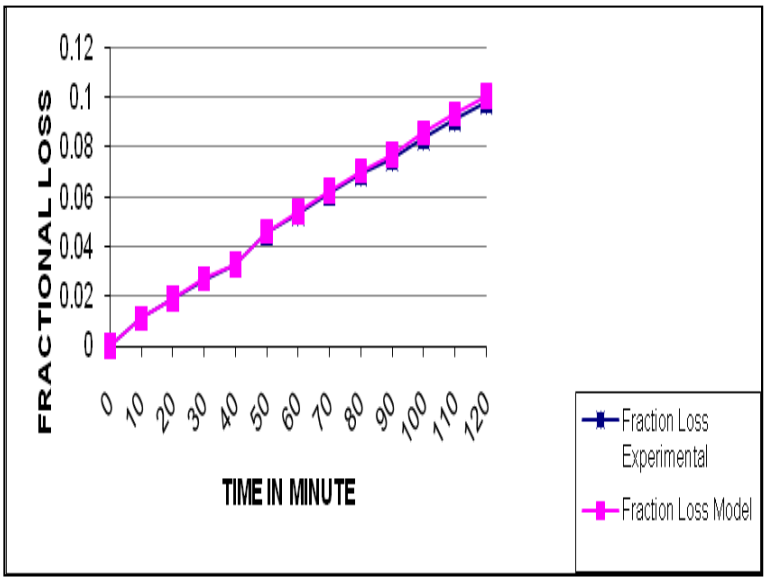

Figure D.51 Comparison of experimental and model fractional loss vs time on addition of coal (+50µm-100µm) to xstrata chromite (+100µm-150µm) at 1100 ºC

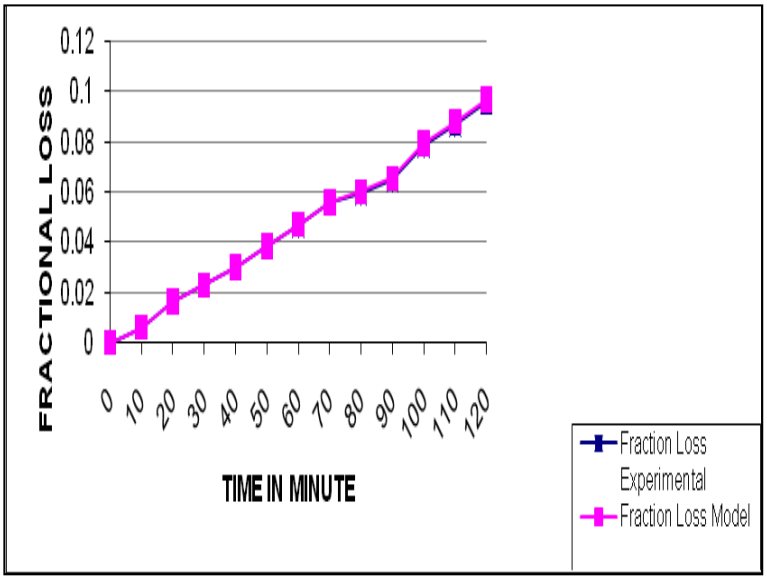

Figure D.52 Comparison of experimental and model fractional loss vs time on addition of coal (+100µm-150µm) to xstrata chromite (+100µm-150µm) at 1100 ºC

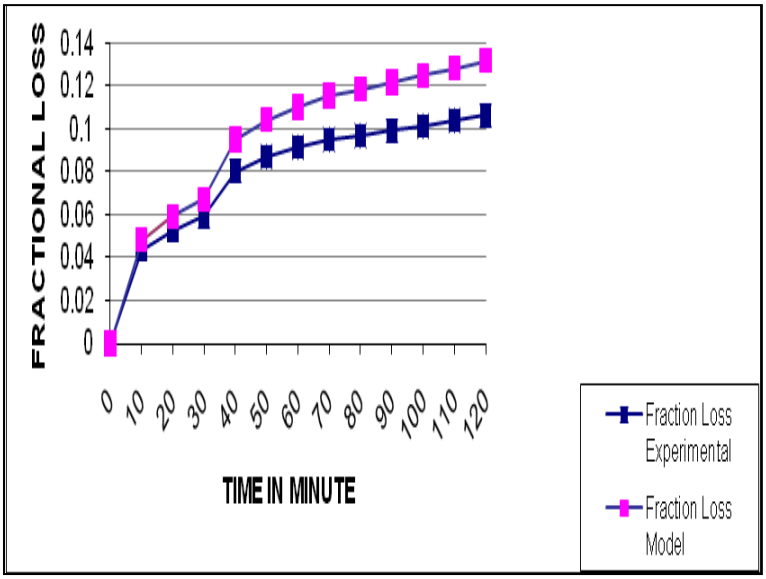

Figure D.53 Comparison of experimental and model fractional loss vs time on addition of coal (+100µm-150µm) to xstrata chromite (+150µm-200µm) at 1200 ºC

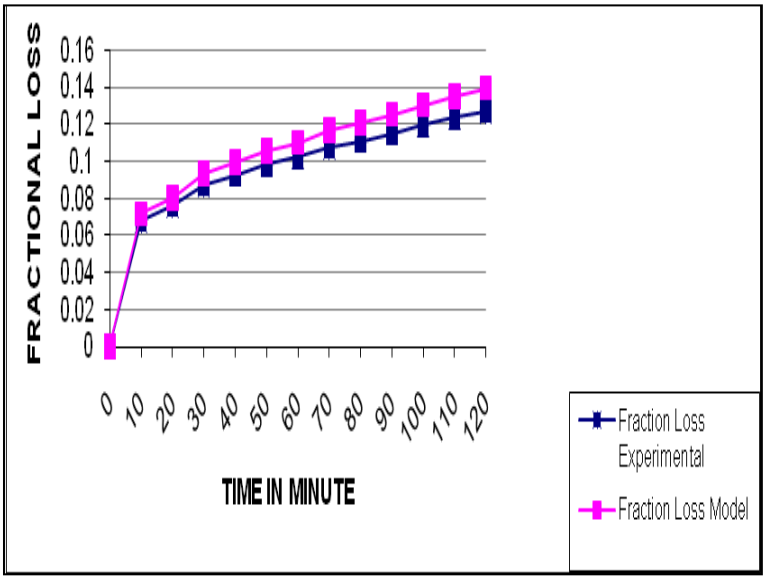

Figure D.54 Comparison of experimental and model fractional loss vs time on addition of coal (+150µm-200µm) to xstrata chromite (+100µm-150µm) at 1200 ºC

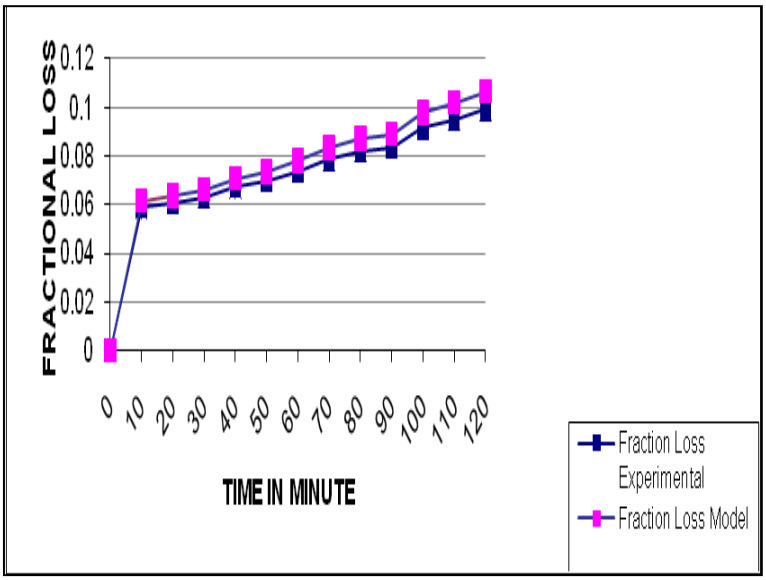

Figure D.55 Comparison of experimental and model fractional loss vs time on addition of coal (+150µm-200µm) to xstrata chromite (+150µm-200µm) at 1200 ºC

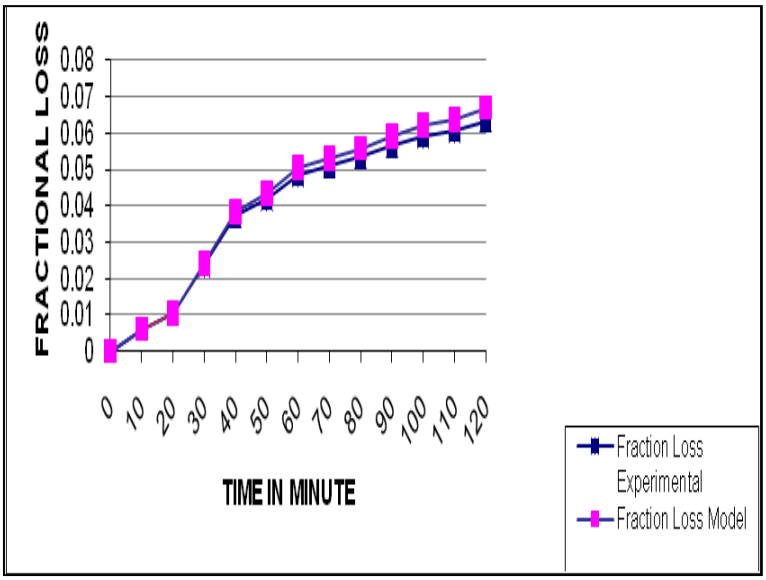

Figure D.56 Comparison of experimental and model fractional loss vs time on addition of charcoal (+50µm-100µm) to xstrata chromite (+50µm-100µm) at 1200 ºC

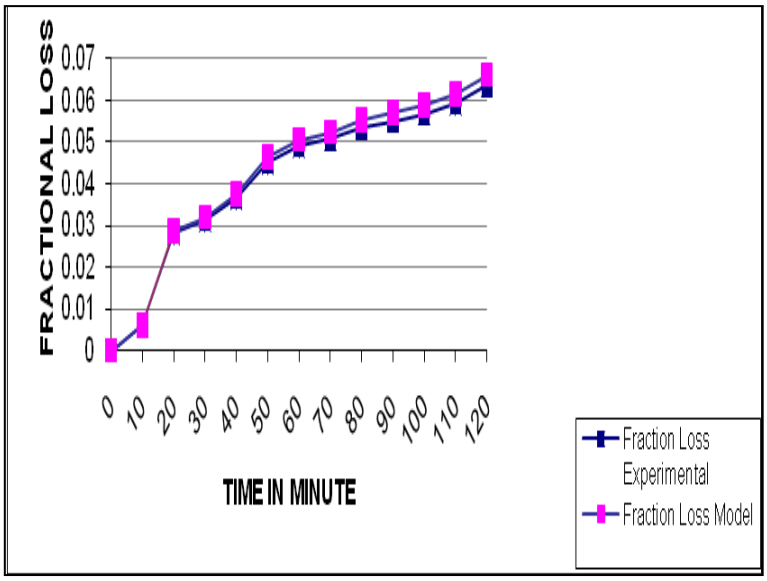

Figure D.57 Comparison of experimental and model fractional loss vs time on addition of charcoal (+100µm-150µm) to xstrata chromite (+50µm-100µm) at 1200 ºC

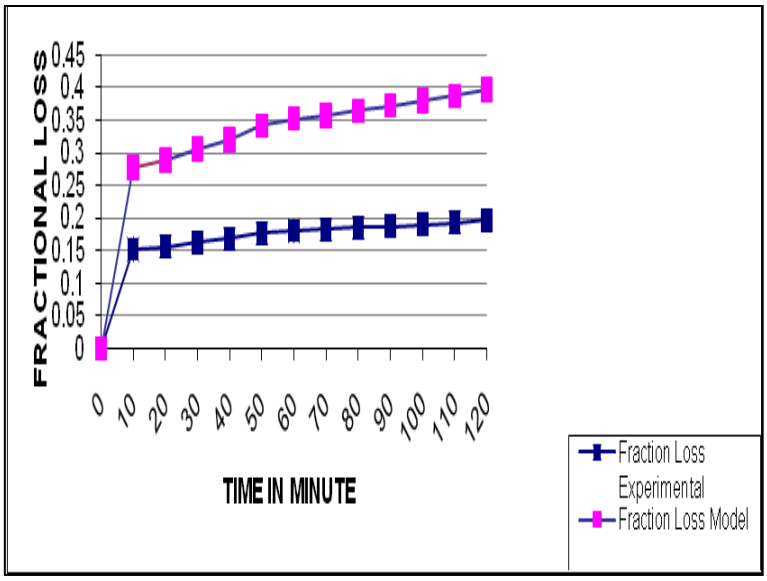

Figure D.58 Comparison of experimental and model fractional loss vs time on addition of charcoal (+150µm-200µm) to xstrata chromite (+50µm-100µm) at 1200 ºC

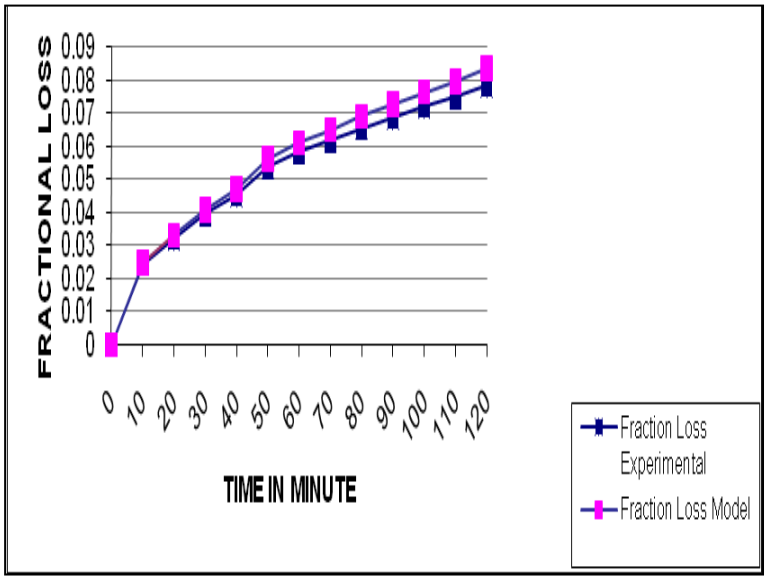

Figure D.59 Comparison of experimental and model fractional loss vs time on addition of charcoal (+50µm-100µm) to xstrata chromite (+100µm-150µm) at 1200 ºC

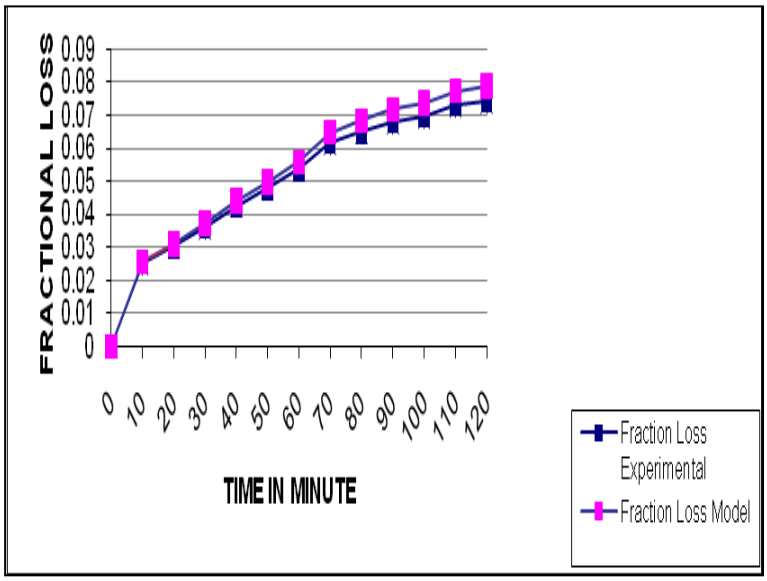

Figure D.60 Comparison of experimental and model fractional loss vs time on addition of charcoal (+100µm-150µm) to xstrata chromite (+100µm-150µm) at 1200 ºC

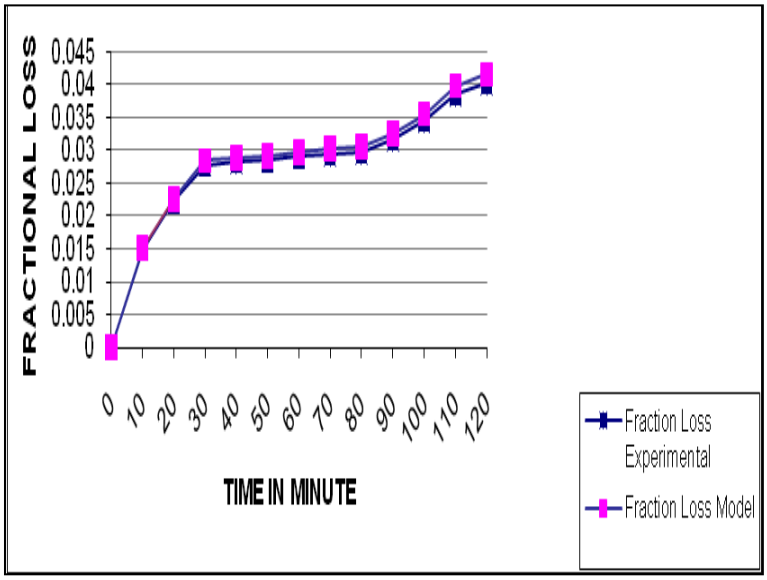

Figure D.61 Comparison of experimental and model fractional loss vs time on addition of charcoal (+50µm-100µm) to xstrata chromite (+150µm-200µm) at 1200 ºC

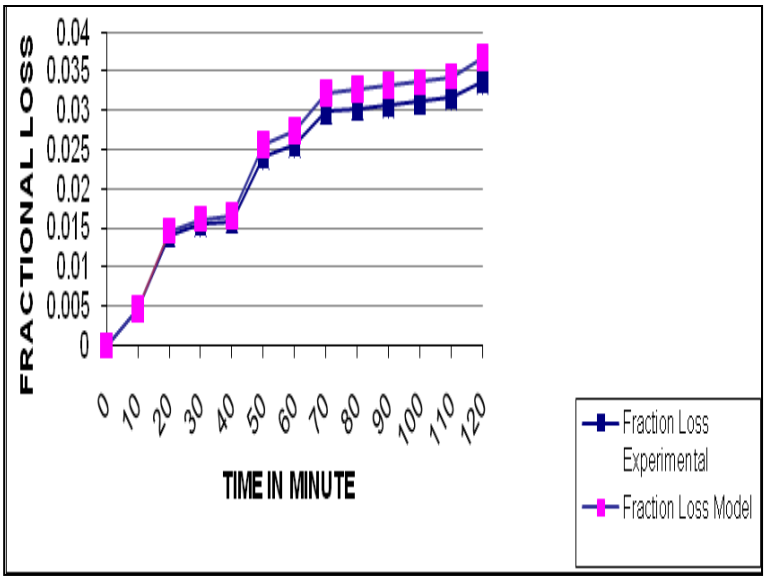

Figure D.62 Comparison of experimental and model fractional loss vs time on addition of charcoal (+100µm-150µm) to xstrata chromite (+150µm-200µm) at 1200 ºC

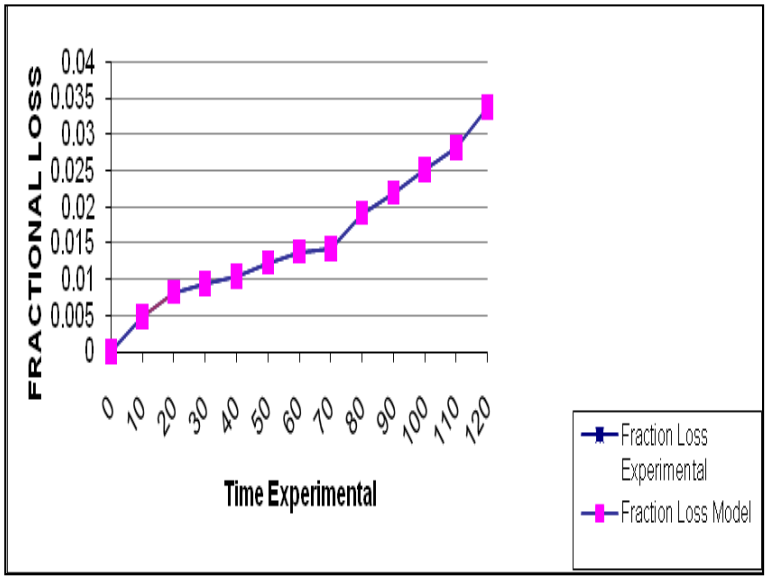

Figure D.63 Comparison of experimental and model fractional loss vs time on addition of charcoal (+150µm-200µm) to xstrata chromite (+150µm-200µm) at 1200 ºC

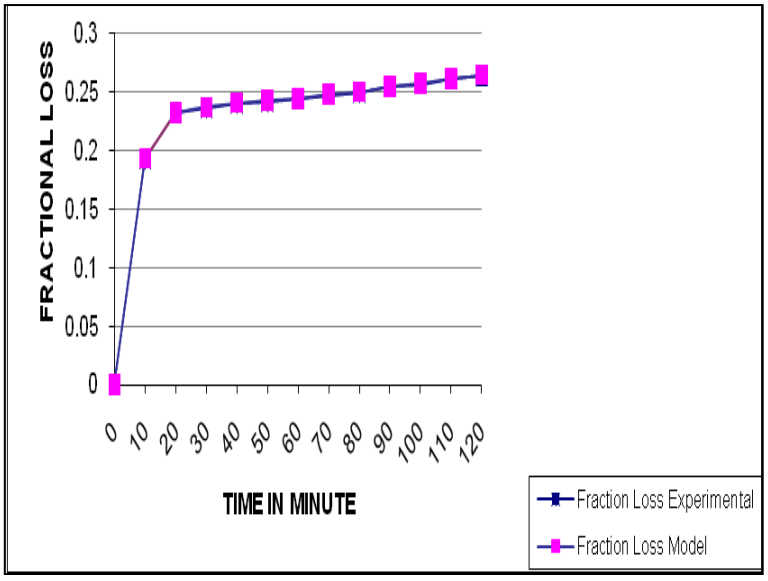

Figure D.64 Comparison of experimental and model fractional loss vs time on addition of charcoal (+100µm-150µm) to xstrata chromite (+100µm-150µm) at 1200 ºC

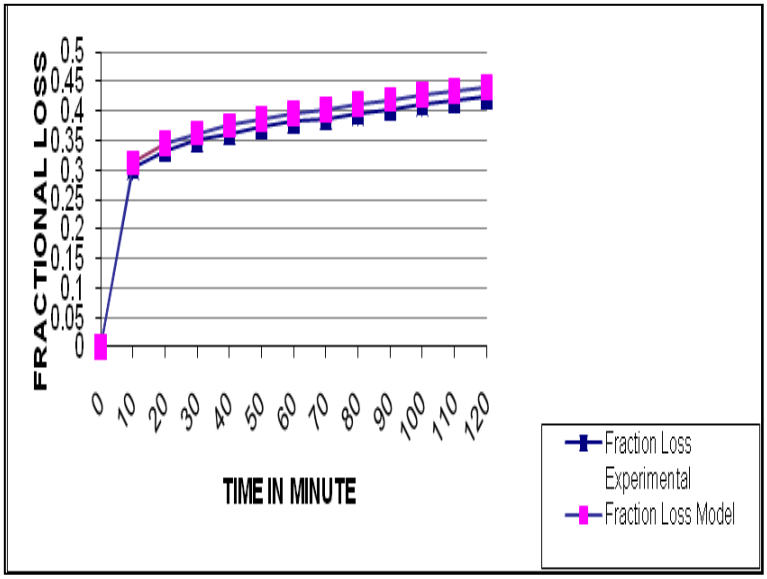

Figure D.65 Comparison of experimental and model fractional loss vs time on addition of charcoal (+50µm-100µm) to xstrata chromite (+50µm-100µm) at 1300 ºC

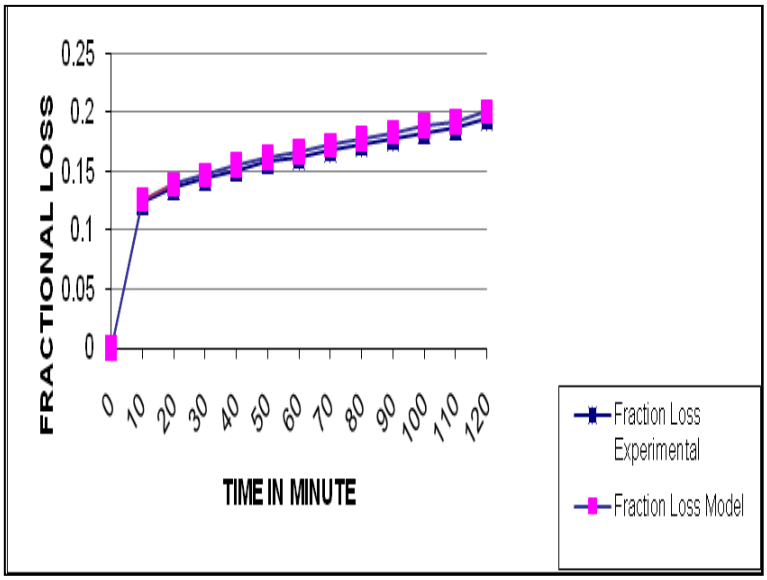

Figure D.66 Comparison of experimental and model fractional loss vs time on addition of charcoal (+100µm-150µm) to xstrata chromite (+50µm-100µm) at 1300 ºC

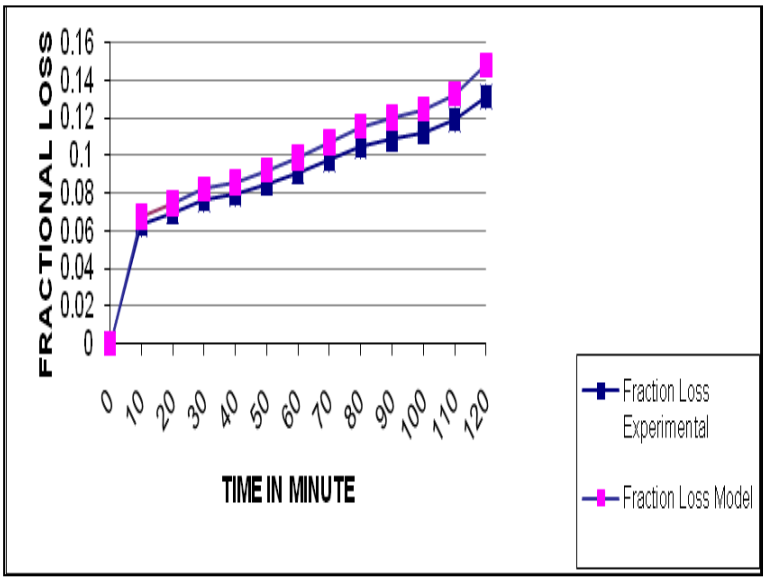

Figure D.67 Comparison of experimental and model fractional loss vs time on addition of charcoal (+50µm-100µm) to xstrata chromite (+100µm-150µm) at 1300 ºC

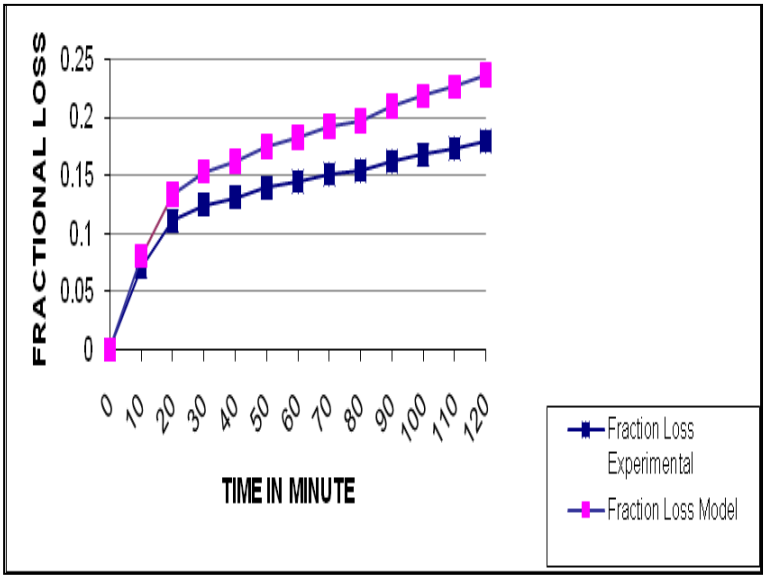

Figure D.68 Comparison of experimental and model fractional loss vs time on addition of coke (+150µm-200µm) to xstrata chromite (+100µm-150µm) at 1300 ºC

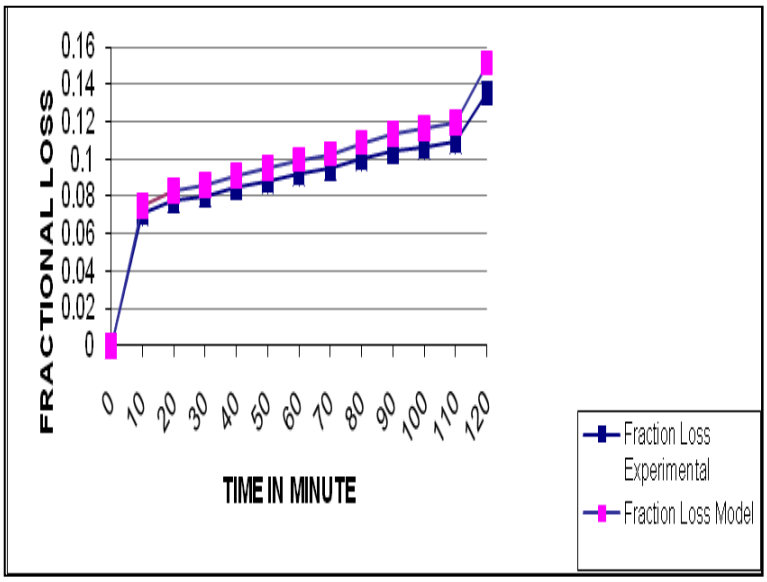

Figure D.69 Comparison of experimental and model fractional loss vs time on addition of coke (+150µm-200µm) to xstrata chromite (+150µm-200µm) at 1300 ºC

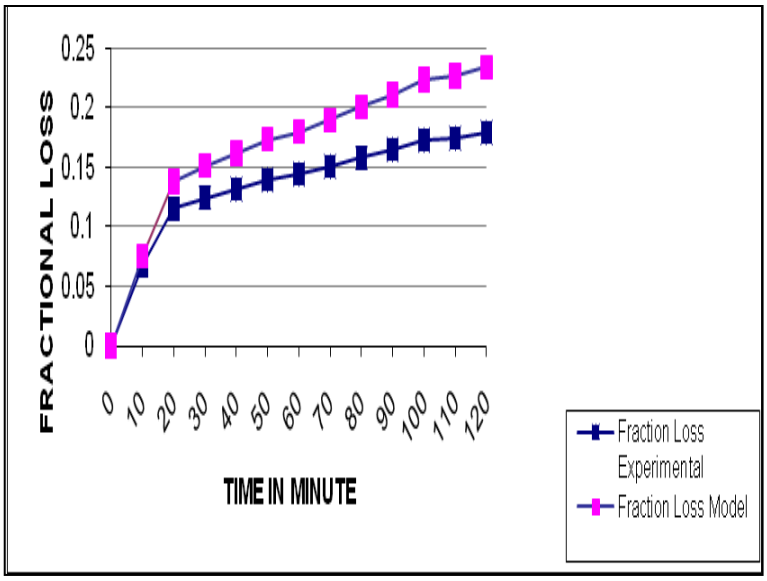

Figure D.70 Comparison of experimental and model fractional loss vs time on addition of coke (+100µm-150µm) to xstrata chromite (+100µm-150µm) at 1300 ºC

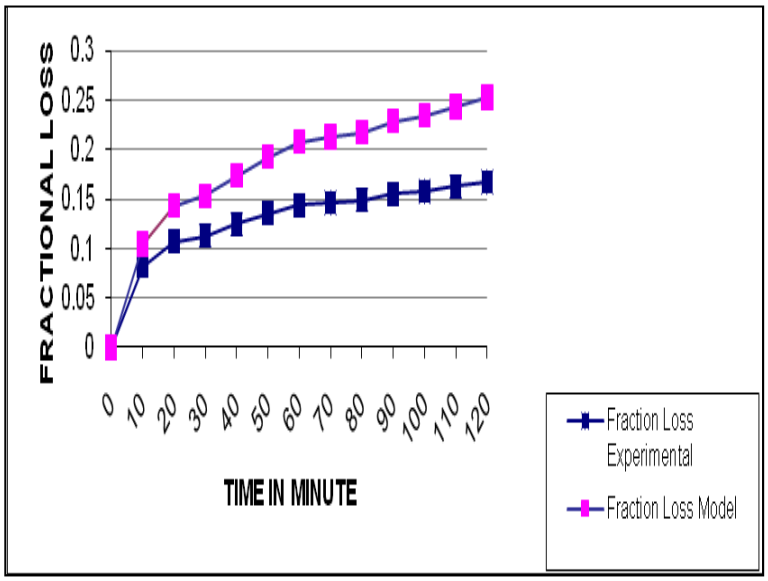

Figure D.71 Comparison of experimental and model fractional loss vs time on addition of coke (+50µm-100µm) to xstrata chromite (+150µm-200µm) at 1300 ºC

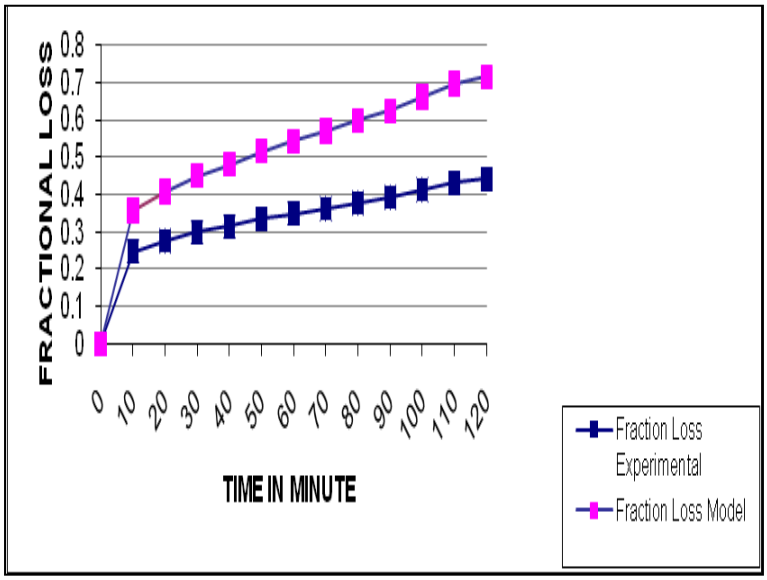

Figure D.72 Comparison of experimental and model fractional loss vs time on addition of coal (+50µm-100µm) to xstrata chromite (+50µm-100µm) at 1300 ºC

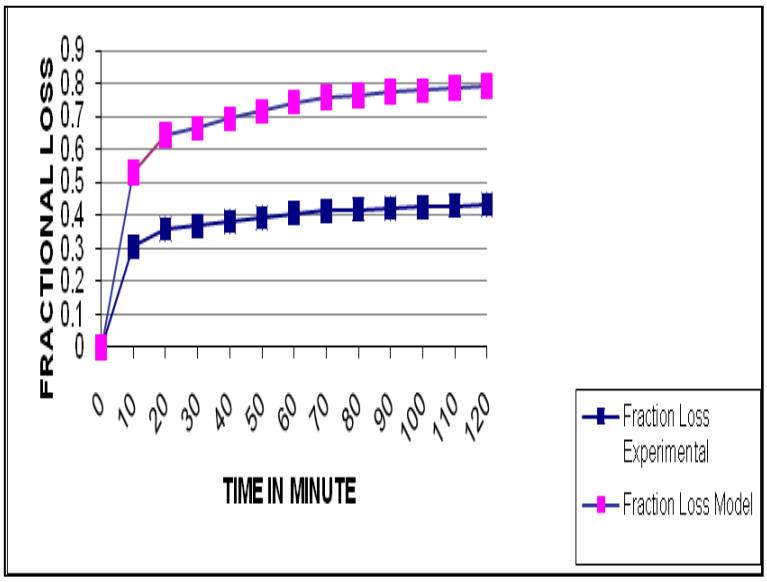

Figure D.73 Comparison of experimental and model fractional loss vs time on addition of coal (+100µm-150µm) to xstrata chromite (+50µm-100µm) at 1300 ºC

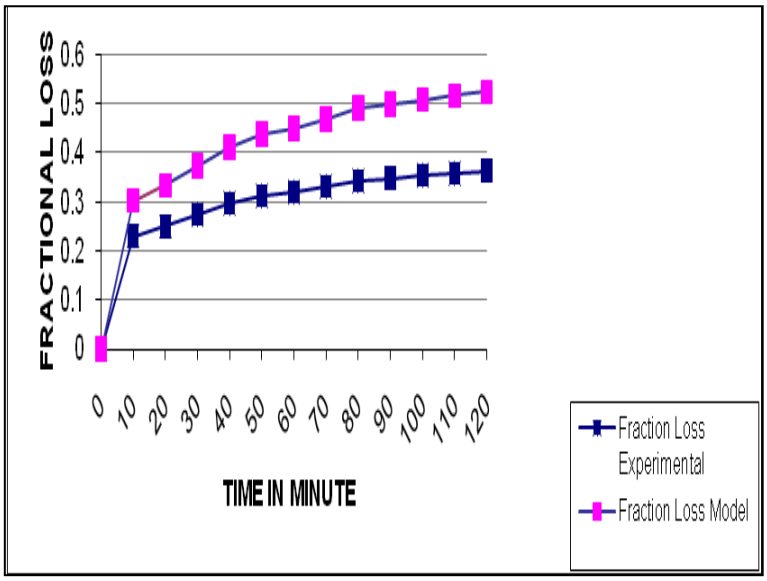

Figure D.74 Comparison of experimental and model fractional loss vs time on addition of coal (+150µm-200µm) to xstrata chromite (+50µm-100µm) at 1300 ºC

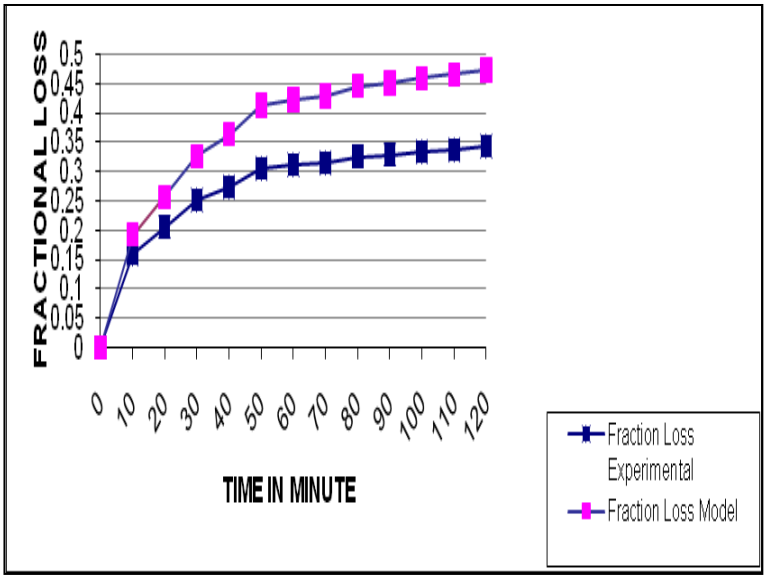

Figure D.75 Comparison of experimental and model fractional loss vs time on addition of coal (+100µm-150µm) to xstrata chromite (+100µm-150µm) at 1300 ºC

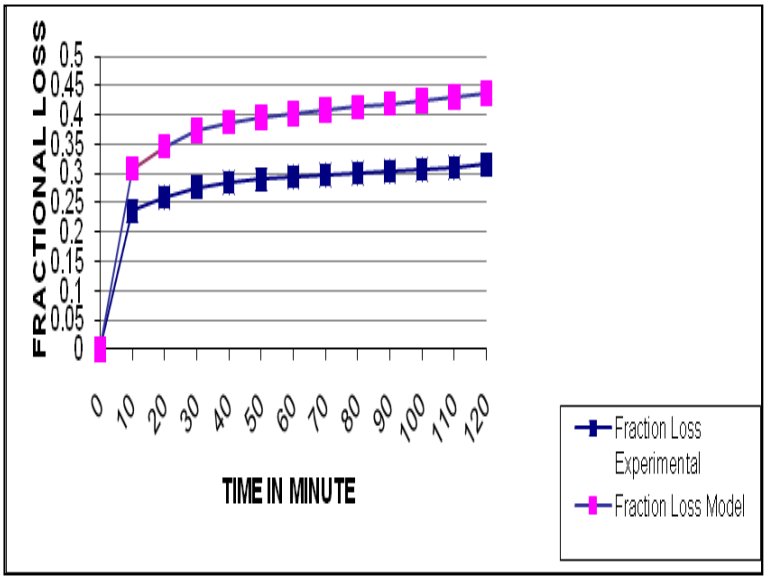

Figure D.76 Comparison of experimental and model fractional loss vs time on addition of coal (+150µm-200µm) to xstrata chromite (+100µm-150µm) at 1300 ºC

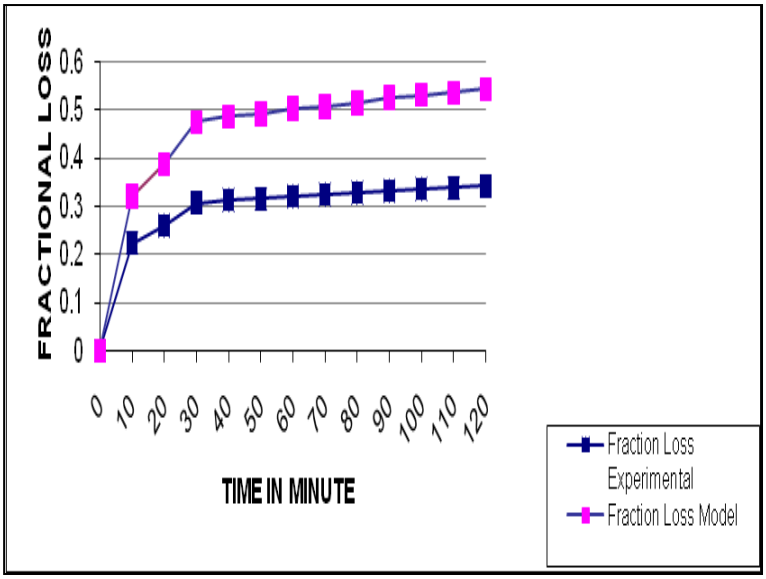

Figure D.77 Comparison of experimental and model fractional loss vs time on addition of coal (+100µm-150µm) to xstrata chromite (+150µm-200µm) at 1300 ºC

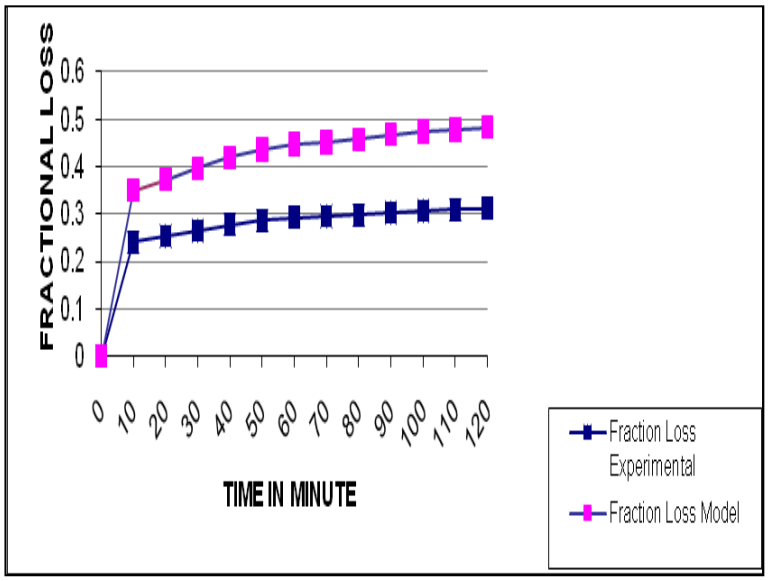

Figure D.78 Comparison of experimental and model fractional loss vs time on addition of coal (+150µm-200µm) to xstrata chromite (+150µm-200µm) at 1300 ºC

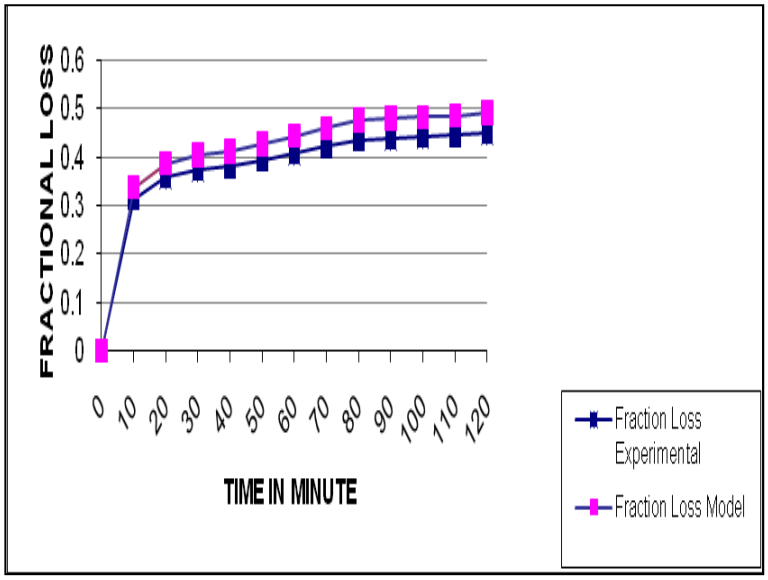

Figure D.79 Comparison of experimental and model fractional loss vs time on addition of coal (+50µm-100µm) to xstrata chromite (+50µm-100µm) at 1300 ºC

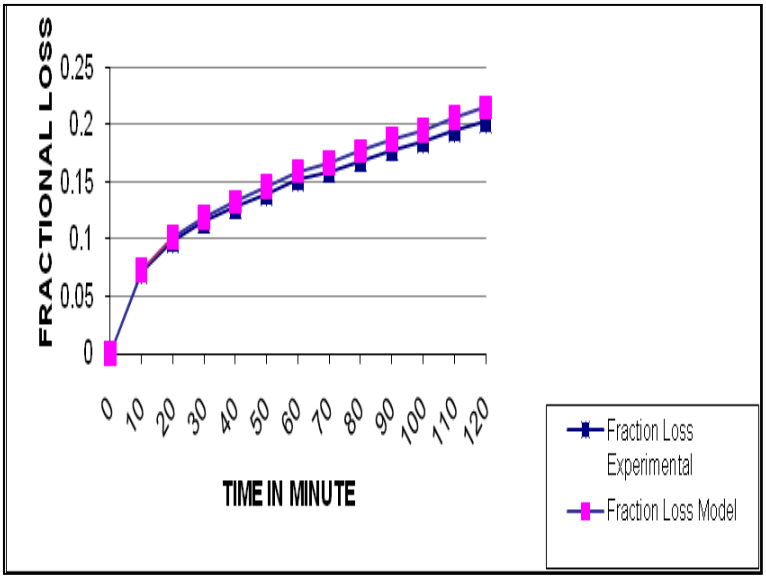

Figure D.80 Comparison of experimental and model fractional loss vs time on addition of charcoal (+50µm-100µm) to xstrata chromite (+50µm-100µm) at 1300 ºC

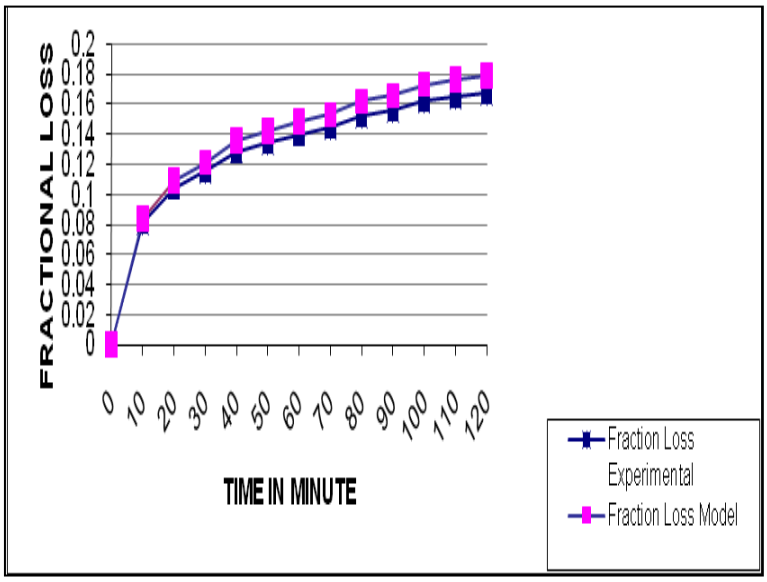

Figure D.81 Comparison of experimental and model fractional loss vs time on addition of charcoal (+50µm-100µm) to xstrata chromite (+100µm-150µm) at 1300 ºC

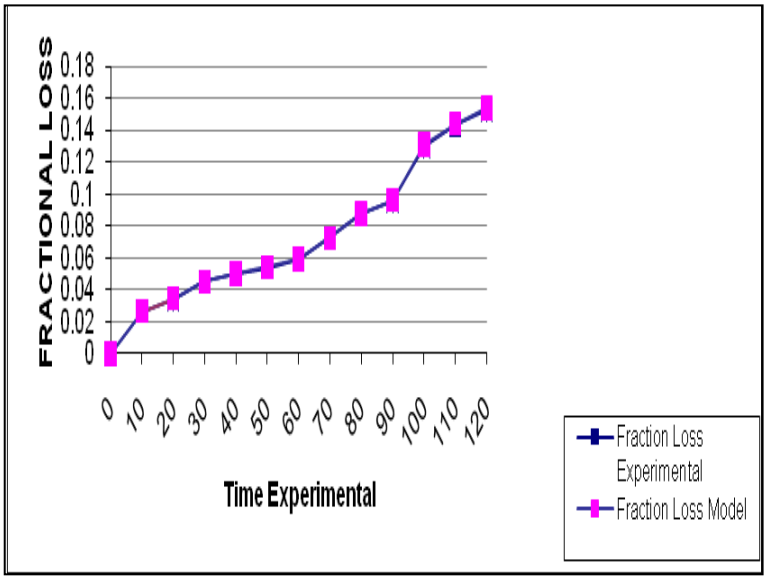

Figure D.82 Comparison of experimental and model fractional loss vs time on addition of charcoal (+50µm-100µm) to xstrata chromite (+150µm-200µm) at 1300 ºC

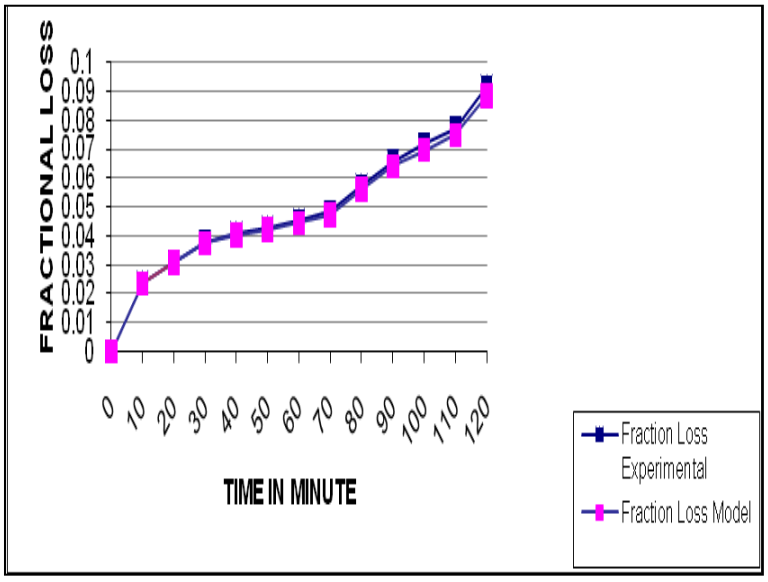

Figure D.83 Comparison of experimental and model fractional loss vs time on addition of charcoal (+100µm-150µm) to xstrata chromite (+150µm-200µm) at 1300 ºC

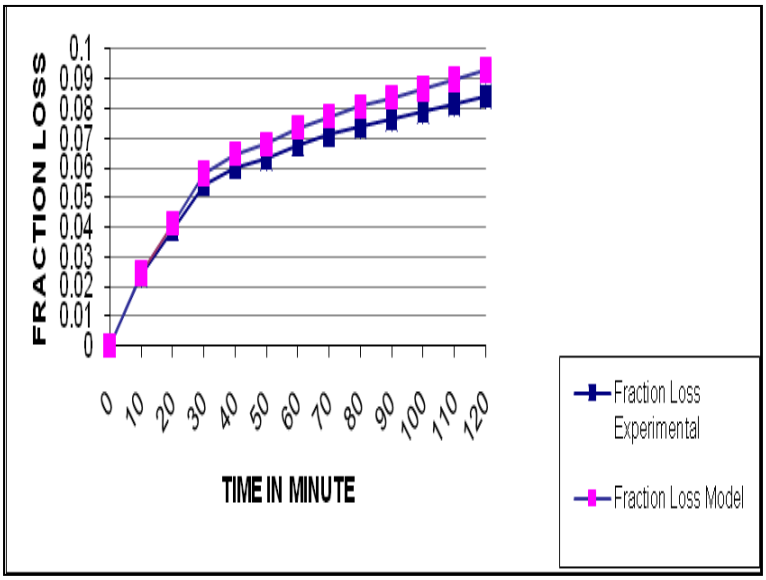

Figure D.84 Comparison of experimental and model fractional loss vs time on addition of charcoal (+150µm-200µm) to xstrata chromite (+150µm-200µm) at 1300 ºC

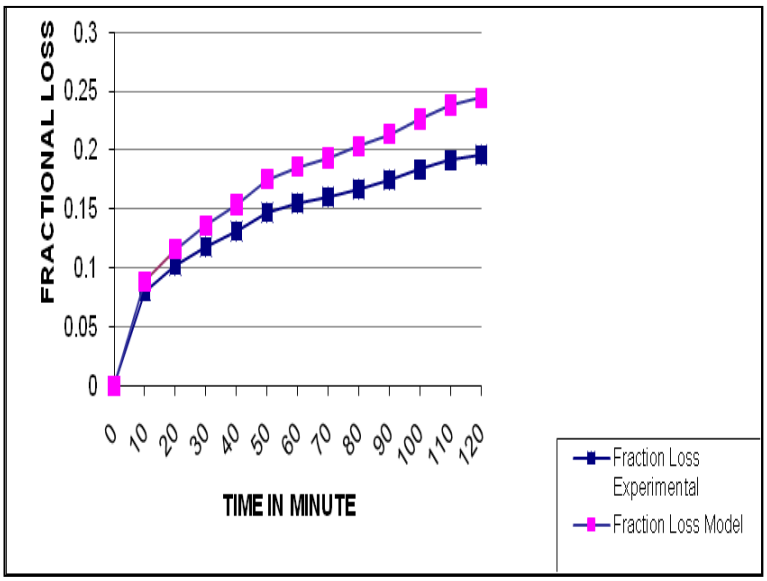

Figure D.85 Comparison of experimental and model fractional loss vs time on addition of charcoal (+100µm-150µm) to xstrata chromite (+50µm-100µm) at 1300 ºC

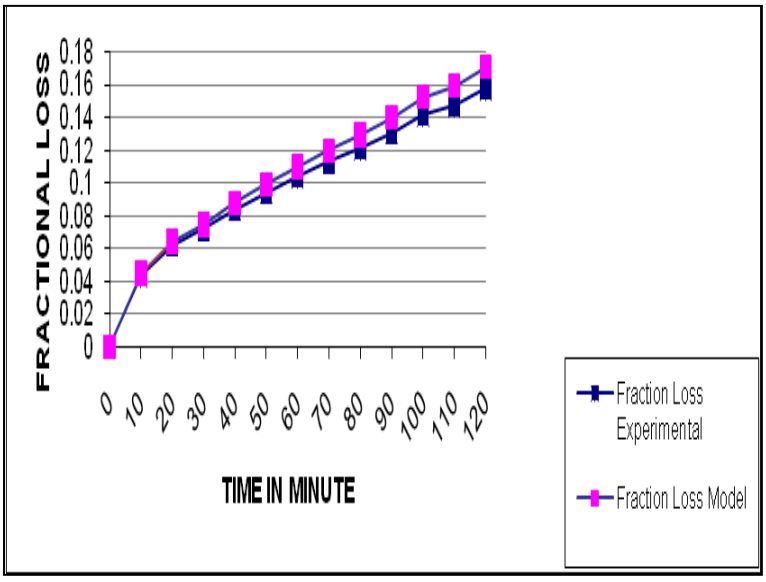

Figure D.86 Comparison of experimental and model fractional loss vs time on addition of charcoal (+150µm-200µm) to xstrata chromite (+50µm-100µm) at 1300 ºC

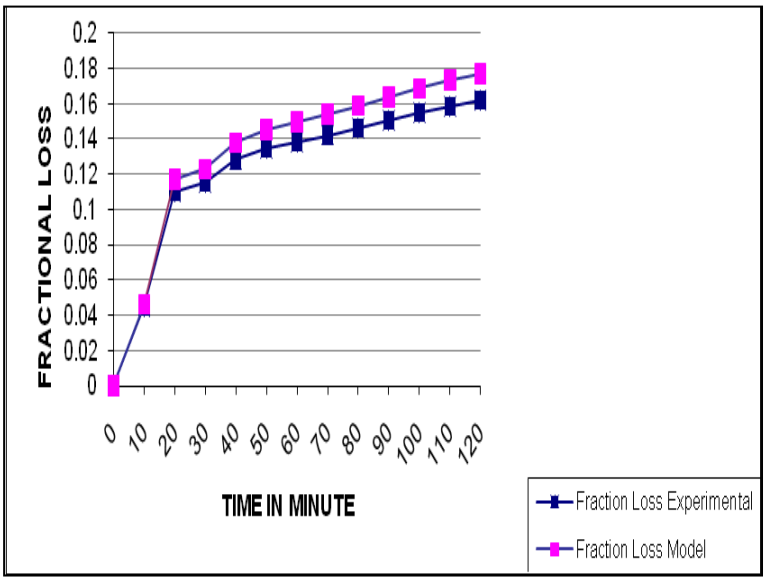

Figure D.87 Comparison of experimental and model fractional loss vs time on addition of charcoal (+100µm-150µm) to xstrata chromite (+100µm-150µm) at 1300 ºC

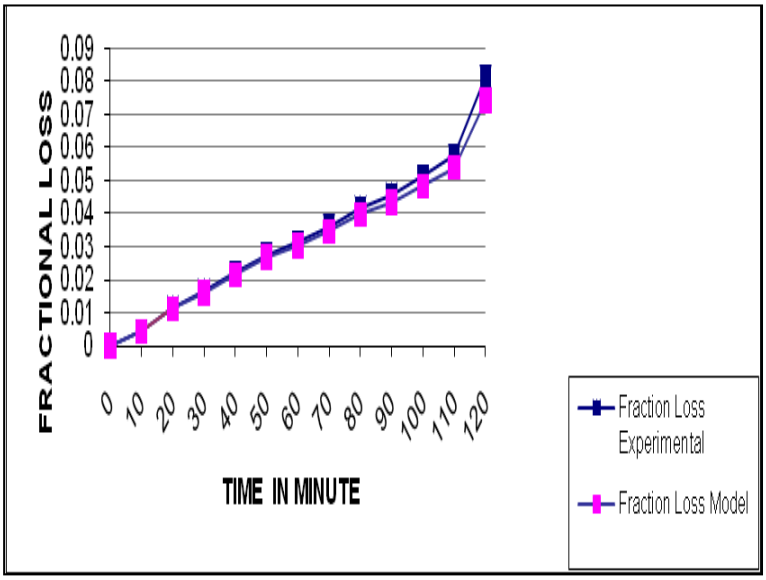

Figure D.88 Comparison of experimental and model fractional loss vs time on addition of charcoal (as received) to xstrata chromite (as received) at 1300 ºC

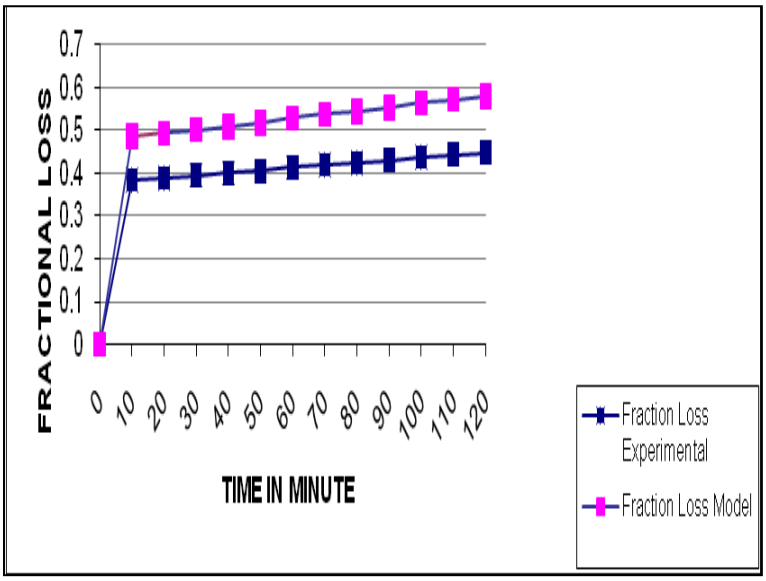

Figure D.89 Comparison of experimental and model fractional loss vs time on addition of coal (as received) to xstrata chromite (as received) at 1300 ºC

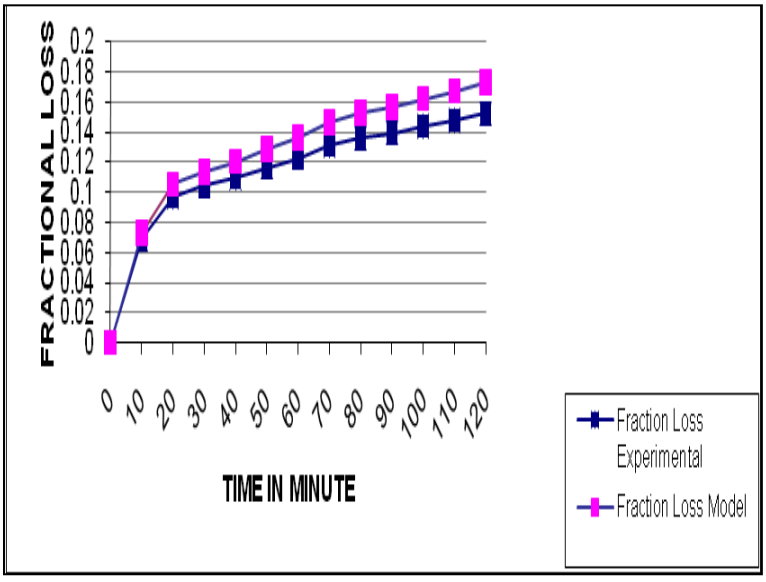

Figure D.90 Comparison of experimental and model fractional loss vs time on addition of coke (as received) to xstrata chromite (as received) at 1300 ºC

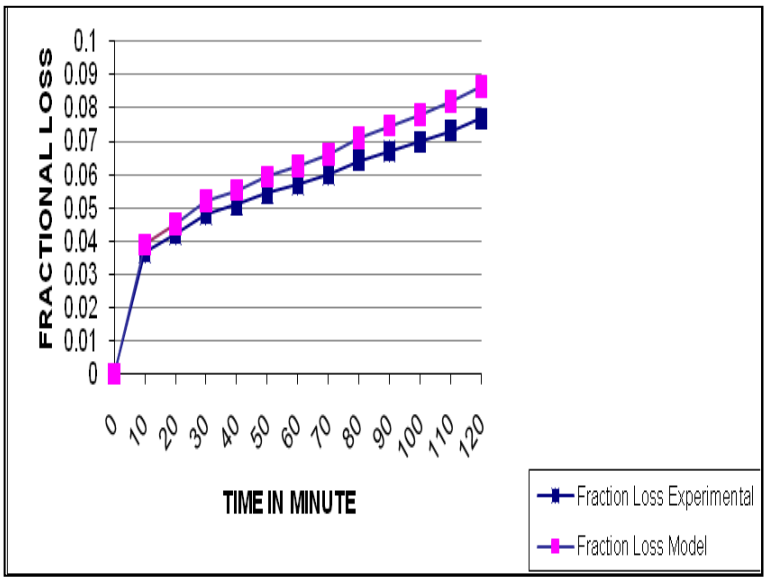

Figure D.91 Comparison of experimental and model fractional loss vs time on addition of graphite (as received) to xstrata chromite (as received) at 1300 ºC

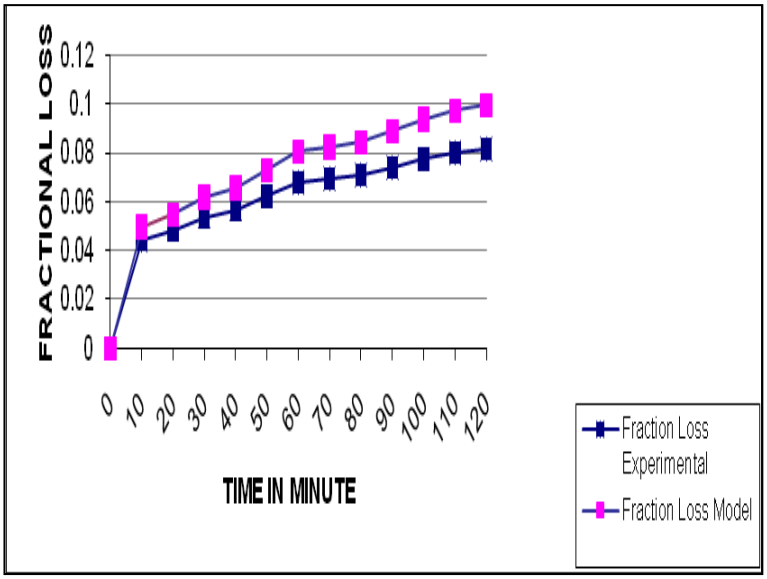

Figure D.92 Comparison of experimental and model fractional loss vs time on addition of charcoal (as received) to xstrata chromite (as received) at 1300 ºC

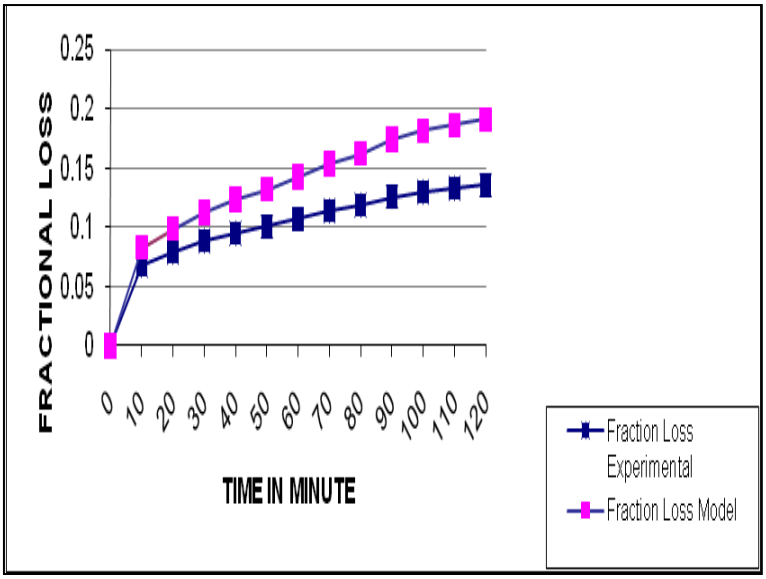

Figure D.93 Comparison of experimental and model fractional loss vs time on addition of coke (as received) to xstrata chromite (as received) at 1200 ºC

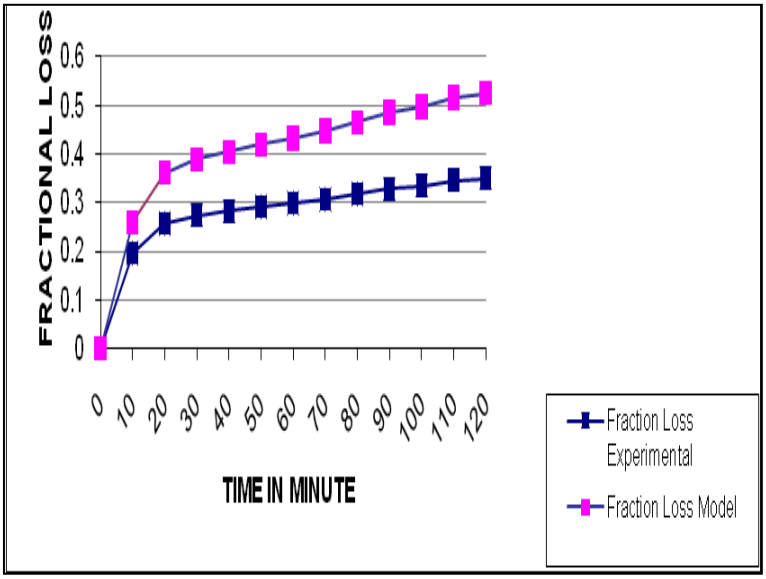

Figure D.94 Comparison of experimental and model fractional loss vs time on addition of coal (as received) to xstrata chromite (as received) at 1200 ºC

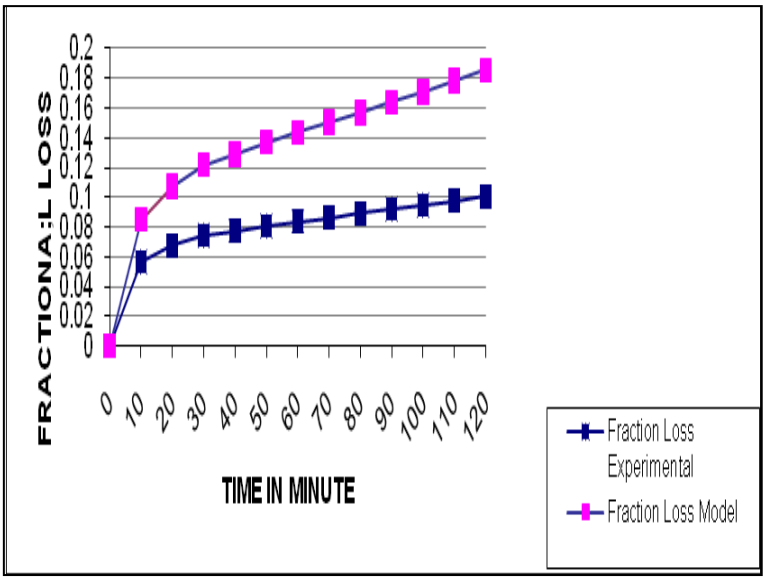

Figure D.95 Comparison of experimental and model fractional loss vs time on addition of coke (as received) to xstrata chromite (as received) at 1200 ºC

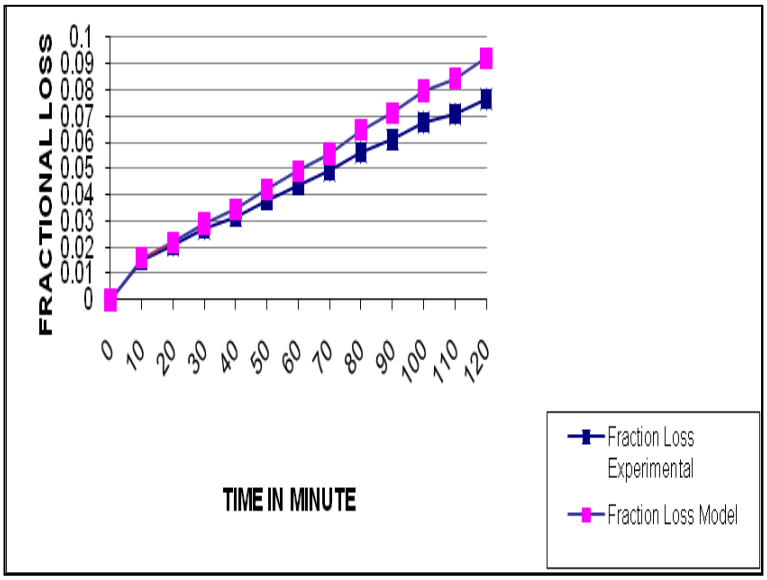

Figure D.96 Comparison of experimental and model fractional loss vs time on addition of charcoal (as received) to xstrata chromite (as received) at 1200 ºC

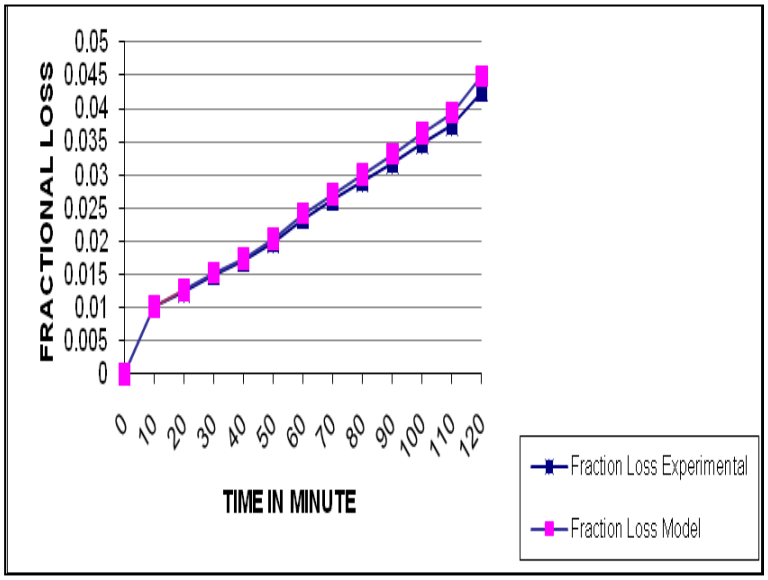

Figure D.97 Comparison of experimental and model fractional loss vs time on addition of graphite (as received) to xstrata chromite (as received) at 1100 ºC

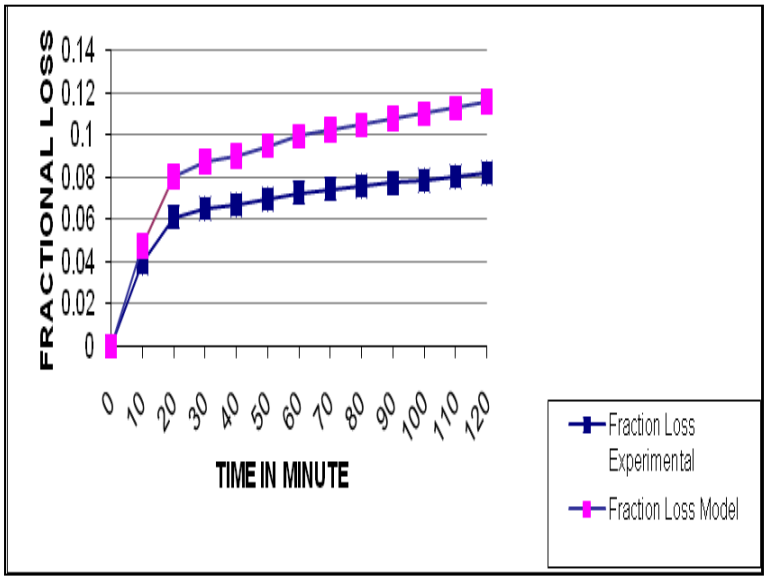

Figure D.98 Comparison of experimental and model fractional loss vs time on addition of charcoal (as received) to xstrata chromite (as received) at 1000 ºC

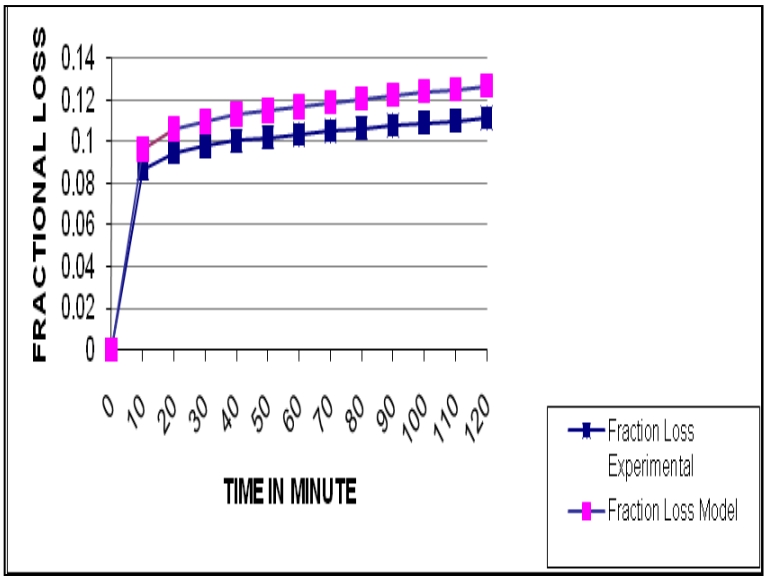

Figure D.99 Comparison of experimental and model fractional loss vs time on addition of coke (as received) to xstrata chromite (as received) at 1000 ºC

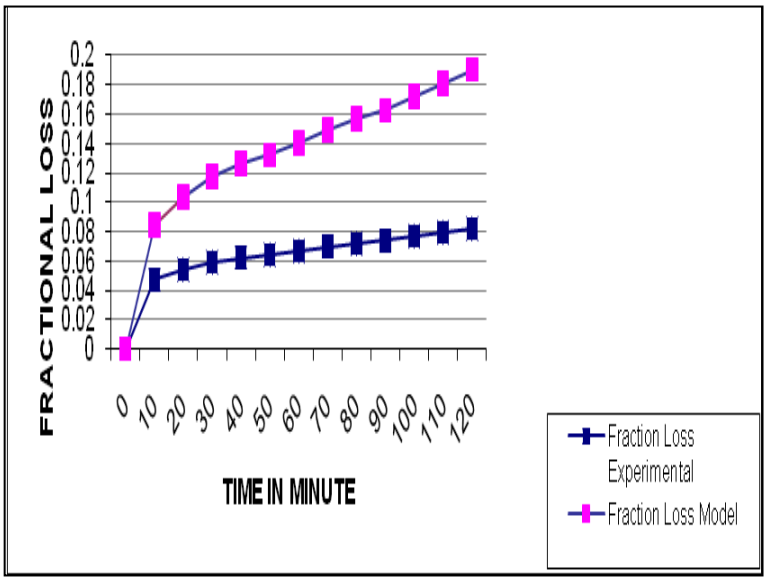

Figure D.100 Comparison of experimental and model fractional loss vs time on addition of coal (as received) to xstrata chromite (as received) at 1000 ºC

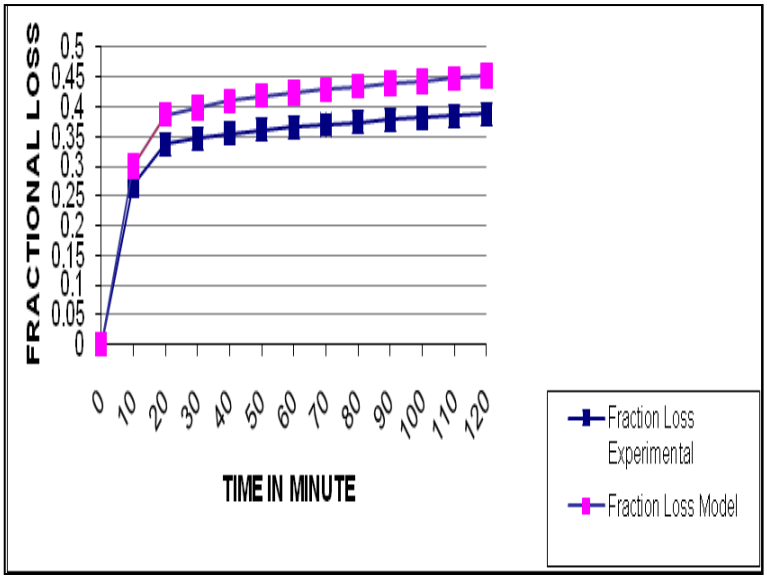

Figure D.101 Comparison of experimental and model fractional loss vs time on addition of coal (+50µm-100µm) to xstrata chromite (+150µm-200µm) received) at 1000 ºC

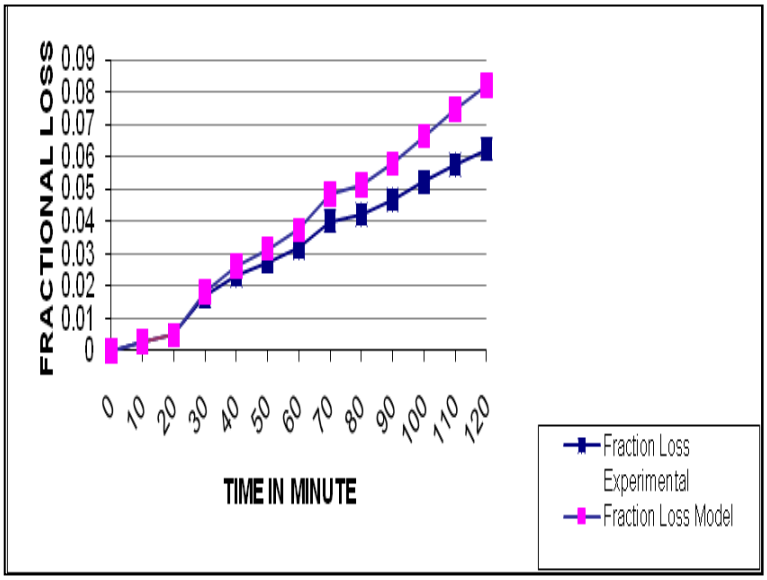

Figure D.102 Comparison of experimental and model fractional loss vs time on addition of graphite (as received) to xstrata chromite (as received) at 1000 ºC

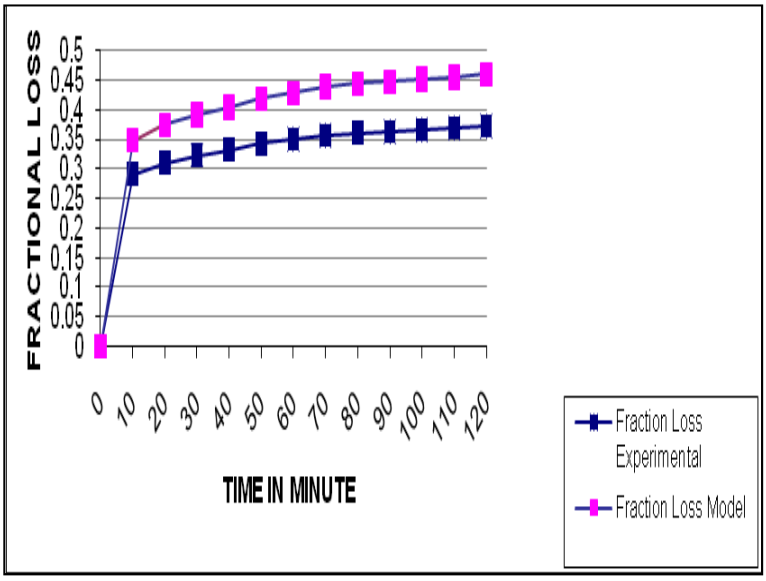

Figure D.103 Comparison of experimental and model fractional loss vs time on addition of coal (+50µm-100µm) to xstrata chromite (+100µm-150µm) received) at 1000 ºC

Table of Calculation of Reactivity of Reductants

Table E1: Chromite (+50µm-100µm) and Coke (+50µm-100µm) at1100ºC Run 33

At °C	Mass (read)	Mass loss	Fraction loss(Exp)	Chemical Factor	Diffusion Factor	Time (Exp)	Time (model)	Fraction loss (Model)
1100	35.646	0	0	0	0	0	0	0
1100	35.284	0.362	0.050535	0.017137068	0.00087097	10	26.4895	0.052048871
1100	35.174	0.472	0.065891	0.022464613	0.00149130	20	35.0391	0.068453947
1100	34.898	0.748	0.104421	0.036094039	0.00381429	30	57.5739	0.110784716
1100	34.806	0.840	0.117264	0.040723925	0.00484024	40	65.4421	0.125257022
1100	34.783	0.863	0.120475	0.041888406	0.00511692	50	67.4378	0.128902726
1100	34.705	0.941	0.131364	0.045858744	0.00611619	60	74.2927	0.141347664
1100	34.664	0.982	0.137087	0.047959032	0.00667959	70	77.9502	0.147939055
1100	34.626	1.020	0.142392	0.049913951	0.0072255	80	81.3739	0.154078456
1100	34.601	1.045	0.145882	0.051204481	0.00759719	90	83.6442	0.158133313
1100	34.533	1.113	0.155375	0.054732605	0.00865905	100	89.8921	0.169225225
1100	34.502	1.144	0.159702	0.056349790	0.00916804	110	92.7759	0.174311958
1100	34.469	1.177	0.164309	0.058077422	0.00972717	120	95.8706	0.179747369

Table E2: Chromite (+50µm-100µm) and Coke (+100µm-150µm) at1100ºC Run 34

At	Mass (read)	Mass Loss	Fraction loss (Exp)	Chemical Factor	Diffusion Factor	Time (Exp)	Time (model)	Fraction loss (Mode)
1100	40.77	0	0	0	0	0	0	0
1100	40.42	0.349	0.0487204	0.016511254	0.00080886	10	30.12469	0.049372228
1100	40.35	0.415	0.057934	0.019696748	0.0011486	20	36.02845	0.058853535
1100	40.26	0.508	0.0709168	0.024220846	0.00173153	30	44.46329	0.072290012
1100	40.17	0.598	0.0834808	0.028639314	0.00241365	40	52.75759	0.085377307
1100	40.09	0.675	0.0942300	0.032451723	0.00309099	50	59.95860	0.09663922
1100	40.02	0.746	0.1041416	0.035993882	0.00379341	60	66.68569	0.107076098
1100	39.95	0.816	0.1139136	0.039511822	0.00456018	70	73.40137	0.117414761
1100	39.86	0.903	0.1260588	0.043920357	0.00561755	80	81.86542	0.130330933
1100	39.79	0.976	0.1362496	0.047651094	0.00659548	90	89.06971	0.14122493
1100	39.7	1.066	0.1488136	0.052291247	0.00791716	100	98.08282	0.154725533
1100	39.63	1.133	0.1581668	0.055775316	0.00898564	110	104.8884	0.164825198
1100	39.58	1.183	0.1651468	0.058392219	0.00983076	120	110.0214	0.172389255

Table E3: Chromite (+50µm-100µm) and Coke (+150µm-200µm) at1100ºC Run 35

At °C	Mass (read)	Mass loss	Fraction loss (Exp)	Chemical Factor	Diffusion Factor	Time (Exp)	Time (model)	Fraction loss (Model)
1100	40.856	0	0	0	0	0	0	0
1100	40.703	0.153	0.0213588	0.007170899	0.0001535	10	15.8834	0.021503248
1100	40.625	0.231	0.0322476	0.010866861	0.0003517	20	24.1533	0.032576019
1100	40.532	0.324	0.0452304	0.015310000	0.0006960	30	34.1692	0.045874442
1100	40.449	0.407	0.0568172	0.019309525	0.0011042	40	43.2539	0.057830510
1100	40.367	0.489	0.0682644	0.023293159	0.0016024	50	52.3667	0.069722809
1100	40.251	0.605	0.0844580	0.028984660	0.0024716	60	65.4964	0.086680699
1100	40.196	0.660	0.0921360	0.031706689	0.0029522	70	71.8213	0.094775573
1100	40.123	0.733	0.1023268	0.035343371	0.0036592	80	80.3168	0.105573182
1100	40.038	0.818	0.1141928	0.039612714	0.0045832	90	90.3562	0.118221798
1100	39.954	0.902	0.1259192	0.043869453	0.0056047	100	100.436	0.130800949
1100	39.87	0.986	0.1376456	0.048164435	0.0067360	110	110.677	0.143457827
1100	39.843	1.013	0.1414148	0.049553230	0.0071232	120	114.003	0.147542421

Table E4: Chromite (+100µm-150µm) and Coke (+50µm-100µm) at1100ºC Run 36

At °C	Mass (read)	Mass loss	Fraction loss (Exp)	Chemical Factor	Diffusion Factor	Time (Exp)	Time (model)	Fraction loss (Model)
1100	40.48	0	0	0	0	0	0	0
1100	40.42	0.057	0.0079572	0.002659466	2.118E-05	10	8.49758	0.007945349
1100	40.37	0.116	0.0161936	0.005427269	8.805E-05	20	17.3144	0.016144609
1100	40.28	0.203	0.0283388	0.009536931	0.0002711	30	30.3555	0.028189180
1100	40.22	0.266	0.0371336	0.012534319	0.0004674	40	39.8294	0.036877220
1100	40.16	0.317	0.0442532	0.014974173	0.0006660	50	47.5178	0.043889685
1100	40.10	0.384	0.0536064	0.018197957	0.0009814	60	57.6446	0.053074148
1100	40.03	0.451	0.0629596	0.021443051	0.0013597	70	67.8019	0.062227030
1100	39.95	0.535	0.0746860	0.025542182	0.0019239	80	80.5807	0.073658013
1100	39.85	0.627	0.0875292	0.030071639	0.0026585	90	94.6341	0.086121645
1100	39.80	0.679	0.0947884	0.032650592	0.0031286	100	102.605	0.093140624
1100	39.80	0.684	0.0954864	0.032899294	0.0031759	110	103.372	0.093814554
1100	39.68	0.800	0.1116800	0.038705450	0.0043784	120	121.230	0.109402186

TableE 5: Chromite (+100µm-150µm) and Coke (+100µm-150µm) at1100ºC Run 37

At °C	Mass (read)	Mass loss	Fraction loss (Exp)	Chemical Factor	Diffusion Factor	Time (Exp)	Time (model)	Fraction loss (Model)
1100	37.5	0	0	0	0	0	0	0
1100	37.09	0.411	0.0573756	0.019503098	0.0011263	10	30.9441	0.060620187
1100	37.00	0.497	0.0693812	0.023683549	0.0016562	20	38.0096	0.074109103
1100	36.92	0.577	0.0805492	0.027604743	0.0022440	30	44.7731	0.086899967
1100	36.83	0.671	0.0936716	0.032252935	0.0030537	40	52.9599	0.102224110
1100	36.76	0.744	0.1038624	0.035893746	0.0037726	50	59.4995	0.114341179
1100	36.68	0.822	0.1147512	0.039814561	0.0046294	60	66.6659	0.127493793
1100	36.60	0.897	0.1252212	0.043615014	0.0055409	70	73.7338	0.140337532
1100	36.50	0.997	0.1391812	0.048729751	0.0068923	80	83.4331	0.157756905
1100	36.48	1.021	0.1425316	0.049965504	0.0072402	90	85.8085	0.161986766
1100	36.42	1.082	0.1510472	0.053120934	0.0081657	100	91.9300	0.172821954
1100	36.35	1.147	0.1601212	0.056506586	0.0092181	110	98.5871	0.184498852
1100	36.30	1.203	0.1679388	0.059443064	0.0101804	120	104.435	0.194665483

TableE 6: Chromite (+100µm-150µm) and Coke (+150µm-200µm) at1100ºC Run 38

At °C	Mass (read)	Mass loss	Fraction loss (Exp)	Chemical Factor	Diffusion Factor	Time (Exp)	Time (model)	Fraction loss (Model)
1100	37.5	0	0	0	0	0	0	0
1100	37.26	0.244	0.0340624	0.011485546	0.0003927	10	25.6217	0.034533294
1100	37.21	0.291	0.0406236	0.013728818	0.0005603	20	30.7076	0.041292294
1100	37.13	0.369	0.0515124	0.017474375	0.0009054	30	39.2585	0.052584661
1100	37.06	0.437	0.0610052	0.020763193	0.0012754	40	46.8269	0.062505372
1100	36.97	0.527	0.0735692	0.025150301	0.0018658	50	57.0099	0.075743605
1100	36.88	0.617	0.0861332	0.029577256	0.0025727	60	67.3854	0.089103360
1100	36.80	0.701	0.0978596	0.033745839	0.0033395	70	77.2464	0.101680708
1100	36.75	0.748	0.1044208	0.036094039	0.0038143	80	82.8397	0.108763115
1100	36.70	0.803	0.1120988	0.038856542	0.0044122	90	89.4553	0.117091699
1100	36.64	0.864	0.1206144	0.041939099	0.0051291	100	96.8822	0.126379670
1100	36.56	0.943	0.1316428	0.045960982	0.0061431	110	106.643	0.138486856
1100	36.52	0.985	0.1375060	0.048113076	0.0067219	120	111.898	0.144959249

Table E7: Chromite (+150µm-200µm) and Coke (+50µm-100µm) at1100ºC Run 39

At °C	Mass (read)	Mass loss	Fraction loss (Exp)	Chemical Factor	Diffusion Factor	Time (Exp)	Time (model)	Fraction loss (Model)
1100	39.83	0	0	0	0	0	0	0
1100	39.39	0.439	0.0612844	0.020860258	0.0012873	10	32.8351	0.064243245
1100	39.3	0.527	0.0735692	0.025150301	0.0018658	20	39.9644	0.077818189
1100	39.23	0.599	0.0836204	0.028688634	0.0024219	30	45.9392	0.089093280
1100	39.16	0.668	0.0932528	0.032103897	0.0030258	40	51.7868	0.100038942
1100	39.07	0.756	0.1055376	0.036494874	0.0038984	50	59.4204	0.114195265
1100	39.00	0.832	0.1161472	0.040319551	0.0047459	60	66.1744	0.126595951
1100	38.93	0.903	0.1260588	0.043920357	0.0056175	70	72.6216	0.138324808
1100	38.86	0.968	0.1351328	0.047240819	0.0064842	80	78.6423	0.149182572
1100	38.78	1.049	0.1464404	0.051411292	0.0076576	90	86.3060	0.162870929
1100	38.72	1.114	0.1555144	0.054784686	0.0086752	100	92.5873	0.173979895
1100	38.63	1.197	0.1671012	0.059127564	0.0100748	110	100.781	0.188323020
1100	38.59	1.244	0.1736624	0.061604669	0.0109178	120	105.508	0.196522068

Table E8: Chromite (+150µm-200µm) and Coke (+100µm-150µm) at1100ºC Run 40

At °C	Mass (read)	Mass loss	Fraction loss (Exp)	Chemical Factor	Diffusion Factor	Time (Exp)	Time (model)	Fraction loss (Model)
1100	48.039	0	0	0	0	0	0	0
1100	47.916	0.123	0.0171708	0.005756676	9.904E-05	10	20.84288	0.017268696
1100	47.891	0.148	0.0206608	0.006934915	0.0001436	20	25.13803	0.020802420
1100	47.864	0.175	0.0244300	0.008210562	0.0002011	30	29.79938	0.024627830
1100	47.836	0.203	0.0283388	0.009536931	0.0002711	40	34.65830	0.028604753
1100	47.780	0.259	0.0361564	0.012200377	0.0004429	50	44.45286	0.036588509
1100	47.701	0.338	0.0471848	0.015982341	0.0007581	60	58.44620	0.047918712
1100	47.657	0.382	0.0533272	0.018101418	0.0009711	70	66.33045	0.054263174
1100	47.604	0.435	0.0607260	0.020666148	0.0012636	80	75.91447	0.061937407
1100	47.532	0.507	0.0707772	0.024171977	0.0017246	90	89.08864	0.072418473
1100	47.466	0.573	0.0799908	0.027407932	0.0022124	100	101.3234	0.082082007
1100	47.404	0.635	0.0886460	0.030467508	0.0027282	110	112.9569	0.091208125
1100	47.363	0.676	0.0943696	0.032501432	0.0031004	120	120.7256	0.097268608

Table E9: Chromite (+150µm-200µm) and Coke (+150µm-200µm) at1100ºC Run 41

At °C	Mass (read)	Mass loss	Fraction loss (Exp)	Chemical Factor	Diffusion Factor	Time (Exp)	Time (model)	Fraction loss (Model)
1100	39.52	0	0	0	0	0	0	0
1100	39.31	0.21	0.0293160	0.009869078	0.0002903	10	27.4303	0.030169467
1100	39.26	0.261	0.0364356	0.012295766	0.0004498	20	34.4131	0.037751537
1100	39.21	0.312	0.0435552	0.014734437	0.0006449	30	41.5242	0.045432116
1100	39.17	0.349	0.0487204	0.016511254	0.0008089	40	46.7643	0.051065586
1100	39.12	0.400	0.0558400	0.018970955	0.0010660	50	54.0999	0.058914574
1100	39.05	0.471	0.0657516	0.022415919	0.0014849	60	64.5322	0.070002344
1100	38.98	0.539	0.0752444	0.025738240	0.0019533	70	74.7671	0.080795306
1100	38.95	0.574	0.0801304	0.027457127	0.0022203	80	80.1290	0.086416120
1100	38.88	0.639	0.0892044	0.030665564	0.0027635	90	90.2584	0.096971920
1100	38.84	0.678	0.0946488	0.032600867	0.0031192	100	96.4441	0.103377874
1100	38.77	0.746	0.1041416	0.035993882	0.0037934	110	107.426	0.114675787
1100	38.73	0.788	0.1100048	0.038101558	0.0042446	120	114.335	0.121734706

Table E10: Chromite (+50µm-100µm) and Charcoal (+50µm-100µm) at1100ºC Run 42

At °C	Mass (read)	Mass loss	Fraction loss (Exp)	Chemical Factor	Diffusion Factor	Time (Exp)	Time (model)	Fraction loss (Model)
1100	48.85	0	0	0	0	0	0	0
1100	48.82	0.026	0.0036296	0.001211333	4.398E-06	10	3.2816	0.003641788
1100	48.73	0.117	0.0163332	0.005474313	8.958E-05	20	15.0046	0.016579285
1100	48.56	0.291	0.0406236	0.013728818	0.0005603	30	38.4685	0.04213666
1100	48.49	0.356	0.0496976	0.016848132	0.000842	40	47.5950	0.051956585
1100	48.44	0.411	0.0573756	0.019503098	0.0011263	50	55.4741	0.060380103
1100	48.39	0.456	0.0636576	0.021686087	0.0013905	60	62.0286	0.067349427
1100	48.33	0.523	0.0730108	0.024954479	0.0018371	70	71.9698	0.077853882
1100	48.29	0.564	0.0787344	0.026965397	0.0021422	80	78.1620	0.084356843
1100	48.22	0.626	0.0873896	0.030022178	0.0026499	90	87.6846	0.094297519
1100	48.14	0.710	0.0991160	0.034194610	0.0034278	100	100.895	0.107968590
1100	48.11	0.741	0.1034436	0.035743582	0.0037415	110	105.861	0.113072232
1100	48.03	0.817	0.1140532	0.039562266	0.0045717	120	118.247	0.125715810

Table E11: Chromite (+50µm-100µm) and Charcoal (+100µm-150µm) at1100ºC Run 43

At °C	Mass (read)	Mass loss	Fraction loss (Exp)	Chemical Factor	Diffusion Factor	Time (Exp)	Time (model)	Fraction loss (Model)
1100	48.88	0	0	0	0	0	0	0
1100	48.88	5E-04	6.98E-05	2.32672E-05	1.624E-09	10	0.09540	6.98029E-05
1100	48.75	0.130	0.0181480	0.006086301	0.0001107	20	25.2195	0.018339991
1100	48.72	0.162	0.0226152	0.007595952	0.0001722	30	31.5567	0.022913026
1100	48.65	0.226	0.0315496	0.010629111	0.0003365	40	44.3870	0.032127972
1100	48.62	0.261	0.0364356	0.012295766	0.0004498	50	51.4923	0.037206050
1100	48.56	0.320	0.0446720	0.015118071	0.0006788	60	63.6131	0.045827730
1100	48.52	0.361	0.0503956	0.017088900	0.0008661	70	72.1432	0.051864277
1100	48.48	0.401	0.0559796	0.019019307	0.0010714	80	80.5506	0.057789109
1100	48.44	0.441	0.0615636	0.020957342	0.0012992	90	89.0432	0.063748832
1100	48.40	0.476	0.0664496	0.022659439	0.0015171	100	96.5447	0.068992063
1100	48.36	0.517	0.0721732	0.024660894	0.0017945	110	105.416	0.075167750
1100	48.28	0.597	0.0833412	0.028589998	0.0024054	120	122.992	0.087321503

Table E12: Chromite (+50µm-100µm) and Charcoal (+150µm-200µm) at1100ºC Run 44

At °C	Mass (read)	Mass loss	Fraction loss (Exp)	Chemical Factor	Diffusion Factor	Time (Exp)	Time (model)	Fraction loss (Model)
1100	41.3	0	0	0	0	0	0	0
1100	41.25	0.047	0.0065612	0.002191867	1.4392E-05	10	7.697441	0.006583307
1100	41.20	0.097	0.0135412	0.004534262	6.1492E-05	20	15.98060	0.013635212
1100	41.15	0.152	0.0212192	0.007123693	0.00015152	30	25.20566	0.021449634
1100	41.09	0.212	0.0295952	0.009964019	0.00029587	40	35.40662	0.030042560
1100	41.00	0.303	0.0422988	0.014303206	0.00060789	50	51.15543	0.043209765
1100	40.93	0.370	0.0516520	0.017522581	0.00091036	60	62.96768	0.053007121
1100	40.89	0.410	0.0572360	0.019454697	0.00112073	70	70.10875	0.058897523
1100	40.85	0.449	0.0626804	0.021345871	0.00134749	80	77.13602	0.064670161
1100	40.77	0.534	0.0745464	0.025493180	0.00191657	90	92.67596	0.077351710
1100	40.73	0.570	0.0795720	0.027260375	0.00218887	100	99.35128	0.082763802
1100	40.67	0.630	0.0879480	0.030220052	0.00268456	110	110.6024	0.091837792
1100	40.63	0.670	0.0935320	0.032203251	0.00304436	120	118.1912	0.097924245

TableE13: Chromite (+100µm-150µm) and Charcoal (+50µm-100µm) at1100ºC Run 45

At °C	Mass (read)	Mass loss	Fraction loss (Exp)	Chemical Factor	Diffusion Factor	Time (Exp)	Time (model)	Fraction loss (Model)
1100	48.82	0	0	0	0	0	0	0
1100	48.73	0.091	0.0127036	0.004252592	5.41E-05	10	15.009	0.012809345
1100	48.69	0.131	0.0182876	0.006133408	0.0001124	20	21.725	0.018506452
1100	48.66	0.165	0.0230340	0.007737718	0.0001787	30	27.493	0.023380804
1100	48.64	0.185	0.0258260	0.008683858	0.0002249	40	30.911	0.026261678
1100	48.61	0.213	0.0297348	0.010011496	0.0002987	50	35.727	0.030311787
1100	48.58	0.242	0.0337832	0.011390313	0.0003863	60	40.754	0.034527249
1100	48.47	0.354	0.0494184	0.016751858	0.0008325	70	60.546	0.051004153
1100	48.36	0.468	0.0653328	0.022269865	0.0014658	80	81.316	0.068092434
1100	48.29	0.532	0.0742672	0.025395190	0.0019020	90	93.258	0.077824247
1100	48.23	0.592	0.0826432	0.028343497	0.0023645	100	104.64	0.087037151
1100	48.18	0.645	0.0900420	0.030962800	0.0028167	110	114.85	0.095246456
1100	48.15	0.671	0.0936716	0.032252935	0.0030537	120	119.91	0.099297909

Table E14: Chromite (+100µm-150µm) and Charcoal (+100µm-150µm) at1100ºC Run 46

At °C	Mass (read)	Mass loss	Fraction loss (Exp)	Chemical Factor	Diffusion Factor	Time (Exp)	Time (model)	Fraction loss (Model)
1100	48.86	0	0	0	0	0	0	0
1100	48.79	0.073	0.0101908	0.003408538	3.478E-05	10	15.0323	0.010214349
1100	48.75	0.115	0.0160540	0.005380228	8.653E-05	20	23.7595	0.016112363
1100	48.73	0.135	0.0188460	0.006321882	0.0001194	30	27.9357	0.018926376
1100	48.68	0.178	0.0248488	0.008352503	0.0002081	40	36.9591	0.024988338
1100	48.65	0.213	0.0297348	0.010011496	0.0002987	50	44.3493	0.029934377
1100	48.60	0.256	0.0357376	0.012057328	0.0004326	60	53.4849	0.036025477
1100	48.55	0.306	0.0427176	0.014446908	0.0006201	70	64.1865	0.043128215
1100	48.51	0.353	0.0492788	0.016703728	0.0008277	80	74.3241	0.049824356
1100	48.47	0.392	0.0547232	0.018584303	0.0010233	90	82.7942	0.055395048
1100	48.38	0.478	0.0667288	0.022756881	0.0015301	100	101.660	0.067724725
1100	48.33	0.528	0.0737088	0.025199269	0.0018730	110	112.750	0.074921769
1100	48.27	0.586	0.0818056	0.028047861	0.0023159	120	125.727	0.083296492

Table E15: Chromite (+100µm-150µm) and Charcoal (+150µm-200µm) at1100ºC Run 47.

At °C	Mass (read)	Mass loss	Fraction loss (Exp)	Chemical Factor	Diffusion Factor	Time (Exp)	Time (model)	Fraction loss (Model)
1100	48.264	0	0	0	0	0	0	0
1100	48.187	0.08	0.0107492	0.003595982	3.87E-05	10	17.7519	0.010829179
1100	48.139	0.13	0.0174500	0.005850832	0.0001023	20	29.0169	0.017660443
1100	48.099	0.17	0.0230340	0.007737718	0.0001787	30	38.5224	0.023400188
1100	48.072	0.19	0.0268032	0.009015434	0.0002424	40	44.9997	0.027298582
1100	48.031	0.23	0.0325268	0.010961993	0.0003579	50	54.9305	0.033255311
1100	47.996	0.27	0.0374128	0.012629773	0.0004745	60	63.4992	0.038375430
1100	47.962	0.30	0.0421592	0.014255315	0.0006038	70	71.9041	0.043380089
1100	47.941	0.32	0.0450908	0.015262011	0.0006917	80	77.1356	0.046486323
1100	47.917	0.35	0.0484412	0.016415046	0.0007995	90	83.1521	0.050050398
1100	47.844	0.42	0.0586320	0.019938918	0.0011768	100	101.702	0.060983047
1100	47.811	0.45	0.0632388	0.021540251	0.0013720	110	110.212	0.065970345
1100	47.782	0.48	0.0672872	0.022951823	0.0015562	120	117.755	0.070376179

Table E16: Chromite (+150µm-200µm) and Charcoal (+50µm-100µm) at1100ºC Run 48

At °C	Mass (read)	Mass loss	Fraction loss (Exp)	Chemical Factor	Diffusion Factor	Time (Exp)	Time (model)	Fraction loss (Model)
1100	48.59	0	0	0	0	0	0	0
1100	48.54	0.050	0.0069800	0.002332101	1.629E-05	10	28.18070225	0.007028644
1100	48.53	0.063	0.0087948	0.002940237	2.588E-05	20	35.59344784	0.008871994
1100	48.52	0.071	0.0099116	0.003314843	3.289E-05	30	40.17281287	0.010009619
1100	48.51	0.079	0.0110284	0.003689731	4.074E-05	40	44.76567090	0.011149720
1100	48.50	0.087	0.0121452	0.004064901	4.944E-05	50	49.37204353	0.012292297
1100	48.49	0.100	0.0139600	0.004675156	6.537E-05	60	56.88627899	0.014154259
1100	48.48	0.108	0.0150768	0.005051070	7.628E-05	70	61.52823062	0.015303323
1100	48.48	0.111	0.0154956	0.005192111	8.059E-05	80	63.27246585	0.015734859
1100	48.46	0.126	0.0175896	0.005897917	0.0001039	90	72.02235590	0.017897738
1100	48.44	0.146	0.0203816	0.006840553	0.0001397	100	83.76350947	0.020795044
1100	48.41	0.183	0.0255468	0.008589162	0.0002201	110	105.7105959	0.026195526
1100	48.36	0.235	0.0328060	0.011057143	0.0003641	120	137.0546481	0.033873819

Table E17: Chromite (+150µm-200µm) and Charcoal (+100µm-150µm) at1100ºC Run 49.

At °C	Mass (read)	Mass loss	Fraction loss (Exp)	Chemical Factor	Diffusion Factor	Time (Exp)	Time (model)	Fraction loss (Model)
1100	48.702	0	0	0	0	0	0	0
1100	48.698	0.004	0.0005584	0.000186168	1.04E-07	10	1.339360	0.000557963
1100	48.696	0.006	0.0008376	0.000279278	2.339E-07	20	2.008439	0.000836616
1100	48.679	0.023	0.0032108	0.001071414	3.441E-06	30	7.679425	0.003196349
1100	48.652	0.050	0.0069800	0.002332101	1.629E-05	40	16.62659	0.006911761
1100	48.625	0.077	0.0107492	0.003595982	3.87E-05	50	25.50020	0.010587497
1100	48.589	0.113	0.0157748	0.005286161	8.354E-05	60	37.21665	0.015426922
1100	48.534	0.168	0.0234528	0.007879524	0.0001853	70	54.86122	0.022685109
1100	48.473	0.229	0.0319684	0.010771747	0.0003456	80	74.06610	0.030544500
1100	48.436	0.266	0.0371336	0.012534319	0.0004674	90	85.52647	0.035214397
1100	48.406	0.296	0.0413216	0.013968065	0.0005799	100	94.71338	0.038947052
1100	48.367	0.335	0.0467660	0.015838191	0.0007446	110	106.5145	0.043727730
1100	48.301	0.401	0.0559796	0.019019307	0.0010714	120	126.1174	0.051633847

Table E18: Chromite (+150µm-200µm) and Charcoal (+150µm-200µm) at1100ºC Run 50.

At °C	Mass (read)	Mass loss	Fraction loss (Exp)	Chemical Factor	Diffusion Factor	Time (Exp)	Time (model)	Fraction loss (Model)
1100	48.57	0	0	0	0	0	0	0
1100	48.56	0.011	0.0015356	0.000512129	7.866E-07	10	4.91573	0.001535379
1100	48.54	0.031	0.0043276	0.001444619	6.255E-06	20	13.8627	0.004325846
1100	48.52	0.052	0.0072592	0.002425612	1.762E-05	30	23.2700	0.007254268
1100	48.50	0.074	0.0103304	0.003455393	3.574E-05	40	33.1396	0.010320418
1100	48.48	0.094	0.0131224	0.004393407	5.774E-05	50	42.1247	0.013106304
1100	48.45	0.118	0.0164728	0.005521363	9.112E-05	60	52.9231	0.016447455
1100	48.42	0.149	0.0208004	0.006982103	0.0001456	70	66.8972	0.020760028
1100	48.41	0.159	0.0221964	0.007454227	0.0001659	80	71.4113	0.022150442
1100	48.39	0.179	0.0249884	0.008399826	0.0002105	90	80.4489	0.024930190
1100	48.34	0.235	0.0328060	0.011057143	0.0003641	100	105.821	0.032705852
1100	48.31	0.261	0.0364356	0.012295766	0.0004498	110	117.634	0.036312169
1100	48.29	0.284	0.0396464	0.013394067	0.0005334	120	128.103	0.039500366

TableE19: Chromite (+50µm-100µm) and graphite (+150µm-200µm) at1100ºC Run 52

At °C	Mass (read)	Mass loss	Fraction loss (Exp)	Chemical Factor	Diffusion Factor	Time (Exp)	Time (model)	Fraction loss (Model)
1100	40.27	0	0	0	0	0	0	0
1100	40.25	0.011	0.0015356	0.000512129	7.866E-07	10	3.72910	0.001531725
1100	40.24	0.024	0.0033504	0.001118050	3.747E-06	20	8.11679	0.003331961
1100	40.22	0.044	0.0061424	0.002051673	1.261E-05	30	14.8259	0.006080463
1100	40.21	0.060	0.0083760	0.002799832	2.347E-05	40	20.1571	0.008260884
1100	40.18	0.081	0.0113076	0.003783497	4.284E-05	50	27.1055	0.011097934
1100	40.16	0.110	0.0153560	0.005145093	7.914E-05	60	36.6095	0.014969658
1100	40.13	0.133	0.0185668	0.006227636	0.0001159	70	44.0713	0.018002386
1100	40.09	0.176	0.0245696	0.008257871	0.0002035	80	57.8410	0.023582449
1100	40.02	0.250	0.0349000	0.011771354	0.0004124	90	80.9817	0.032912327
1100	39.96	0.305	0.0425780	0.014399003	0.0006160	100	97.7204	0.039623901
1100	39.9	0.365	0.0509540	0.017281600	0.0008856	110	115.528	0.046729867
1100	39.86	0.409	0.0570964	0.019406302	0.0011152	120	128.284	0.051798290

TableE20: Chromite (+50µm-100µm) and Coal (+150µm-200µm) at1100ºC Run 57

At °C	Mass (read)	Mass loss	Fraction loss (Exp)	Chemical Factor	Diffusion Factor	Time (Exp)	Time (model)	Fraction loss (Model)
1100	46.28	0	0	0	0	0	0	0
1100	46.21	0.064	0.0089344	0.002987047	2.6714E-05	10	11.63613	0.008924187
1100	46.16	0.115	0.0160540	0.005380228	8.6529E-05	20	20.93963	0.016021076
1100	46.12	0.151	0.0210796	0.007076492	0.00014952	30	27.52356	0.021022902
1100	46.08	0.195	0.0272220	0.009157606	0.00025005	40	35.58964	0.027127578
1100	46.00	0.275	0.0383900	0.012964006	0.00049984	50	50.30970	0.038202694
1100	45.94	0.337	0.0470452	0.015934286	0.00075361	60	61.76691	0.046764485
1100	45.89	0.388	0.0541648	0.018391092	0.00100226	70	71.22413	0.053793317
1100	45.85	0.422	0.0589112	0.020035820	0.00118822	80	77.54559	0.058472255
1100	45.80	0.479	0.0668684	0.022805609	0.00153657	90	88.17359	0.066303948
1100	45.74	0.536	0.0748256	0.025591189	0.00193121	100	98.84003	0.074120179
1100	45.67	0.601	0.0838996	0.028787289	0.00243841	110	111.0512	0.083014684
1100	45.62	0.652	0.0910192	0.031309806	0.00287953	120	120.6685	0.089979560

Table E21: Chromite (+100µm-150µm) and Coal (+50µm-100µm) at1100ºC Run 58

At °C	Mass (read)	Mass loss	Fraction loss (Exp)	Chemical Factor	Diffusion Factor	Time (Exp)	Time (model)	Fraction loss (Model)
1100	46.30	0	0	0	0	0	0	0
1100	46.22	0.080	0.0111680	0.003736612	4.178E-05	10	12.74208	0.011200932
1100	46.17	0.137	0.0191252	0.006416146	0.0001230	20	21.92557	0.019221602
1100	46.11	0.193	0.0269428	0.009062820	0.0002449	30	31.03401	0.027133770
1100	46.07	0.234	0.0326664	0.011009566	0.0003610	40	37.75739	0.032946743
1100	45.98	0.326	0.0455096	0.015405992	0.0007047	50	53.01462	0.046052018
1100	45.92	0.383	0.0534668	0.018149685	0.0009763	60	62.58758	0.054213994
1100	45.86	0.440	0.0614240	0.020908798	0.0012933	70	72.25384	0.062408152
1100	45.81	0.495	0.0691020	0.023585922	0.0016426	80	81.67052	0.070345092
1100	45.76	0.541	0.0755236	0.025836299	0.0019681	90	89.61466	0.077005957
1100	45.70	0.601	0.0838996	0.028787289	0.0024384	100	100.0714	0.085724890
1100	45.65	0.653	0.0911588	0.031359399	0.0028886	110	109.2217	0.093309344
1100	45.60	0.703	0.0981388	0.033845530	0.0033590	120	118.0979	0.100626458

Table E22: Chromite (+100µm-150µm) and Coal (+100µm-150µm) at1100ºC Run 59

At °C	Mass (read)	Mass loss	Fraction loss (Exp)	Chemical Factor	Diffusion Factor	Time (Exp)	Time (model)	Fraction loss (Model)
1100	46.17	0	0	0	0	0	0	0
1100	46.12	0.043	0.0060028	0.002004950	1.2043E-05	10	7.424338	0.006007663
1100	46.05	0.116	0.0161936	0.005427269	8.8046E-05	20	20.12492	0.016228908
1100	46.00	0.164	0.0228944	0.007690458	0.00017652	30	28.54296	0.022964864
1100	45.95	0.213	0.0297348	0.010011496	0.00029868	40	37.19188	0.029853471
1100	45.89	0.275	0.0383900	0.012964006	0.00049984	50	48.21674	0.038587404
1100	45.83	0.335	0.0467660	0.015838191	0.00074460	60	58.97360	0.047058348
1100	45.77	0.398	0.0555608	0.018874263	0.00105527	70	70.36241	0.055972554
1100	45.74	0.428	0.0597488	0.020326639	0.00122272	80	75.81993	0.060224470
1100	45.70	0.465	0.0649140	0.022123855	0.00144674	90	82.58163	0.065474738
1100	45.60	0.564	0.0787344	0.026965397	0.00214218	100	100.8431	0.079556403
1100	45.54	0.624	0.0871104	0.029923271	0.00263262	110	112.0324	0.088114393
1100	45.48	0.687	0.0959052	0.033048576	0.00320443	120	123.8819	0.097119303

TableE23: Chromite (+100µm-150µm) and Coal (+150µm-200µm) at1100ºC Run 67

At °C	Mass (read)	Mass loss	Fraction loss (Exp)	Chemical Factor	Diffusion Factor	Time (Exp)	Time (model)	Fraction loss (Model)
1200	48.5	0	0	0	0	0	0	0
1200	48.01	0.488	0.0681248	0.023244382	0.00159579	10	46.558004	0.071725982
1200	47.96	0.544	0.0759424	0.025983424	0.00199033	20	52.354001	0.080407343
1200	47.87	0.626	0.0873896	0.030022178	0.00264987	30	61.016948	0.093281708
1200	47.84	0.665	0.0928340	0.031954906	0.00299809	40	65.211455	0.099471924
1200	47.80	0.702	0.0979992	0.033795682	0.00334924	50	69.235662	0.105384272
1200	47.77	0.731	0.1020476	0.035243370	0.00363873	60	72.420504	0.110045040
1200	47.73	0.772	0.1077712	0.037297545	0.00406955	70	76.969662	0.116674262
1200	47.70	0.796	0.1111216	0.038504068	0.00433352	80	79.658011	0.120576315
1200	47.68	0.825	0.1151700	0.039966002	0.00466417	90	82.931660	0.125312376
1200	47.65	0.855	0.1193580	0.041483048	0.00501976	100	86.347428	0.130235886
1200	47.62	0.885	0.1235460	0.043004911	0.00538920	110	89.793129	0.135183784
1200	47.59	0.910	0.1270360	0.044276838	0.00570771	120	92.687558	0.139325547

Table E24: Chromite (+150µm-200µm) and Coal (+50µm-100µm) at1100ºC Run 65

At °C	Mass (read)	Mass loss	Fraction loss (Exp)	Chemical Factor	Diffusion Factor	Time (Exp)	Time (model)	Fraction loss (Model)
1100	48.43	0	0	0	0	0	0	0
1100	48.04	0.388	0.0541648	0.018391092	0.00100226	10	45.74223	0.056094945
1100	47.99	0.435	0.0607260	0.020666148	0.00126362	20	51.62054	0.063147771
1100	47.91	0.516	0.0720336	0.024611980	0.00178743	30	61.92864	0.075430506
1100	47.90	0.523	0.0730108	0.024954479	0.00183710	40	62.83011	0.076499524
1100	47.87	0.558	0.0778968	0.026670597	0.00209602	50	67.36306	0.081862514
1100	47.84	0.585	0.0816660	0.027998606	0.00230787	60	70.88924	0.086019987
1100	47.81	0.616	0.0859936	0.029527845	0.00256419	70	74.96953	0.090815090
1100	47.78	0.646	0.0901816	0.031012357	0.00282565	80	78.95069	0.095477498
1100	47.76	0.669	0.0933924	0.032153571	0.00303507	90	82.02469	0.099066588
1100	47.73	0.695	0.0970220	0.033446889	0.00328125	100	85.52253	0.103138985
1100	47.70	0.729	0.1017684	0.035143390	0.00361837	110	90.13352	0.108488593
1100	47.67	0.760	0.1060960	0.036695416	0.00394084	120	94.37434	0.113389914

Table E25: Chromite (+150µm-200µm) and Coal (+100µm-150µm) at1100ºC Run 68

At °C	Mass (read)	Mass loss	Fraction loss (Exp)	Chemical Factor	Diffusion Factor	Time (Exp)	Time (model)	Fraction loss (Model)
1200	48.55	0	0	0	0	0	0	0
1200	48.12	0.424	0.0591904	0.02013274	0.00119966	10	44.46429	0.065224625
1200	48.06	0.491	0.0685436	0.023390727	0.00161578	20	52.43669	0.076610859
1200	48.00	0.548	0.0765008	0.026179660	0.00202024	30	59.43015	0.086522512
1200	47.96	0.584	0.0815264	0.027949355	0.00229983	40	63.94813	0.092887857
1200	47.93	0.613	0.0855748	0.029379644	0.00253877	50	67.64499	0.098074290
1200	47.90	0.642	0.0896232	0.030814160	0.00279002	60	71.39339	0.103312811
1200	47.88	0.666	0.0929736	0.032004565	0.00300731	70	74.53472	0.107687275
1200	47.85	0.699	0.0975804	0.033646168	0.00332001	80	78.91239	0.113759632
1200	47.82	0.725	0.1012100	0.034943492	0.00357781	90	82.40931	0.118590452
1200	47.80	0.745	0.1040020	0.035943812	0.00378300	100	85.12811	0.122334186
1200	47.78	0.767	0.1070732	0.037046567	0.00401566	110	88.14793	0.126479962
1200	47.76	0.790	0.1102840	0.038202154	0.00426671	120	91.33779	0.130844988

Table E26: Chromite (+50µm-100µm) and Coal (+100µm-150µm) at1100ºC Run 69

At °C	Mass (read)	Mass loss	Fraction loss (Exp)	Chemical Factor	Diffusion Factor	Time (Exp)	Time (model)	Fraction loss (Model)
1200	48.58	0	0	0	0	0	0	0
1200	48.27	0.314	0.0438344	0.014830318	0.0006533	10	32.73111	0.048297547
1200	48.2	0.377	0.0526292	0.017860153	0.0009456	20	40.16444	0.059044875
1200	48.16	0.423	0.0590508	0.020084278	0.0011939	30	45.78003	0.067110185
1200	48.01	0.575	0.0802700	0.027506328	0.0022282	40	65.48506	0.095046476
1200	47.96	0.622	0.0868312	0.029824384	0.0026154	50	71.94126	0.104076779
1200	47.93	0.653	0.0911588	0.031359399	0.0028886	60	76.29502	0.110132342
1200	47.90	0.680	0.0949280	0.032700322	0.0031380	70	80.14924	0.115470296
1200	47.89	0.694	0.0968824	0.033397082	0.0032716	80	82.17066	0.118261331
1200	47.87	0.710	0.0991160	0.034194610	0.0034278	90	84.50011	0.121470382
1200	47.85	0.726	0.1013496	0.034993458	0.0035879	100	86.85016	0.124699918
1200	47.84	0.743	0.1037228	0.035843686	0.0037622	110	89.36975	0.128153633
1200	47.82	0.760	0.1060960	0.036695416	0.0039408	120	91.91276	0.131630235

Table E27: Chromite (+150µm-200µm) and Coal (+150µm-200µm) at1100ºC Run 70

At °C	Mass (read)	Mass loss	Fraction loss (Exp)	Chemical Factor	Diffusion Factor	Time (Exp)	Time (model)	Fraction loss (Model)
1200	48.36	0	0	0	0	0	0	0
1200	47.93	0.423	0.0590508	0.020084278	0.00119393	10	54.60699	0.061693986
1200	47.92	0.436	0.0608656	0.020714668	0.00126952	20	56.39717	0.063672333
1200	47.91	0.452	0.0630992	0.021491649	0.00136582	30	58.60993	0.066113829
1200	47.88	0.482	0.0672872	0.022951823	0.00155618	40	62.78709	0.070711223
1200	47.86	0.501	0.0699396	0.023878861	0.00168337	50	65.45178	0.073636080
1200	47.83	0.529	0.0738484	0.025248242	0.00188023	60	69.40589	0.077964942
1200	47.79	0.563	0.0785948	0.026916251	0.00213445	70	74.25116	0.083251003
1200	47.77	0.589	0.0822244	0.028195657	0.00234015	80	77.98902	0.087315075
1200	47.76	0.600	0.0837600	0.028737959	0.00243014	90	79.57898	0.089040153
1200	47.70	0.655	0.0914380	0.031458599	0.00290666	100	87.60569	0.097715783
1200	47.68	0.681	0.0950676	0.032750057	0.00314745	110	91.44504	0.101845982
1200	47.65	0.710	0.0991160	0.034194610	0.00342785	120	95.76168	0.106474555

Table E28: Chromite (+50µm-100µm) and Charcoal (+50µm-100µm) at1200ºC Run 71

At °C	Mass (read)	Mass loss	Fraction loss (Exp)	Chemical Factor	Diffusion Factor	Time (Exp)	Time (model)	Fraction loss (Model)
1200	48.76	0	0	0	0	0	0	0
1200	48.72	0.044	0.0061424	0.002051673	1.261E-05	10	9.282972	0.006175891
1200	48.69	0.074	0.0103304	0.003455393	3.574E-05	20	15.69221	0.010425037
1200	48.59	0.170	0.0237320	0.007974084	0.0001897	30	36.64235	0.024229862
1200	48.50	0.266	0.0371336	0.012534319	0.0004674	40	58.27399	0.038348410
1200	48.46	0.300	0.0418800	0.014159546	0.0005958	50	66.10116	0.043423297
1200	48.42	0.347	0.0484412	0.016415046	0.0007995	60	77.06577	0.050502329
1200	48.40	0.364	0.0508144	0.017233418	0.0008807	70	81.07332	0.053080970
1200	48.38	0.382	0.0533272	0.018101418	0.0009711	80	85.34087	0.055821759
1200	48.36	0.404	0.0563984	0.019164394	0.0010877	90	90.59075	0.059186190
1200	48.34	0.424	0.0591904	0.020132740	0.0011997	100	95.39598	0.062258638
1200	48.33	0.434	0.0605864	0.020617632	0.0012577	110	97.81027	0.063799805
1200	48.31	0.454	0.0633784	0.021588858	0.0013781	120	102.6623	0.066891999

Table E29: Chromite (+50µm-100µm) and Charcoal (+100µm-150µm) at1200ºC Run 72

At °C	Mass (read)	Mass loss	Fraction loss (Exp)	Chemical Factor	Diffusion Factor	Time (Exp)	Time (model)	Fraction loss (Model)
1200	48.84	0	0	0	0	0	0	0
1200	48.80	0.044	0.0061424	0.002051673	1.2611E-05	10	9.270362	0.006167518
1200	48.64	0.202	0.0281992	0.009489499	0.00026844	20	43.50807	0.028725849
1200	48.62	0.224	0.0312704	0.010534043	0.00033056	30	48.39487	0.031917521
1200	48.58	0.263	0.0367148	0.012391174	0.00045682	40	57.13074	0.037605660
1200	48.52	0.323	0.0450908	0.015262011	0.00069168	50	70.75408	0.046431623
1200	48.49	0.351	0.0489996	0.016607482	0.00081826	60	77.18846	0.050581345
1200	48.48	0.363	0.0506748	0.017185241	0.00087585	70	79.96112	0.052365799
1200	48.46	0.382	0.0533272	0.018101418	0.00097112	80	84.36974	0.055198531
1200	48.45	0.394	0.0550024	0.018680938	0.00103389	90	87.16590	0.056992255
1200	48.43	0.407	0.0568172	0.019309525	0.00110417	100	90.20538	0.058939493
1200	48.42	0.424	0.0591904	0.020132740	0.00119966	110	94.19632	0.061492205
1200	48.39	0.455	0.0635180	0.021637470	0.00138428	120	101.5215	0.066165548

Table E30: Chromite (+50µm-100µm) and Charcoal (+150µm-200µm) at1200ºC Run 73

At °C	Mass (read)	Mass loss	Fraction loss (Exp)	Chemical Factor	Diffusion Factor	Time (Exp)	Time (model)	Fraction loss (Model)
1200	49.86	0	0	0	0	0	0	0
1200	48.77	1.085	0.1514660	0.053276663	0.00821277	10	51.27663	0.277186849
1200	48.74	1.116	0.1557936	0.054888865	0.00870763	20	53.56731	0.288200045
1200	48.7	1.163	0.1623548	0.057343714	0.00948778	30	57.13519	0.305130091
1200	48.66	1.203	0.1679388	0.059443064	0.01018035	40	60.26259	0.319747364
1200	48.60	1.263	0.1763148	0.062609774	0.01126909	50	65.11217	0.342006257
1200	48.57	1.291	0.1802236	0.064094922	0.01179785	60	67.44102	0.352520552
1200	48.56	1.303	0.1818988	0.064732859	0.01202852	70	68.45200	0.357049831
1200	48.54	1.323	0.1846908	0.065798025	0.01241841	80	70.15425	0.364628236
1200	48.52	1.343	0.1874828	0.066865626	0.01281512	90	71.87818	0.372242255
1200	48.50	1.362	0.1901352	0.067882115	0.01319835	100	73.53609	0.379507084
1200	48.48	1.382	0.1929272	0.068954504	0.01360845	110	75.30261	0.387185865
1200	48.45	1.408	0.1965568	0.070352313	0.01415193	120	77.63196	0.397214023

Table E31: Chromite (+100µm-150µm) and Charcoal (+50µm-100µm) at1200ºC Run 74

At °C	Mass (read)	Mass loss	Fraction loss (Exp)	Chemical Factor	Diffusion Factor	Time (Exp)	Time (model)	Fraction loss (Model)
1200	48.97	0	0	0	0	0	0	0
1200	48.80	0.175	0.0244300	0.008210562	0.00020113	10	29.34037	0.024938653
1200	48.74	0.231	0.0322476	0.010866861	0.00035170	20	39.08911	0.033132152
1200	48.69	0.282	0.0393672	0.013298465	0.00052584	30	48.12216	0.040683044
1200	48.65	0.325	0.0453700	0.015357994	0.00070036	40	55.85406	0.047114967
1200	48.59	0.385	0.0537460	0.018246233	0.00098663	50	66.82169	0.056189194
1200	48.56	0.417	0.0582132	0.019793602	0.00115985	60	72.75716	0.061075868
1200	48.53	0.442	0.0617032	0.021005891	0.00130520	70	77.43623	0.064916246
1200	48.51	0.469	0.0654724	0.022318545	0.00147212	80	82.53126	0.069086092
1200	48.48	0.492	0.0686832	0.023439518	0.00162248	90	86.90575	0.072656330
1200	48.46	0.516	0.0720336	0.024611980	0.00178743	100	91.50422	0.076399525
1200	48.44	0.536	0.0748256	0.025591189	0.00193121	110	95.36278	0.079532638
1200	48.41	0.562	0.0784552	0.026867110	0.00212674	120	100.4151	0.083624346

Table E32: Chromite (+100µm-150µm) and Charcoal (+100µm-150µm) at1200ºC Run 75

At °C	Mass (read)	Mass loss	Fraction loss (Exp)	Chemical Factor	Diffusion Factor	Time (Exp)	Time (model)	Fraction loss (Model)
1200	48.847	0	0	0	0	0	0	0
1200	48.667	0.180	0.0251280	0.008447153	0.00021286	10	31.048326	0.025651098
1200	48.631	0.216	0.0301536	0.010153954	0.00030721	20	37.475877	0.030905924
1200	48.589	0.258	0.0360168	0.012152690	0.00043947	30	45.068104	0.037088546
1200	48.542	0.305	0.0425780	0.014399003	0.00061602	40	53.684480	0.044073247
1200	48.504	0.343	0.0478828	0.016222686	0.00078099	50	60.744632	0.049771185
1200	48.464	0.383	0.0534668	0.018149685	0.00097628	60	68.267693	0.055817749
1200	48.405	0.442	0.0617032	0.021005891	0.00130520	70	79.536823	0.064827094
1200	48.382	0.465	0.0649140	0.022123855	0.00144674	80	83.986091	0.068368314
1200	48.36	0.487	0.0679852	0.023195610	0.00158915	90	88.271641	0.071770766
1200	48.347	0.500	0.0698000	0.023830026	0.00167655	100	90.817731	0.073788270
1200	48.324	0.523	0.0730108	0.024954479	0.00183710	110	95.347422	0.077370335
1200	48.314	0.533	0.0744068	0.025444182	0.00190927	120	97.326877	0.078932778

Table E33: Chromite (+150µm-200µm) and Charcoal (+50µm-100µm) at1200ºC Run 77

At °C	Mass (read)	Mass loss	Fraction loss (Exp)	Chemical Factor	Diffusion Factor	Time (Exp)	Time (model)	Fraction loss (Model)
1200	48.88	0	0	0	0	0	0	0
1200	48.78	0.107	0.0149372	0.005004066	7.4871E-05	10	35.4776874	0.015127792
1200	48.72	0.159	0.0221964	0.007454227	0.00016587	20	53.1748008	0.022616523
1200	48.68	0.199	0.0277804	0.009347232	0.00026048	30	66.9934962	0.028437592
1200	48.68	0.202	0.0281992	0.009489499	0.00026844	40	68.0371498	0.028876285
1200	48.68	0.204	0.0284784	0.009584367	0.00027382	50	68.7334827	0.029168911
1200	48.68	0.208	0.0290368	0.009774156	0.00028473	60	70.1275026	0.029754556
1200	48.67	0.211	0.0294556	0.009916546	0.00029306	70	71.1742031	0.030194132
1200	48.67	0.213	0.0297348	0.010011496	0.00029868	80	71.8725683	0.030487346
1200	48.66	0.227	0.0316892	0.010676652	0.00033954	90	76.7737948	0.032543504
1200	48.64	0.247	0.0344812	0.011628430	0.00040252	100	83.8141050	0.035491957
1200	48.61	0.276	0.0385296	0.013011772	0.00050351	110	94.1034792	0.039790321
1200	48.60	0.288	0.0402048	0.013585325	0.00054867	120	98.3892883	0.041576934

Table E34: Chromite (+150µm-200µm) and Charcoal (+100µm-150µm) at1200ºC Run 78

At °C	Mass (read)	Mass loss	Fraction loss (Exp)	Chemical Factor	Diffusion Factor	Time (Exp)	Time (model)	Fraction loss (Model)
1200	48.86	0	0	0	0	0	0	0
1200	48.82	0.033	0.0046068	0.001537964	7.0887E-06	10	12.452576	0.004662451
1200	48.76	0.101	0.0140996	0.004722130	6.6685E-05	20	39.177424	0.014619705
1200	48.75	0.111	0.0154956	0.005192111	8.0594E-05	30	43.229367	0.016123572
1200	48.74	0.114	0.0159144	0.005333192	8.5025E-05	40	44.451073	0.016576704
1200	48.68	0.173	0.0241508	0.008115957	0.00019654	50	69.054937	0.025672717
1200	48.67	0.184	0.0256864	0.008636508	0.00022248	60	73.764131	0.027407279
1200	48.64	0.214	0.0298744	0.010058977	0.00030151	70	86.803599	0.032199430
1200	48.64	0.217	0.0302932	0.010201449	0.00031009	80	88.123385	0.032683587
1200	48.64	0.220	0.0307120	0.010343962	0.00031878	90	89.446057	0.033168641
1200	48.63	0.223	0.0311308	0.010486516	0.00032759	100	90.771617	0.033654591
1200	48.63	0.227	0.0316892	0.010676652	0.00033954	110	92.543526	0.034303918
1200	48.62	0.242	0.0337832	0.011390313	0.00038626	120	99.234012	0.036753067

Table E35: Chromite (+150µm-200µm) and Charcoal (+150µm-200µm) at1200ºC Run 79.

At °C	Mass (read)	Mass loss	Fraction loss (Exp)	Chemical Factor	Diffusion Factor	Time (Exp)	Time (model)	Fraction loss (Model)
1200	48.86	0	0	0	0	0	0	0
1200	48.83	0.035	0.0048860	0.001631326	7.975E-06	10	18.76033	0.004886021
1200	48.80	0.059	0.0082364	0.002753039	2.2696E-05	20	31.66017	0.008236459
1200	48.79	0.067	0.0093532	0.003127504	2.9283E-05	30	35.96659	0.009353276
1200	48.79	0.075	0.0104700	0.003502251	3.6711E-05	40	40.27626	0.010470095
1200	48.77	0.088	0.0122848	0.004111817	5.0582E-05	50	47.28640	0.012284931
1200	48.76	0.099	0.0138204	0.004628187	6.4062E-05	60	53.22479	0.013820566
1200	48.76	0.102	0.0142392	0.004769108	6.8016E-05	70	54.84542	0.014239376
1200	48.72	0.137	0.0191252	0.006416146	0.00012297	80	73.78690	0.019125517
1200	48.70	0.157	0.0219172	0.007359767	0.00016170	90	84.63893	0.021917616
1200	48.68	0.180	0.0251280	0.008447153	0.00021286	100	97.14439	0.025128546
1200	48.66	0.202	0.0281992	0.009489499	0.00026844	110	109.1319	0.028199887
1200	48.62	0.242	0.0337832	0.011390313	0.00038626	120	130.9925	0.033784185

Table E36: Chromite (+50µm-100µm) and Coke (+100µm-150µm) at1300ºC Run 91

At °C	Mass (read)	Mass loss	Fraction loss (Exp)	Chemical Factor	Diffusion Factor	Time (Exp)	Time (model)	Fraction loss (Model)
1300	54.73	0	0	0	0	0	0	0
1300	53.84	0.883	0.1232668	0.042903303	0.00536414	10	52.55679	0.125721372
1300	53.75	0.973	0.1358308	0.047497200	0.00655365	20	58.30737	0.138800328
1300	53.70	1.028	0.1435088	0.050326539	0.00734335	30	61.86052	0.146815944
1300	53.64	1.084	0.1513264	0.053224747	0.00819706	40	65.50911	0.154994957
1300	53.60	1.130	0.1577480	0.055618762	0.00893623	50	68.52976	0.161726635
1300	53.57	1.161	0.1620756	0.057238991	0.00945384	60	70.57756	0.166269862
1300	53.53	1.201	0.1676596	0.059337874	0.01014509	70	73.23447	0.172139956
1300	53.49	1.235	0.1724060	0.061129318	0.01075353	80	75.50589	0.177136457
1300	53.45	1.273	0.1777108	0.063139643	0.01145642	90	78.05886	0.182728251
1300	53.42	1.311	0.1830156	0.065158634	0.01218366	100	80.62709	0.188327868
1300	53.39	1.336	0.1865056	0.066491688	0.01267550	110	82.32512	0.192016063
1300	53.33	1.395	0.1947420	0.069652883	0.01387873	120	86.35921	0.200733416

Table E37: Chromite (+100µm-150µm) and Coke (+50µm-100µm) at1300ºC Run 94.

At °C	Mass (read)	Mass loss	Fraction loss (Exp)	Chemical Factor	Diffusion Factor	Time (Exp)	Time (model)	Fraction loss (Model)
1300	54.32	0	0	0	0	0	0	0
1300	53.87	0.455	0.0635180	0.021637470	0.00138428	10	46.0435	0.067487448
1300	53.82	0.500	0.0698000	0.023830026	0.00167655	20	51.0131	0.074584554
1300	53.77	0.548	0.0765008	0.026179660	0.00202024	30	56.3998	0.082236418
1300	53.75	0.569	0.0794324	0.027211200	0.00218105	40	58.7845	0.085610432
1300	53.71	0.609	0.0850164	0.029182112	0.00250508	50	63.3744	0.092081170
1300	53.67	0.652	0.0910192	0.031309806	0.00287953	60	68.3787	0.099101229
1300	53.62	0.701	0.0978596	0.033745839	0.00333949	70	74.1707	0.107181016
1300	53.57	0.750	0.1047000	0.036194216	0.00383523	80	80.0589	0.115345420
1300	53.54	0.778	0.1086088	0.037598892	0.00413472	90	83.4672	0.120048455
1300	53.52	0.805	0.1123780	0.038957296	0.00443476	100	86.7841	0.124609270
1300	53.47	0.852	0.1189392	0.041331127	0.00498358	110	92.6294	0.132608306
1300	53.38	0.942	0.1315032	0.045909860	0.00612962	120	104.079	0.148135036

Table E38: Chromite (+100µm-150µm) and Coke (+150µm-200µm) at1300ºC Run 95

At °C	Mass (read)	Mass loss	Fraction loss (Exp)	Chemical Factor	Diffusion Factor	Time (Exp)	Time (model)	Fraction loss (Model)
1300	54.632	0	0	0	0	0	0	0
1300	54.124	0.508	0.0709168	0.024220846	0.00173153	10	30.27914	0.080327216
1300	53.837	0.795	0.1109820	0.038453736	0.00432235	20	51.37604	0.133674145
1300	53.739	0.893	0.1246628	0.043411560	0.00549007	30	59.28186	0.153121079
1300	53.694	0.938	0.1309448	0.045705427	0.00607600	40	63.03557	0.162251771
1300	53.634	0.998	0.1393208	0.048781177	0.00690665	50	68.16326	0.174618162
1300	53.595	1.037	0.1447652	0.050791130	0.00747716	60	71.57228	0.182771947
1300	53.549	1.083	0.1511868	0.053172838	0.00818138	70	75.67101	0.192504081
1300	53.526	1.106	0.1543976	0.054368199	0.00854629	80	77.75223	0.197416059
1300	53.469	1.163	0.1623548	0.057343714	0.00948778	90	83.00242	0.209718700
1300	53.429	1.203	0.1679388	0.059443064	0.01018035	100	86.76611	0.218460260
1300	53.393	1.239	0.1729644	0.061340526	0.01082637	110	90.20996	0.226402263
1300	53.347	1.285	0.1793860	0.063776279	0.01168343	120	94.68911	0.236651072

Table E39: Chromite (+150µm-200µm) and Coke (+150µm-200µm) at1300ºC Run 96

At °C	Mass (read)	Mass loss	Fraction loss (Exp)	Chemical Factor	Diffusion Factor	Time (Exp)	Time (model)	Fraction loss (Model)
1300	54.468	0	0	0	0	0	0	0
1300	53.962	0.506	0.0706376	0.024123112	0.00171770	10	51.33808	0.075047335
1300	53.912	0.556	0.0776176	0.026572370	0.00208075	20	56.89009	0.082930782
1300	53.892	0.576	0.0804096	0.027555533	0.00223608	30	59.13600	0.086107054
1300	53.862	0.606	0.0845976	0.029034016	0.00247997	40	62.53198	0.090895851
1300	53.836	0.632	0.0882272	0.030319019	0.00270199	50	65.50162	0.095069708
1300	53.809	0.659	0.0919964	0.031657061	0.00294306	60	68.61162	0.099427145
1300	53.789	0.679	0.0947884	0.032650592	0.00312857	70	70.93261	0.102669946
1300	53.752	0.716	0.0999536	0.034494024	0.00348743	80	75.26542	0.108702761
1300	53.724	0.744	0.1038624	0.035893746	0.00377259	90	78.57816	0.113296997
1300	53.706	0.762	0.1063752	0.036795719	0.00396214	100	80.72328	0.116263492
1300	53.686	0.782	0.1091672	0.037799896	0.00417848	110	83.12105	0.119571529
1300	53.498	0.970	0.1354120	0.047343355	0.00651195	120	106.4082	0.151270900

Table E40: Chromite (+100µm-150µm) and Coke (+100µm-150µm) at1300ºC Run 97

At °C	Mass (read)	Mass loss	Fraction loss (Exp)	Chemical Factor	Diffusion Factor	Time (Exp)	Time (model)	Fraction loss (Model)
1300	54.65	0	0	0	0	0	0	0
1300	54.17	0.483	0.0674268	0.023000570	0.0015627	10	28.4261	0.075539606
1300	53.83	0.823	0.1148908	0.039865036	0.0046410	20	53.1334	0.138022529
1300	53.76	0.890	0.1242440	0.043259026	0.0054521	30	58.4892	0.151184493
1300	53.71	0.942	0.1315032	0.045909860	0.0061296	40	62.7601	0.161583888
1300	53.65	0.999	0.1394604	0.048832608	0.0069210	50	67.5578	0.173164411
1300	53.62	1.031	0.1439276	0.050481352	0.0073878	60	70.3051	0.179747394
1300	53.57	1.078	0.1504888	0.052913376	0.0081032	70	74.4111	0.189520724
1300	53.52	1.130	0.1577480	0.055618762	0.0089362	80	79.0531	0.200476186
1300	53.47	1.178	0.1644488	0.058129874	0.0097444	90	83.4317	0.210718916
1300	53.41	1.236	0.1725456	0.061182111	0.0107717	100	88.8437	0.223258049
1300	53.40	1.251	0.1746396	0.061974720	0.0110465	110	90.2652	0.226529306
1300	53.36	1.284	0.1792464	0.063723193	0.0116644	120	93.4244	0.233766388

Table E41: Chromite (+150µm-200µm) and Coke (+50µm-100µm) at1300ºC Run 98

At °C	Mass (read)	Mass loss	Fraction loss (Exp)	Chemical Factor	Diffusion Factor	Time (Exp)	Time (model)	Fraction loss (Model)
1300	54.231	0	0	0	0	0	0	0
1300	53.641	0.590	0.0823640	0.028244932	0.00234826	10	35.99419722	0.104142478
1300	53.465	0.766	0.1069336	0.036996387	0.00400492	20	50.21262763	0.143200560
1300	53.423	0.808	0.1127968	0.039108467	0.00446879	30	53.85546079	0.153021353
1300	53.337	0.894	0.1248024	0.043462415	0.00550275	40	61.62147392	0.173706793
1300	53.261	0.970	0.1354120	0.047343355	0.00651195	50	68.83278859	0.192610634
1300	53.202	1.029	0.1436484	0.050378138	0.00735816	60	74.66004961	0.207673944
1300	53.181	1.050	0.1465800	0.051463009	0.00767273	70	76.78301931	0.213114846
1300	53.165	1.066	0.1488136	0.052291247	0.00791716	80	78.41786028	0.217287718
1300	53.122	1.109	0.1548164	0.054524338	0.00859452	90	82.88625163	0.228617802
1300	53.101	1.130	0.1577480	0.055618762	0.00893623	100	85.10833023	0.234211183
1300	53.067	1.164	0.1624944	0.057396084	0.00950477	110	88.76182522	0.243348815
1300	53.033	1.198	0.1672408	0.059180133	0.01009233	120	92.48483045	0.252585224

Table E42: Chromite (+50µm-100µm) and Coal (+50µm-100µm) at1300ºC Run 99

At °C	Mass (read)	Mass loss	Fraction loss (Exp)	Chemical Factor	Diffusion Factor	Time (Exp)	Time (model)	Fraction loss (Model)
1300	52.196	0	0	0	0	0	0	0
1300	50.423	1.773	0.2475108	0.090435663	0.02305655	10	40.9646299	0.356255632
1300	50.223	1.973	0.2754308	0.101827081	0.02899462	20	47.9448983	0.406907118
1300	50.055	2.141	0.2988836	0.111624222	0.03459823	30	54.2462063	0.450285835
1300	49.941	2.255	0.3147980	0.118397376	0.03873444	40	58.7598780	0.480022138
1300	49.801	2.395	0.3343420	0.126860333	0.04419737	50	64.5765207	0.516734761
1300	49.701	2.495	0.3483020	0.133007256	0.04836675	60	68.9222247	0.543005715
1300	49.599	2.597	0.3625412	0.139368231	0.05285647	70	73.5243526	0.569769926
1300	49.491	2.705	0.3776180	0.146207489	0.05787904	80	78.5896721	0.597996475
1300	49.393	2.803	0.3912988	0.152509733	0.06268314	90	83.3628047	0.623439026
1300	49.244	2.952	0.4120992	0.162275243	0.07045329	100	90.9545484	0.661656059
1300	49.104	3.092	0.4316432	0.171663078	0.07828743	110	98.4713804	0.696857780
1300	49.030	3.166	0.4419736	0.176712386	0.08264531	120	102.600903	0.715113597

Table E43: Chromite (+50µm-100µm) and Coal (+100µm-150µm) at1300ºC Run 100

At °C	Mass (read)	Mass loss	Fraction loss (Exp)	Chemical Factor	Diffusion Factor	Time (Exp)	Time (model)	Fraction loss (Model)
1300	56.80	0	0	0	0	0	0	0
1300	54.62	2.182	0.3046072	0.114048264	0.03605417	10	44.4421530	0.529471662
1300	54.24	2.558	0.3570968	0.136925015	0.05111111	20	58.0516711	0.642479569
1300	54.17	2.630	0.3671480	0.141446455	0.05436143	30	60.9061505	0.663617191
1300	54.07	2.728	0.3808288	0.147678228	0.05898519	40	64.9267593	0.691952299
1300	53.99	2.811	0.3924156	0.153028354	0.06308589	50	68.4572076	0.715481059
1300	53.89	2.911	0.4063756	0.159565418	0.06825794	60	72.8678464	0.743151979
1300	53.84	2.959	0.4130764	0.162739651	0.07083253	70	75.0474454	0.756137270
1300	53.82	2.986	0.4168456	0.164535786	0.07230744	80	76.2916216	0.763349539
1300	53.78	3.024	0.4221504	0.167076838	0.07441622	90	78.0650997	0.773382160
1300	53.76	3.044	0.4249424	0.168420485	0.07554173	100	79.0091351	0.778605026
1300	53.73	3.074	0.4291304	0.170444134	0.07725039	110	80.4390631	0.786362276
1300	53.70	3.100	0.4327600	0.172205984	0.07875120	120	81.6919166	0.793008139

Table E44: Chromite (+50µm-100µm) and Coal (+150µm-200µm) at1300ºC Run 101

At °C	Mass (read)	Mass loss	Fraction loss (Exp)	Chemical Factor	Diffusion Factor	Time (Exp)	Time (model)	Fraction loss (Model)
1300	60.271	0	0	0	0	0	0	0
1300	58.621	1.650	0.2303400	0.083569280	0.01978421	10	45.2982	0.302715407
1300	58.482	1.789	0.2497444	0.091336503	0.02350315	20	50.6365	0.333726323
1300	58.312	1.959	0.2734764	0.101020251	0.02855343	30	57.5402	0.372449070
1300	58.149	2.122	0.2962312	0.110505358	0.03393544	40	64.5634	0.410272568
1300	58.030	2.241	0.3128436	0.117559974	0.03821160	50	69.9510	0.438233962
1300	57.981	2.290	0.3196840	0.120497871	0.04006002	60	72.2352	0.449817052
1300	57.901	2.370	0.3308520	0.125337055	0.04319020	70	76.0489	0.468799789
1300	57.810	2.461	0.3435556	0.130907539	0.04692368	80	80.5172	0.490478671
1300	57.780	2.491	0.3477436	0.132759703	0.04819560	90	82.0212	0.497640803
1300	57.739	2.532	0.3534672	0.135303859	0.04996735	100	84.1020	0.507438068
1300	57.701	2.570	0.3587720	0.137675300	0.05164433	110	86.0567	0.516525474
1300	57.670	2.601	0.3630996	0.139619602	0.05303751	120	87.6703	0.523942212

Table E45: Chromite (+100µm-150µm) and Coal (+100µm-150µm) at1300ºC Run 102

At°C	Mass (read)	Mass loss	Fraction loss (Exp)	Chemical Factor	Diffusion Factor	Time (Exp)	Time (model)	Fraction loss (Model)
1300	57.356	0	0	0	0	0	0	0
1300	56.210	1.146	0.1599816	0.056454315	0.00920142	10	30.925293	0.192324687
1300	55.888	1.468	0.2049328	0.073594171	0.01545112	20	42.388048	0.256804301
1300	55.560	1.796	0.2507216	0.091731182	0.02370007	30	55.499071	0.326237945
1300	55.390	1.966	0.2744536	0.101423485	0.02877354	40	62.904692	0.363473951
1300	55.169	2.187	0.3053052	0.114344788	0.03623414	50	73.195637	0.412902505
1300	55.125	2.231	0.3114476	0.116962802	0.03784072	60	75.337692	0.422858279
1300	55.099	2.257	0.3150772	0.118517135	0.03880948	70	76.618397	0.428756585
1300	55.025	2.331	0.3254076	0.122971281	0.04164668	80	80.325085	0.445601044
1300	55.003	2.353	0.3284788	0.124304249	0.04251325	90	81.444864	0.450623772
1300	54.963	2.393	0.3340628	0.126738275	0.04411628	100	83.501993	0.459771724
1300	54.938	2.418	0.3375528	0.128266459	0.04513630	110	84.801687	0.465498724
1300	54.901	2.455	0.3427180	0.130538052	0.04667176	120	86.745182	0.473986843

Table E46: Chromite (+100µm-150µm) and Coal (+150µm-200µm) at 1300ºC Run 103

At °C	Mass (read)	Mass loss	Fraction loss (Exp)	Chemical Factor	Diffusion Factor	Time (Exp)	Time (model)	Fraction loss (Model)
1300	54.055	0	0	0	0	0	0	0
1300	52.368	1.687	0.2355052	0.085623944	0.02073888	10	52.011048	0.308208044
1300	52.198	1.857	0.2592372	0.095185146	0.02545584	20	59.379612	0.345925559
1300	52.078	1.977	0.2759892	0.102057871	0.02912140	30	64.854949	0.373046368
1300	52.016	2.039	0.2846444	0.105650379	0.03112747	40	67.775525	0.387201157
1300	51.980	2.075	0.2896700	0.107749666	0.03232803	50	69.500567	0.395460754
1300	51.950	2.105	0.2938580	0.109506649	0.03334878	60	70.954696	0.402365280
1300	51.927	2.128	0.2970688	0.110858379	0.03414393	70	72.079828	0.407671433
1300	51.902	2.153	0.3005588	0.112332328	0.03502071	80	73.313011	0.413450976
1300	51.879	2.176	0.3037696	0.113692698	0.03583890	90	74.456998	0.418778756
1300	51.858	2.197	0.3067012	0.114938432	0.03659566	100	75.509475	0.423651773
1300	51.83	2.225	0.310610	0.116604885	0.03761921	110	76.924688	0.430161234
1300	51.799	2.256	0.3149376	0.118457252	0.03877195	120	78.50753	0.437383448

Table E47: Chromite (+150µm-200µm) and Coal (+100µm-150µm) at 1300ºC Run 104

At °C	Mass (read)	Mass loss	Fraction loss (Exp)	Chemical Factor	Diffusion Factor	Time (Exp)	Time (model)	Fraction loss (Model)
1300	58.02	0	0	0	0	0	0	0
1300	56.42	1.601	0.2234996	0.080862339	0.0185587	10	42.22083	0.319992756
1300	56.15	1.866	0.2604936	0.095696985	0.0257210	20	52.78467	0.387636244
1300	55.83	2.195	0.3064220	0.114819639	0.0365232	30	67.57926	0.474605400
1300	55.78	2.239	0.3125644	0.117440475	0.0381373	40	69.70711	0.486391595
1300	55.76	2.261	0.3156356	0.118756750	0.0389598	50	70.78472	0.492292677
1300	55.72	2.298	0.3208008	0.120979395	0.0403667	60	72.61784	0.502226854
1300	55.70	2.318	0.3235928	0.122185520	0.0411396	70	73.61964	0.507600745
1300	55.68	2.344	0.3272224	0.123758454	0.0421575	80	74.93355	0.514589992
1300	55.64	2.384	0.3328064	0.126189437	0.0437525	90	76.98068	0.525347221
1300	55.62	2.404	0.3355984	0.127410017	0.0445634	100	78.01603	0.530726751
1300	55.60	2.422	0.3381112	0.128511466	0.0453008	110	78.95462	0.535568248
1300	55.57	2.451	0.3421596	0.130291902	0.0465043	120	80.48037	0.543367239

TableE48: Chromite (+150µm-200µm) and Coal (+150µm-200µm) at1300 ºC Run 105

At °C	Mass (read)	Mass loss	Fraction loss (Exp)	Chemical Factor	Diffusion Factor	Time (Exp)	Time (model)	Fraction loss (Model)
1300	55.500	0	0	0	0	0	0	0
1300	53.777	1.723	0.2405308	0.087631978	0.02169217	10	53.49114	0.349925608
1300	53.689	1.811	0.2528156	0.092578081	0.02412519	20	57.53764	0.372435222
1300	53.597	1.903	0.2656588	0.097807322	0.02682751	30	61.92632	0.396254193
1300	53.507	1.993	0.2782228	0.102982217	0.02963169	40	66.37982	0.419801027
1300	53.446	2.054	0.2867384	0.106523884	0.03162449	50	69.49037	0.435878846
1300	53.401	2.099	0.2930204	0.109154698	0.03314314	60	71.83355	0.447792169
1300	53.386	2.114	0.2951144	0.110035098	0.03365862	70	72.62387	0.451772174
1300	53.364	2.136	0.2981856	0.111329511	0.03442309	80	73.79143	0.457616918
1300	53.325	2.175	0.3036300	0.113633464	0.03580309	90	75.88602	0.467997914
1300	53.301	2.199	0.3069804	0.115057256	0.03666822	100	77.19089	0.474397562
1300	53.286	2.214	0.3090744	0.115949458	0.03721512	110	78.01263	0.478401270
1300	53.267	2.233	0.3117268	0.117082172	0.03791472	120	79.06038	0.483476591

Table E49: Chromite (+50µm-100µm) and Charcoal (+50µm-100µm) at1300 ºC Run 107

At °C	Mass (read)	Mass loss	Fraction loss (Exp)	Chemical Factor	Diffusion Factor	Time (Exp)	Time (model)	Fraction loss (Model)
1300	55	0	0	0	0	0	0	0
1300	54.49	0.513	0.0716148	0.024465268	0.00176636	10	32.51139	0.073165618
1300	54.30	0.704	0.0982784	0.033895383	0.00336881	20	45.41152	0.101177720
1300	54.18	0.824	0.1150304	0.039915517	0.00465255	30	53.75119	0.118983161
1300	54.09	0.914	0.1275944	0.044480660	0.00575957	40	60.12869	0.132439487
1300	54.00	1.001	0.1397396	0.048935487	0.00694968	50	66.39600	0.145529160
1300	53.91	1.091	0.1523036	0.053588273	0.00830733	60	72.98769	0.159153529
1300	53.86	1.140	0.1591440	0.056140809	0.00910148	70	76.62365	0.166606344
1300	53.79	1.206	0.1683576	0.059600894	0.01023336	80	81.57451	0.176683395
1300	53.73	1.274	0.1778504	0.063192663	0.01147524	90	86.74056	0.187111497
1300	53.67	1.326	0.1851096	0.065958010	0.01247748	100	90.73641	0.195116771
1300	53.60	1.398	0.1951608	0.069814197	0.01394151	110	96.33506	0.206244453
1300	53.55	1.454	0.2029784	0.072835708	0.01514233	120	100.7434	0.214933679

Table E50: Chromite (+100µm-150µm) and Charcoal (+50µm-100µm) at1300 ºC Run 108

At °C	Mass (read)	Mass loss	Fraction loss (Exp)	Chemical Factor	Diffusion Factor	Time (Exp)	Time (model)	Fraction loss (Model)
1300	54.515	0	0	0	0	0	0	0
1300	53.934	0.581	0.0811076	0.027801635	0.00227582	10	40.28778	0.083870438
1300	53.765	0.750	0.1047000	0.036194216	0.00383523	20	52.97304	0.109272719
1300	53.688	0.827	0.1154492	0.040066990	0.00468745	30	58.90625	0.120991034
1300	53.593	0.922	0.1287112	0.044888567	0.00586405	40	66.36242	0.135570930
1300	53.552	0.963	0.1344348	0.046984577	0.00641521	50	69.62753	0.141904475
1300	53.511	1.004	0.1401584	0.049089847	0.00699284	60	72.92149	0.148262557
1300	53.480	1.035	0.1444860	0.050687848	0.00744731	70	75.43138	0.153086055
1300	53.423	1.092	0.1524432	0.053640228	0.00832315	80	80.09021	0.161991072
1300	53.399	1.116	0.1557936	0.054888865	0.00870763	90	82.06899	0.165754395
1300	53.352	1.163	0.1623548	0.057343714	0.00948778	100	85.97387	0.173147771
1300	53.332	1.183	0.1651468	0.058392219	0.00983076	110	87.64756	0.176303273
1300	53.315	1.200	0.1675200	0.059285288	0.01012749	120	89.0759	0.178989827

Table E51: Chromite (+150µm-200µm) and Charcoal (+50µm-100µm) at1300 ºC Run 109

At ºC	Mass (read)	Mass loss	Fraction loss (Exp)	Chemical Factor	Diffusion Factor	Time (Exp)	Time (model)	Fraction loss (Model)
1300	54.855	0	0	0	0	0	0	0
1300	54.666	0.189	0.0263844	0.008873303	0.00023481	10	20.43207694	0.026414486
1300	54.609	0.246	0.0343416	0.011580797	0.00039924	20	26.67575726	0.034392475
1300	54.533	0.322	0.0449512	0.015214026	0.00068736	30	35.06099565	0.045038145
1300	54.498	0.357	0.0498372	0.016896276	0.00084681	40	38.94611596	0.049943948
1300	54.468	0.387	0.0540252	0.018342801	0.00099703	50	42.28814585	0.054150515
1300	54.431	0.424	0.0591904	0.02013274	0.00119966	60	46.42526915	0.059340632
1300	54.337	0.518	0.0723128	0.024709812	0.00180155	70	57.01272361	0.072536297
1300	54.229	0.626	0.0873896	0.030022178	0.00264987	80	69.31599643	0.087714755
1300	54.169	0.686	0.0957656	0.03299881	0.0031949	90	76.21675387	0.096155221
1300	53.923	0.932	0.1301072	0.04539894	0.00599605	100	105.0171681	0.130819699
1300	53.83	1.025	0.1430900	0.050171776	0.00729904	110	116.1249889	0.143948626
1300	53.762	1.093	0.1525828	0.053692189	0.00833898	120	124.3259326	0.153556454

Table E52: Chromite (+150µm-200µm) and Charcoal (+100µm-150µm) at1300ºC Run 110

At ºC	Mass (read)	Mass loss	Fraction loss (Exp)	Chemical Factor	Diffusion Factor	Time (Exp)	Time (model)	Fraction loss (Model)
1300	54.79	0	0	0	0	0	0	0
1300	54.62	0.170	0.0237320	0.007974084	0.00018974	10	31.59274	0.023507907
1300	54.57	0.222	0.0309912	0.010438993	0.00032464	20	41.23655	0.030609670
1300	54.52	0.272	0.0379712	0.012820735	0.00048890	30	50.50070	0.037399355
1300	54.50	0.292	0.0407632	0.013776658	0.00056416	40	54.20398	0.040104583
1300	54.49	0.307	0.0428572	0.014494818	0.00062421	50	56.98054	0.042129523
1300	54.47	0.324	0.0452304	0.015310000	0.00069601	60	60.12638	0.044420336
1300	54.45	0.345	0.0481620	0.016318856	0.00079022	70	64.01107	0.047244134
1300	54.38	0.411	0.0573756	0.019503098	0.00112628	80	76.21035	0.056075676
1300	54.32	0.471	0.0657516	0.022415919	0.00148489	90	87.28785	0.064047682
1300	54.28	0.513	0.0716148	0.024465268	0.00176636	100	95.03490	0.069596152
1300	54.24	0.553	0.0771988	0.026425067	0.00205795	110	102.4076	0.074856074
1300	54.14	0.657	0.0917172	0.031557820	0.00292483	120	121.5515	0.088421452

Table E53: Chromite (+150µm-200µm) and Charcoal (+150µm-200µm) at1300ºC Run 111

At °C	Mass (read)	Mass loss	Fraction loss (Exp)	Chemical Factor	Diffusion Factor	Time (Exp)	Time (model)	Fraction loss (Model)
1300	54.77	0	0	0	0	0	0	0
1300	54.60	0.170	0.0237320	0.007974084	0.00018974	10	32.84505	0.024432070
1300	54.49	0.282	0.0393672	0.013298465	0.00052584	20	55.82308	0.041285738
1300	54.38	0.391	0.0545836	0.018535994	0.00101801	30	79.23403	0.058256166
1300	54.34	0.431	0.0601676	0.020472114	0.00124016	40	88.08927	0.064622684
1300	54.32	0.452	0.0630992	0.021491649	0.00136582	50	92.79569	0.067994684
1300	54.29	0.486	0.0678456	0.023146842	0.00158253	60	100.5000	0.073497063
1300	54.26	0.510	0.0711960	0.024318600	0.00174542	70	106.0015	0.077412924
1300	54.24	0.530	0.0739880	0.025297220	0.00188747	80	110.6262	0.080696170
1300	54.22	0.548	0.0765008	0.026179660	0.00202024	90	114.8198	0.083666602
1300	54.21	0.565	0.0788740	0.027014547	0.00214993	100	118.8078	0.086485456
1300	54.19	0.585	0.0816660	0.027998606	0.00230787	110	123.5338	0.089818419
1300	54.17	0.603	0.0841788	0.028885965	0.00245499	120	127.8188	0.092833434

Table E54: Chromite (+50µm-100µm) and Charcoal (+100µm-150µm) at1300ºC Run 112

At °C	Mass (read)	Mass loss	Fraction loss (Exp)	Chemical Factor	Diffusion Factor	Time (Exp)	Time (model)	Fraction loss (Model)
1300	54.83	0	0	0	0	0	0	0
1300	54.26	0.574	0.0801304	0.027457127	0.00222028	10	33.5332630	0.088694717
1300	54.10	0.732	0.1021872	0.035293368	0.00364894	20	44.2961161	0.116008066
1300	53.99	0.844	0.1178224	0.040926241	0.00488777	30	52.3505228	0.136087125
1300	53.89	0.940	0.1312240	0.045807633	0.00610278	40	59.5425624	0.153757365
1300	53.78	1.055	0.1472780	0.051721678	0.00774867	50	68.5168525	0.175466406
1300	53.72	1.110	0.1549560	0.054576396	0.00861063	60	72.9499785	0.186051865
1300	53.68	1.148	0.1602608	0.056558863	0.00923486	70	76.0670422	0.193440314
1300	53.63	1.198	0.1672408	0.059180133	0.01009233	80	80.2366450	0.203253528
1300	53.58	1.251	0.1746396	0.061974720	0.01104652	90	84.7419796	0.213767066
1300	53.52	1.315	0.1835740	0.065371667	0.01226164	100	90.3012923	0.226612149
1300	53.46	1.372	0.1915312	0.068418001	0.01340254	110	95.3636049	0.238186496
1300	53.43	1.402	0.1957192	0.070029368	0.01402547	120	98.0705157	0.244327852

Table E55: Chromite (+50µm-100µm) and Charcoal (+150µm-200µm) at 1300ºC Run 113

At °C	Mass (read)	Mass loss	Fraction loss (Exp)	Chemical Factor	Diffusion Factor	Time (Exp)	Time (model)	Fraction loss (Model)
1300	53.29	0	0	0	0	0	0	0
1300	52.98	0.315	0.043974	0.014878265	0.00065750	10	27.43838	0.045037076
1300	52.84	0.447	0.0624012	0.021248710	0.00133534	20	39.58301	0.064531567
1300	52.78	0.515	0.0718940	0.024563071	0.00178039	30	45.99392	0.074714478
1300	52.69	0.602	0.0840392	0.028836625	0.00244669	40	54.35262	0.087879853
1300	52.62	0.676	0.0943696	0.032501432	0.00310036	50	61.60294	0.099197838
1300	52.54	0.747	0.1042812	0.036043958	0.00380385	60	68.68297	0.110159256
1300	52.48	0.808	0.1127968	0.039108467	0.00446879	70	74.86403	0.119655858
1300	52.42	0.868	0.1211728	0.042141928	0.00517814	80	81.03361	0.129067219
1300	52.35	0.937	0.1308052	0.045654332	0.00606264	90	88.24044	0.139975597
1300	52.28	1.016	0.1418336	0.049707791	0.00716695	100	96.64097	0.152575388
1300	52.23	1.058	0.1476968	0.051876947	0.00779443	110	101.1729	0.159321384
1300	52.16	1.129	0.1576084	0.055566589	0.00891980	120	108.9397	0.170799035

Table E56: Chromite (+100µm-150µm) and Charcoal (+100µm-150µm) at1300ºC Run 114.

At °C	Mass (read)	Mass loss	Fraction loss (Exp)	Chemical Factor	Diffusion Factor	Time (Exp)	Time (model)	Fraction loss (Model)
1300	53.81	0	0	0	0	0	0	0
1300	53.49	0.322	0.0449512	0.015214026	0.00068736	10	21.8838897	0.046164851
1300	53.02	0.788	0.1100048	0.038101558	0.00424456	20	56.9500566	0.117138900
1300	52.98	0.825	0.1151700	0.039966002	0.00466417	30	59.9169479	0.122976890
1300	52.89	0.918	0.1281528	0.044684570	0.00581169	40	67.4983330	0.137777849
1300	52.84	0.965	0.1347140	0.047087057	0.00644277	50	71.3982355	0.145326246
1300	52.82	0.991	0.1383436	0.048421314	0.00680681	60	73.5756288	0.149521437
1300	52.79	1.018	0.1421128	0.049810859	0.00719619	70	75.8519660	0.153892562
1300	52.76	1.048	0.1463008	0.051359581	0.00764247	80	78.3995099	0.158766680
1300	52.73	1.079	0.1506284	0.052965257	0.00811879	90	81.0523283	0.163822284
1300	52.70	1.109	0.1548164	0.054524338	0.00859452	100	83.6394149	0.168733071
1300	52.67	1.136	0.1585856	0.055931921	0.00903519	110	85.9845982	0.173168031
1300	52.65	1.159	0.1617964	0.057134292	0.00941997	120	87.9949855	0.176957280

Table E57: Chromite (+as received) and Charcoal (+as received) at1300ºC Run 115.

At °C	Mass (read)	Mass loss	Fraction loss (Exp)	Chemical Factor	Diffusion Factor	Time (Exp)	Time (model)	Fraction loss (Model)
1300	53.179	0	0	0	0	0	0	0
1300	53.147	0.032	0.0044672	0.001491290	6.6652E-06	10	8.0129721	0.004445049
1300	53.097	0.082	0.0114472	0.003830386	4.3903E-05	20	20.420668	0.011301968
1300	53.061	0.118	0.0164728	0.005521363	9.112E-05	30	29.268640	0.016172382
1300	53.021	0.158	0.0220568	0.007406995	0.00016378	40	39.015104	0.021518832
1300	52.981	0.198	0.0276408	0.009299819	0.00025785	50	48.671912	0.026796964
1300	52.955	0.224	0.0312704	0.010534043	0.00033056	60	54.900471	0.030191224
1300	52.920	0.259	0.0361564	0.012200377	0.00044292	70	63.224543	0.034715102
1300	52.880	0.299	0.0417404	0.014111669	0.00059180	80	72.652230	0.039821746
1300	52.852	0.327	0.0456492	0.015453996	0.00070910	90	79.196999	0.043356203
1300	52.812	0.367	0.0512332	0.017377978	0.00089549	100	88.468164	0.048348170
1300	52.767	0.412	0.0575152	0.019551503	0.00113184	110	98.787100	0.053883844
1300	52.596	0.583	0.0813868	0.027900110	0.00229181	120	136.90972	0.074148830

Table E58: Chromite (+as received) and Coal (+as received) at1300ºC Run 117.

At °C	Mass (read)	Mass loss	Fraction loss (Exp)	Chemical Factor	Diffusion Factor	Time (Exp)	Time (model)	Fraction loss (Model)
1300	55.303	0	0	0	0	0	0	0
1300	52.560	2.743	0.3829228	0.148640147	0.05971360	10	59.520444	0.484924706
1300	52.520	2.783	0.3885068	0.151215949	0.0616833	20	60.785610	0.493011464
1300	52.480	2.823	0.3940908	0.153807480	0.06369305	30	62.065508	0.501105806
1300	52.440	2.863	0.3996748	0.156414982	0.06574335	40	63.360333	0.509206419
1300	52.406	2.897	0.4044212	0.158644102	0.06751836	50	64.472820	0.516095869
1300	52.343	2.960	0.4132160	0.162806037	0.07088681	60	66.563513	0.528868163
1300	52.302	3.001	0.4189396	0.165536985	0.07313523	70	67.944902	0.537182709
1300	52.266	3.037	0.4239652	0.167949715	0.07514657	80	69.171557	0.544483405
1300	52.221	3.082	0.4302472	0.170985444	0.07771020	90	70.723183	0.553607726
1300	52.167	3.136	0.4377856	0.174657920	0.08086015	100	72.612414	0.564551809
1300	52.130	3.173	0.4429508	0.177193239	0.08306550	110	73.924347	0.572045482
1300	52.095	3.208	0.4478368	0.179605980	0.08518735	120	75.178632	0.579129009

Table E59: Chromite (+as received) and Coke (+as received) at1300ºCRun 118.

At °C	Mass (read)	Mass loss	Fraction loss (Exp)	Chemical Factor	Diffusion Factor	Time (Exp)	Time (model)	Fraction loss (Model)
1300	52.83	0	0	0	0	0	0	0
1300	52.34	0.493	0.0688228	0.023488315	0.00162919	10	37.51333	0.073165973
1300	52.14	0.694	0.0968824	0.033397082	0.00327160	20	54.67586	0.105414210
1300	52.09	0.745	0.1040020	0.035943812	0.00378300	30	59.21191	0.113810603
1300	52.05	0.785	0.1095860	0.037950703	0.00421145	40	62.82208	0.120455479
1300	52.00	0.835	0.1165660	0.040471151	0.00478117	50	67.40036	0.128834362
1300	51.95	0.880	0.1228480	0.042750931	0.00532666	60	71.58372	0.136443819
1300	51.90	0.938	0.1309448	0.045705427	0.00607600	70	77.06454	0.146346104
1300	51.86	0.974	0.1359704	0.047548492	0.00656758	80	80.51735	0.152545300
1300	51.84	0.999	0.1394604	0.048832608	0.00692098	90	82.93828	0.156873919
1300	51.81	1.029	0.1436484	0.050378138	0.00735816	100	85.86862	0.162093618
1300	51.78	1.058	0.1476968	0.051876947	0.00779443	110	88.72762	0.167165421
1300	51.74	1.092	0.1524432	0.053640228	0.00832315	120	92.11275	0.173144057

Table E60: Chromite (+as received) and graphite (+as received) at1300ºC Run 119

At °C	Mass (read)	Mass loss	Fraction loss (Exp)	Chemical Factor	Diffusion Factor	Time (Exp)	Time (model)	Fraction loss (Model)
1300	52.3	0	0	0	0	0	0	0
1300	52.04	0.263	0.0367148	0.012391174	0.00045682	10	43.44905638	0.038981364
1300	52.00	0.302	0.0421592	0.014255315	0.00060385	20	50.42408992	0.045143212
1300	51.96	0.345	0.0481620	0.016318856	0.00079022	30	58.27747877	0.052049424
1300	51.94	0.365	0.0509540	0.017281600	0.00088564	40	61.98885638	0.055301562
1300	51.91	0.390	0.0544440	0.018487688	0.00101275	50	66.68074822	0.05940223p
1300	51.89	0.409	0.0570964	0.019406302	0.00111520	60	70.28589681	0.062545021
1300	51.87	0.430	0.0600280	0.020423618	0.00123433	70	74.31020970	0.06604494p
1300	51.84	0.460	0.0642160	0.021880602	0.00141533	80	80.13184160	0.071092545
1300	51.82	0.481	0.0671476	0.022903080	0.00154963	90	84.25806621	0.074659124
1300	51.80	0.500	0.0698000	0.023830026	0.00167655	100	88.02774179	0.077909522
1300	51.78	0.524	0.0731504	0.025003428	0.00184425	110	92.8391184p	0.082047057
1300	51.75	0.550	0.0767800	0.026277808	0.00203528	120	98.11432738	0.086569218

Table E61: Chromite (+as received) and Charcoal (+as received) at1200ºC Run 120.

At ^{o}C	Mass (read)	Mass loss	Fraction loss (Exp)	Chemical Factor	Diffusion Factor	Time (Exp)	Time (model)	Fraction loss (Model)
1200	53.355	0	0	0	0	0	0	0
1200	53.037	0.318	0.0443928	0.015022135	0.00067021	10	45.586366	0.049801138
1200	53.009	0.346	0.0483016	0.016366949	0.00079486	20	50.152230	0.054696028
1200	52.970	0.385	0.0537460	0.018246233	0.00098663	30	56.664524	0.061648481
1200	52.949	0.406	0.0566776	0.019261143	0.00109868	40	60.245212	0.065456618
1200	52.909	0.446	0.0622616	0.021200136	0.00132928	50	67.209974	0.072834251
1200	52.868	0.487	0.0679852	0.023195610	0.00158915	60	74.546762	0.080563861
1200	52.858	0.497	0.0693812	0.023683549	0.00165616	70	76.366803	0.082474676
1200	52.848	0.507	0.0707772	0.024171977	0.00172461	80	78.198888	0.084395460
1200	52.825	0.530	0.0739880	0.025297220	0.00188747	90	82.458519	0.088850951
1200	52.800	0.555	0.0774780	0.026523264	0.00207313	100	87.161312	0.093753168
1200	52.782	0.573	0.0799908	0.027407932	0.00221241	110	90.594467	0.097320781
1200	52.771	0.584	0.0815264	0.027949355	0.00229983	120	92.712009	0.099516581

Table E62: Chromite (+as received) and Coke (+as received) at1200ºC Run 121.

At ^{o}C	Mass (read)	Mass loss	Fraction loss (Exp)	Chemical Factor	Diffusion Factor	Time (Exp)	Time (model)	Fraction loss (Model)
1200	53.530	0	0	0	0	0	0	0
1200	53.042	0.488	0.0681248	0.023244382	0.00159579	10	39.7231708	0.082728724
1200	52.964	0.566	0.0790136	0.027063703	0.00215769	20	47.5987750	0.098568854
1200	52.898	0.632	0.0882272	0.030319019	0.00270199	30	54.6055720	0.112507346
1200	52.848	0.682	0.0952072	0.032799798	0.00315691	40	60.1257957	0.123386870
1200	52.809	0.721	0.1006516	0.034743676	0.00353749	50	64.5598491	0.132061044
1200	52.763	0.767	0.1070732	0.037046567	0.00401566	60	69.9356421	0.142500530
1200	52.716	0.814	0.1136344	0.039410952	0.00453724	70	75.5929186	0.153395884
1200	52.679	0.851	0.1187996	0.041280498	0.00497155	80	80.1646628	0.162132878
1200	52.629	0.901	0.1257796	0.043818554	0.00559193	90	86.5096522	0.174158791
1200	52.599	0.931	0.1299676	0.045347879	0.00598278	100	90.4095434	0.181493000
1200	52.579	0.951	0.1327596	0.046370157	0.00625116	110	93.0484608	0.186431085
1200	52.560	0.970	0.1354120	0.047343355	0.00651195	120	95.5844701	0.191157850

Table E63: Chromite (+as received) and Coal (+as received) at1200ºC Run 122.

At ^{o}C	Mass (read)	Mass loss	Fraction loss (Exp)	Chemical Factor	Diffusion Factor	Time (Exp)	Time (model)	Fraction loss (Model)
1200	54.859	0	0	0	0	0	0	0
1200	53.45	1.409	0.1966964	0.070406159	0.01417307	10	38.083613	0.259295867
1200	53.009	1.850	0.2582600	0.094787405	0.02525072	20	55.590481	0.361669692
1200	52.896	1.963	0.2740348	0.101250626	0.02867909	30	60.575612	0.388988819
1200	52.832	2.027	0.2829692	0.104952803	0.03073314	40	63.494321	0.404615918
1200	52.770	2.089	0.2916244	0.108568730	0.03280207	50	66.388942	0.419848607
1200	52.720	2.139	0.2986044	0.111506314	0.03452811	60	68.772204	0.432193512
1200	52.660	2.199	0.3069804	0.115057256	0.03666822	70	71.690657	0.447070513
1200	52.586	2.273	0.3173108	0.119476379	0.03941286	80	75.379553	0.465500086
1200	52.509	2.350	0.3280600	0.124122241	0.04239446	90	79.325016	0.484753236
1200	52.460	2.399	0.3349004	0.127104552	0.04435981	100	81.893687	0.497036013
1200	52.382	2.477	0.3457892	0.131894376	0.04759948	110	86.077384	0.516620932
1200	52.350	2.509	0.3502564	0.133874809	0.04896866	120	87.827986	0.524662667

Table E64: Chromite (+as received) and Coke (+as received) at1100ºC Run 125.

At ^{o}C	Mass (read)	Mass loss	Fraction loss (Exp)	Chemical Factor	Diffusion Factor	Time (Exp)	Time (model)	Fraction loss (Model)
1100	52.76	0	0	0	0	0	0	0
1100	52.36	0.407	0.0568172	0.019309525	0.00110417	10	40.835507	0.084977118
1100	52.28	0.485	0.0677060	0.023098080	0.00157592	20	52.036278	0.107413108
1100	52.23	0.532	0.0742672	0.025395190	0.00190199	30	59.328159	0.121820376
1100	52.21	0.555	0.0774780	0.026523264	0.00207313	40	63.046735	0.129107458
1100	52.19	0.579	0.0808284	0.027703179	0.00225988	50	67.032899	0.136874028
1100	52.17	0.599	0.0836204	0.028688634	0.00242189	60	70.437706	0.143471213
1100	52.15	0.619	0.0864124	0.029676092	0.00258974	70	73.918299	0.150180408
1100	52.13	0.639	0.0892044	0.030665564	0.00276346	80	77.474992	0.157000006
1100	52.11	0.659	0.0919964	0.031657061	0.00294306	90	81.108098	0.163928349
1100	52.09	0.679	0.0947884	0.032650592	0.00312857	100	84.817934	0.170963737
1100	52.07	0.699	0.0975804	0.033646168	0.00332001	110	88.604818	0.178104421
1100	52.05	0.719	0.1003724	0.034643800	0.00351742	120	92.469071	0.185348606

Table E65: Chromite (+as received) and Charcoal (+as received) at1100ºC Run126.

At ^{o}C	Mass (read)	Mass loss	Fraction loss (Exp)	Chemical Factor	Diffusion Factor	Time (Exp)	Time (model)	Fraction loss (Model)
1100	53.524	0	0	0	0	0	0	0
1100	53.415	0.109	0.0152164	0.005098080	7.7706E-05	10	19.6477275	0.015846145
1100	53.376	0.148	0.0206608	0.006934915	0.00014361	20	27.1096685	0.021820154
1100	53.330	0.194	0.0270824	0.009110211	0.00024748	30	36.2072825	0.029070910
1100	53.297	0.227	0.0316892	0.010676652	0.00033954	40	42.9329519	0.034408140
1100	53.251	0.273	0.0381108	0.012868488	0.00049253	50	52.5879768	0.042035746
1100	53.210	0.314	0.0438344	0.014830318	0.00065329	60	61.4704194	0.049017428
1100	53.172	0.352	0.0491392	0.016655602	0.00082299	70	69.9378914	0.055641280
1100	53.121	0.403	0.0562588	0.019116027	0.00108230	80	81.6604974	0.064760656
1100	53.086	0.438	0.0611448	0.020811723	0.00128136	90	89.9450628	0.071169943
1100	53.040	0.484	0.0675664	0.023049323	0.00156932	100	101.132656	0.079778568
1100	53.016	0.508	0.0709168	0.024220846	0.00173153	110	107.105584	0.084352756
1100	52.976	0.548	0.0765008	0.026179660	0.00202024	120	117.269148	0.092101333

Table E66: Chromite (as received) & graphite (+as received) at1100ºC Run 127.

At ^{o}C	Mass (read)	Mass loss	Fraction loss (Exp)	Chemical Factor	Diffusion Factor	Time (Exp)	Time (model)	Fraction loss (Model)
1100	52.308	0	0	0	0	0	0	0
1100	52.236	0.072	0.0100512	0.003361688	3.3827E-05	10	26.898989	0.010180065
1100	52.219	0.089	0.0124244	0.004158738	5.1741E-05	20	33.376617	0.012621191
1100	52.201	0.107	0.0149372	0.005004066	7.4871E-05	30	40.288319	0.015221471
1100	52.186	0.122	0.0170312	0.005709604	9.7426E-05	40	46.089881	0.017400573
1100	52.166	0.142	0.0198232	0.006651883	0.00013215	50	53.884629	0.020323263
1100	52.140	0.168	0.0234528	0.007879524	0.00018528	60	64.119589	0.024152118
1100	52.120	0.188	0.0262448	0.008825935	0.00023232	70	72.071278	0.027119915
1100	52.100	0.208	0.0290368	0.009774156	0.00028473	80	80.091656	0.030107247
1100	52.080	0.228	0.0318288	0.010724197	0.00034256	90	88.180999	0.033114065
1100	52.059	0.249	0.0347604	0.011723708	0.00040911	100	96.749339	0.036292143
1100	52.039	0.269	0.0375524	0.012677507	0.00047808	110	104.98094	0.039338754
1100	52.003	0.305	0.0425780	0.014399003	0.00061602	120	119.97396	0.044871336

Table E67: Chromite (+as received) and Charcoal (+as received) at1000ºC Run 128.

At °C	Mass (read)	Mass loss	Fraction loss (Exp)	Chemical Factor	Diffusion Factor	Time (Exp)	Time (model)	Fraction loss (Model)
1000	53.652	0	0	0	0	0	0	0
1000	53.369	0.283	0.0395068	0.013346264	0.00052961	10	33.85290	0.047585877
1000	53.215	0.437	0.0610052	0.020763193	0.00127543	20	57.63241	0.080093171
1000	53.184	0.468	0.0653328	0.022269865	0.00146575	30	62.88998	0.087179112
1000	53.172	0.480	0.0670080	0.022854342	0.00154309	40	64.96809	0.089969837
1000	53.152	0.500	0.0698000	0.023830026	0.00167655	50	68.48506	0.094679866
1000	53.132	0.520	0.0725920	0.024807665	0.00181573	60	72.06909	0.099462955
1000	53.120	0.532	0.0742672	0.025395190	0.00190199	70	74.25180	0.102367646
1000	53.110	0.542	0.0756632	0.025885336	0.00197546	80	76.08930	0.104808072
1000	53.099	0.553	0.0771988	0.026425067	0.00205795	90	78.13007	0.107513292
1000	53.089	0.563	0.0785948	0.026916251	0.00213445	100	80.00311	0.109991368
1000	53.078	0.574	0.0801304	0.027457127	0.00222028	110	82.08307	0.112737823
1000	53.066	0.586	0.0818056	0.028047861	0.00231592	120	84.37561	0.115758420

Table E68: Chromite (+as received) and Coke (+as received) at1000ºC Run 129.

At °C	Mass (read)	Mass loss	Fraction loss (Exp)	Chemical Factor	Diffusion Factor	Time (Exp)	Time (model)	Fraction loss (Model)
1000	53.57	0	0	0	0	0	0	0
1000	52.94	0.622	0.0868312	0.029824384	0.00261542	10	56.455387	0.096355255
1000	52.89	0.680	0.0949280	0.032700322	0.00313800	20	62.494147	0.106279296
1000	52.87	0.700	0.0977200	0.033696001	0.00332974	30	64.608636	0.109736976
1000	52.85	0.720	0.1005120	0.034693736	0.00352745	40	66.739734	0.113212780
1000	52.84	0.730	0.1019080	0.035193377	0.00362854	50	67.811534	0.114957453
1000	52.83	0.740	0.1033040	0.035693537	0.00373114	60	68.887513	0.116706625
1000	52.81	0.752	0.1049792	0.036294415	0.00385623	70	70.184218	0.118811558
1000	52.80	0.762	0.1063752	0.036795719	0.00396214	80	71.269424	0.120570593
1000	52.79	0.772	0.1077712	0.037297545	0.00406955	90	72.358839	0.122334094
1000	52.78	0.782	0.1091672	0.037799896	0.00417848	100	73.452472	0.124102050
1000	52.78	0.787	0.1098652	0.038051267	0.00423351	110	74.000873	0.124987695
1000	52.77	0.797	0.1112612	0.038554406	0.00434471	120	75.100850	0.126762313

Table E69: Chromite (+as received) and Coal (+as received) at1000ºC Run 130.

At °C	Mass (read)	Mass loss	Fraction loss (Exp)	Chemical Factor	Diffusion Factor	Time (Exp)	Time (model)	Fraction loss (Model)
1000	54.29	0	0	0	0	0	0	0
1000	53.95	0.338	0.0471848	0.015982341	0.00075814	10	40.5706561	0.084442102
1000	53.90	0.389	0.0543044	0.018439388	0.00100749	20	49.9949961	0.103351910
1000	53.86	0.424	0.0591904	0.020132740	0.00119966	30	56.9777011	0.117193416
1000	53.84	0.446	0.0622616	0.021200136	0.00132928	40	61.5829281	0.126243749
1000	53.83	0.460	0.0642160	0.021880602	0.00141533	50	64.6007899	0.132140867
1000	53.81	0.479	0.0668684	0.022805609	0.00153657	60	68.8054163	0.140312685
1000	53.79	0.499	0.0696604	0.023781195	0.00166974	70	73.3673638	0.149120767
1000	53.77	0.516	0.0720336	0.024611980	0.00178743	80	77.3551228	0.156770765
1000	53.76	0.529	0.0738484	0.025248242	0.00188023	90	80.4730827	0.162720121
1000	53.74	0.549	0.0766404	0.026228732	0.00202775	100	85.3862527	0.172038007
1000	53.72	0.567	0.0791532	0.027112864	0.00216546	110	89.9290591	0.180591748
1000	53.70	0.587	0.0819452	0.028097121	0.00232398	120	95.1115425	0.190277772

Table E70: Chromite (+150µm-200µm) and Coal (+50µm-100µm) at1300ºC Run 133

At °C	Mass (read)	Mass loss	Fraction loss (Exp)	Chemical Factor	Diffusion Factor	Time (Exp)	Time (model)	Fraction loss (Model)
1300	55.267	0	0	0	0	0	0	0
1300	53.356	1.911	0.2667756	0.098264911	0.02707029	10	44.72002	0.299299825
1300	52.855	2.412	0.3367152	0.127899206	0.04489022	20	60.13773	0.386621001
1300	52.787	2.480	0.3462080	0.132079658	0.04772684	30	62.37723	0.398666764
1300	52.726	2.541	0.3547236	0.135864340	0.05036148	40	64.41803	0.409505480
1300	52.676	2.591	0.3617036	0.138991448	0.05258562	50	66.11370	0.418411500
1300	52.648	2.619	0.3656124	0.140752596	0.05385690	60	67.07242	0.423407014
1300	52.620	2.647	0.3695212	0.142520994	0.05514686	70	68.03777	0.428408125
1300	52.587	2.680	0.3741280	0.144614585	0.05669138	80	69.18411	0.434309201
1300	52.561	2.706	0.3777576	0.146271328	0.05792687	90	70.09390	0.438963592
1300	52.537	2.730	0.3811080	0.147806358	0.05908199	100	70.93894	0.443263753
1300	52.514	2.753	0.3843188	0.149282636	0.06020230	110	71.75351	0.447388036
1300	52.492	2.775	0.3873900	0.150699537	0.06128617	120	72.53705	0.451335909

Table E71: Chromite (+100µm-200µm) and Coal (+50µm-100µm) at1300ºC Run 132

At ^{o}C	Mass (read)	Mass loss	Fraction loss (Exp)	Chemical Factor	Diffusion Factor	Time (Exp)	Time (model)	Fraction loss (Model)
1300	54.946	0	0	0	0	0	0	0
1300	52.86	2.086	0.2912056	0.108393089	0.03270015	10	53.1672812	0.348101162
1300	52.723	2.223	0.3103308	0.116485644	0.03754555	20	57.8579230	0.374194338
1300	52.634	2.312	0.3227552	0.121823335	0.04090683	30	61.0013836	0.391285281
1300	52.568	2.378	0.3319688	0.125823927	0.04351098	40	63.3828641	0.404024115
1300	52.492	2.454	0.3425784	0.130476502	0.04662986	50	66.1795581	0.418755563
1300	52.443	2.503	0.3494188	0.133502788	0.04871014	60	68.0141584	0.428286150
1300	52.393	2.553	0.3563988	0.136612782	0.05088993	70	69.9120927	0.438035516
1300	52.364	2.582	0.3604472	0.138426892	0.05218094	80	71.0250389	0.443700642
1300	52.345	2.601	0.3630996	0.139619602	0.05303751	90	71.7590949	0.447416223
1300	52.325	2.621	0.3658916	0.140878669	0.05394842	100	72.5359928	0.451330597
1300	52.305	2.641	0.3686836	0.142141437	0.05486886	110	73.317233	0.455248164
1300	52.280	2.666	0.3721736	0.143725144	0.05603291	120	74.2999321	0.460149419